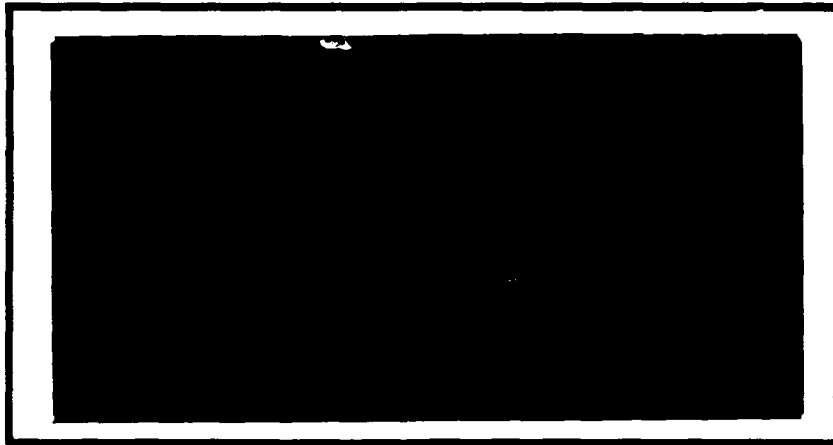


AD-A205 771

1



DTIC
 ELECTE
 MAR 29 1989
 S
 as D

DEPARTMENT OF THE AIR FORCE
 AIR UNIVERSITY

AIR FORCE INSTITUTE OF TECHNOLOGY

Wright-Patterson Air Force Base, Ohio

80

(1)

AFIT/GAE/AA/88D-02

DTIC
ELECTRONIC
MAR 29 1969
S
D
S

Navier-Stokes Solution For A NACA 0012

Airfoil With Mass Flux (Fan)

Thesis

Paul D. Boyles
Captain, USAF

AFIT/GAE/AA/88D-02

Approved for public release; distribution unlimited

J

A-1

AFIT/GAE/AA/88D-02

NAVIER-STOKES SOLUTION FOR A NACA 0012 AIRFOIL
WITH MASS FLUX (FAN)

THESIS

Presented to the Faculty of the School of Engineering
of the Air Force Institute of Technology
Air University
In Partial Fulfillment of the
Requirements for the Degree of
Master of Science in Aeronautical Engineering

Paul D. Boyles
Captain, USAF

December 1988

Approved for public release; distribution unlimited

Preface

The purpose of this study was to numerically simulate the flow field for NACA 0012 airfoil with mass transfer through the surface (fan). Recent emphasis in V/STOL and the advancements in today's technology has created an environment where a detailed knowledge of the flow characteristics involved in lift augmentation is needed. One particular area especially lacking in research is the "Fan-in-wing" device. Such a device was not practical in the 60's when it was studied for its vertical take off and hovering performance. However, with today's advances in material science, propulsion and aviation technology, such a device could be practical.

In two-dimensions, a "fan" is characterized by suction normal to the upper airfoil surface and vectored blowing on the lower airfoil surface. This study examines the lift and drag effects of such a device with varying suction velocity, ejection angle and angle of attack. The current "state of the art" in computational fluid dynamics (CFD) makes it possible to do this initial study by numerical simulation. It is hoped that the results obtained in this work can be an aid in the design of future experimental tests which will verify these numerical results and perhaps lead to V/STOL applications.

I would like to thank Dr. Halim for supervising this

work, and Capt Beran for his support and aid in this research. I would also like to thank Dr Shang, the sponsor of this research, and the wonderful group of people that work for him at the Flight Dynamics Laboratory. Without their technical guidance and sharing of computer resources, this thesis could not have been accomplished.

Finally, My wife and two small children need a special thanks for their patience, understanding and support during the many late nights and busy weekends over the past five months. I can now begin to try and make it up to them.

Table of Contents

	Page
Preface.....	ii
List of Figures.....	vi
List of Tables.....	ix
List of Symbols.....	x
Abstract.....	xiv
I. Introduction.....	1
II. Analysis.....	14
Governing Equations.....	14
III. Numerical Solutions of the NS Equations.....	28
Implicit Navier-Stokes Code.....	28
Grid Generation.....	33
Convergence Criteria.....	34
IV. Results and Discussion.....	37
Code and Grid Verification.....	37
Suction and Ejection Separately.....	44
Convergence Criterion for Periodic Solutions.....	55
The Effect of Varying Suction Rate....	70
The Effect of Varying Ejection Angle..	78
The Effect of Varying Angle of Attack.	85
V. Conclusions and Recommendations.....	91
Appendix A: Non-Dimensional Variables.....	93
Appendix B: Jacobian Matrices for the Navier-Stokes Equations.....	96
Appendix C: Boundary and Initial Conditions.....	98
Boundary Conditions Without Blowing..	98
Boundary Conditions for Suction and Blowing.....	100
Initial Conditions.....	103
Appendix D: Derivation of Force Coefficients C_1 and C_d	105

Appendix E: Computer Resource Requirements.....	109
Appendix F: Navier-Stokes Code, Fortran Listing..	111
Appendix G: Hyperbolic Grid Generating Code, Fortran Listing.....	112
Appendix H: Data Reduction Program 1, Fortran Listing.....	113
Appendix I: Data Reduction Program 2, Fortran Listing.....	114
Appendix J: Geometric Progression Program, Fortran Listing.....	115
Appendix K: Grid Redistribution Program, Fortran Listing.....	116
Bibliography.....	117
Vita.....	121

List of Figures

Figure	Page
1. A "Fan-in-Wing".....	2
2. A "Fan-in-Wing" Aircraft.....	2
3. Propulsion System for the Ryan XV-5A.....	3
4. V/STOL Aircraft Configurations.....	4
5. Effect of Boundary Layer Geometry on Stability.....	5
6. Effect of Suction on the Boundary Layer.....	6
7. Boundary Layer Control a)Blowing, b)Slotted Wing, c)Suction.....	7
8. Blowing Non-Tangent to the Surface.....	8
9. Three-Dimensional Effects of a Fan.....	9
10. General Transformation from the Physical Domain to the Computational Domain b.....	18
11. Final Grid Configuration for a NACA 0012 Airfoil.....	39
12. Final Grid Configuration, Close-Up.....	40
13. Comparisons of C_p with Experimental Data....	43
14. Comparisons of C_p for Transition Point Effects.....	45
15. Comparisons of C_f for Transition Point Effects.....	46
16. Comparisons of C_p for Suction and Blowing Effects.....	48
17. Comparison of C_f for Suction and Blowing Effects.....	49

18.	Velocity Boundary Layer Profile above Suction Surface.....	51
19.	Velocity Profiles above Suction and Blowing Surfaces.....	53
20.	Velocity Profiles of Trailing Edge Vortex and Shear Layer.....	54
21.	Streamline Comparisons for one Period in C_1 .	56
22.	Vorticity Contour Comparisons for one Period in C_1	57
23.	Force Coefficients vs Iterations, Number 3..	59
24.	Force Coefficients vs Iterations, Number 4..	60
25.	Force Coefficients vs Iterations, Number 5..	61
26.	Force Coefficients vs Iterations, Number 6..	62
27.	Force Coefficients vs Iterations, Number 7..	63
28.	Force Coefficients vs Iterations, Number 8..	64
29.	Force Coefficients vs Iterations, Number 9..	65
30.	Force Coefficients vs Iterations, Number 10.	66
31.	Force Coefficients vs Iterations, Number 11.	67
32.	Force Coefficients vs Iterations, Number 14.	68
33.	Force Coefficients vs Iterations, Number 17.	69
34.	Force Coefficients vs Suction Velocity.....	71
35.	Comparisons of C_p for Different Suction Velocities.....	73
36.	Comparisons of C_f for Different Suction Velocities.....	75
37.	C_p Comparisons for one Period in C_1	77
38.	Streamline and Vorticity Comparisons for Different Suction Velocities.....	79
39.	Force Coefficients vs Ejection Angle.....	80

40.	Streamline and Vorticity Comparisons for Different Ejection Angles.....	83
41.	Streamline and Vorticity Comparisons for Different Ejection Angles.....	84
42.	Force Coefficients vs Angle of Attack.....	86
43.	Comparisons of C_p for Different Angles of Attack.....	87
44.	C_l vs C_d for Angle of Attack.....	88
45.	Streamline and Vorticity Comparisons for Different Angles of Attack.....	90
46.	Boundary Conditions.....	101

List of Tables

Table	Page
1. NACA 0012 Grid Configurations.....	38
2. Separation Point Comparison.....	41
3. Lift and Drag Comparison with Experimental Data.....	42
4. C_l and C_d vs Re and Transition Point.....	42
5. C_l and C_d Comparison with Experimental and Theoretical Data.....	44
6. C_l and C_d Comparison, $C_v = .05$, $\delta = 90^\circ$	47
7. Velocity and density Comparison at the Suction Surface.....	50
8. List of Model Configurations for $M = .3$ and $Re = 1,000,000$	58
9. C_l and C_d Component Comparison vs Suction Velocity.....	74
10. C_l and C_d Component Comparison vs Ejection Angle.....	81
11. C_d Calculation for Surface Blowing.....	82
12. C_l and C_d Component Comparison vs Angle of Attack.....	89
13. Computer Resource Comparison.....	109

List of Symbols

<u>Symbol</u>	<u>Definition</u>
A	Area
A	Jacobian matrix
a	Speed of sound
B	Jacobian matrix
C_d	Drag coefficient
C_l	Lift coefficient
C_p	Pressure coefficient
c	Airfoil cord
c_p	Specific heat at constant pressure
CFL	Courant number
C_r	Fan compression ratio
C_v	Suction velocity
D_i, D_e	Damping Coefficients
d	Indicates derivative
E_t	Total internal energy
e	Specific internal energy
F, \hat{F}	Flux vectors
\bar{f}	Body force vector
G, \hat{G}	Flux vectors
I	Identity matrix
IL	number of grid points in η - direction
J	Transformation Jacobian
JL	Number of grid points in ξ - direction

k	Coefficient for thermal conductivity
k_t	Coefficient for turbulent thermal conductivity
L	Reference length
M	Mach number
M	Jacobian matrix
\dot{m}	Mass flow rate
N	Number of iterations
N	Jacobian matrix
P	Pressure
Pr	Molecular Prandtl number
Pr_t	Turbulent Prandtl number
Q	Internal heat generation
\bar{q}	Heat conduction vector
R	Perfect gas constant
Re	Reynolds number
s	Surface area
T	Temperature
t	Time
U, \hat{U}	Vectors of dependable variables
U_∞	Free stream velocity
u	Stream wise velocity component
u	Contravariant velocity
\bar{V}	Velocity vector
v	Normal velocity component
v	Contravariant velocity
x	Stream wise direction coordinate

γ	Normal direction coordinate
α	Angle of attack
γ	Specific heat ratio
Δ	Difference operator
δ	Ejection angle
δ	Finite difference operator
ϵ	Turbulent eddy viscosity
η	Coordinate in computational space normal to the body
θ	Slope on the airfoil surface
ξ	Coordinate in computational space tangent to the body
λ	Coefficient of viscosity
λ_t	Coefficient of viscosity including turbulent properties
μ	Molecular dynamic viscosity
ρ	Density
σ	Shear stress tensor
τ	Viscous stress tensor
ω	Damping coefficients
∂	Indicates partial derivative

Superscripts

τ	Transpose of matrix
--------	---------------------

Subscripts

i,j,k	Index notation
i,j	Mesh indices

x	Partial derivative with respect to x
y	Partial derivative with respect to y
η	Partial derivative with respect to η
ξ	Partial derivative with respect to ξ
∞	Denotes free stream conditions

Abstract

The purpose of this study was to determine, through numerical simulation, the two-dimensional effect of mass transfer (fan) on a NACA 0012 airfoil. A "fan" is characterized by suction on the upper surface of an airfoil and corresponding blowing from the lower surface. The results are presented through the comparisons of lift and drag coefficients, pressure and skin friction coefficient profiles, and streamline and vorticity contours. The numerical code used in this study is based on the Beam-Warming approximate factorization algorithm which is used to solve the mass-averaged, compressible Navier-Stokes equations for viscous, unsteady flows. The grid used in this study was a c-grid produced from a hyperbolic grid generating code.

This study examined the effect of varying suction velocity (1, 5 and 10 percent of the free stream velocity), ejection angle (15, 45 and 90 degrees) and angle of attack (0, 2 and 4 degrees). The results indicate that suction has only a small influence on lift; but, produces a large viscous drag proportional to the suction velocity. Blowing produces a large lift component due to a modified pressure distribution surrounding the leading edge and only a small drag penalty. Blowing also creates an unsteady periodic solution. The unsteady behavior is the result of vortex

shedding caused by the interaction of a broad shear layer formed behind the ejection surface which induces a circulation around the trailing edge. The shedding of the trailing edge vortex creates periodic oscillations in lift and drag, but is not responsible for the large mean increase seen in lift.

Increasing suction velocities produced a linear increase in lift. A maximum drag penalty occurred at medium values of suction (5%). The mass flow for the suction velocities studied were too small to provide substantial lift; but, did provide a substantial thrust component at an ejection angle of 15° and a suction velocity of 10%.

Ejection angles mildly affected lift; but reduced drag considerably at lower ejection angles (15°) due to thrust. Increasing angles of attack (α) produced a large linear increase in lift and a corresponding reduction in drag near that of a clean airfoil.

The results indicate that, in two-dimensions, a "fan" type device can produce aerodynamic benefits and warrants additional experimental and numerical studies, with an emphasis on the lift curve slope and stall behavior. The effect of different fan geometries, boundary conditions and cambered airfoils should also be investigated.

NAVIER-STOKES SOLUTION FOR A NACA 0012 AIRFOIL
WITH MASS FLUX (FAN)

I Introduction

The effect of mass flux on a NACA 0012 airfoil section is the focus of this research project. This study is accomplished through the use of numerical analysis based on the mass averaged, compressible Navier-Stokes (NS) equations. For this report mass flux is defined by the intake of mass, suction, on the upper surface of the airfoil, and the ejection of mass, blowing, on the lower surface. The mechanism providing the suction and blowing will be referred to as a "fan" (see Figure 1). Though in two-dimensions this behavior could be contributed to a variety of devices.

The concept of a "fan-in-wing" (see Figure 2) has been around since the late 50's, reached its peak in the late 60's and was essentially discarded in the mid 70's as being impractical. The "fan-in-wing" was first considered in the 50's for its vertical/short take off and landing (V/STOL) ability (23:8). However, the technology and material sciences of the times forced designs that were heavy and large. A typical size fan covered between 40 to 50 percent of the wing area, "flying fan".

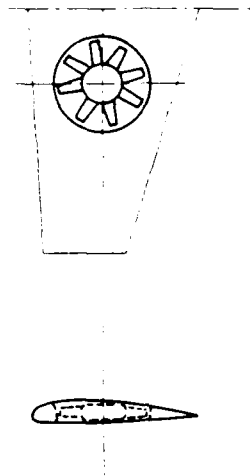


Figure 1. A "Fan-in-Wing" (23:23)

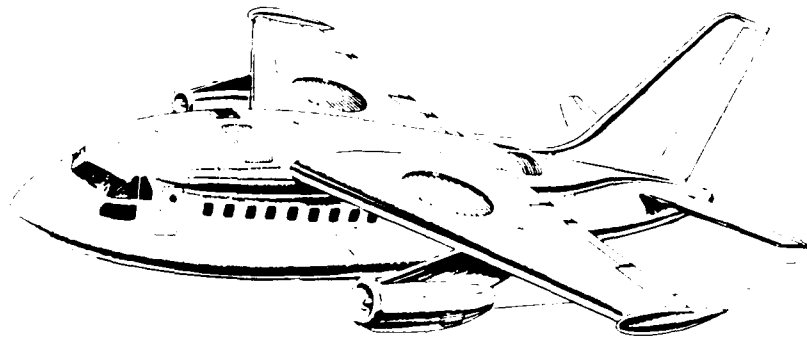


Figure 2. A "Fan-in-Wing" Aircraft (29:8)

The 60's technology produced some aircraft employing a "fan-in-wing" concept. The most notable being the Ryan XV-5a which employed a jet powered wing lifting fan (see Figure 3) (20:38). But, most research and development concentrated on the "tilt wing" concept (28:2-28) which has found many applications with the implementation of the modern turbo fan.

1. Nose fan
2. Gas generator
3. Diverter valve
4. Engine tail pipe
5. Wing fan
6. Crossover ducts
7. Nose fan supply duct
8. Left wing fan scroll
9. Right wing fan scroll
10. Nose fan scroll

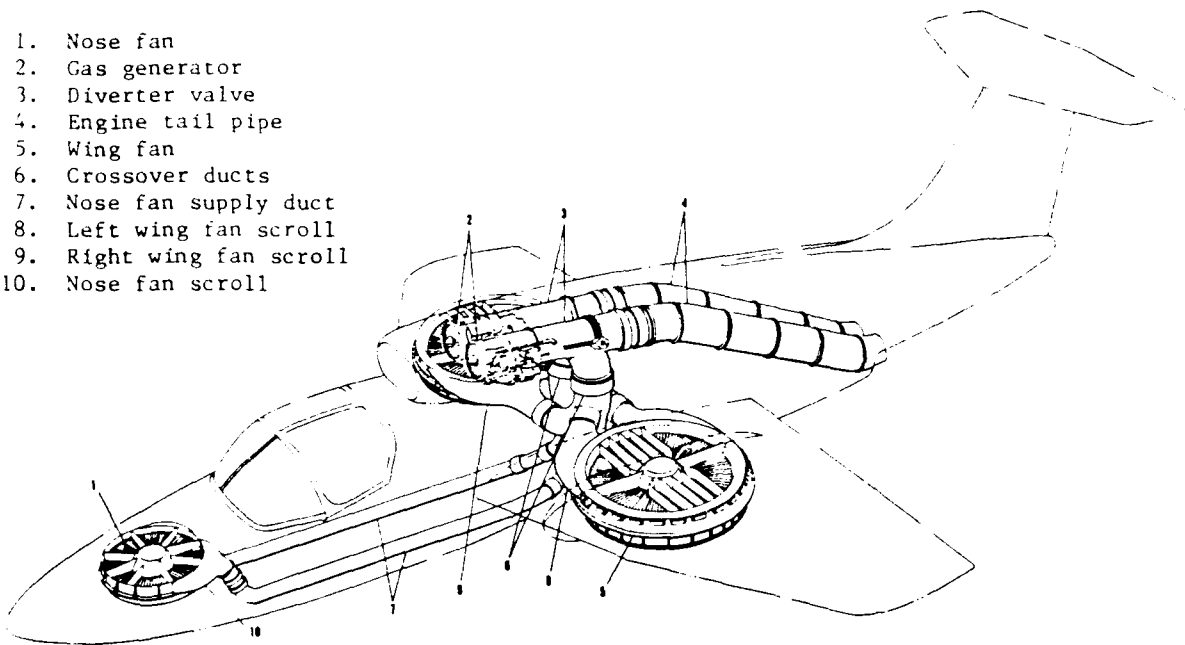


Figure 3. Propulsion System for the Ryan XV-5A (20:38)

In the 70's the fan gave way to jet technology which was lighter and more powerful (see Figure 4) and led to the development of the Harrier. "But in 1980 there is still only one true VSTOL aircraft in the free world that has reached the operational stage, the Hawker Siddeley Harrier (20:3)." Renewed interest in VSTOL and current

development in material science and compressor technology suggest that a second look is warranted for the "fan-in-wing"; with an emphasis on the flow characteristics and possible applications to future STOL technology.

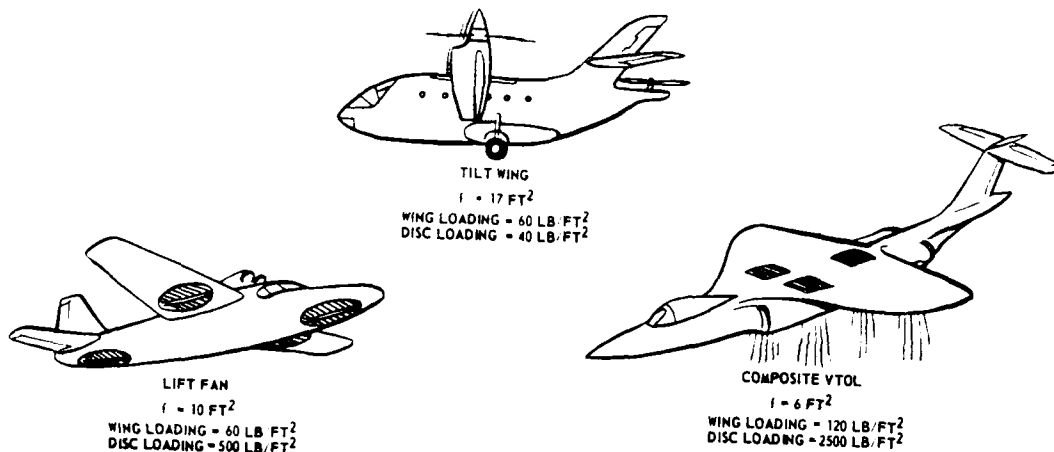


Figure 4. V/STOL Aircraft Configurations (28:14)

The positive effect of suction on boundary layer control and thus aircraft performance has been well documented and is in practical use (31:43-44). The fluid particles in the boundary layer over an airfoil surface have a much lower kinetic energy than do the fluid particles outside the boundary layer, due to the no slip condition and skin friction at the airfoil surface

(31:24-25). As the low energy particles over the airfoil surface mix with the outer boundary they increase the thickness of the low energy boundary layer thus decreasing its stability (see Figure 5) (31:25). And under unfavorable conditions separation can occur causing a substantial increase in drag and a decrease in lift which can lead to early stall behavior at high angles of attack (22:411-413). In boundary layer control the low energy boundary layer is sucked away and the the outer boundary is free to accelerate while a new smaller boundary layer reforms, thus improving lift performance and delaying separation (31:381,382).

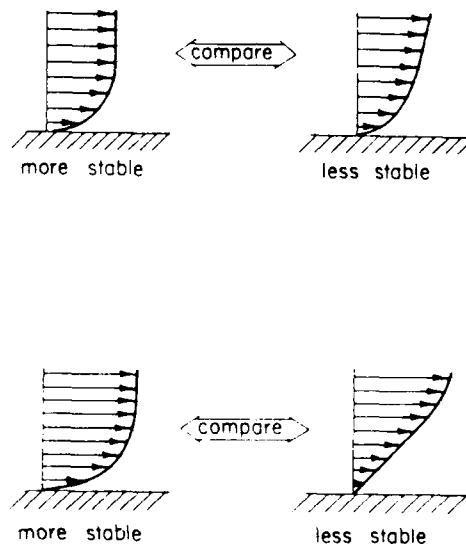


Figure 5. Effect of Boundary Layer Geometry Stability (23:265)

In principle the effects of boundary layer control by suction can be extended to a fan, the results are not as promising. The effect of suction produced by a fan is

not as well understood. The best results for suction are obtained when the slot widths are of the same order as the displacement thickness (see Figure 6) which is much smaller than a fan width (23:269).

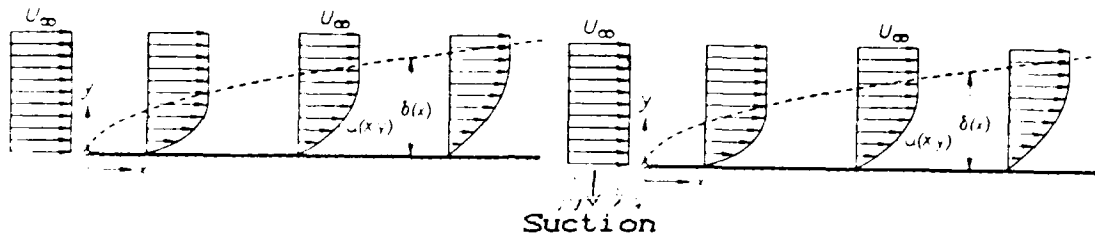


Figure 6. Effect of Suction on the Boundary Layer

The effect of blowing on the other hand is not well understood. Most research on blowing has concentrated on surface blowing which is tangent to the airfoil. This research has led to practical applications such as the "jet flap" and "slotted wing" (see Figure 7) (31:380,381); while the effect of blowing normal to the surface has been carefully ignored.

"It is mandatory to pay careful attention to the shape of the slit in order to prevent the jet from dissolving into vortices at a short distance behind the exit section (31:380).

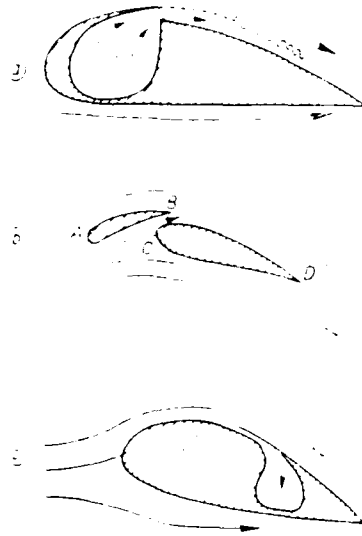


Figure 7. Boundary Layer Control a) Blowing
 b) Slotted Wing c) Suction (31:381)

At the very least, blowing which is non-tangent to the surface will produce vortices which will cause separation and produce a large separated area behind the blowing exit (see Figure 8) (31:28-29). What is not understood is the effect of blowing on the pressure distribution of the airfoil surface and the effective camber produced by turning the flow. If the blowing configuration is such that vortices are shed then an unsteady solution can be expected.

Some studies were done in the 60's on the optimal configuration for a "fan-in-wing" (23:254). These studies focused on the macroscopic behavior of lift and drag and did not study the flow interaction. These studies do

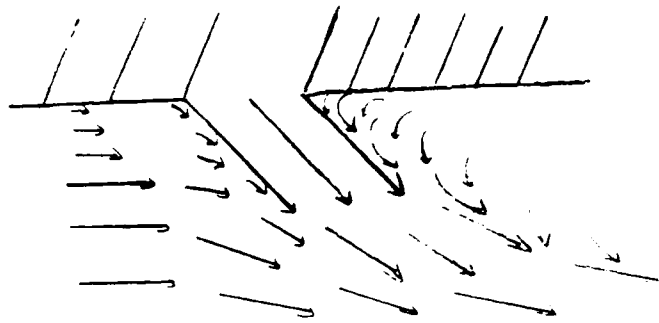


Figure 8. Blowing Non-Tangent to the Surface.

indicate that a horizontal "fan-in-wing" can produce additional lift and reduce drag (see Figure 9).

The effect of the fan on the wing is somewhat similar to the section of a jet flap. The efflux from the fan is discharged in a direction normal to the plane of the wing and then turns in the downstream direction. (23:254)

These experimental results suggest that the use of inlet vanes to guide the incoming flow is detrimental to both lift and drag. However, the use of exit vanes or vectoring on the ejecting flow can reduce drag without significantly affecting lift or pitching moments. These results also indicate that ejection angles of 20 to 30 degrees with respect to the cord produce the best performance (23:257).

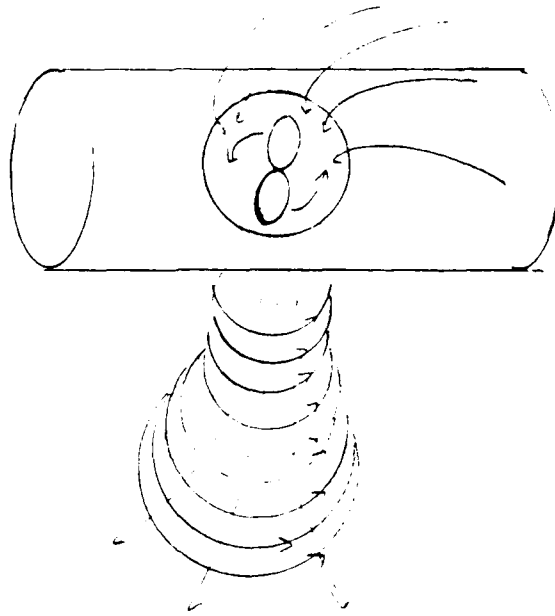


Figure 9. Three-Dimensional Effects of a Fan

As long as the concept has been around, the performance and flow field characteristics of the fan are still not well understood. "There is still no acceptable theory for predicting the performance of a fan-in-wing configuration. At best we will probably have to resort to a numerical solution (23:258-259)." With the current "state of the art" in Computational Fluid Dynamics (CFD), it is possible to numerically simulate complex flow field such as a "fan-in-wing".

In a numerical study many more configurations can be tested in less time and at lower cost than in an experimental study (2:45). The problem with numerical studies is that they can only simulate a problem but can not ensure its validity. This is why numerical solutions must be compared with experimental studies to validate their accuracy before small departures from the validated

model configuration and test conditions can be introduced (32). The new solutions can then provide valuable insight for future experimental and numerical studies. This can then become a continuous cycle of validation, insight, test, validation...

The main difficulty in predicting the effect of the fan on the wing is that it is characterized by a three-dimensional flow field. A vortex is produced in the plane of the wing and interacts with the flow normal to the fan (see Figure 9). This problem can be simplified into two dimensions by ignoring the vortex formed by a rotating fan and calculating only the effects of suction and blowing normal to the plane of the airfoil.

This report looks only at the two-dimensional problem, suction and blowing and as such can be described by any number of mechanisms; however, the term "fan" will be retained in describing the model. The focus of this report is on the effect of mass flux on the lift and drag performance of an airfoil section, and the characteristic behavior of the flow. The problem is further simplified by keeping the geometry and flow condition fixed (appendix C).

The model used for this report is based on the NACA 0012 airfoil section because its behavior has been well documented over a wide range of conditions (1:462,463; 24) that will serve as a basis for validating the numerical

solution without blowing. The fan model used assumes no inlet vanes but ejection vanes are used in order to allow smooth, vectored, parallel ejection. The effect of varying suction velocities, ejection angles and angles of attack was studied.

The model conditions were picked for optimum numerical performance. Compressible codes perform better at higher Mach numbers (34) and for this reason $M = 0.3$ was chosen. The Reynolds number (Re) can also have a dramatic affect on the solution. If Re is too low current turbulence models have difficulty in describing the physics correctly and if it is too high then the strong compressible effects require extremely high numerical resolution. For these reasons $Re = 1,000,000$ was chosen. This value is well above the laminar flow region (18) and much smaller than the critical Re for stall (22:413) for this airfoil which could create problems at high angles of attack (34).

Boundary conditions on the upper surface were chosen such that the velocity on the surface was normal to the surface with a constant fractional value of the free stream velocity (see appendix C). Because enhancements were being sought, the velocity ejecting from the lower surface was chosen to be constant in magnitude and direction. The ejection angle was measured from the cord assigned a value between 15 and 90 degrees. The

parameters considered for comparison and analysis were the coefficients of lift, C_l , drag, C_d and pressure, C_p .

The Navier-Stokes code used in the analysis (appendix F). was a modified version of a code developed by Miguel Visbal (36) at the Air Force Wright Aeronautical Laboratories (AFWAL) Flight Dynamics Lab (FDL). This code is based on the "full" compressible Navier-Stokes equations for viscous flow and uses the Beam-Warming Implicit Factored Scheme (4). The turbulence model is based on work done by Baldwin and Lomax (8). The "full" NS code was chosen over the approximate NS (ANS) and the parabolized NS (PNS) codes because of the large stream wise variation and the dynamic behavior of the flow field. The suction and blowing alter dramatically both the direction of the flow and the viscous behavior at the surface. And for the first numerical attempt at this problem a more accurate code was needed to insure numerical accuracy. A compressible code was also needed because of the compressibility imposed on the flow by the fan boundary conditions. Changes to the code involved boundary conditions, input/output, turbulence modeling, force and residual calculations and loop structure to reduce memory requirements.

Tests on different grids were performed in order to determine an optimum spacing configuration. The grids were developed using a hyperbolic grid generator (appendix

G) also provided by the Flight Dynamics Laboratory (FDL) The grids were tested using the above code in order to determine the optimum spacing needed to resolve the problem accurately. Tests were done on the code using a symmetric grid representing a NACA 0012 airfoil and comparing results with known solutions for both laminar and turbulent cases. The results from the final unsymmetric grid were then compared for grid effects. Details on the grid analysis are presented in the Results and Discussion section. After the grid was verified the fan modifications were added and results were obtained. There was no available fan data for comparison and as such the results remain to be verified through future experiments and additional numerical simulations.

Computer resources were provided by FDL and included accounts on the Aeronautical Systems Division Cyber Computer and Cray XMP. The Cray was used for running the Code (appendix E) and performing data analysis too large for the Cyber; all other analysis and plots were performed on the Cyber.

II Analysis

Governing Equations

The mathematical equations which describe the behavior of a fluid (gas) in motion are based on the Principles of Conservation of Mass, Momentum, and Energy. These equations are often grouped together and referred to as the Navier-Stokes (NS) Equations though only the momentum equation is credited to Navier and Stokes (41:71). These equations are listed below in vector notation and are valid for unsteady compressible and viscous flows (6:88-96).

Continuity (Conservation of Mass)

$$\frac{\partial \rho}{\partial t} + \bar{\nabla} \cdot (\rho \bar{V}) = 0 \quad (1)$$

Momentum (Conservation of Momentum)

$$\frac{\partial (\rho \bar{V})}{\partial t} + \bar{\nabla} \cdot (\rho \bar{V} \bar{V}) = \rho \bar{f} + \bar{\nabla} \cdot \underline{\underline{\sigma}} \quad (2)$$

Energy (Conservation of Energy)

$$\frac{\partial E_t}{\partial t} + (\bar{V} \cdot \bar{\nabla}) E_t = \frac{\partial Q}{\partial t} + \rho \bar{f} \cdot \bar{V} + \bar{\nabla} \cdot (\underline{\underline{\sigma}} \cdot \bar{V}) - \bar{\nabla} \cdot \bar{q} \quad (3)$$

where the shear stress term $\underline{\sigma}$ is related to the pressure, P , and viscous stress tensor, $\underline{\tau}$ (16:6)

$$\underline{\sigma} = -PI + \underline{\tau} \quad (4)$$

The definition of variables used can be found in the list of symbols near the beginning of this report.

Three additional equations are needed to relate P , τ and heat conduction, q . If a perfect fluid/gas is assumed then the equation of state can be used (16:7)

$$P = \rho RT = \rho e(\gamma-1) \quad (5)$$

and if a Newtonian fluid is assumed then Stoke's law of friction can be used (14:12)

$$\underline{\tau} = \lambda(\nabla \cdot \underline{V})\underline{I} + \mu(\nabla \underline{V} + (\nabla \underline{V})^T) \quad (6)$$

and the third equation relates the heat flux vector to the temperature gradient by Fourier's law of heat conduction

$$\underline{q} = -k \nabla T \quad ; \quad \nabla \cdot \underline{q} = -\nabla \cdot (k \nabla T) \quad (7)$$

where the conductivity k is a function of the temperature. (14:11-12)

Total internal energy, E_t can be related to the specific internal energy, e , and velocity by the following

relationship (15:13)

$$Et = \rho \left(e + \frac{u^2 + v^2}{2} \right) \quad (8)$$

The above equations can be non-dimensionalized (see appendix A) by applying the following definitions (an * represents a dimensional quantity)

$$\begin{aligned} x &= \frac{x^*}{L^*} & y &= \frac{y^*}{L^*} & u &= \frac{u^*}{U_\infty^*} & v &= \frac{v^*}{U_\infty^*} \\ P &= \frac{P^*}{\gamma M_\infty^2 P_\infty^*} & T &= \frac{\gamma P M_\infty^2}{\rho} & \rho &= \frac{\rho^*}{\rho_\infty^*} & \mu &= \frac{\mu^*}{\mu_\infty^*} \\ Et &= \frac{Et^*}{\gamma M_\infty^2 P_\infty^*} & e &= \frac{Et}{\rho} & \varepsilon &= \frac{\varepsilon^*}{\mu_\infty^*} & q &= \frac{q^*}{q_\infty^*} \quad (9) \\ M_\infty &= \frac{U_\infty}{\sqrt{\gamma RT}} & Re &= \frac{\rho_\infty^* U_\infty^* L^*}{\mu_\infty^*} & t &= \frac{t^* U_\infty^*}{L^*} L^* = 1 \end{aligned}$$

The non-dimensional NS equations are written below in conservation-law form for a 2-D cartesian coordinate system.

$$\frac{\partial \rho}{\partial t} + \frac{\partial(\rho u)}{\partial x} + \frac{\partial(\rho v)}{\partial y} = 0 \quad (10)$$

$$\begin{aligned} \frac{\partial(\rho u)}{\partial t} + \frac{\partial(\rho u^2 + P - \tau_{xx})}{\partial x} + \frac{\partial(\rho uv - \tau_{xy})}{\partial y} & \quad (11) \\ & = \rho \bar{f}_x \end{aligned}$$

$$\begin{aligned} \frac{\partial(\rho v)}{\partial t} + \frac{\partial(\rho v^2 + P - \tau_{yy})}{\partial y} + \frac{\partial(\rho uv - \tau_{yx})}{\partial x} & \quad (12) \\ & = \rho \bar{f}_y \end{aligned}$$

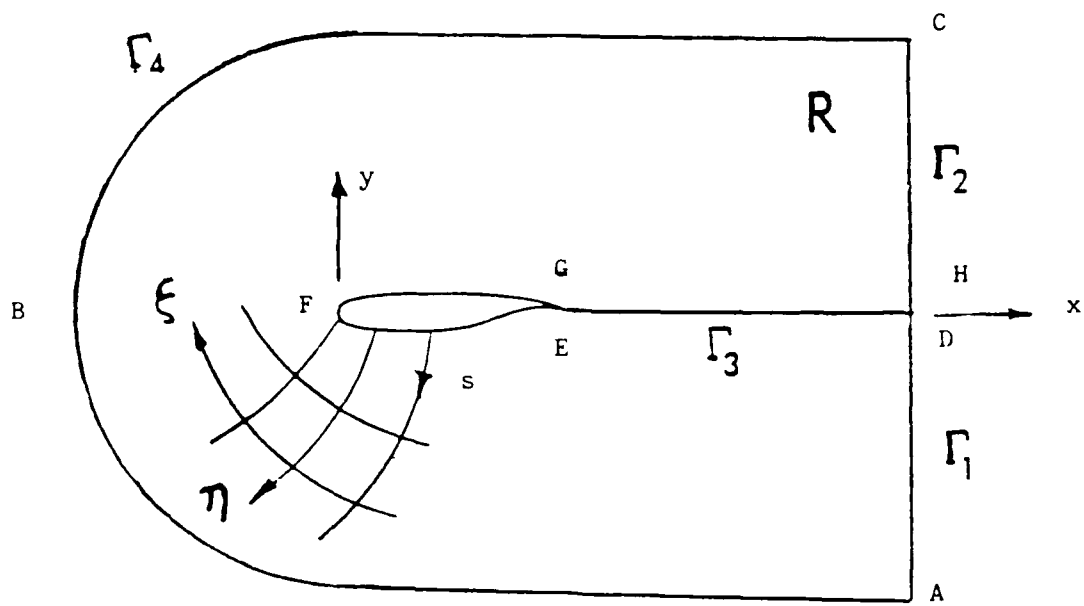
$$\begin{aligned} \frac{\partial Et}{\partial t} - \rho(\bar{f}_x u + \bar{f}_y v) + & \quad (13) \\ \frac{\partial(Etu + Pu - u\tau_{xy} - v\tau_{xy} + q_x)}{\partial x} + \\ \frac{\partial(Etv + Pv - u\tau_{xy} - v\tau_{yy} + q_x)}{\partial y} & = 0 \end{aligned}$$

where the internal heat generation, Q , is assumed constant in time (15:32).

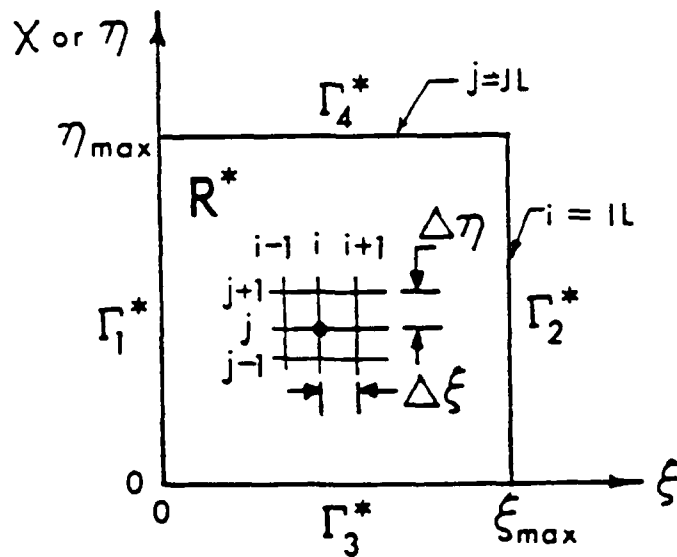
The non-dimensionalized stress terms in index notation are (16:6)

$$\tau_{ij} = -P\delta_{ij} + \frac{\mu}{Re} \left[\frac{\partial u_i}{\partial x_j} + \frac{\partial u_j}{\partial x_i} \right] + \delta_{ij} \lambda \frac{\partial u_k}{\partial x_k} \quad (14)$$

The above equations can be transformed for varying geometries by applying a coordinate transformation. For any given geometry the coordinates can be related to a square with unit axes of 1 (see Figure 10) by using the chain rule of partial differentiation to relate the



(a) Physical Plane



(b) Transformed Plane

Figure 10 General Transformation from The Physical Domain a to the Computation Domain b (34:47)

physical domain (x,y) to the computational domain (ξ,η) .

Where (2:252)

$$\xi = \xi(x,y) \quad , \quad \eta = \eta(x,y) \quad (15)$$

$$\frac{\partial}{\partial x} = \xi_x \frac{\partial}{\partial \xi} + \eta_x \frac{\partial}{\partial \eta} \quad (16)$$

$$\frac{\partial}{\partial y} = \xi_y \frac{\partial}{\partial \xi} + \eta_y \frac{\partial}{\partial \eta} \quad (17)$$

The metrics are determined in the following manner (2:252)

$$d\xi = \xi_x dx + \xi_y dy \quad (18)$$

$$d\eta = \eta_x dx + \eta_y dy \quad (19)$$

In matrix form

$$\begin{bmatrix} d\xi \\ d\eta \end{bmatrix} = \begin{bmatrix} \xi_x & \xi_y \\ \eta_x & \eta_y \end{bmatrix} = \begin{bmatrix} dx \\ dy \end{bmatrix} \quad (20)$$

and

$$\begin{bmatrix} dx \\ dy \end{bmatrix} = \begin{bmatrix} x_\xi & x_\eta \\ y_\xi & y_\eta \end{bmatrix} = \begin{bmatrix} d\xi \\ d\eta \end{bmatrix} \quad (21)$$

Therefore

$$\begin{bmatrix} \xi_x & \xi_y \\ \eta_x & \eta_y \end{bmatrix} = \begin{bmatrix} x_\xi & x_\eta \\ y_\xi & y_\eta \end{bmatrix}^{-1} = J \begin{bmatrix} y_\eta & -x_\eta \\ -y_\xi & x_\xi \end{bmatrix} \quad (22)$$

Where the Jacobian J is given by (21:416)

$$J = \frac{\partial(\xi, \eta)}{\partial(x, y)} = \begin{vmatrix} \frac{\partial \xi}{\partial x} & \frac{\partial \xi}{\partial y} \\ \frac{\partial \eta}{\partial x} & \frac{\partial \eta}{\partial y} \end{vmatrix} = \xi_x \eta_y - \xi_y \eta_x \quad (23)$$

$$J = \frac{1}{\frac{\partial(x, y)}{\partial(\xi, \eta)}} = \frac{1}{\begin{vmatrix} \frac{\partial x}{\partial \xi} & \frac{\partial x}{\partial \eta} \\ \frac{\partial y}{\partial \xi} & \frac{\partial y}{\partial \eta} \end{vmatrix}} = \frac{1}{(x_\xi y_\eta - x_\eta y_\xi)} \quad (24)$$

and the transformation metrics are given by (35:7)

$$\xi_x = y_\eta J \quad \xi_y = -x_\eta J \quad (25)$$

$$\eta_x = -y_\xi J \quad \eta_y = x_\xi J \quad (26)$$

Further simplifications can be applied after the coordinate transformation is completed. The chain-rule conservative NS equations without body forces \bar{f} written in terms of general curvilinear coordinates (ξ, η) are as follows (35:5-6)

$$\frac{\partial U}{\partial t} + \xi_x \frac{\partial F}{\partial \xi} + \xi_y \frac{\partial G}{\partial \xi} + \eta_x \frac{\partial F}{\partial \eta} + \eta_y \frac{\partial G}{\partial \eta} = 0 \quad (27)$$

Where

$$U = [\rho, \rho u, \rho v, \rho e]^T \quad (28)$$

$$F = \begin{bmatrix} \rho u \\ \rho u^2 - \tau_{xx} \\ \rho v^2 - \tau_{xy} \\ (\rho e + p)u - F_4 \end{bmatrix} \quad (29)$$

$$G = \begin{bmatrix} \rho v \\ \rho uv - \tau_{xy} \\ \rho v^2 - \tau_{yy} \\ (\rho e + p)v - G_4 \end{bmatrix} \quad (30)$$

Stokes hypothesis gives (31:60)

$$\lambda = -\frac{2}{3} \mu \quad (31)$$

Where μ is defined as the molecular dynamic viscosity. It can be extended to include turbulent eddy viscosity, ϵ

(35:6)

$$\lambda_t = -\frac{2}{3} (\mu + \epsilon) \quad (32)$$

The thermal conductivity, k , is separated into k for the fluid and k_t for the turbulent properties. Then the viscous stress and heat conduction terms can be written in the following form (35:6)

$$\tau_{xx} = -\frac{3}{2} \lambda_t u_x + \lambda_t (u_x + v_y) \quad (33)$$

$$\tau_{xy} = -\frac{3}{2} \lambda_t (u_x + v_y) \quad (34)$$

$$\tau_{yy} = -\frac{3}{2} \lambda_t v_y + \lambda_t (u_x + v_y) \quad (35)$$

$$F_4 = u\tau_{xx} + v\tau_{xy} - q_x \quad (36)$$

$$G_4 = u\tau_{xy} + v\tau_{yy} - q_y \quad (37)$$

$$P = \rho(\gamma-1) \left(e - \frac{1}{2} (u^2 + v^2) \right) \quad (38)$$

$$q_x = -(k + k_t) T_x \quad ; \quad q_y = -(k + k_t) T_y \quad (39)$$

$$k = c_p \frac{\mu}{Pr} \quad , \quad k_t = c_p \frac{\epsilon}{Pr_t} \quad (40)$$

where the molecular Prandtl number is defined by (35:6)

$$Pr = \frac{\mu c_p}{k} \cong .72 \quad (41)$$

and the turbulent Prandtl number is defined by (35:7)

$$Pr_t = \frac{\varepsilon C_p}{k} \cong .9 \quad (42)$$

where the specific heat at constant pressure, c_p for a perfect gas is defined by (12)

$$c_p = \frac{\gamma R}{\gamma - 1} \cong 1,000 \text{ J/Kg-K} \quad (43)$$

The NS equations can be written in the following strong conservation form by applying the coordinate transformation identities previously discussed (35:7)

$$\frac{\partial \hat{U}}{\partial t} + \frac{\partial \hat{F}}{\partial \xi} + \frac{\partial \hat{G}}{\partial \eta} = 0 \quad (44)$$

where

$$\hat{U} = \frac{U}{J} \quad (45)$$

$$\hat{F} = \frac{(\xi_x F + \xi_y G)}{J} \quad (46)$$

$$\hat{G} = \frac{(\eta_x F + \eta_y G)}{J} \quad (47)$$

Rewriting equation (44) allows for an easier implementation of the implicit algorithm scheme (section III)

$$\frac{\partial \hat{U}}{\partial t} + \frac{\partial E_1}{\partial \xi} + \frac{\partial E_2}{\partial \eta} = \quad (48)$$

$$\frac{\partial v_1(\hat{U}, \hat{U}_\xi)}{\partial \xi} + \frac{\partial v_2(\hat{U}, \hat{U}_\eta)}{\partial \xi} + \frac{\partial w_1(\hat{U}, \hat{U}_\xi)}{\partial \eta} + \frac{\partial w_2(\hat{U}, \hat{U}_\eta)}{\partial \eta}$$

where (35:8)

$$E_1 = \frac{1}{J} \begin{bmatrix} \rho u \\ \rho u u + \xi_x P \\ \rho v u + \xi_y P \\ (P + \rho e) u \end{bmatrix} \quad (49)$$

$$E_2 = \frac{1}{J} \begin{bmatrix} \rho v \\ \rho u v + \eta_x P \\ \rho v v + \eta_y P \\ (P + \rho e) v \end{bmatrix} \quad (50)$$

$$v_1 = \frac{1}{J} \begin{bmatrix} 0 \\ b_{1u}\xi + b_{2v}\xi \\ b_{2u}\xi + b_{3v}\xi \\ b_{1uu}\xi + b_2(vu_\xi + uv_\xi) + b_{3vv}\xi + b_4T_\xi \end{bmatrix} \quad (51)$$

$$v_2 = \frac{1}{J} \begin{bmatrix} 0 \\ c_{1u}\eta + c_{2v}\eta \\ c_{3u}\eta + c_{4v}\eta \\ c_{1uu}\eta + c_{2uv}\eta + c_{3vu}\eta + c_{4vv}\eta + c_5T_\eta \end{bmatrix} \quad (52)$$

$$W_1 = \frac{1}{J} \begin{pmatrix} 0 \\ c_{1u}\xi + c_{3v}\xi \\ c_{2u}\xi + c_{4v}\xi \\ c_{1uu}\xi + c_{2vu}\xi + c_{3uv}\xi + c_{4vv}\xi + c_{5T}\xi \end{pmatrix} \quad (53)$$

$$W_2 = \frac{1}{J} \begin{pmatrix} 0 \\ d_{1u}\eta + d_{2v}\eta \\ d_{2u}\eta + d_{3v}\eta \\ d_{1uu}\eta + d_{2(vu_\eta + uv_\xi)} + d_{3vv}\eta + d_{4T}\eta \end{pmatrix} \quad (54)$$

u and v denote the contravariant velocities (35:9)

$$u = \xi_x u + \xi_y v \quad (55)$$

$$u = \eta_x u + \eta_y v \quad (56)$$

The viscous coefficients are (35:4):

$$b_1 = -\frac{3}{2} \lambda_t \left(\frac{4}{3} \xi_x^2 + \xi_y^2 \right) \quad (57)$$

$$b_2 = -\frac{1}{2} \lambda_t \xi_x \xi_y \quad (58)$$

$$b_3 = -\frac{3}{2} \lambda_t \left(\frac{4}{3} \xi_y^2 + \xi_x^2 \right) \quad (59)$$

$$b_4 = c_p \left(\frac{\mu}{Pr} + \frac{\epsilon}{Pr_t} \right) \left(\xi_x^2 + \xi_y^2 \right) \quad (60)$$

$$c_1 = \frac{\sqrt{3}}{2} \lambda_t \left[\frac{4}{3} \xi_x \eta_x + \xi_y \eta_y \right] \quad (61)$$

$$c_2 = \frac{\sqrt{3}}{2} \lambda_t \left[\frac{2}{3} \xi_x \eta_y - \xi_y \eta_x \right] \quad (62)$$

$$c_3 = - \frac{\sqrt{3}}{2} \lambda_t \left[\xi_x \eta_y + \frac{2}{3} \xi_y \eta_x \right] \quad (63)$$

$$c_4 = \frac{\sqrt{3}}{2} \lambda_t \left[\xi_x \eta_x + \frac{2}{3} \xi_y \eta_y \right] \quad (64)$$

$$c_5 = - c_p \left(\frac{\mu}{\bar{P}_r} + \frac{\epsilon}{\bar{P}_r} \right) \left[\xi_x \eta_x + \xi_y \eta_y \right] \quad (65)$$

$$d_1 = - \frac{\sqrt{3}}{2} \lambda_t \left[\frac{4}{3} \eta_x^2 + \eta_y^2 \right] \quad (66)$$

$$d_2 = - \frac{1}{2} \lambda_t \eta_x \eta_y \quad (67)$$

$$d_3 = - \frac{\sqrt{3}}{2} \lambda_t \left[\frac{4}{3} \eta_y^2 + \eta_x^2 \right] \quad (68)$$

$$d_4 = c_p \left(\frac{\mu}{\bar{P}_r} + \frac{\epsilon}{\bar{P}_r} \right) \left[\eta_x^2 + \eta_y^2 \right] \quad (69)$$

The above NS equations written in terms of general curvilinear coordinates are valid for both subsonic and supersonic, unsteady, compressible, viscous flows. The governing equations form a hybrid hyperbolic-parabolic system. Their parabolic nature comes from the second-order derivatives in the momentum and energy equations which provide dissipative effects. The continuity equation contains only first-order terms and is

hyperbolic; without the unsteady density term it would be elliptic. These relationships dictate the manner in which the initial and boundary conditions can be applied. (25:312)

Additional approximations must be made in order to solve a finite difference problem (discussed in section III). The main difficulties are in the area of turbulent flow, where at best, turbulent models are only approximate and rely heavily on empirical data.

III Numerical Solution of the NS Equations

The numerical method for solving the NS equations as previously presented is discussed in this chapter. The finite-difference scheme presented is the result of work by R. F. Warming and Richard M. Beam and is known as the Beam-Warming approximate factorization algorithm (4). The original two-dimensional Navier-Stokes code was written and verified by Dr Miguel Visbal of the Flight Dynamics Laboratory (36). Modifications made by the Author and discussed in this chapter concern the airfoil surface boundary conditions for mass exchange (fan). Finally, critical details such as convergence criteria and time steps will be presented.

Implicit Navier-Stokes Code

The implicit code solves the strong conservative formulation of the NS equations (1 - 3) using the Beam-Warming approximate factorization algorithm (4:85). The scheme is written in "delta" form with a first-order Euler time-differencing written as follows (35:19):

$$\left\{ I + \Delta t \left[\frac{\partial A^n}{\partial \xi} - \frac{\partial^2 M^n}{\partial \xi^2} \right] \right\} \left\{ I + \Delta t \left[\frac{\partial B^n}{\partial \eta} - \frac{\partial^2 N^n}{\partial \eta^2} \right] \right\} \Delta \hat{U}^n =$$

$$- \Delta t \left[\frac{\partial}{\partial \xi} (E_1 - V_1 - V_2)^n + \frac{\partial}{\partial \eta} (E_2 - W_1 - W_2)^n \right] \quad (70)$$

$$\hat{U}^{n+1} = \hat{U}^n + \Delta \hat{U} \quad (71)$$

where n represents the temporal index (i.e. $\hat{U}^n = \hat{U}(n\Delta t)$) and A , B , M and N represent the Jacobian matrices. See appendix B for details.

$$A = \frac{\partial E_1}{\partial \hat{U}} \quad , \quad B = \frac{\partial E_2}{\partial \hat{U}} \quad (72)$$

$$M = \frac{\partial V_1}{\partial \hat{U}_\xi} \quad , \quad N = \frac{\partial W_2}{\partial \hat{U}_\eta} \quad (73)$$

After applying second order differencing the space derivatives become (35:19-20):

$$\left\{ I + \Delta t \left[\mu_\xi A_{i,j} - \delta_\xi^2 M_{i,j} \right] \right\} \Delta \hat{U}_{i,j}^* =$$

$$- \Delta t \left[\mu_\eta (E_1 - V_2)_{i,j} + \mu_\eta (E_2 - W_1)_{i,j} \right] \quad (74)$$

$$\left\{ I + \Delta t \left[\mu_{\eta}^B{}_{i,j} - \delta_{\eta}^2 N_{i,j} \right] \right\} \Delta \hat{U}_{i,j} = \Delta \hat{U}_{i,j}^* \quad (75)$$

$$\xi_i = (i - 1) \Delta \xi \quad ; \quad 1 \leq i \leq IL \quad (76)$$

$$\eta_j = (j - 1) \Delta \eta \quad ; \quad 1 \leq j \leq JL \quad (77)$$

and the finite-difference operators are (35:20):

$$\delta_{\xi} f_{i,j} = (f_{i+1/2,j} - f_{i-1/2,j}) / \Delta \xi \quad (78)$$

$$\delta_{\eta} f_{i,j} = (f_{i,j+1/2} - f_{i,j-1/2}) / \Delta \eta \quad (79)$$

$$\mu_{\xi} f_{i,j} = (f_{i+1,j} - f_{i-1,j}) / 2\Delta \xi \quad (80)$$

$$\mu_{\eta} f_{i,j} = (f_{i,j+1} - f_{i,j-1}) / 2\Delta \eta \quad (81)$$

The transformation derivatives (x_{ξ} , x_{η} , y_{ξ} , y_{η}) are computed from the body-fitted grid by using one-sided approximations at the boundaries and second-order central-differencing approximations at the interior points. A solution is arrived at by first solving equation (74) during a sweep along each η line ($2 \leq i \leq IL-1$), and then solving equation (75) during a sweep along each ξ line ($2 \leq j \leq JL-1$). The boundaries ($i=1, IL$; $j=1, JL$) are then solved explicitly.

Artificial damping is needed to maintain the stability of the algorithm and to speed up convergence of the solution. Instabilities can occur in compressible flow computations at high Reynolds numbers. These instabilities can be caused by nonlinear effects, rapid changes of flow direction in separated regions, large pressure gradients and the presence of walls and outer boundaries in the computational domain. They can create finite oscillations which can slow down convergence considerably. (25:322)

These instabilities and oscillations are removed by adding an explicit fourth-order damping term D_e to right-hand-side of equation (74) and inserting two second order damping terms D_{i_ξ} and D_{i_η} within the respective implicit operators in equation (75) (35:20):

$$D_e = -\omega_e \Delta t J_{i,j}^{-1} (\delta_\xi^4 + \delta_\eta^4) U^n \quad (82)$$

$$D_{i_\xi} = -\omega_i \Delta t J_{i,j}^{-1} \delta_\xi^2 J_{i,j} I \quad (83)$$

$$D_{i_\eta} = -\omega_i \Delta t J_{i,j}^{-1} \delta_\eta^2 J_{i,j} I \quad (84)$$

Where ω_i is of order one and $\omega_i \geq 2\omega_e$.

For certain well posed problems convergence to steady-state can be accelerated by employing local time $\Delta t_{i,j}$ which is dependent upon the flow conditions and metrics at each individual point in the grid (35:22):

$$\Delta t_{i,j} = (\text{CFL}) \Delta t_{\max_{i,j}} \quad (85)$$

Where $\Delta t_{\max_{i,j}}$ is calculated using the modified Courant-Friedrichs-Levy stability criteria (35:22).

$$\Delta t_{\max_{i,j}} = \left[\frac{|u|}{\Delta \xi} + \frac{|v|}{\Delta \eta} + a \sqrt{\frac{1}{\Delta S_{\xi}^2} + \frac{1}{\Delta S_{\eta}^2}} + \frac{2\gamma}{\rho \Delta S_{\eta}^2} \left(\frac{\mu}{Pr} + \frac{\epsilon}{Pr_t} \right) \right]^{-1} \quad (86)$$

$$\Delta S_{\xi} = \left(x_{\xi}^2 + y_{\xi}^2 \right)^{1/2} \Delta \xi \quad (87)$$

$$\Delta S_{\eta} = \left(x_{\eta}^2 + y_{\eta}^2 \right)^{1/2} \Delta \eta \quad (88)$$

$$u = \xi_x u + \xi_y v \quad (89)$$

$$v = \eta_x u + \eta_y v \quad (90)$$

The Courant Number (CFL) for an explicit algorithm must be less than one for stability. However, for the implicit scheme CFL can be much higher and is typically set equal to 20.

Grid Generation

As previously mentioned the grids used for this report were numerically generated from a "hyperbolic grid generator" code (appendix G). This code is based on an algorithm developed by Steger and Chaussee (33) which solves a system of hyperbolic partial differential equations. The advantage of using a hyperbolic grid generator over an elliptic one is that only the inner boundary needs to be specified (2:530), in this case the airfoil surface. Also, systems of hyperbolic equations are easier to solve than elliptic equations and the above algorithm is unconditionally stable.

The detailed theory is beyond the scope of this thesis. An excellent reference for theory used in this code is AFWAL-TM-84-191 (19), prepared by Kinsey and Barth. The purpose of using a grid generator is to produce a body conformal grid in the physical domain that can be related to a uniform rectangular computational domain with grid spacing of unity. For best results the grid coordinates should be orthogonal (2-193).

The particular grid topology used in this study was the C-grid. C-grids require less points than many other type grids (19:11) and therefore require less computer resources to resolve a typical problem. C-grids also allow uniform boundary conditions which are easy to implement.

However, for unsteady flows they can present a problem in the wake region of the airfoil. Where along the branch cut all variables are obtained by numerical averaging (see appendix C).

Convergence Criteria

There are three types of converged solutions in numerical simulations, steady-state, periodic and unsteady. Even though no solution is perfectly steady, there is always some oscillation, the unsteady behavior may be so small as not to affect the solution visibly. When this is the case the solution can be said to have reached a steady-state (27). The steady-state solution is the easiest to resolve. It is characterized by the uniform convergence of some criteria after an initial transition region. In most cases local time can be used with a CFL = 20 or more and convergence can be expected in less than 2,000 iterations. Even faster convergence can be achieved if restart solutions are used where the restart solutions represent a variation in parameters such as Reynolds number or transition point.

The criteria for convergence for this report were the coefficients of lift (C_l) and drag (C_d). When the variations in C_d were within 1-2 drag counts (1 drag count = 0.0001) and the amplitude in C_l was less than 0.1% then

the solution was considered converged to a steady state (35:25).

The periodic solutions can be characterized by an initial unsteady behavior in a transition region followed by periodic oscillations in C_l and C_d . Local time can not be used to resolve such a problem, and a fixed constant time step must be used. The oscillations in C_l and C_d may have more than one harmonic mode on an overriding wave (27). If one harmonic dominates or if a superposition period can be found then convergence is determined when the change in the maximum value of C_l and C_d over one characteristic time unit is less than one percent (7). A characteristic time unit is non-dimensionless and represents the time it takes a particle to travel the length of an airfoil.

$$t = t_{min} N \quad (91)$$

Where t_{min} is the smallest constant time step in the computation and N is the number of iterations. Care should be taken to insure that at least four periods are in the analysis, to take into account any unsteady trends (7). Periodic solutions can result from disturbances in the flow field, such as vortex shedding, large separated regions and stall characteristics at high angles of attack.

A truly unsteady solution is characterized by oscillations which are not periodic. Such a solution can not be resolved and often results when the model does not represent true physical behavior such as laminar separation at a turbulent Reynolds number or when numerical instability predominates the solution. This type of behavior can not be resolved except as a function of time and depending on the problem might not represent physical behavior.

IV Results and Discussion

In this chapter the numerical results obtained from the Navier-Stokes code previously mentioned are presented. The verification of both the code and grid are discussed and the final results for a "fan-in-wing" are presented. The results are presented through the comparison of lift and drag coefficients, streamline and vorticity contour plots and surface pressure and skin friction profiles. Data reduction was performed with two codes written by the author and included in appendices J and K. This investigation concentrated on the effect of mass flux on varying suction rates C_v , ejection angles δ and angle of attack α .

Code and Grid Verification

Before the fan problem could be resolved it was necessary to determine a compatible grid configuration and to insure that the NS code was predicting the flow field accurately. This was done by testing the various grids listed in Table 1 under known, verifiable conditions.

grid	wall spacing	η_{pt}	ξ_{pt}	outer boundary	symmetry
1	.001	199	40	5	yes
2	.0005	137	44	5	yes
3	.0001	199	50	10	yes
4	.0001	299	100	20	no
5	.0001	299	100	20	no

Table 1. NACA 0012 Grid Configurations

Grids 1, 3, 4 and 5 were produced using the hyperbolic generator and grid 2 was produced from an elliptical grid generator. Grid 4 and 5 are unsymmetrical because points on the body were clustered over the suction and ejection surfaces which, is evident in Figure 11. The number of points in the η direction, η_{pt} , were increased on grid 4 to allow better resolution and a greater cord distance to the outer boundary. The resolution on the airfoil surface was improved by increasing the number of points in the ξ direction, ξ_{pt} . At the leading edge the spacing is 0.003, at the trailing edge it is 0.005, and over the injection and suction surfaces it is 0.005. The wall spacing on 4 was refined to 0.0001 in order to resolve the boundary layer better. This resolution can be seen on the blown-up portions of the grid in Figure 12. Grid 5 was produced from grid 4 by using two codes (appendix I) to redistribute the points in the η direction in order to force a maximum spacing at the outer boundary of less than one cord length.

All of the grids in Table 1 were tested against

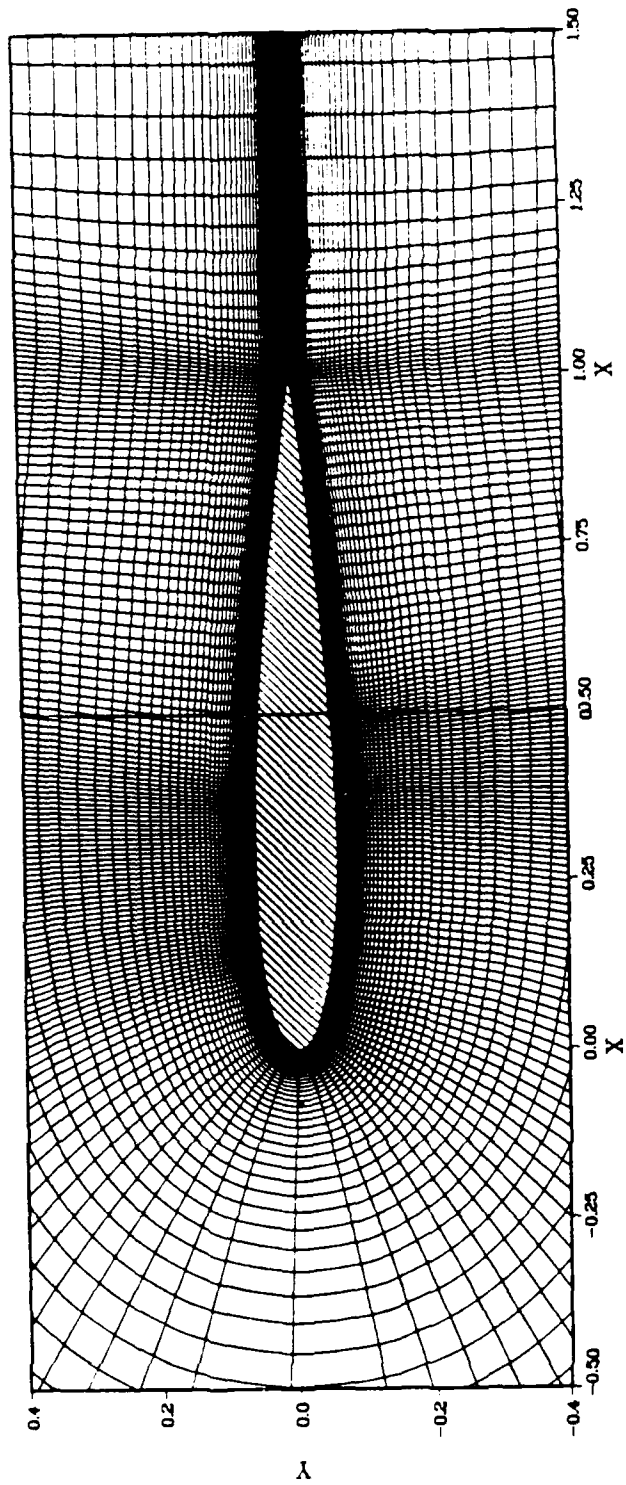


Figure 11. Final Grid Configuration for a NACA 0012 Airfoil

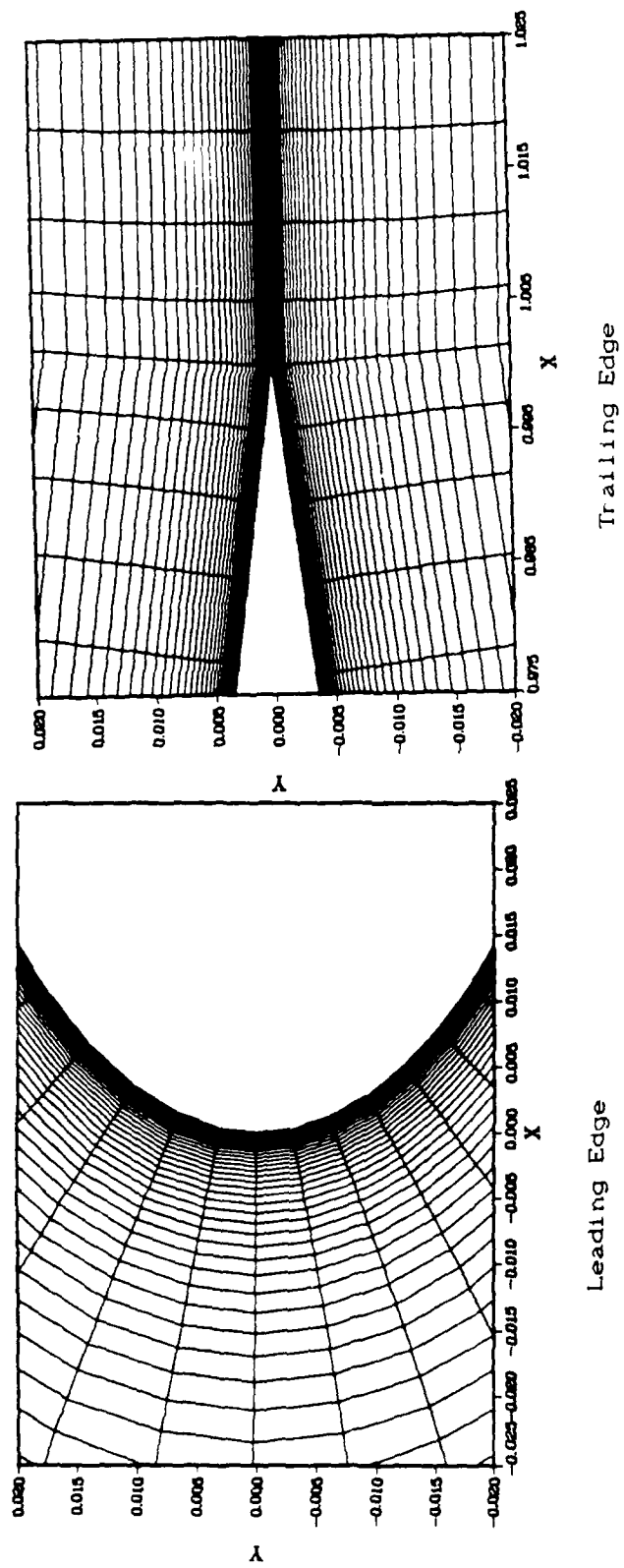


Figure 12. Final Grid Configuration, Close-up

separation point results from a PNS code (13:5). The results are compared in Table 2. The conditions of the test were laminar flow at $Re = 12,500$ and $M = 0.3$. From Table 2 it is obvious that a wall spacing of 0.001 is too coarse. The other grids predict reasonably well. Grid 2 has similar spacing to the grid used for the PNS analysis and for this reason gave the best results. Grid 4 and 5, with smaller wall spacing, predicted separation early. This may be due to better numerical resolution of the boundary layer.

grid	separation
1	.000
2	.817
3	.784
4	.787
5	.787
ref(13:5)	.817

Table 2. Separation Point Comparison

C_l and C_d were then compared at an extreme case for grid 4 and 5 (Table 3). The numerical data was computed using a interactive boundary layer code (10:8). Both the experimental data and the numerical solution fixed the transition at 5 percent cord. For this case $Re = 6,000,000$ and $M = 0.3$. These conditions are near stall ($\cong 14^\circ$), presented a difficult case and were a good test for the code's turbulence model.

grid	Cl	Cd
4	1.08	.0129
5	1.07	.0124
ref (10:8)	.95	.0092
ref (1:462)	1.11	.0111

Table 3. Lift and Drag Comparison with Experimental Data, $\alpha = 10^\circ$, $M = .9$, $Re = 6,000,000$

The C_l results in Table 3 are in good agreement with the experimental data, but the C_d results are higher than expected. Considering the extreme Re and the high angle of attack, this comparison still indicates that the code predicts a reasonable solution. The next case compares surface C_p from grid 5 with experimental data, Figure 13. The difference in Re has only a small effect, C_l and C_d are compared in Table 4 for transition effects. The effect of transition is more pronounced both in the C_p and the C_l , C_d comparisons. Though not in perfect agreement, the NS solution predicts slightly higher values for C_p , the agreement is still reasonable.

$Re \times 10^6$	transition % lower surface	Transition % upper surface	Cl	Cd
1.00	5	40	.455	.0128
1.00	5	5	.465	.0108
1.86	5	5	.460	.0098

Table 4. Cl and Cd vs Re and Transition Point, $\alpha^\circ = 4.04$

A final comparison was made for c_l and c_d versus inviscid theory and experimental data for grid 5, Table 5, and transition points. The transition point on the

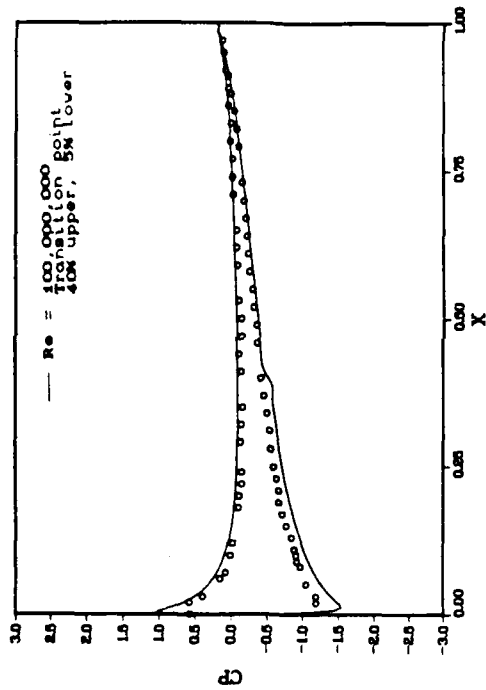
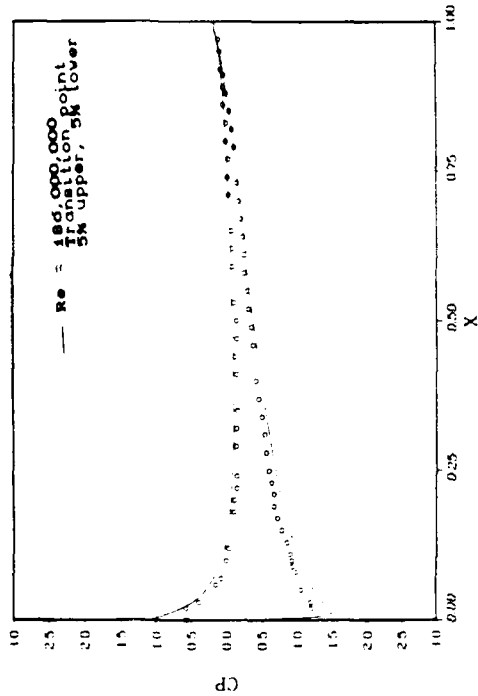
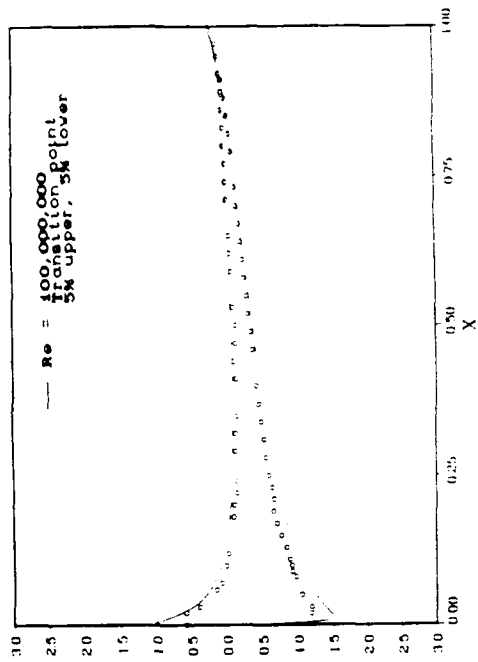


Figure 13. Comparisons of Cp with Experimental Data (25: A1-10)
 ($Re=1,860,000$, $M=3$, $\alpha=4.04^\circ$)

upper surface was fixed at 40 percent of the cord as measured from the leading edge, which is 5 grid points behind the suction region of the fan.

surface		$\alpha=0$	$\alpha=2$	$\alpha=4$	
Transition %c	lower upper	Cl	Cl	Cl	
5	40	0.023	.246	.478	
5	5	0.000	.229	.454	
exp (1:460)		0.0	.22	.44	
inviscid theory					
flat plate $2\pi\alpha$		(31:93)	0.0	.219	.439
Joukowski $t/c = .12$		(27:95)	0.0	.238	.477

Table 5. Cl and Cd Comparison with Experimental and Theoretical Data
(exp Re = 3,000,000, num Re = 1,000,000)

The C_p and C_f surface comparisons are presented in Figures 14 and 15. From this data it is also apparent that the transition point has an effect on the solution. The C_p curves in Figure 14 indicate a pressure difference around the leading edge. This pressure difference is responsible for the lift created by the unsymmetrical transition points. The C_f plots in Figure 15 also indicate a small change due to transition. These differences are small when compared with angle of attack which will be presented later.

Suction and Ejection Separately

The first step taken in determining the effect of a

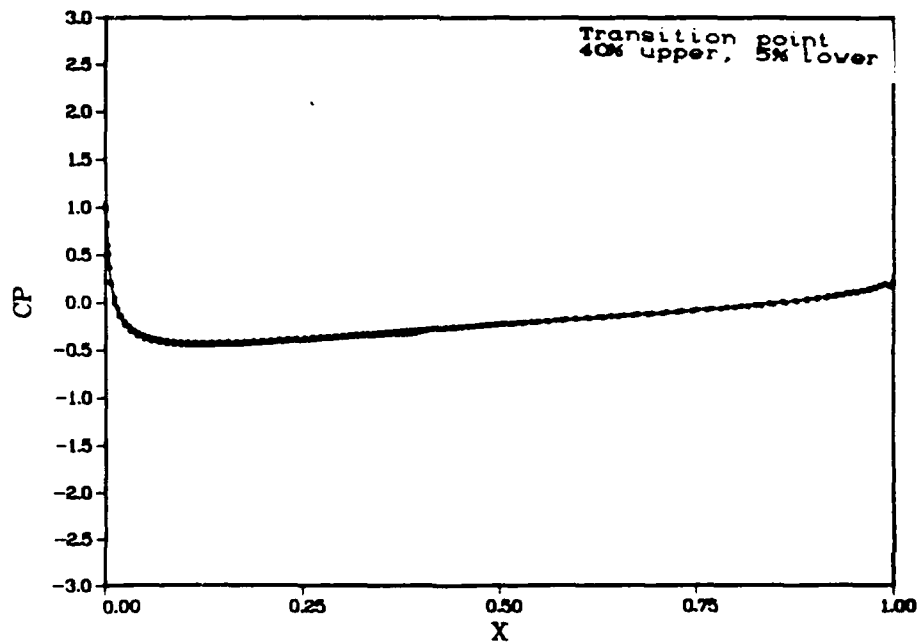
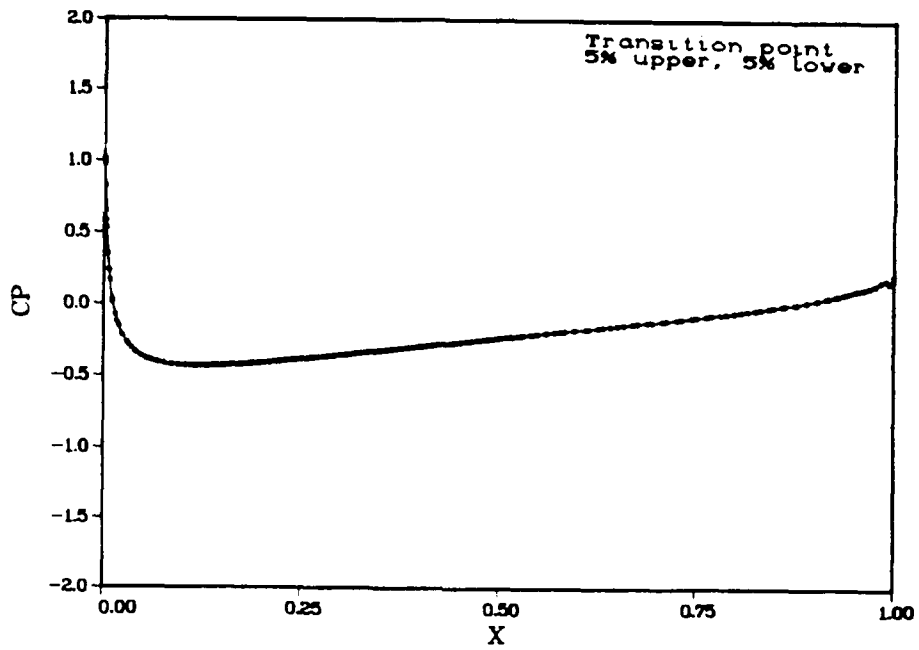


Figure 14. Comparisons of C_p for Transition Point Effects
($Re=1,000,000$, $M=.3$, $\alpha=0^\circ$)

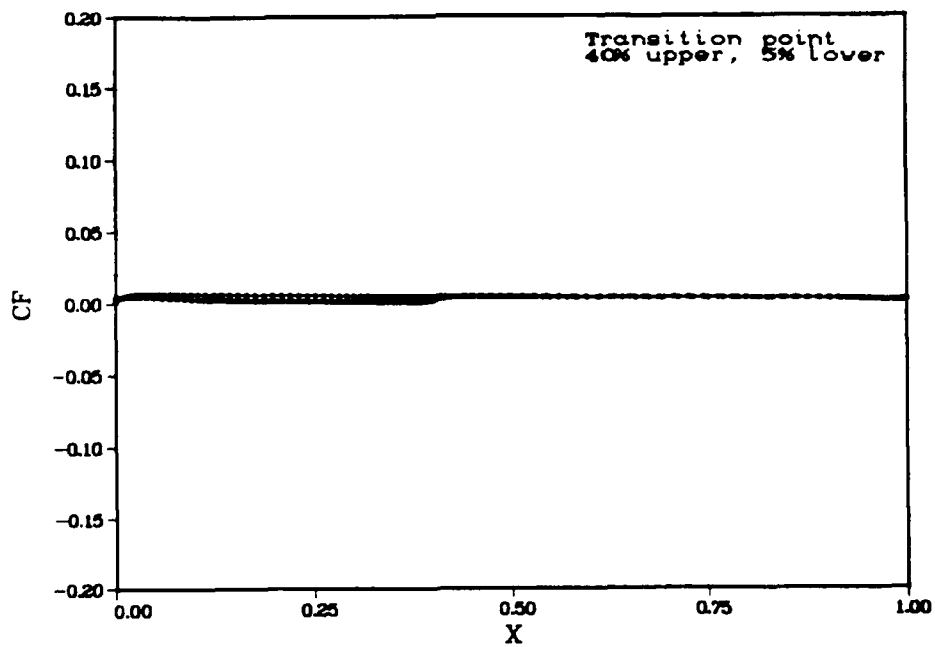
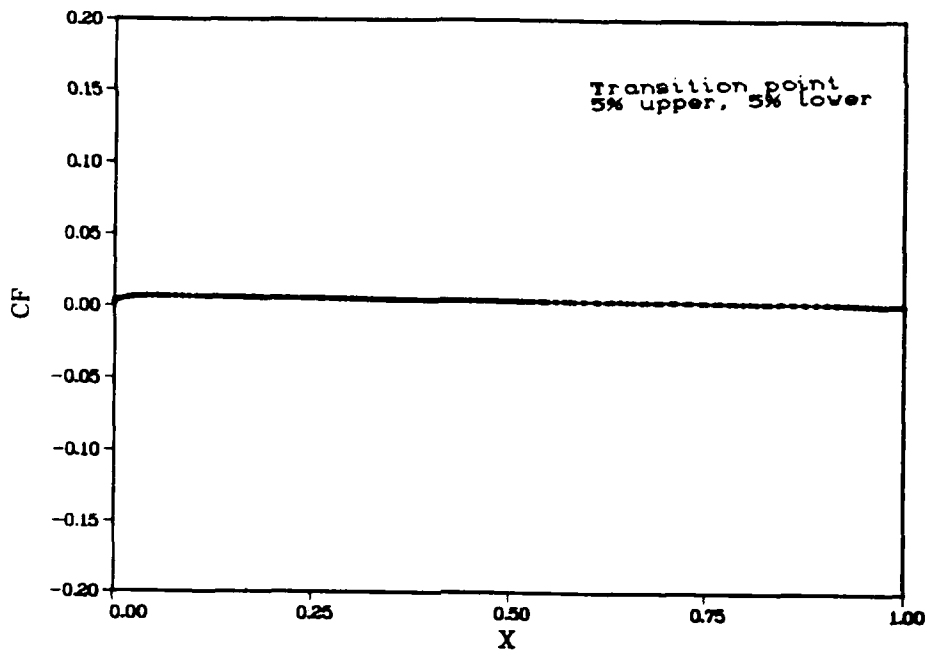


Figure 15. Comparisons of Cf for Transition Point Effects
($Re=1,000,000$, $M=0.3$, $\alpha=0^\circ$)

fan was a comparison of the components, suction and ejection separately see Table 6. For this analysis ejection was set at $\delta = 90^\circ$ and suction velocity $C_v = 0.05$. As with the solutions above, the solution for suction reached a steady-state condition quickly; however, blowing converged to a periodic solution which is discussed in some detail in the following section on convergence. Suction has the effect of increasing lift only marginally while ejection has a surprisingly high effect on lift. The differences can be clearly seen by comparing the C_p curves in Figure 16. The drag effects are reversed. Normal ejection has almost no effect on drag while suction produced an astonishingly high skin friction profile, Figure 17, which results in a large viscous drag component.

case	Cl total	Cl press	Cl viscous	Cl mass
no fan	.01907	.01921	-.00014	.00000
suction	.09968	.09477	.00018	-.00126
ejection	.21473	.21264	-.00018	.00226
fan	.22849	.22725	.00010	.00107

case	Cd total	Cd press	Cd viscous	Cd mass
no fan	.00954	.00164	.00790	.0000
suction	.01484	-.00926	.01806	.00004
ejection	.02694	.02151	.00543	.00000
fan	.03971	.01800	.01567	.00004

Table 6. Cl and Cd Comparison for Suction and Blowing Only
($C_v = .05$, $\delta = 90^\circ$)

The skin friction profile of suction indicates the effect is related to the immediate suction surface.

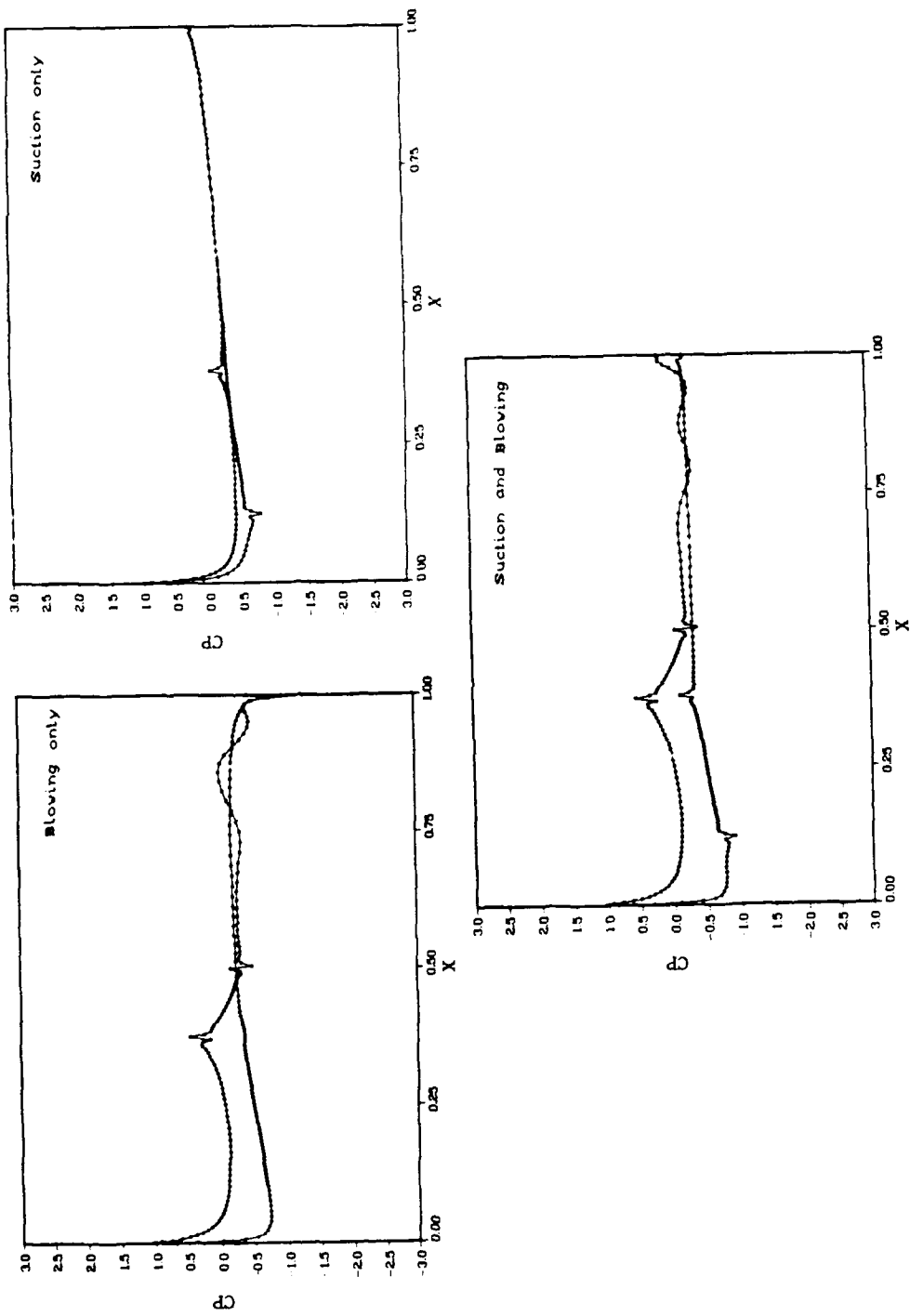


Figure 16. Comparisons of C_p for Suction and Blowing effects
 ($Re=1,000,000$, $M=3$, $\alpha=0^\circ$)

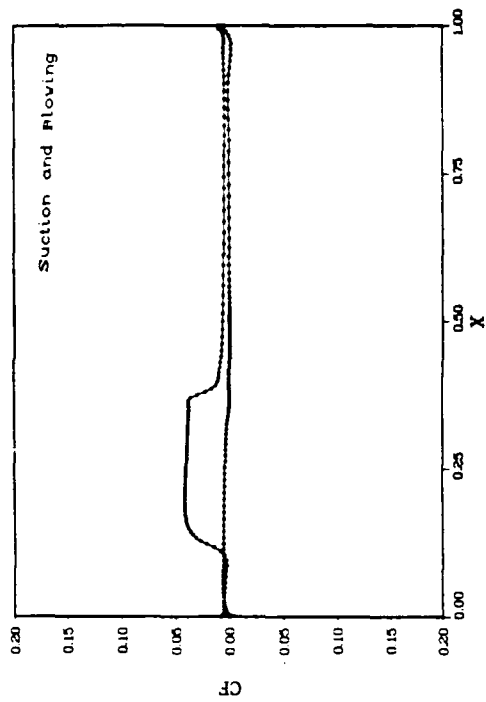
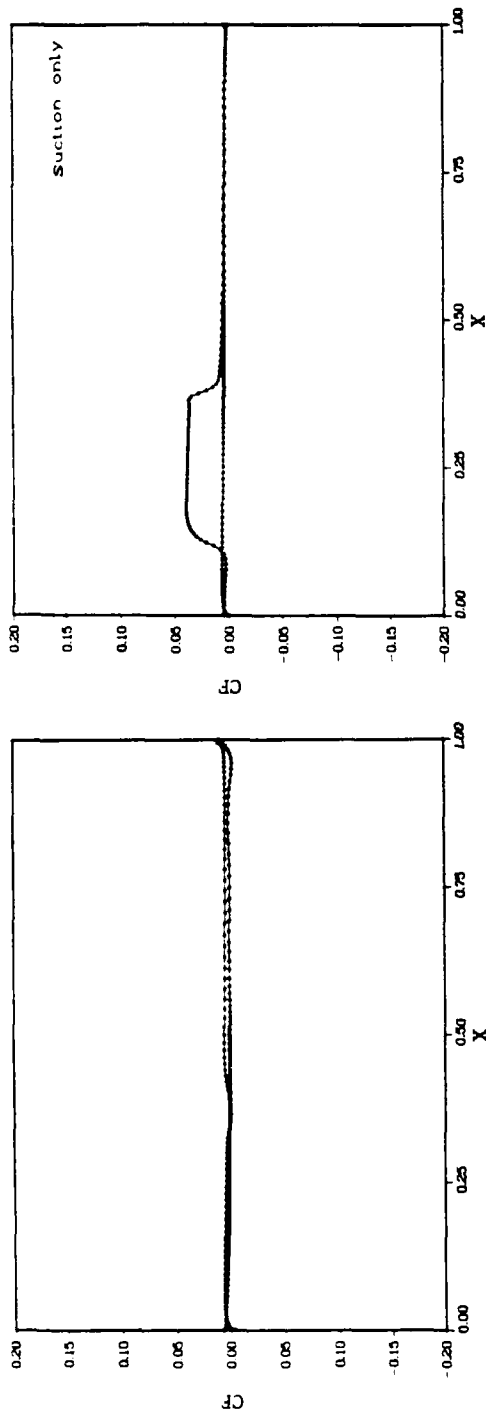


Figure 17. Comparisons of C_f for Suction and Blowing effects:
 ($Re=1,000,000$, $M=3$, $\alpha=0^\circ$, $\delta=90^\circ$, $Cv=0.05$)

Analysis of the velocities at one point above the surface indicate that suction creates a large velocity gradient above the surface, see Table 7 and Figure 18. This result can be directly linked to the boundary conditions by considering the continuity equation at the suction surface

$$\frac{\partial \rho}{\partial t} + \frac{\partial(\rho u)}{\partial x} + \frac{\partial(\rho v)}{\partial y} = 0 \quad (10)$$

surface values $\eta = 1$				
x	y	ρ	u	v
.1110	.0483	.9338	.0000	.0000
.1176	.0492	.9370	.0000	.0000
.1234	.0500	.9360	.0065	-.0496
.1284	.0507	.9504	.0062	-.4961
.1334	.0513	.9613	.0059	-.4965

one point above surface $\eta = 2$				
x	y	ρ	u	v
.1110	.0484	.9344	.2510	.0371
.1176	.0493	.9384	.4547	.0587
.1234	.0501	.9379	.7839	.0594
.1284	.0506	.9526	1.0575	.0796
.1334	.0514	.9638	1.2623	.0999

Table 7. Velocity and Density Comparison at the Suction Surface (Suction begins at x=.12345)

As v increases suddenly at the suction surface so must u along the surface and the growth is very fast as indicated by Table 7. The velocity of u before the suction indicates that it is in the boundary layer and at the point above suction the boundary layer is removed see Figure 18 and $u > 1$. The velocity profile quickly reduces to the free stream value, as can be seen in Figure 19. The effect of suction is confined very close to the body with

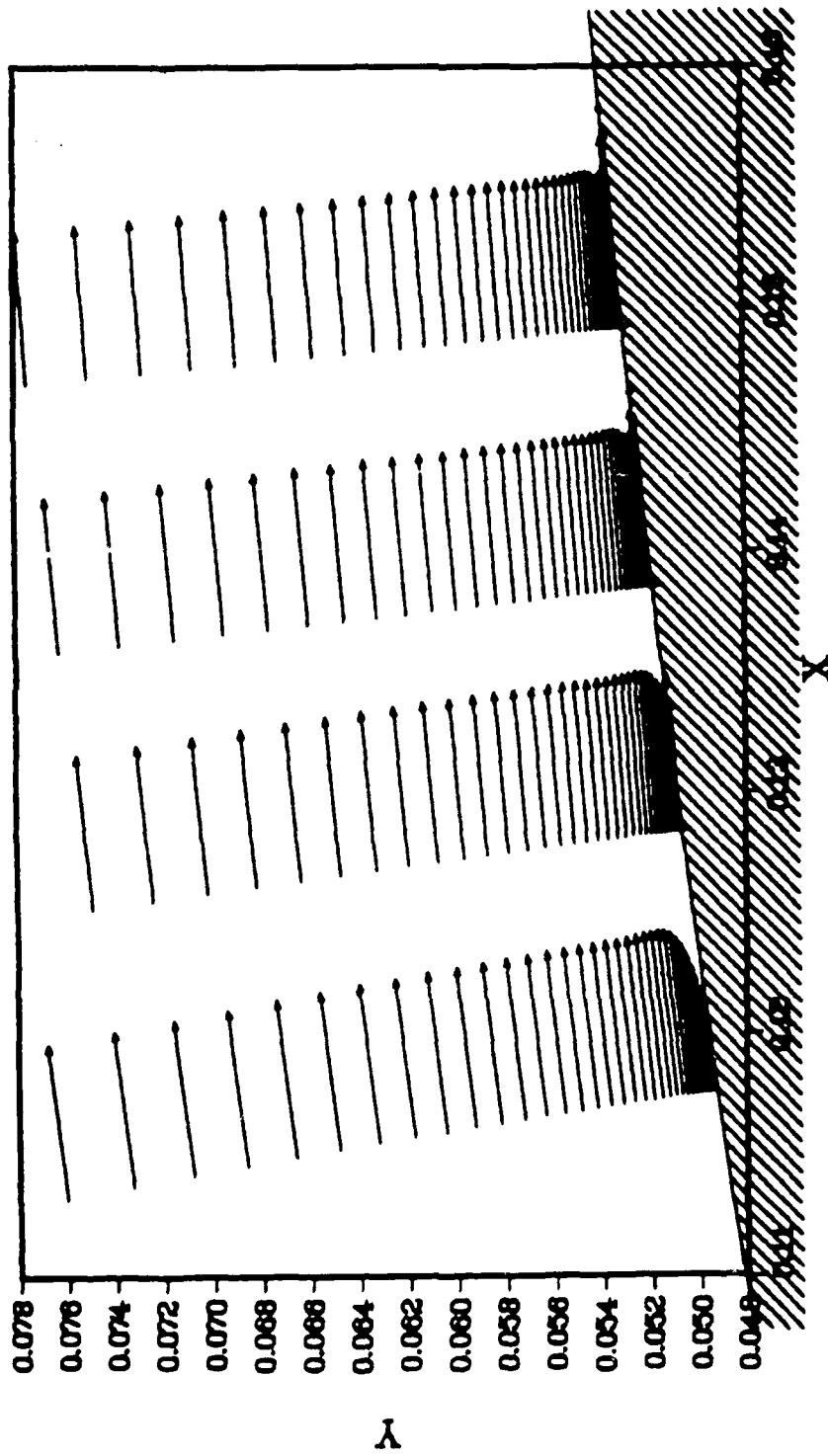
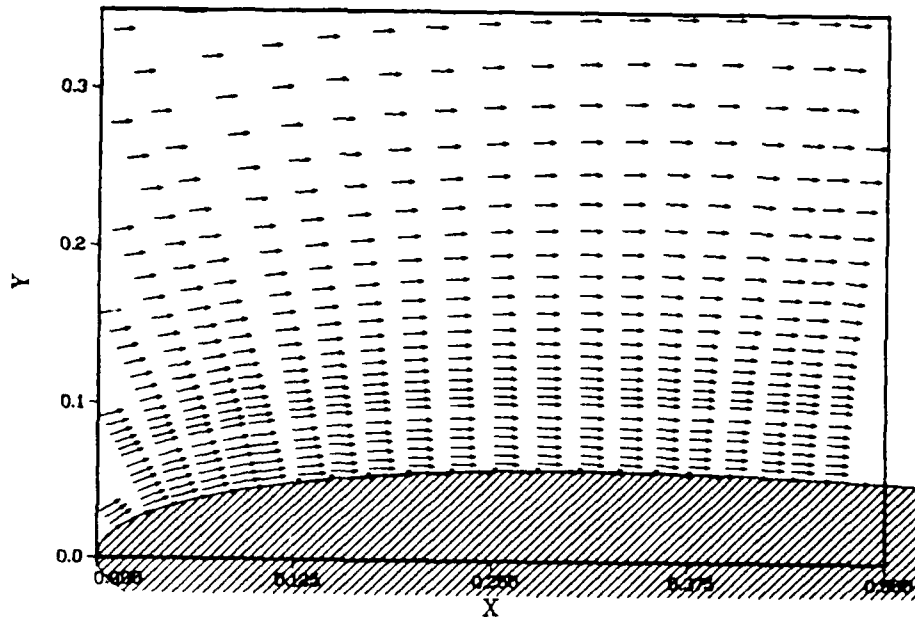


Figure 18. Velocity Boundary Layer Profile above Suction Surface ($C_v = .05$)

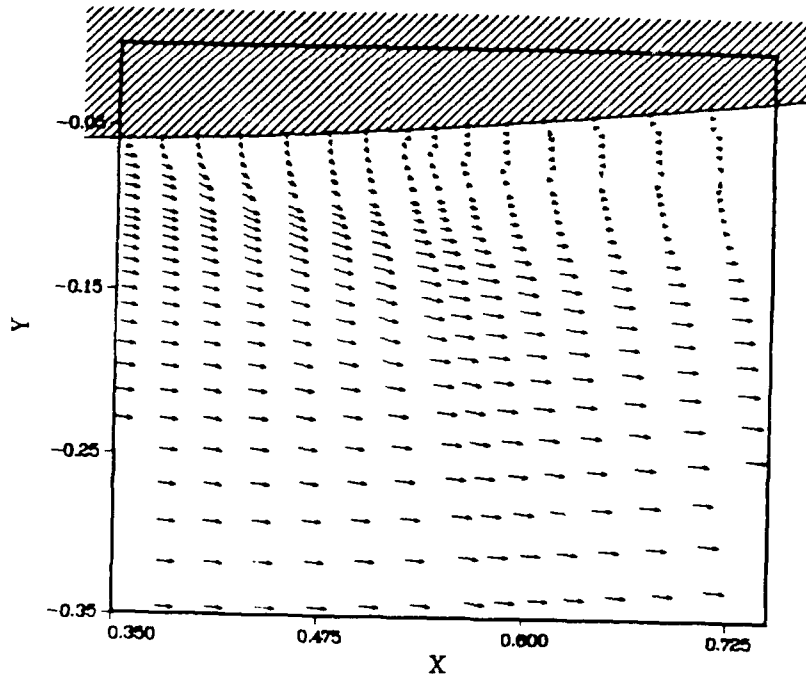
a dimension less than 0.002 as shown in Figure 18. This large surface gradient in velocity produces vorticity and thus has a large effect on the viscous force drag. A better model of suction might decrease drag but should still only have a small effect on lift.

The results for blowing can be explained in this way: at a 90 degrees ejection angle, density is constant along the ejection surface and there is no v component to velocity; therefore, continuity is satisfied if $du = 0$ with both du/dx and $dv/dy \cong 0$ the skin friction is negligible right above the surface. However the effect of blowing produces vortices immediately behind the ejection surfaces shown in Figure 19. The vortices are shed through interaction with a shear layer formed by blowing as it turns the free stream. At the trailing edge these counter-clockwise rotating vortices induce circulation around the trailing edge which leads to the formation of a clockwise rotating vortex. (5:196)

The trailing edge vortex is more powerful than the vortex produced by ejection as shown in Figure 20. This is due to the higher energy of the flow on the upper surface and the lower energy flow between the shear layer and the lower surface. These vortices are shed in a complex interaction as shown graphically by the streamline and

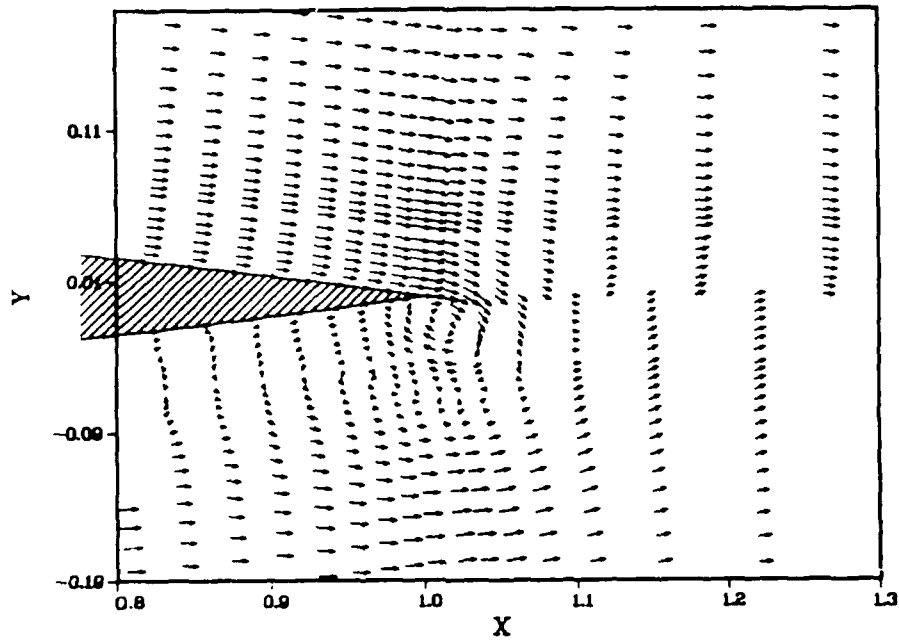


Upper Surface, Suction

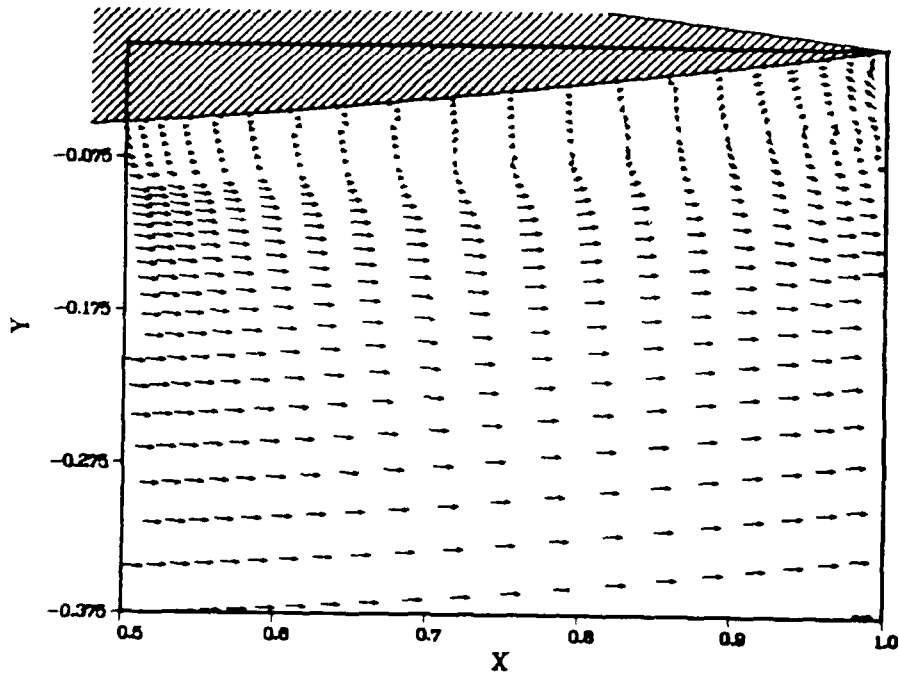


Lower Surface, Blowing

Figure 19. Velocity Profiles above Suction and Blowing Surfaces ($C_v = .05$)



Trailing Edge Vortex



Ejection induced Shear Layer

Figure 20. Velocity Profiles of Trailing Edge Vortex and Shear Layer ($C_v = .05$)

vorticity plots in Figures 21 and 22. As the vortices shed they produce oscillations in lift and drag. But these oscillations can not account for the higher mean values seen in lift due to blowing only.

An analysis of the surface pressure (Figure 16) reveal that the primary component to lift (Table 6) due to blowing is the pressure difference between the upper and lower surfaces on the forward portion of the airfoil. The primary effect of the vortex shedding is confined in the airfoil region behind the ejecting surface. The C_p difference producing lift can be explained by the compression effect the shear layer has on the flow by forcing it to turn.

Convergence Criterion for Periodic Solutions

Before an analysis could be performed, each case had to meet a convergence test as discussed in chapter three. Seventeen cases were run for $Re = 1,000,000$ and $M = 0.3$. Table 8 contains information on each case and pertinent information including the "number" by which they will be referred to. Of the seventeen cases listed the ten with ejection converged periodically. The remaining seven converged to a steady-state solution. Whenever possible, restarts from different converged solutions were used to reduce the transition period and thereby the number of

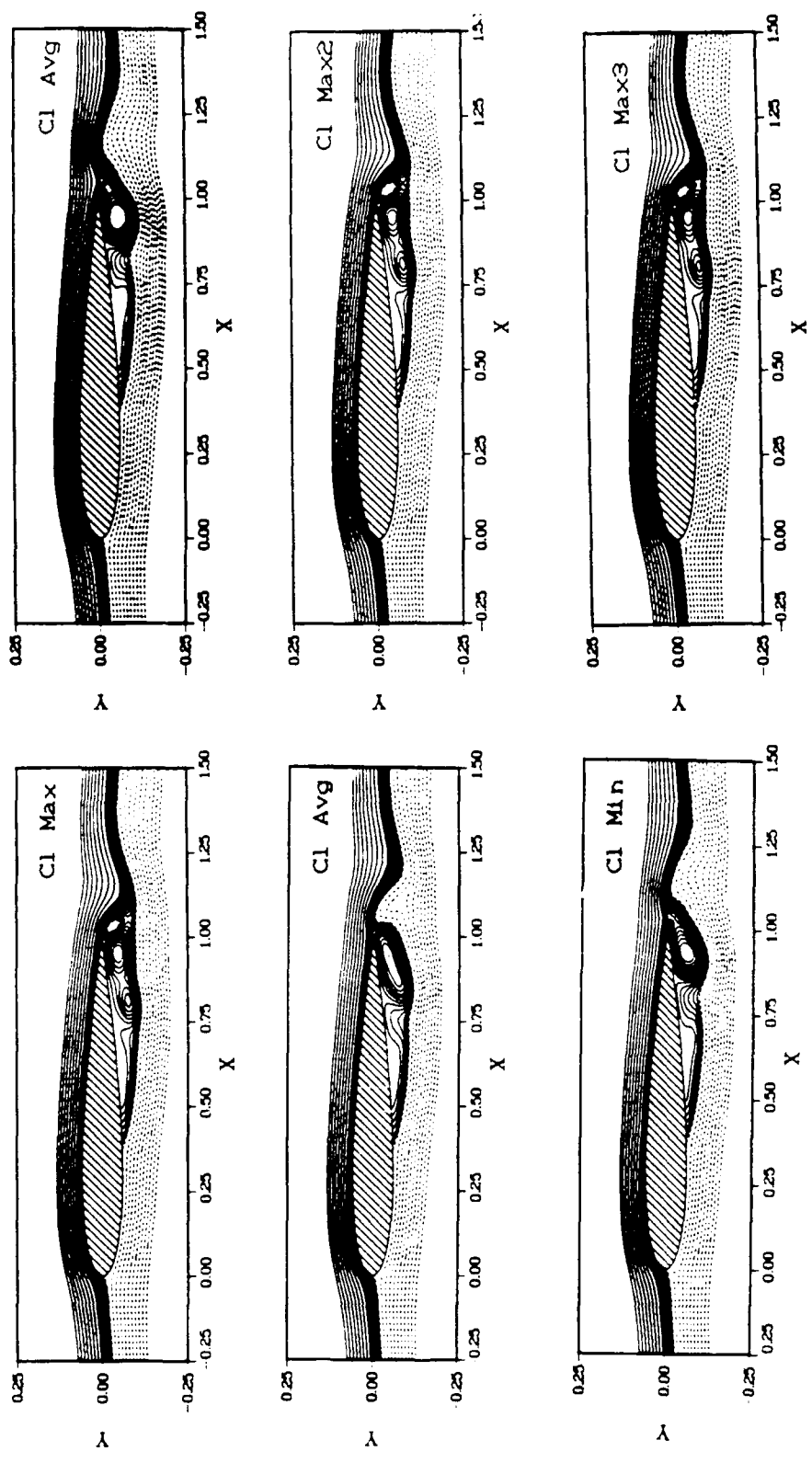


Figure 21. Streamline Comparisons for One Period in CI ($C_v=0.05$, $\delta=90^\circ$)

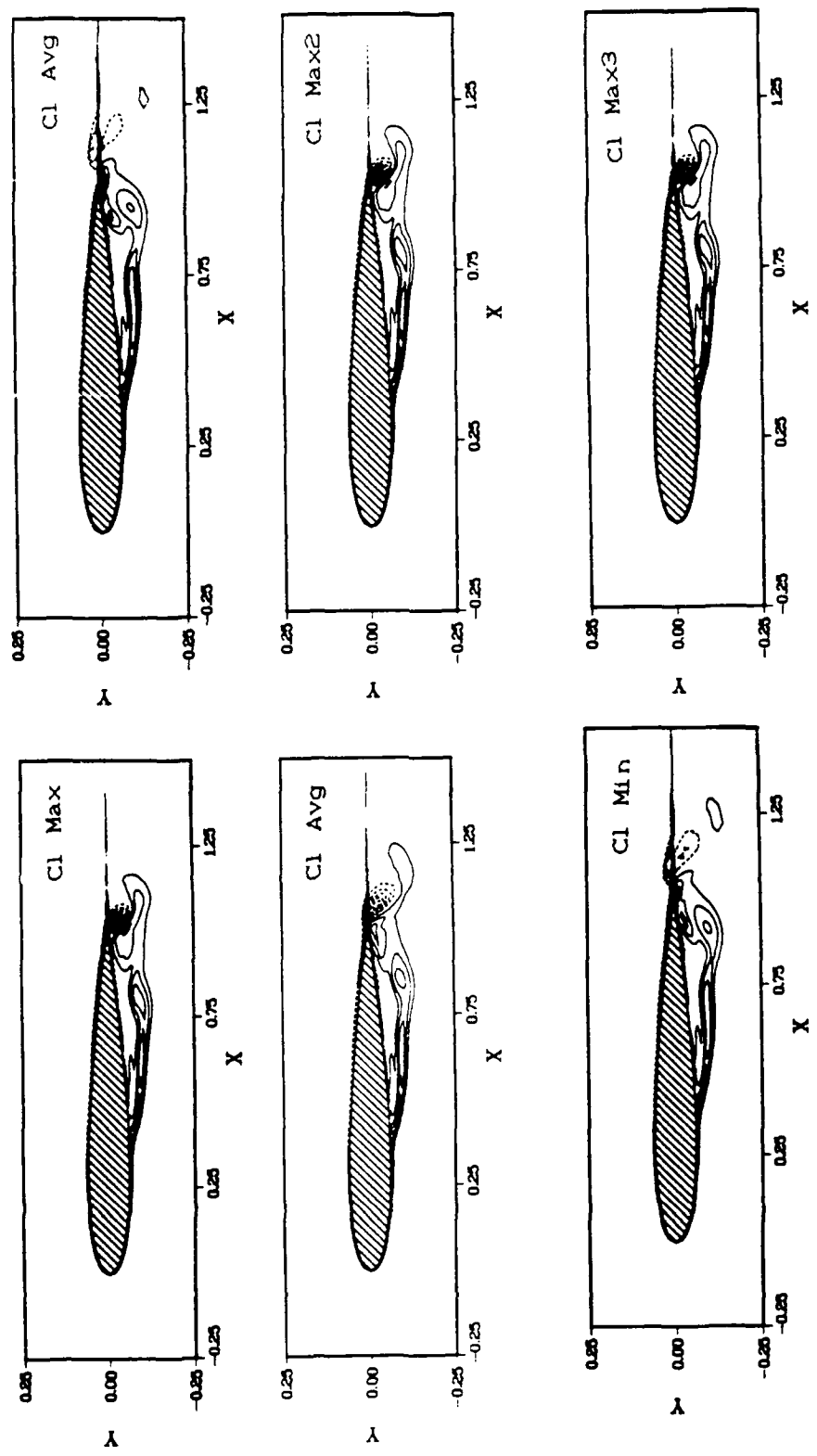


Figure 22. Vorticity Contour Comparisons for One Period in C1
($Cv=0.05$, $\delta=90^\circ$)

#		restart	Cv	δ°	α°	transition % upper	lower
1	clean	2	0.00	0	0	1.5	1.5
2	clean	nev	0.00	0	0	5	40
3	suction	2	0.05	0	0	5	40
4	blowing	2	0.05	90	0	5	40
5	fan	6	0.01	90	0	5	40
6	fan	2	0.05	90	0	5	40
7	fan	6	0.05	45	0	5	40
8	fan	7	0.05	15	0	5	40
9	fan	6	0.10	90	0	5	40
10	fan	9	0.10	45	0	5	40
11	fan	10	0.10	15	0	5	40
12	clean	13	0.00	00	2	5	5
13	clean	nev	0.00	00	2	5	40
14	fan	13	0.05	45	2	5	40
15	clean	16	0.00	00	4	5	5
16	clean	nev	0.00	00	4	5	40
17	fan	16	0.05	45	4	5	40

Table 8. List of Model Configurations for $M=3$,
 $Re = 1,000,000$

iterations needed to converge to the new solution.

Plots of C_1 and C_D for each case can be found in Figures 23-33. A comparison of the amplitude and slope of convergence provides some interesting insight into the behavior characteristics of different Cv, δ and α . The plots indicate that as the suction rate increased the amplitudes in C_1 and C_D decreased. Increasing δ and α had the opposite effect. From the figures it appears, in general, that as the amplitudes decreased in size they increased in frequency. Even for the cases of Number 11 (Figure 31) and number 5 (Figure 25) which may look similar to steady state solutions (Figure 23), detailed analysis shows that low amplitude and high frequency oscillations are present.

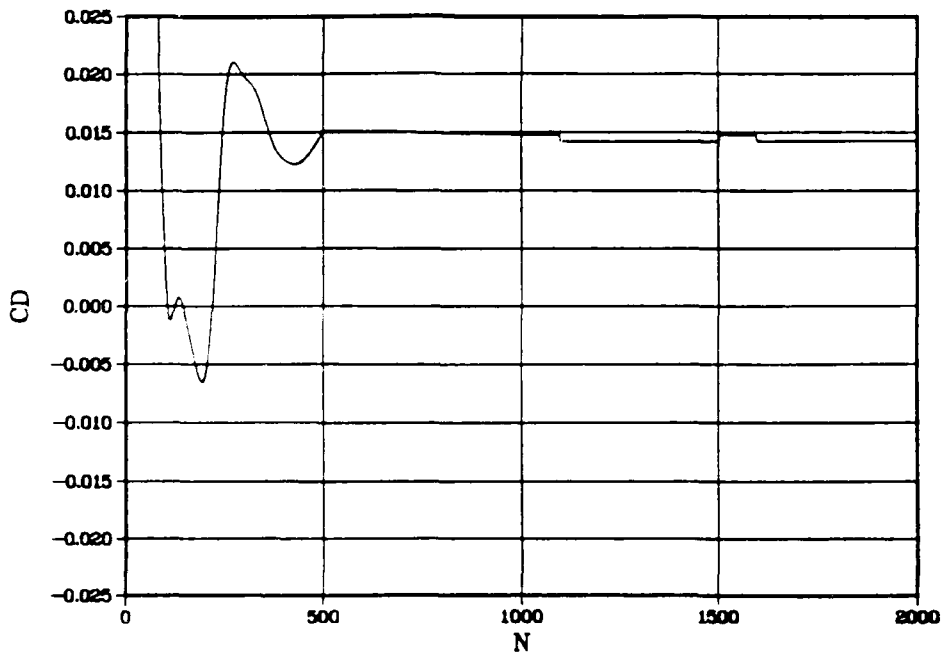
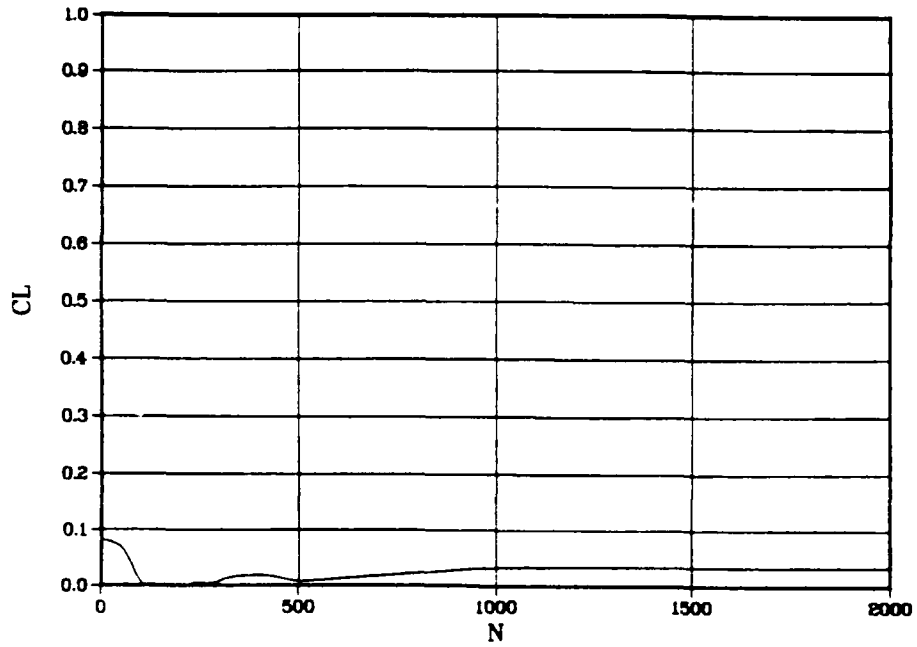


Figure 23. Force Coefficients vs Iterations, Number 3
 (Suction only $C_v=0.05$, $\alpha=0^\circ$)

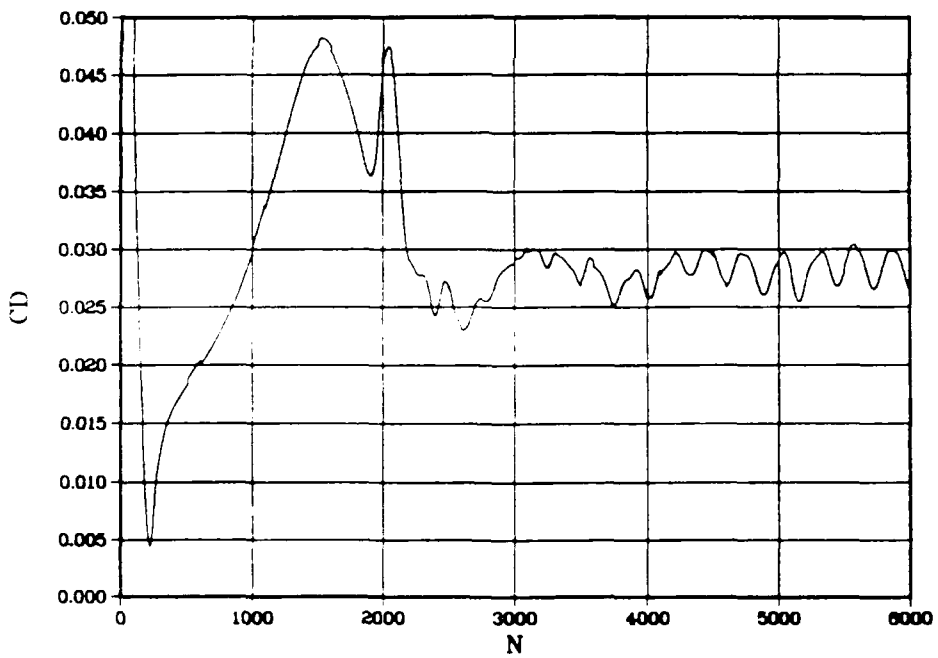
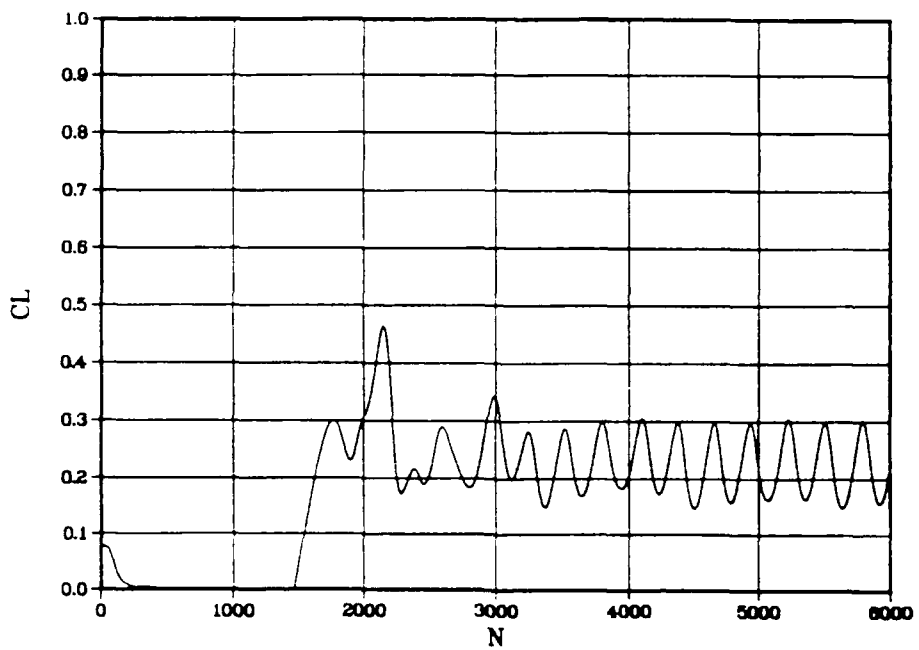


Figure 24. Force Coefficients vs Iterations, Number 4
 (Blowing only $C_v = .05$, $\delta = 90^\circ$, $\alpha = 0^\circ$)

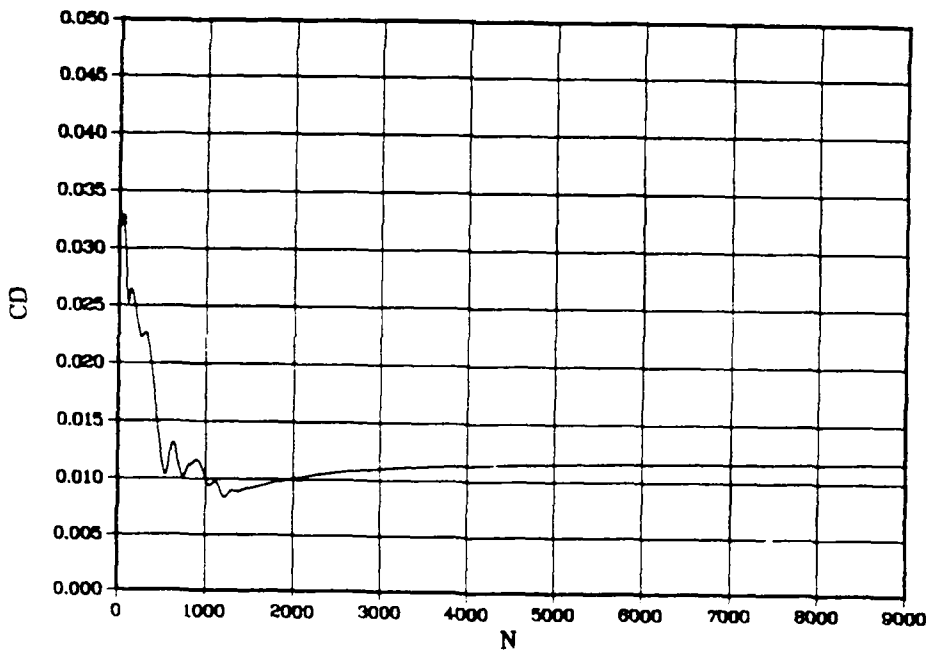
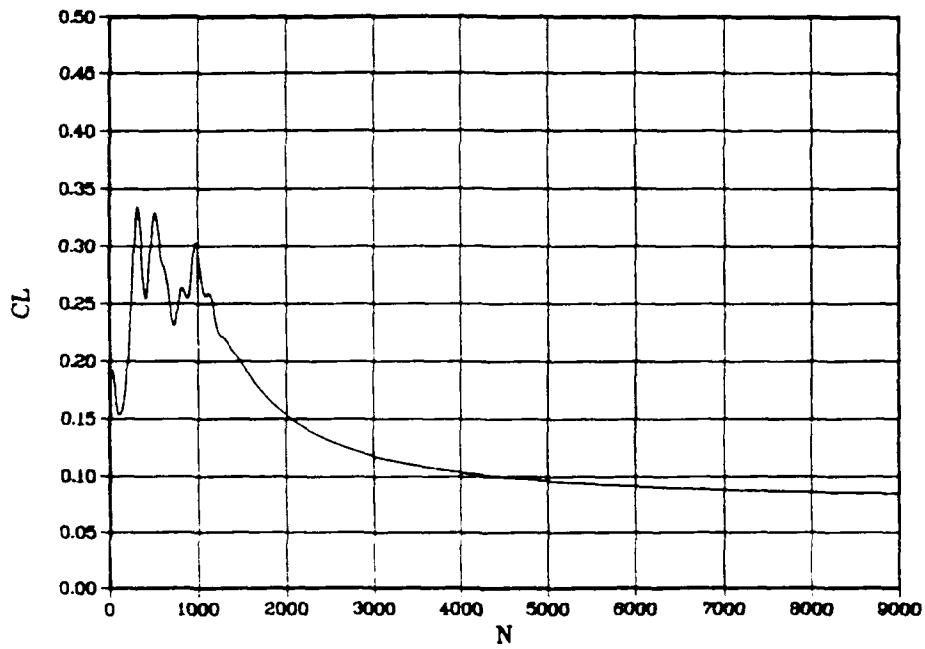


Figure 25. Force Coefficients vs Iterations, Number 5
 ($C_v = .01$, $\delta = 90^\circ$, $\alpha = 0^\circ$)

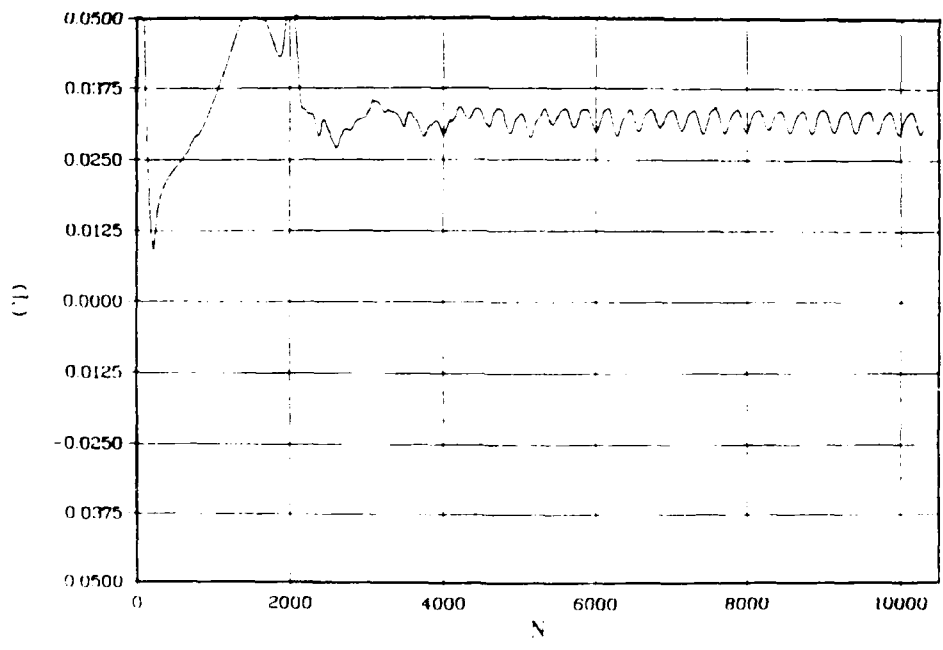
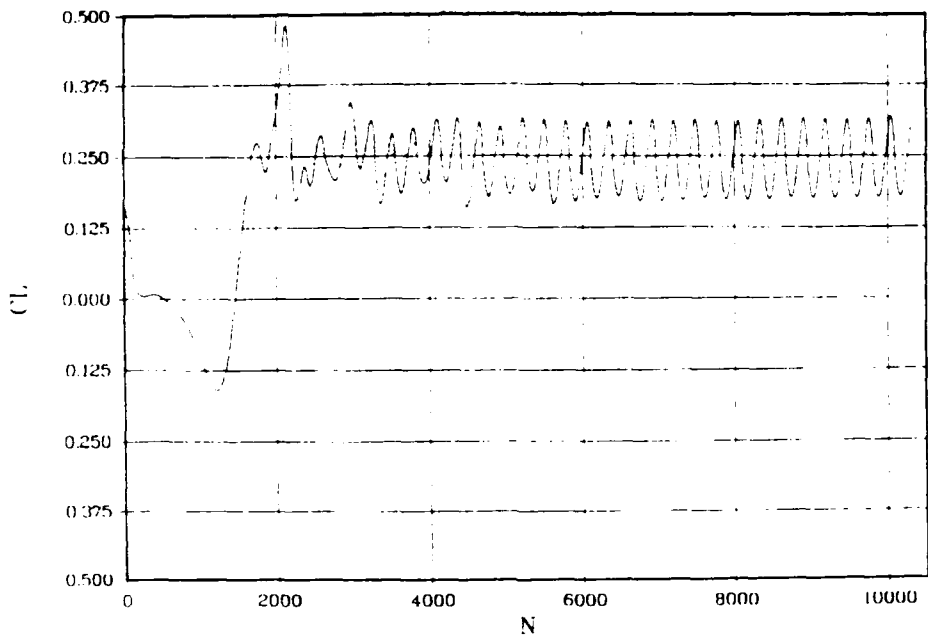


Figure 26. Force Coefficients vs Iterations, Number 6
 ($C_v = .05$, $\delta = 90^\circ$, $\alpha = 0^\circ$)

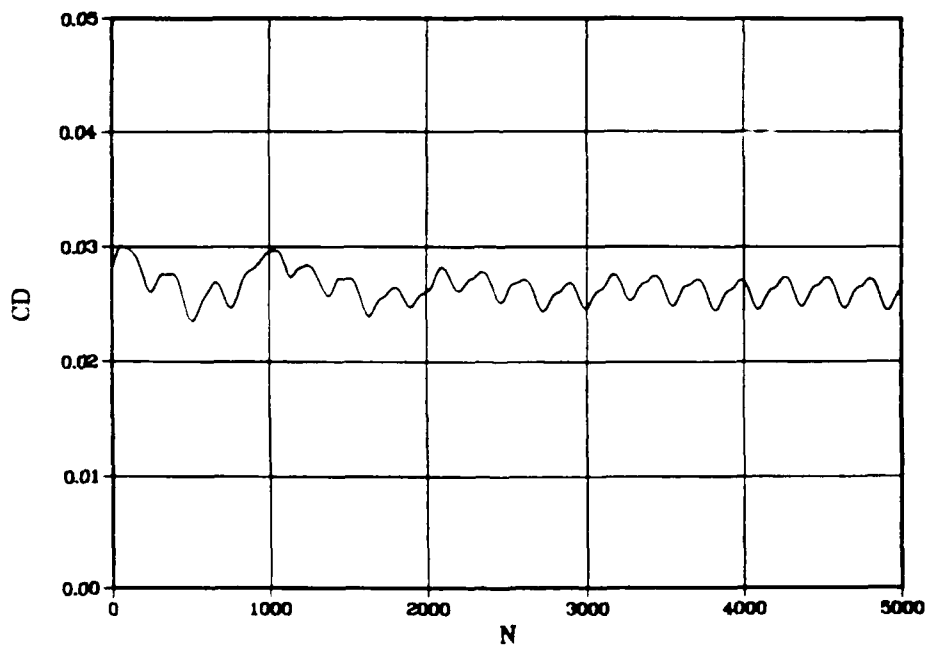
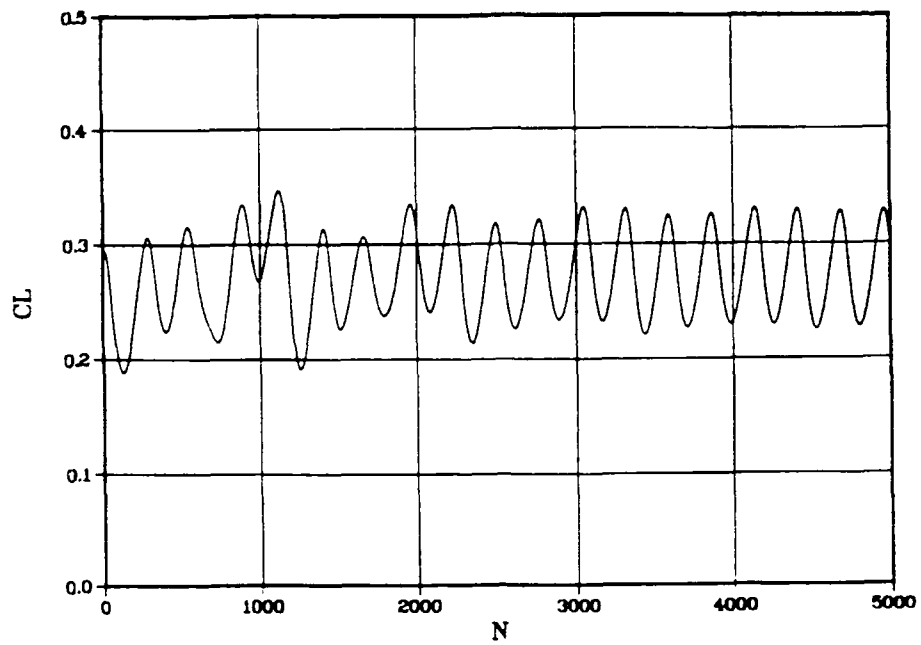


Figure 27. Force Coefficients vs Iterations, Number 7
 ($C_v = .05$, $\delta = 45^\circ$, $\alpha = 0^\circ$)

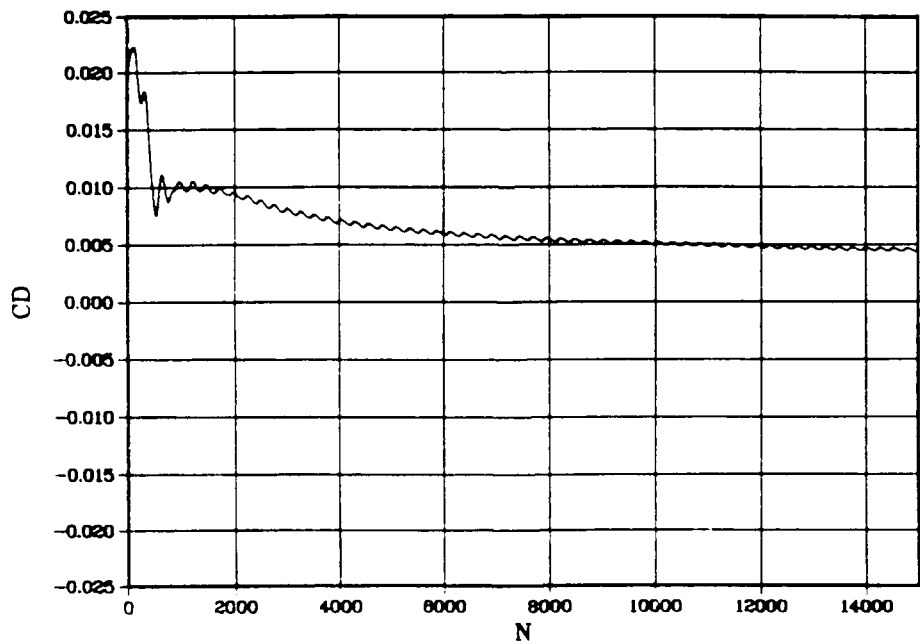
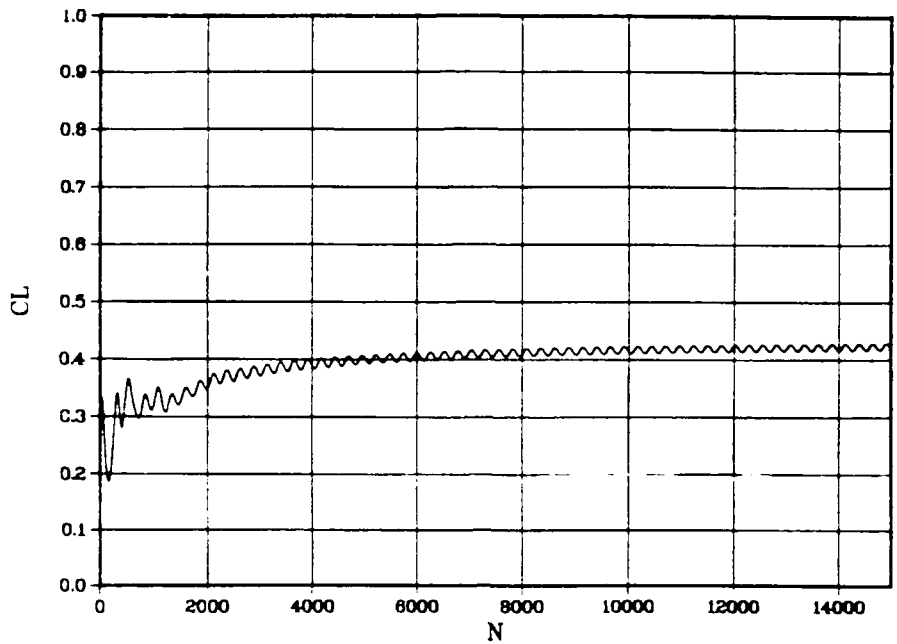


Figure 28. Force Coefficients vs Iterations, Number 8
 ($C_v = 0.5$, $\delta = 15^\circ$, $\alpha = 0^\circ$)

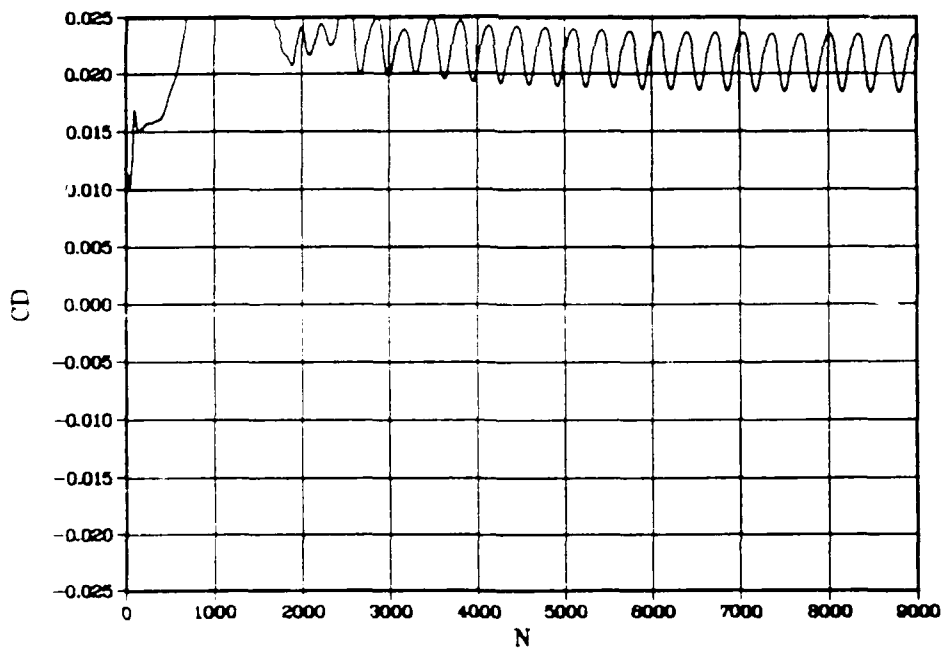
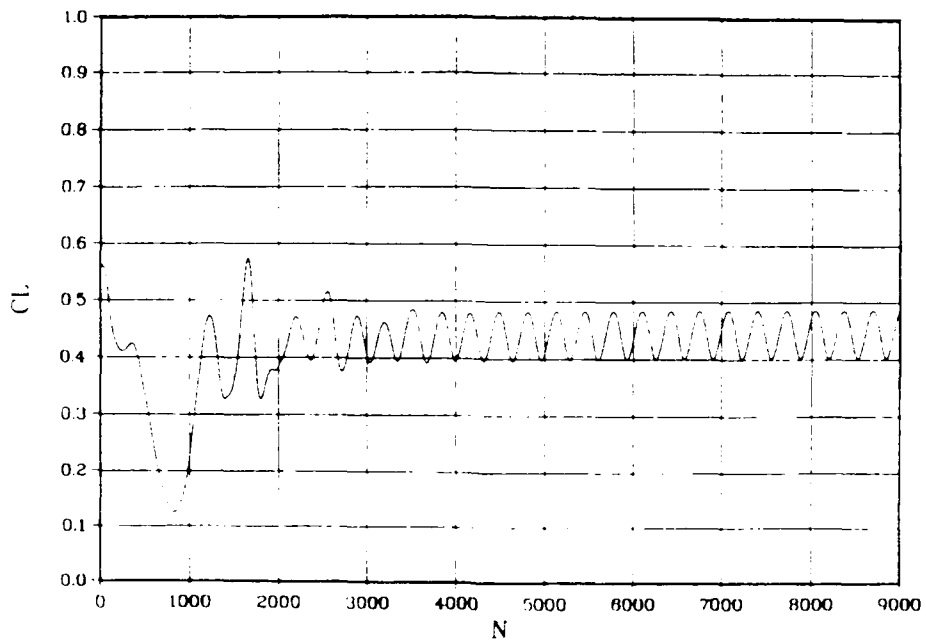


Figure 29. Force Coefficients vs Iterations, Number 9
 ($C_v=0.10$, $\delta=90^\circ$, $\alpha=0^\circ$)

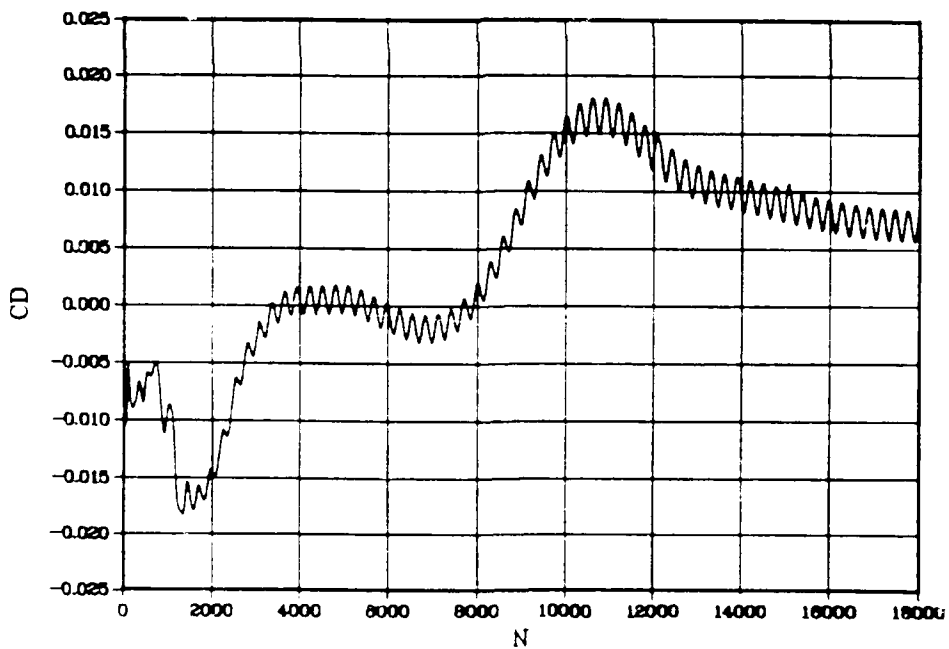
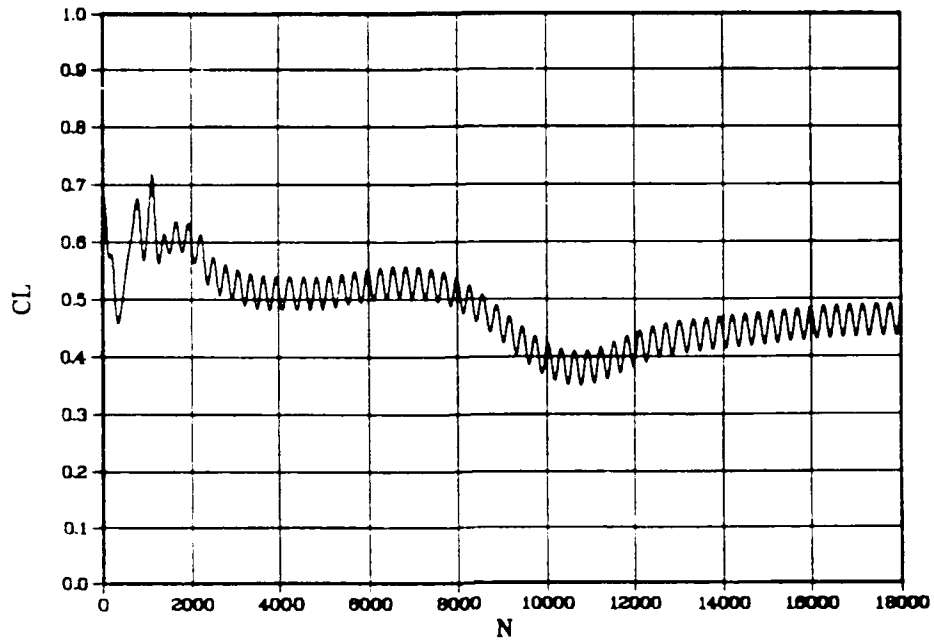


Figure 30. Force Coefficients vs Iterations, Number 10
 ($C_v=10$, $\delta=45^\circ$, $\alpha=0^\circ$)

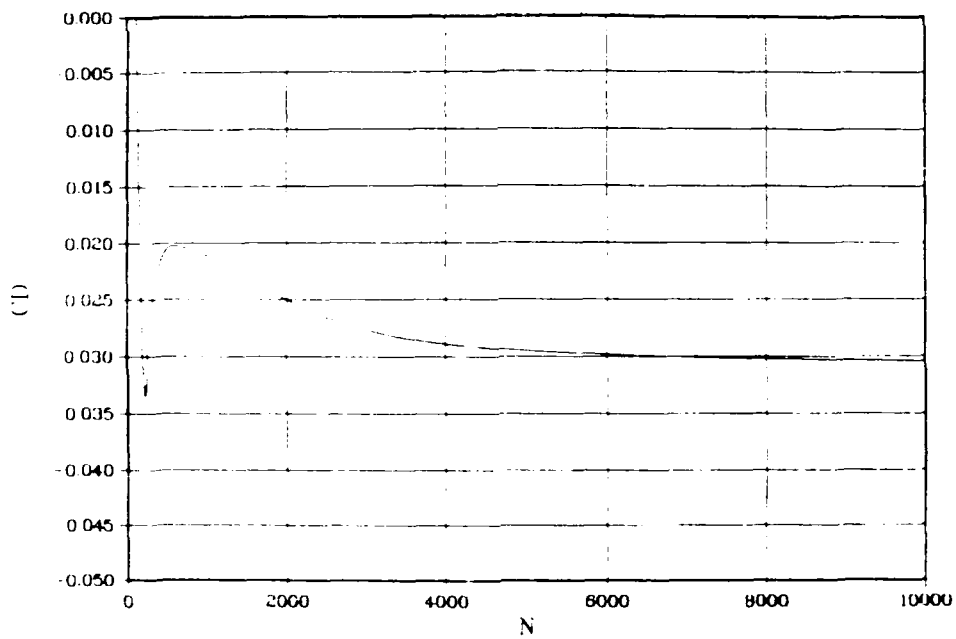
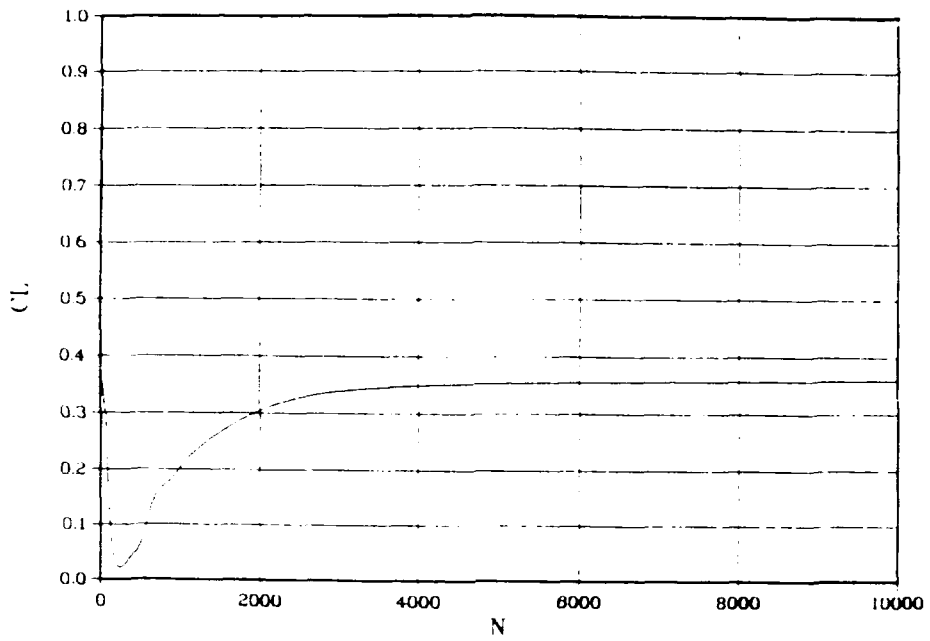


Figure 31. Force Coefficients vs Iterations, Number 11
 (Cv=1.0, $\delta=15^\circ$, $\alpha=0^\circ$)

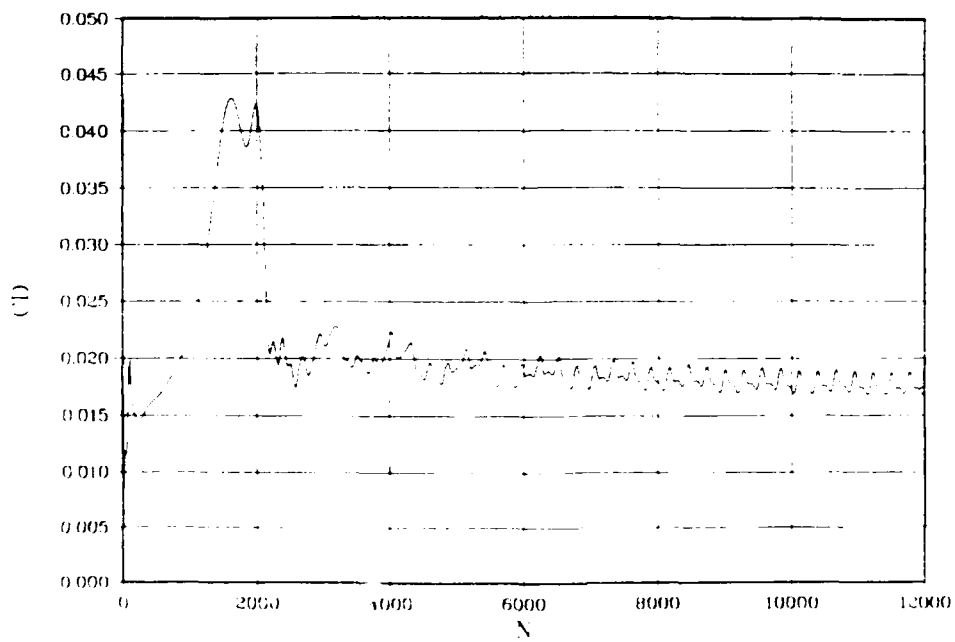
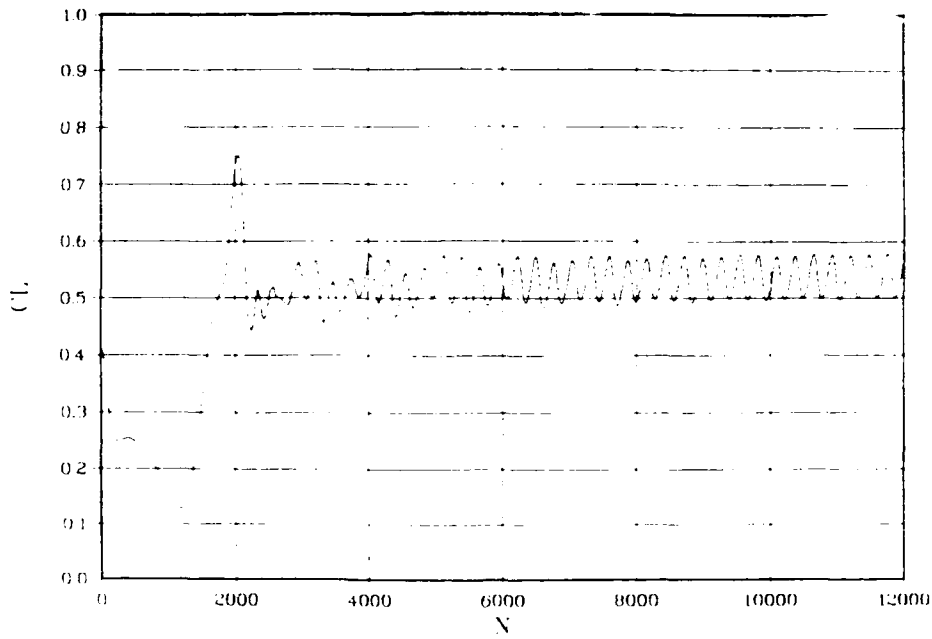


Figure 32. Force Coefficients vs Iterations, Number 14
 ($C_v=0.05$, $\delta=45^\circ$, $\alpha=2^\circ$)

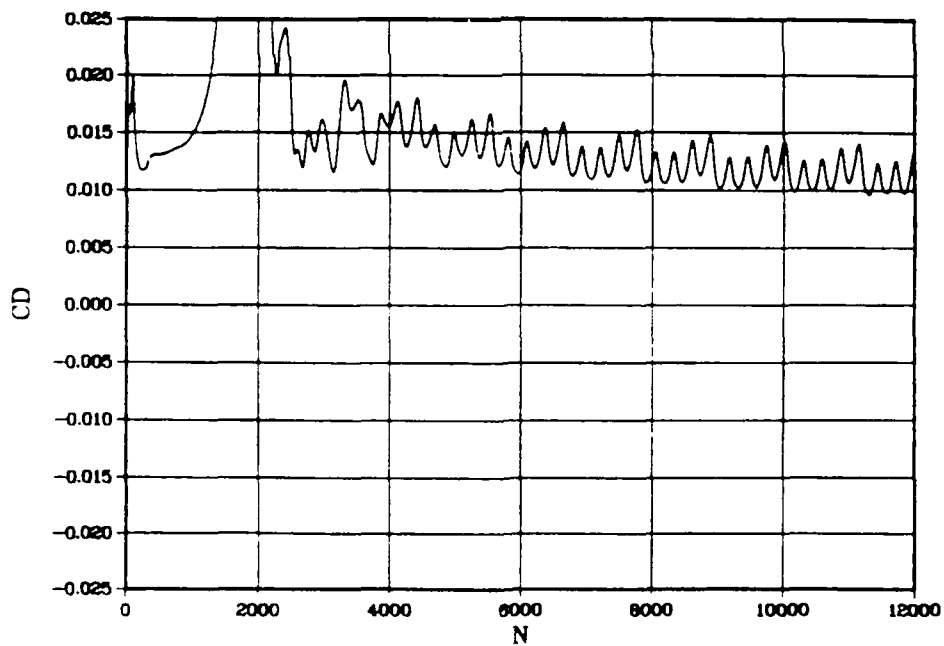
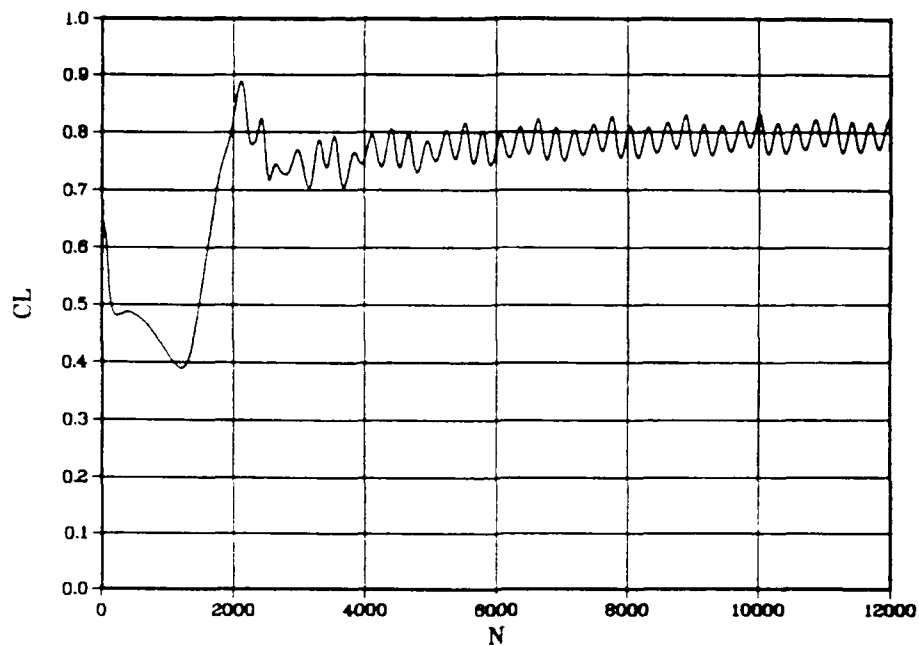


Figure 33. Force Coefficients vs Iterations, Number 17
 ($C_v = .05$, $\delta = 45^\circ$, $\alpha = 4^\circ$)

Upon close inspection, small harmonics or secondary waves riding on the dominant wave can be seen, especially in the C_d plots. This is probably due to the interaction of the shedding vortices as mentioned above. Except at angle of attack, these harmonics are too small to affect the convergence criterion used. At angle of attack the harmonics are more pronounced. For Number 14, Figure 32, a set of four distinct oscillations with the same frequency formed early and later converged to a single oscillation. At four degrees, Number 17 (Figure 33), a similar quartet persisted and became periodic. This is true for both C_l and C_d . This behavior is probably due to a more complex interaction of the shedding vortices induced by the angle of attack. A Fourier analysis could provide more information on the interactions but it is beyond the scope of this report.

The Effect of Varying Suction Rate

In this study three different suction, C_v , cases were studied, at 1%, 5% and 10% of free stream velocity. For purpose of comparison all three cases were run at an ejection angle of 90° . The ejection velocities were almost twice that for suction as a result of a 2:1 area ratio. The C_l vs C_v plot, Figure 34, indicates the expected result that increasing suction velocities and

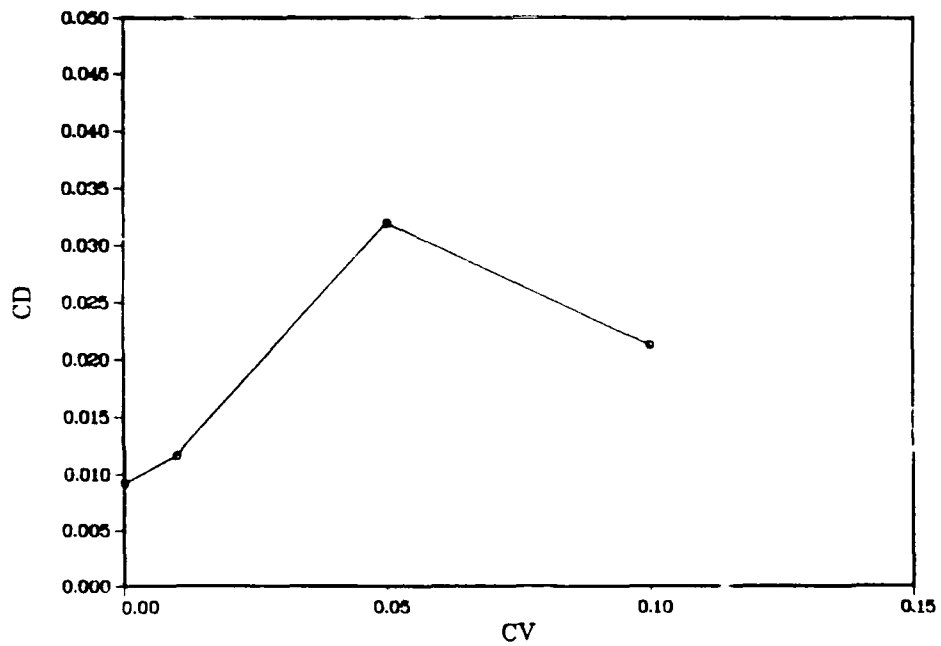
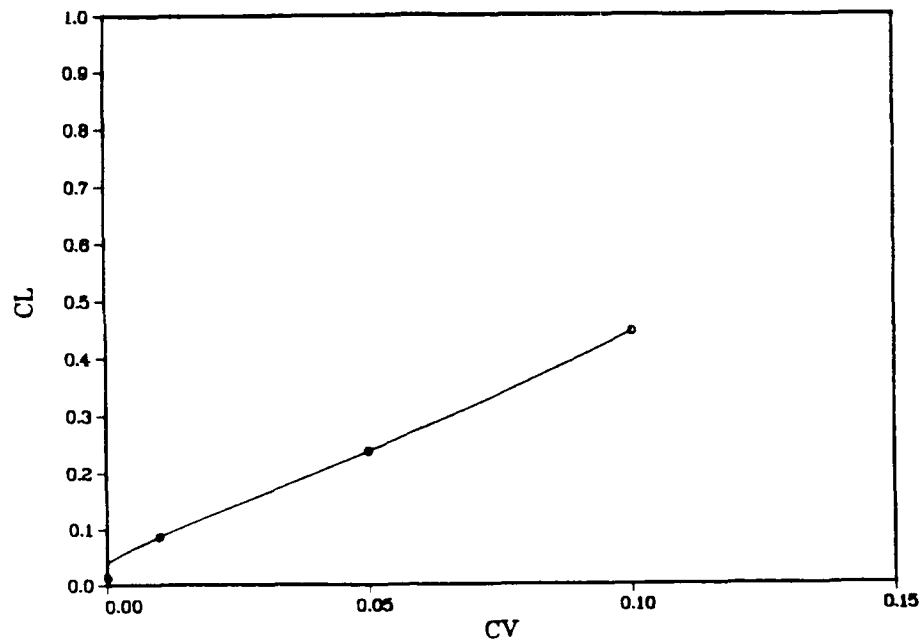


Figure 34. Force Coefficients vs Suction Velocity
 ($\delta=90^\circ$, $\alpha=0^\circ$)

corresponding increasing ejection velocities produce a near linear increase in lift. The surprising results in the C_d plot, Figure 34, suggests that there is a maximum drag produced near C_v equal 5%. C_v increasing beyond this critical value reduces drag. More points are need to draw firm conclusions concerning this particular behavior.

The normal (90°) blowing produced no induced drag due to mass flux at the ejection surface and minimal shear drag on the suction surface. The mass flux component of lift is almost negligible due to the small values of C_v as is demonstrated by an approximation to the momentum flux

$$\text{Lift} \cong \dot{m} \cdot \bar{V} \hat{j} = -\rho A (\bar{V} \cdot \bar{V} \hat{j}) = (\rho A V^2)_{\text{lower}} - (\rho A V^2)_{\text{upper}} \quad (92)$$

$$C_l = \frac{2L}{\rho_\infty V_\infty^2} = 2L \quad , \quad v_{\text{lower}} \cong C_v \quad , \quad v_{\text{upper}} \cong 1.82C_v \quad (93)$$

For $C_v = 0.1$, $\rho \cong 1$ and $A = 0.25$ and 0.125 , $C_l = 0.0012$ a very small value.

The lift and drag behavior can be directly related to the pressure distribution forward of the fan as the lift coefficients in Table 9 and the C_p surface distribution in Figure 35 indicate.

The biggest surprise is that varying the suction rate does not affect the pressure distribution on the lower surface nearly as much as on the upper surface. Since the

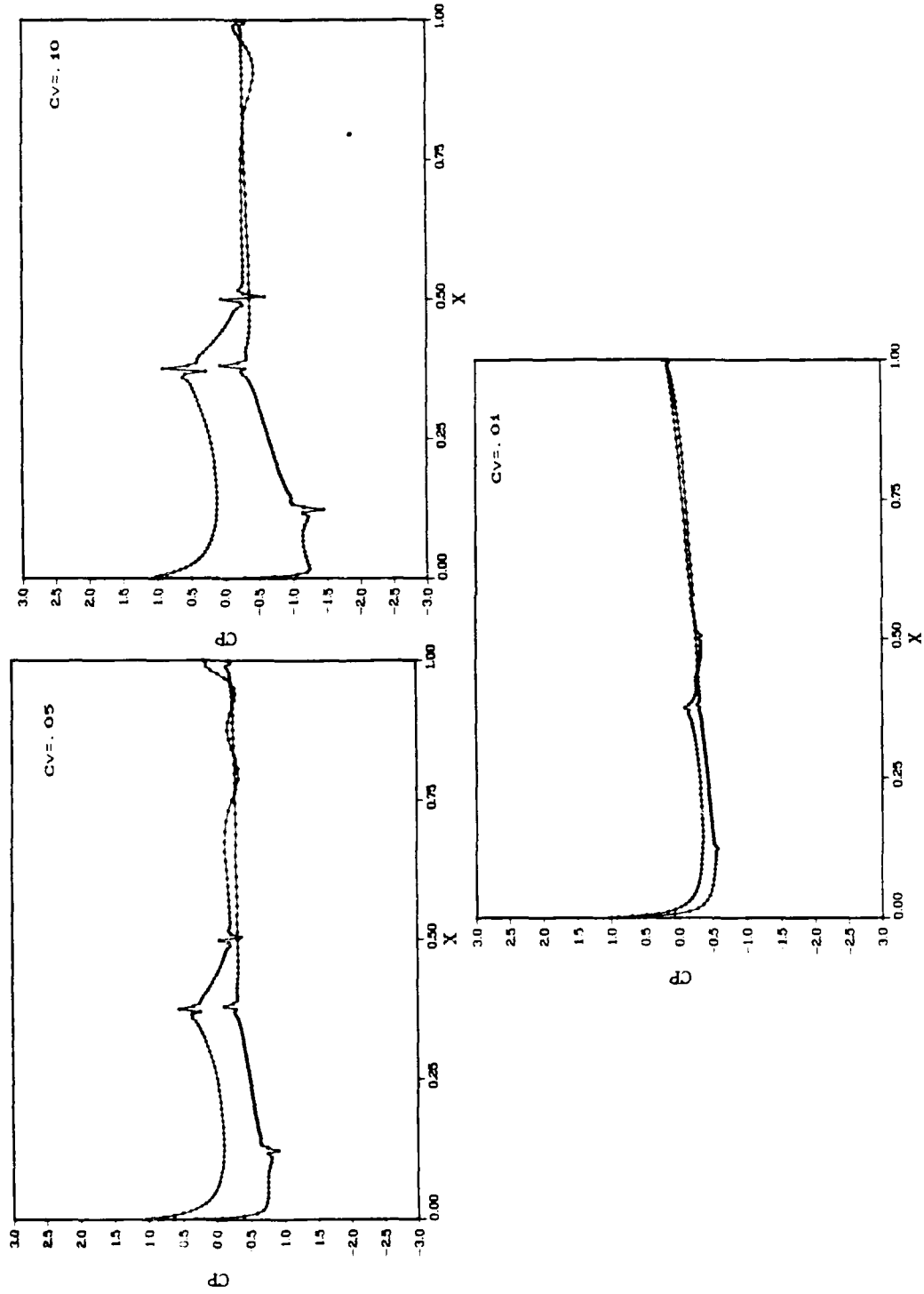


Figure 35. Comparisons of Cp for Different Suction Velocities ($\delta=90^\circ$, $\alpha=0^\circ$)

Number	Cl total	Cl press	Cl viscous	Cl mass
5	.08445	.08456	-.00016	.00004
6	.31719	.31599	.00011	.00108
9	.48454	.47984	.00036	.00434
	Cd total	Cd press	Cd viscous	Cd mass
5	.01223	.00190	.01033	.00000
6	.03232	.01629	.01599	.00004
9	.02992	.00578	.01797	.00016

Table 9. Cl and Cd Component Comparison vs Suction Velocity

negative pressure coefficient on the upper surface exerts a force normal to the surface and the greatest changes near the leading edge where the surface area has the largest vertical component (y) component. This trend can be verified. The following equation approximates pressure drag and lift (see appendix D)

$$P_{lift} \cong \sum P_v dy, \quad P_{drag} \cong \sum P_i dx \quad (94)$$

If the above equations are applied to the C_p curves the lift coefficients in Table 9 can be obtained. The mechanism creating these pressure differences in the C_p curves can not be easily explained. On the other hand The viscous drag is directly related to the suction velocity as is evident in the c_f surface plots of Figure 36. The larger the suction the greater the drag over the suction region. Here again it is the pressure distribution which influences the total drag.

Some mechanism relating the ejection velocity to

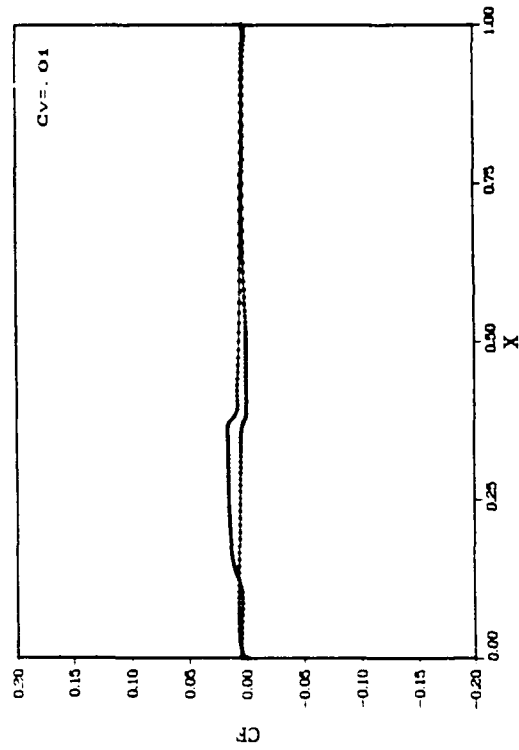
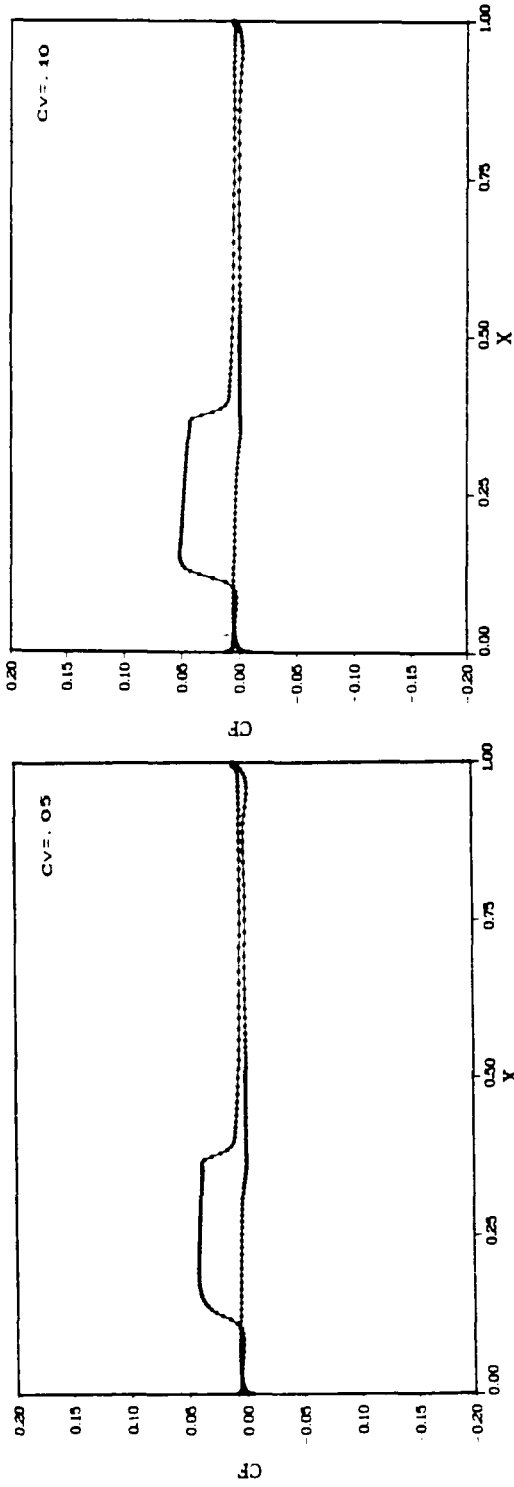


Figure 36. Comparisons of C_f for Different Suction Velocities
 ($\delta=90^\circ$, $\alpha=0^\circ$)

pressure distribution must account for this; but it is not the vortex shedding. Figure 37 compares the C_p plots for different points in the lift curve, Figure 25, for Number 6. The corresponding streamlines and vorticity contours were discussed earlier, see Figures 21 and 22. A comparison indicates that vortex shedding has no discernible effect on the pressure on the forward section of the airfoil. The amplitudes in the lift curve can be accounted for in the region near the trailing edge. The C_p differences near the trailing edge are not nearly as large as at the leading edge and the mean value seems to be near zero.

The streamline and vorticity contours demonstrate the period of the oscillations very well. The streamlines do not depict the shear layer in the ejection wake but do reveal the vortex at the trailing edge and the oscillations in the airfoil wake.

The vorticity contours reveal the shear layer by many small vortex cells. The maximum lift corresponds to a well formed vortex at the tail and the location of the wake at a minimum point below the cord. As the vortex breaks down the lift drops to a minimum and no tail vortex is present. As the vortex reforms the lift begins to climb again and the wake moves to a maximum point above the cord. The drag behavior is similar except that it is slightly out of phase, but with the same period.

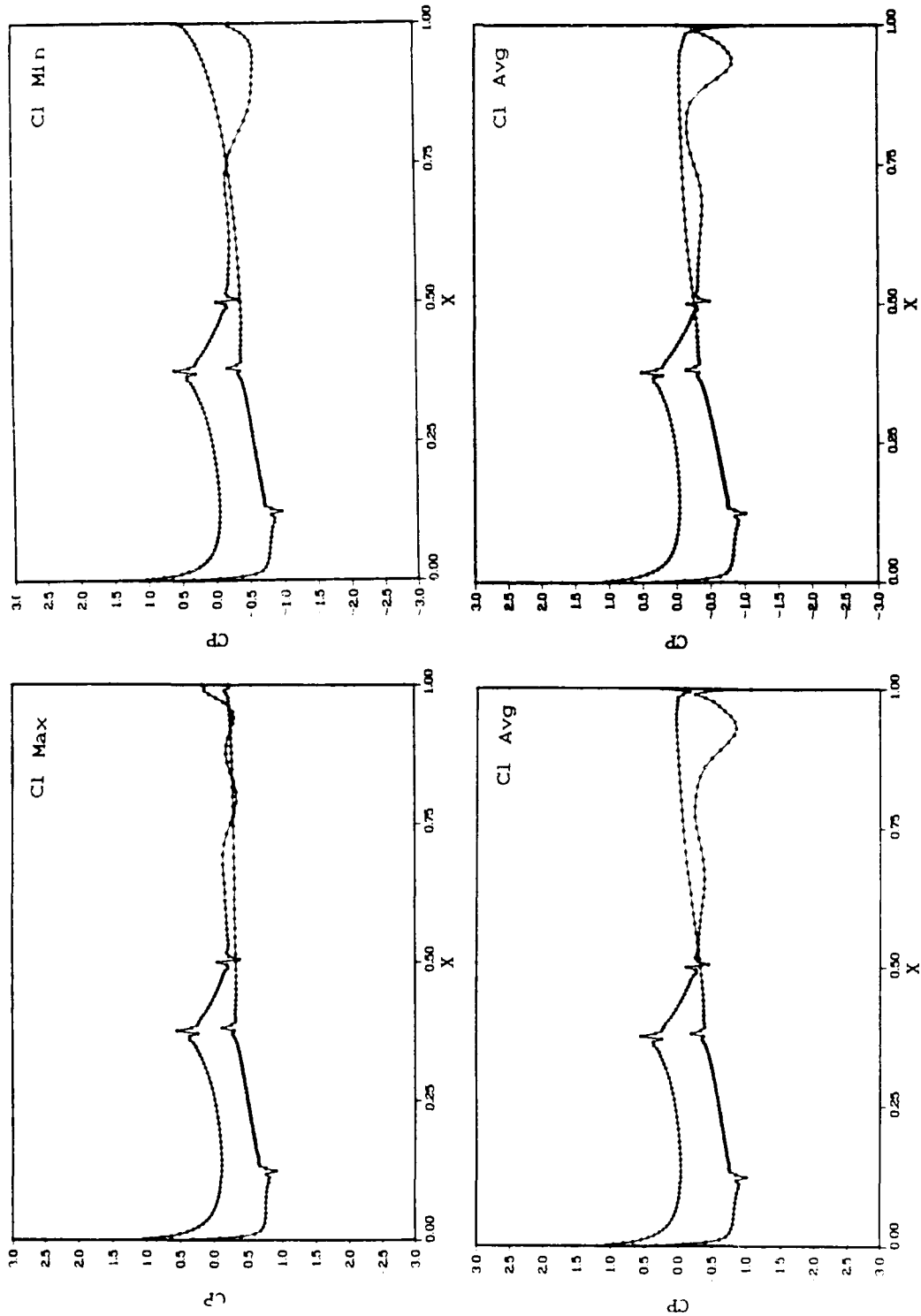


Figure 37. Cp Comparisons for Ore Period in Cl ($C_v=0.05$, $\delta=90^\circ$)

The streamline and vorticity comparison in Figure 38 demonstrate that Number 9, $C_v = 0.1$, has the strongest vortex and the broadest shear layer. Figure 38 also indicates that for $C_v = 0.01$ that there is no trailing edge vortex and a very thin shear layer. It is evident that the greater the suction velocity the greater the disturbance at the blowing surface which creates stronger ejection vortices and a wider shear layer. This broad shear layer may act as a buffer on the rear body and decrease the shedding effects. This could account for the decreasing trend in amplitude with increasing suction velocity shown in the C_l and C_d plots.

The Effect of Varying Ejection Angle

For this portion of the study, suction rates of 5 and 10 percent were compared at ejection angles of 90, 45 and 15 degrees. The C_l and C_d vs δ curves in Figure 39 indicate different behavior for the two suction rates. For $C_v = 0.1$ the trend is an increase in both lift and drag. For $C_v = 0.05$ the trend in lift is reversed. The drag can be explained by examining the mass flux component of lift, Table 10. At any ejection angle the normal component of velocity v does not change; it must satisfy the constant mass flow condition

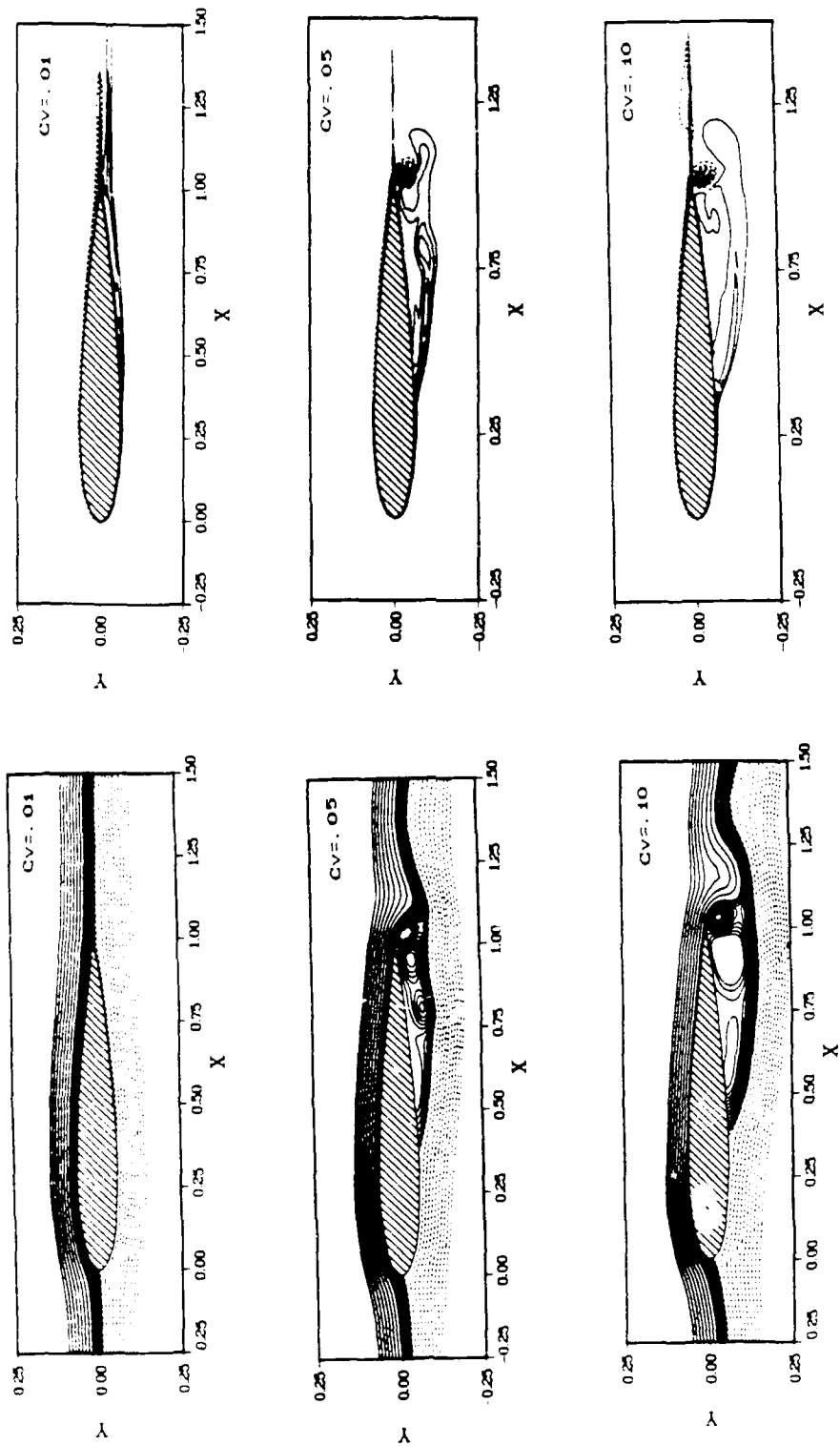


Figure 38. Streamline and Vorticity Comparisons for Different Suction Velocities ($\delta=90^\circ$, $\alpha=0^\circ$)

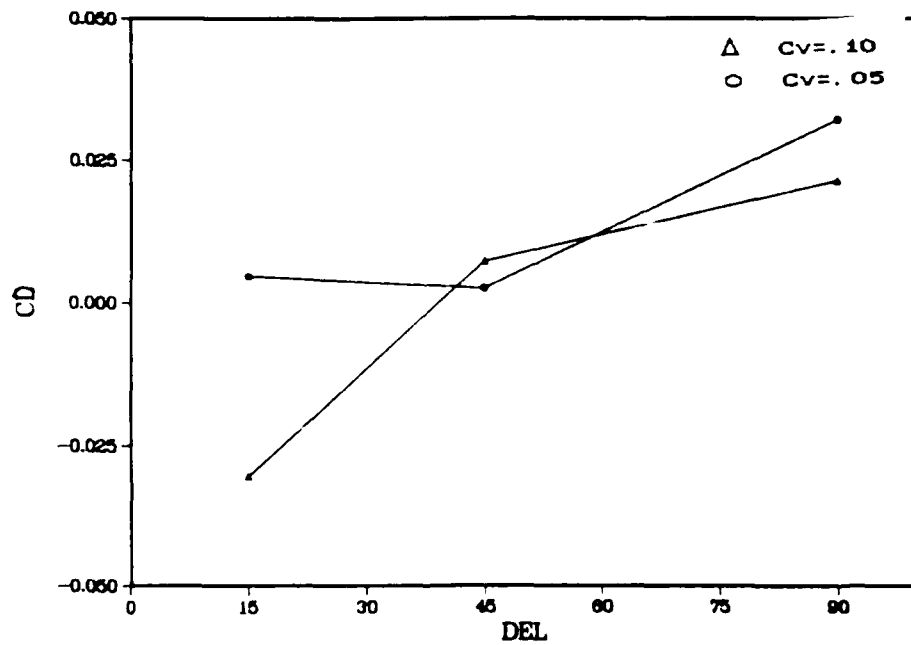
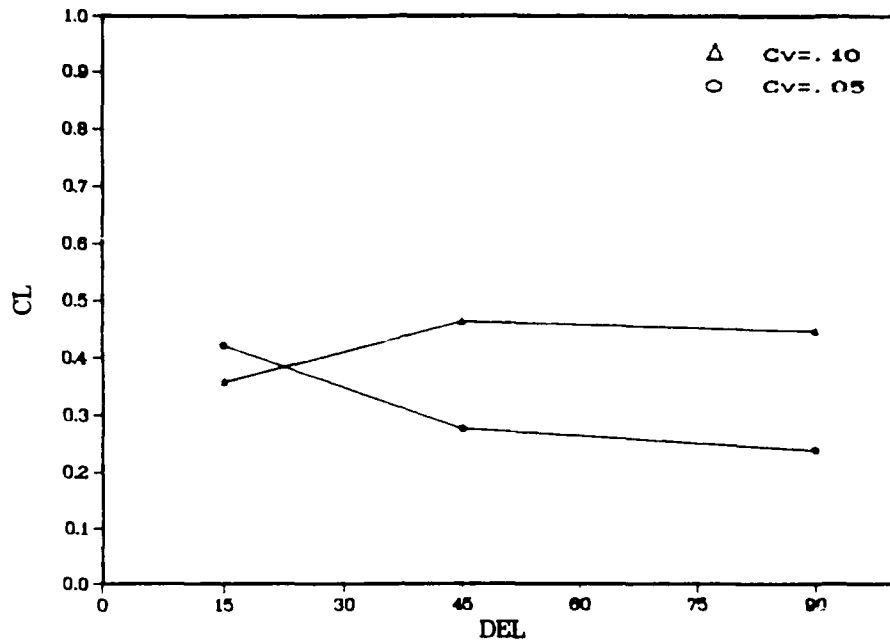


Figure 39. Force Coefficients vs Ejection Angle
 ($Cv = .05$, $\alpha = 0^\circ$)

Number	Cl total	Cl press	Cl viscous	Cl mass
6	.31719	.31599	.00011	.00108
7	.29903	.29773	.00012	.00119
8	.41154	.40985	.00020	.00620
9	.48454	.47984	.00036	.00434
10	.43543	.43027	.00037	.00479
11	.35953	.35320	.00029	.00605

code	Cd total	Cd press	Cd viscous	Cd mass
6	.03232	.01629	.01599	.00004
7	.02675	.01320	.01595	-.00240
8	.00620	.00003	.01638	-.01020
9	.02392	.00578	.01797	.00016
10	.00889	.00048	.01809	-.00967
11	-.07989	-.00056	.01810	-.04128

Table 10. Cl and Cd Component Comparison vs Ejection Angle

$$\dot{m}_{in} = \dot{m}_{out} = \rho AV_{normal} \quad (95)$$

Where A is the surface area of the airfoil and does not change with ejection angle and V_{normal} is equal to v ; therefore the mass flux component to lift does not change. Drag behaves differently. The velocity u is equal to $v/\tan(\delta)$ which is approximately $2CvCr/\tan(\delta)$ and for 45° approximately $1.8Cv$ and for 15° approximately $6.78Cv$. As δ goes to zero u would go to infinity.

$$C_d = 2 \text{ drag} \cong -2 \dot{m} \cdot \bar{V} \hat{i} = -2 \rho A \left(\frac{v^2}{\tan^2 \delta} \right) \quad (96)$$

The approximate calculations are listed in Table 11.

c_v	δ	c_d
.05	90	-0.0000
.05	45	-0.0011
.05	15	-0.0042
.10	90	-0.0000
.10	45	-0.0001
.10	15	-0.0334

Table 11. C_d Calculations for Surface Blowing
 ($A = .125$, $\rho = 1.1$ and $v = 2 C_v/C_r$, $C_r = 1.1$)

This explains the decrease in drag vs δ but does not account for the lift behavior.

As with the effect of varying suction velocities the lift comes mostly from the leading edge pressure differences. The influence of this pressure by changing the ejection angle can not be determined without more data.

The streamline and vortex plots are presented in Figures 40 and 41 for comparison. The vortex patterns at 90° are discussed above. As shown in Figures 40 and 41 the trend at 45° is a smaller and weaker vortex structures which accounts for the reduced amplitude in the C_l and C_d curves. The shear layer is also much smaller with a higher energy imparted by the u component of the ejection. These two reasons account for the smaller frequencies seen in the same curves. The smaller higher energy shear layer is closer to the body and prevents the build up of a strong trailing edge vortex. The smaller trailing edge vortices then must shed at a quicker rate than the ones at 90° where time was required for them to build in strength.

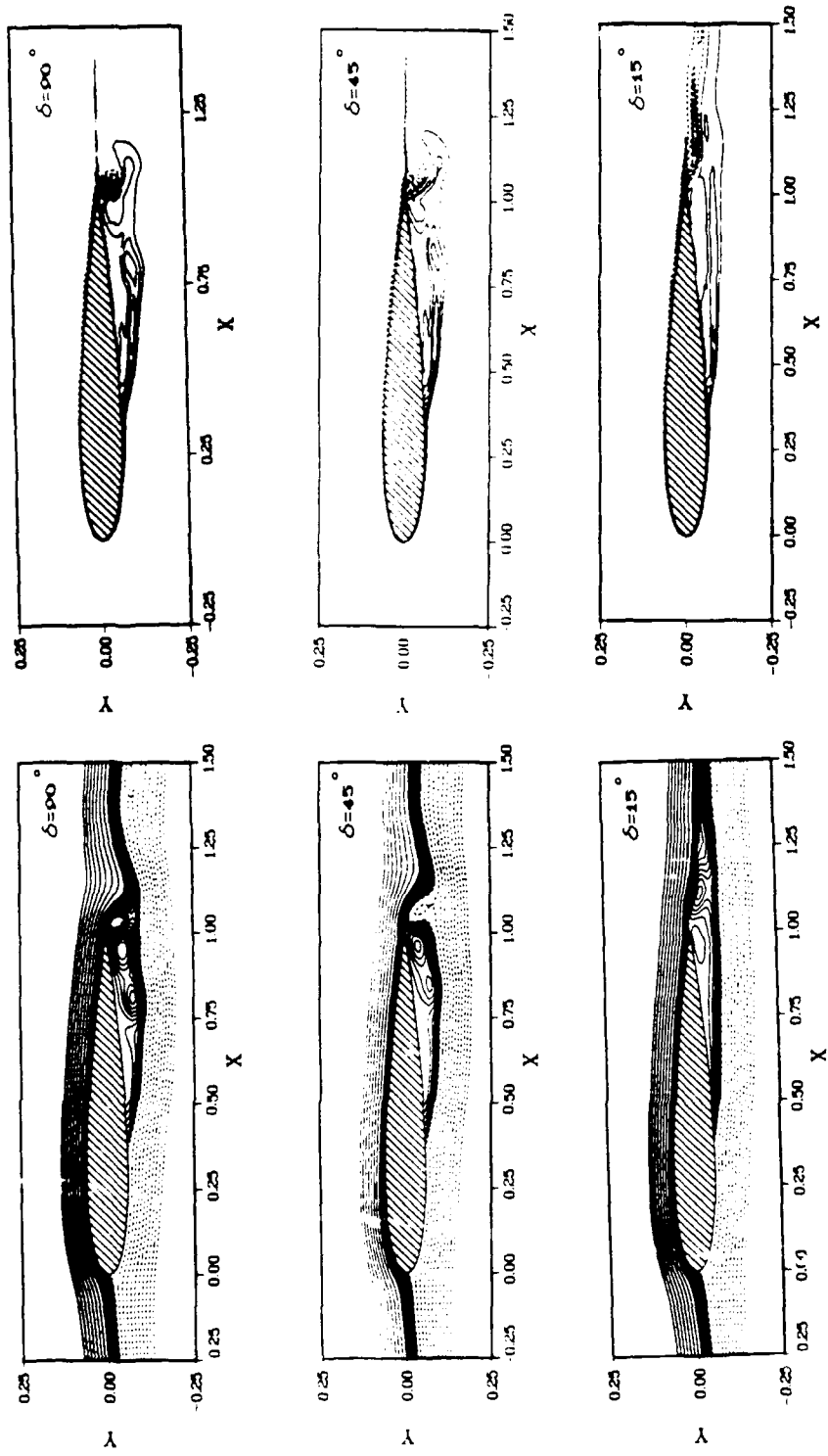


Figure 40. Streamline and Vorticity Comparisons for Different Ejection Angles ($C_v = .05$, $\alpha = 0^\circ$)

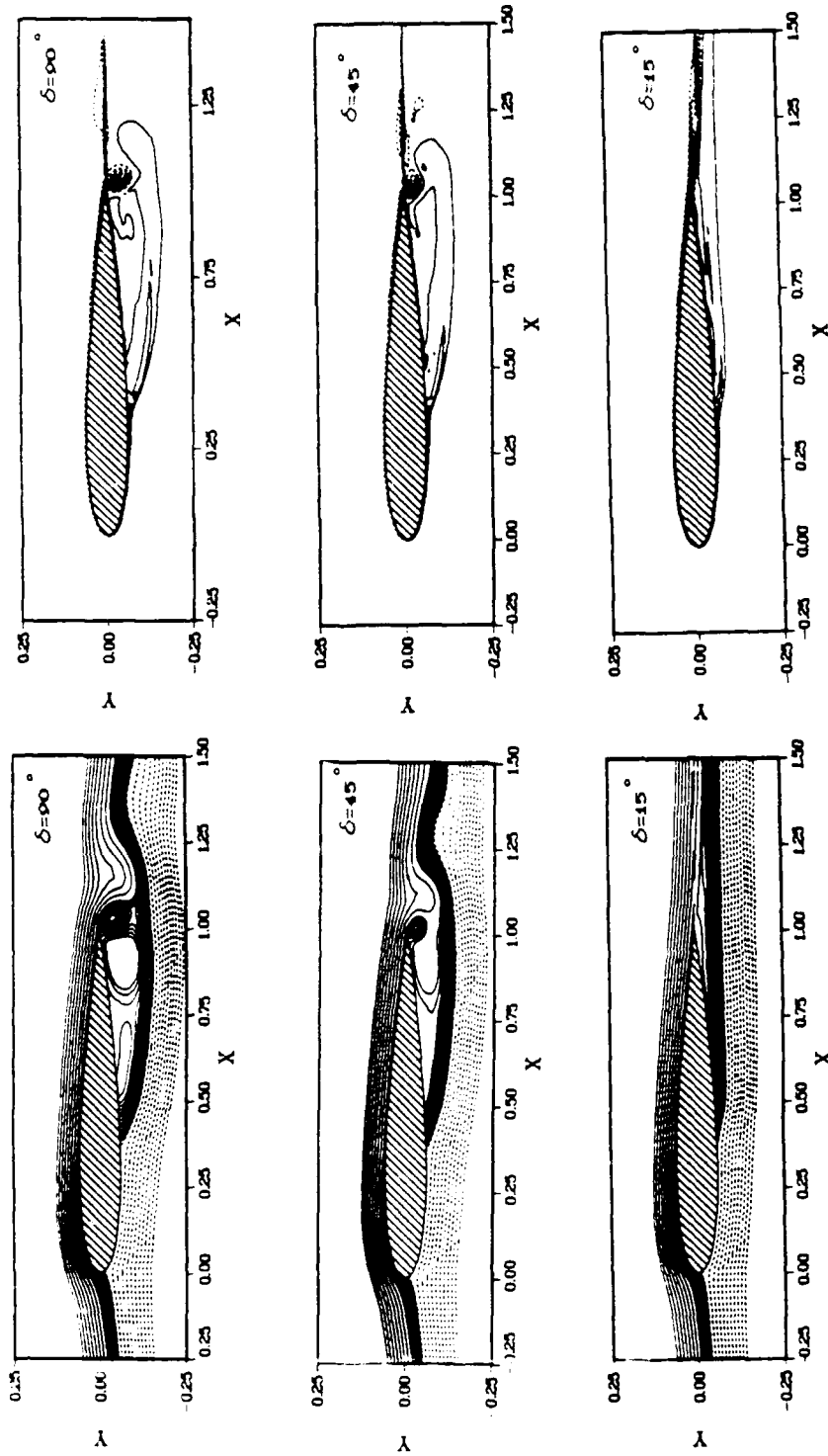


Figure 41. Streamline and Vorticity Comparisons for Different Ejection Angles ($C_v=0.10$, $\alpha=0^\circ$)

At 15° the trend is even more pronounced. For $C_v = 0.1$ A trailing edge vortex was prevented from forming as shown in Figure 41.

The Effect of varying Angle of Attack

The most interesting results were obtained by varying the angle of attack. The C_l and C_d vs α curves are given by Figure 42. The lift curve shows the expected behavior. A delta C_l above that of a clean airfoil and constant with respect to α . Here again the major contributor to lift is the pressure distribution around the leading edge, see Figure 43 and Table 12. The drag curve behavior is unexpected. The trend for increasing α is a decrease in drag almost to the level of a clean airfoil. This behavior is unusual and cannot be explained by thrust due to mass flux. As α goes up the thrust component actually goes down because the direction is increasing the ejection angle by α . This is in agreement with the data in Table 12. Also from this figure the viscous components of drag are nearly constant; it is the contribution of pressure drag that is exhibiting the unusual behavior. At 4° angle of attack the pressure drag is acting as a thrust component. The mechanism causing this behavior is not known. The C_l vs C_d curve, Figure 44 is instructive. The fan curve retains the

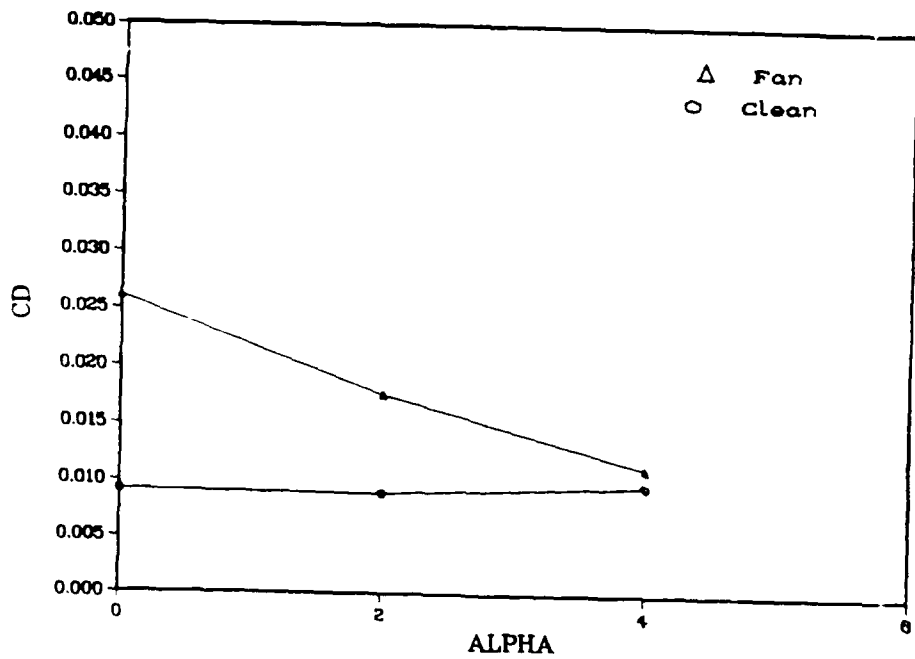
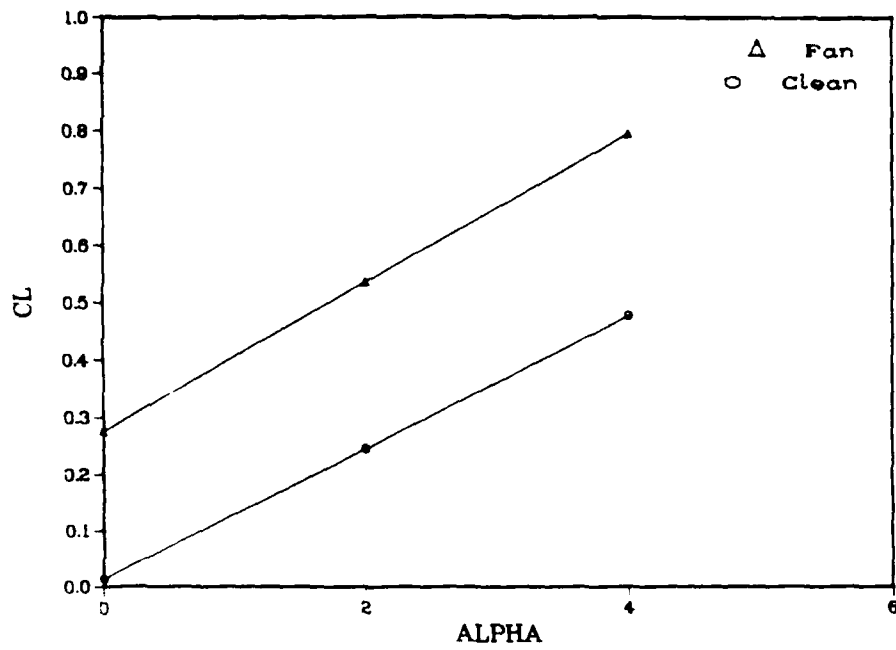


Figure 42. Force Coefficients vs Angle of Attack
($C_v = .05$, $\delta = 45^\circ$)

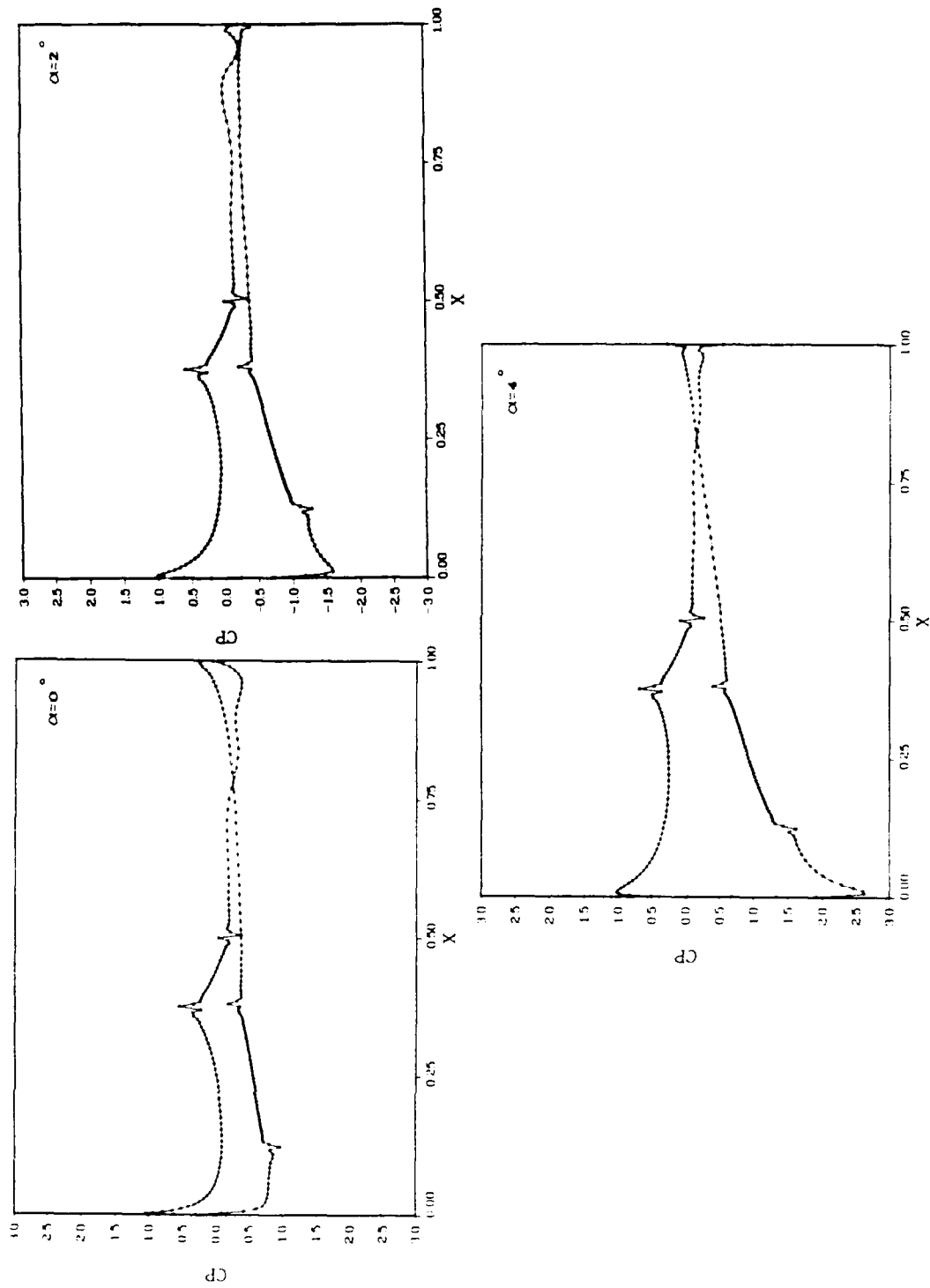


Figure 43. Comparisons of C_p for Different Angles of Attack
 ($CV = .05, \delta = 45^\circ$)

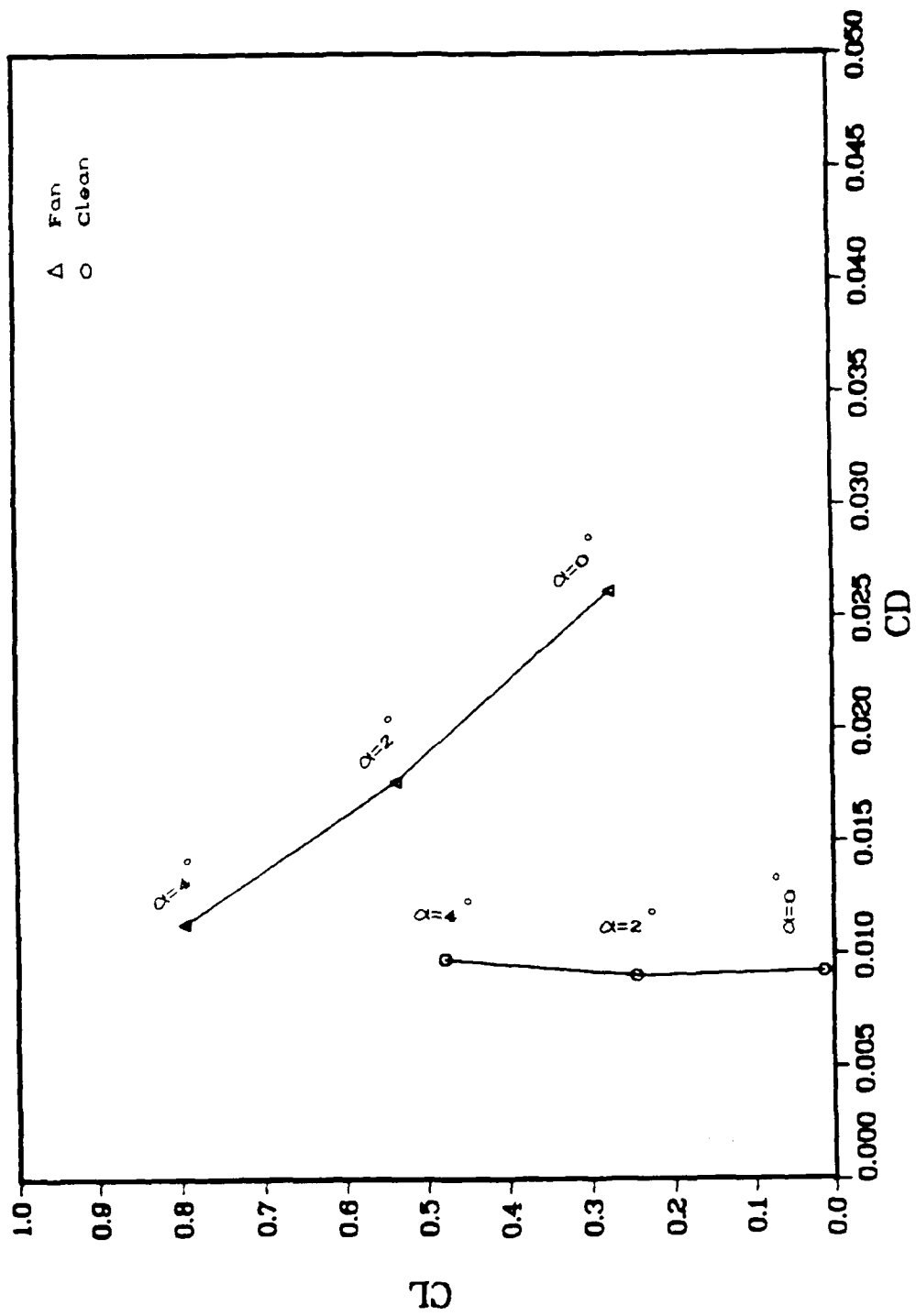


Figure 44. C_l vs C_d for Angle of Attack ($C_v = 0.05$, $\delta = 45^\circ$)

Number	Cl total	Cl press	Cl viscous	Cl mass
2	.01307	.01321	-.00014	.00000
13	.24582	.24601	-.00018	.00000
16	.47828	.47849	-.00021	.00000
7	.29903	.29773	.0012	.00119
14	.56600	.56494	-.00021	.00126
17	.82326	.82255	-.00062	.00133
code	Cd total	Cd press	Cd viscous	Cd mass
2	.00954	.00164	.00790	.00000
13	.00951	.00196	.00755	.00000
16	.01020	.00831	.00698	.00000
7	.02675	.01320	.01595	-.00240
14	.01763	.00845	.01652	-.00234
17	.01983	-.00049	.01653	-.00227

Table 12. Cl and Cd component comparison vs α

general shape of the clean airfoil but is rotated and shifted up. The lift and drag oscillations contain strong harmonics as discussed above (Figures 32 and 33). At four degrees this is especially pronounced. As shown in Figure 45 the vortex pattern of shedding seems to be only mildly affected by the normal component of the free stream velocity, and the thickness of the shear layer above the surface is reduced by a small amount with increasing angle of attack. The streamlines in Figure 45 indicate the stagnation point at the leading edge is also affected by a small amount.

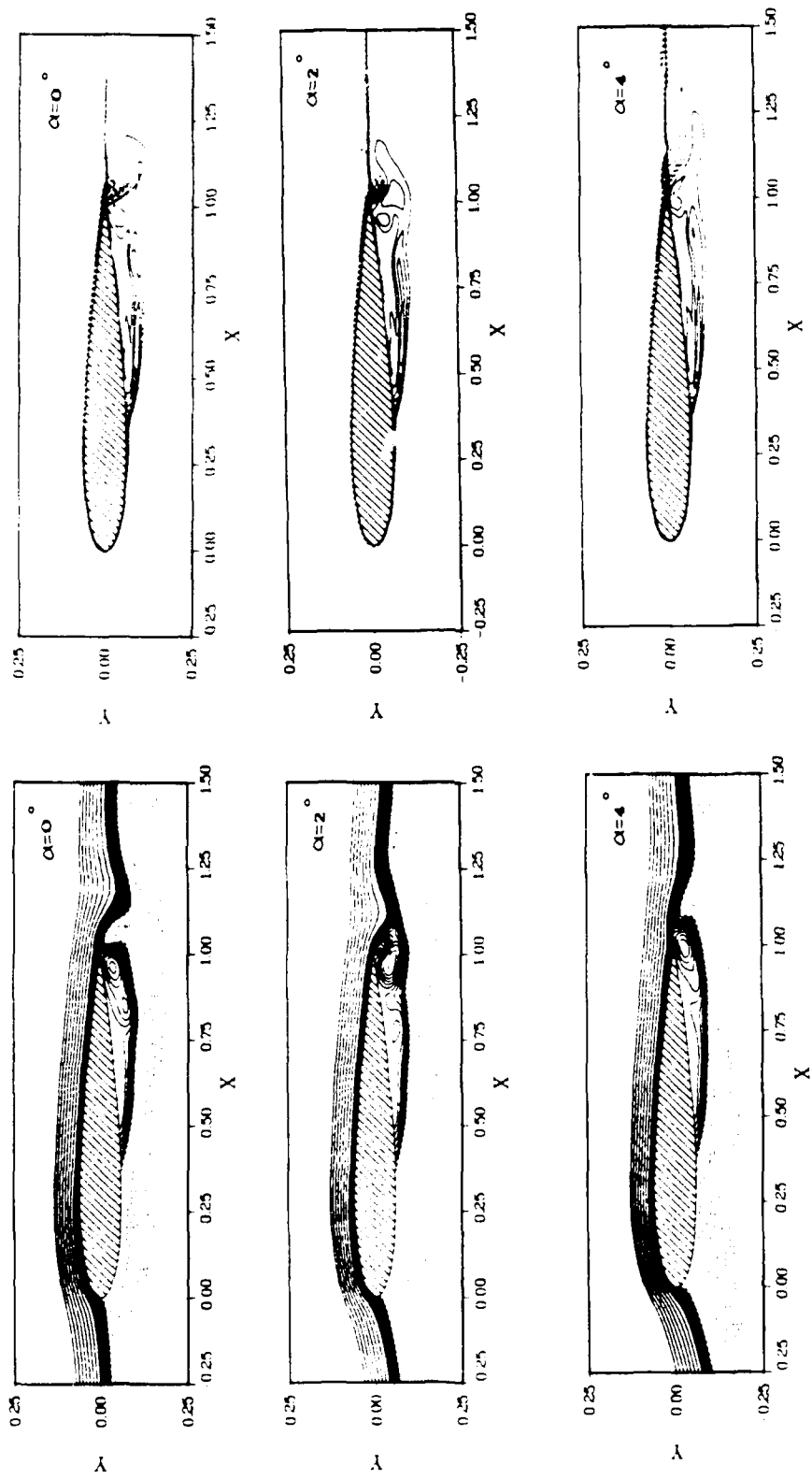


Figure 45. Streamline and Vorticity Comparisons for Different Angles of Attack ($C_v = 0.05$, $\delta = 45^\circ$)

V Conclusions and Recommendations

The solutions obtained using the implicit compressible Navier-Stokes equations compared favorably with both experimental and other numerical results. For lack of verifying data such comparisons could not be made with solutions obtained from the model with mass flux. However, based on the codes performance the solutions should give a fair approximation to the physical problem.

The results indicate that a fan type device imbedded in an airfoil can produce favorable aerodynamic effects, improved lift performance with minor drag penalties. The best lift performance was achieved at an angle of attack of four degrees. The best drag performance was achieved with ejection angles of 15 degrees where thrust was produced.

Because the model only represented one possible configuration out of a multitude the results simply indicate trends in the "fan-in-wing" behavior. Many more tests both experimental and numerical are needed before firm conclusions can be drawn. At best the fan-like device tested indicates interesting and unusual behavior with possible applications to V/STOL technology.

Experimental tests should be performed to confirm this behavior. Emphasis should be given to high angles of attack in order to determine the maximum C_l and the

airfoil stall effects for a fan-like device.

Appendix A: Non-Dimensional Variables (2:191-193)

The variables used in the Navier-Stokes equations can be written in a non-dimensional form by dividing by L as the length scale, the free stream velocity U_∞ as the velocity scale and ρ_∞ as the mass scale. All other units can be expressed in terms of the three scalar factors, except viscosity and heat. The non-dimensional relationships are as follows (an * represents a non-dimensional quantity)

$$\begin{aligned}x^* &= \frac{x}{L} \quad , \quad y^* = \frac{y}{L} \quad , \quad u^* = \frac{u}{U_\infty} \quad , \quad v^* = \frac{v}{U_\infty} \\T^* &= \frac{T}{T_\infty} \quad , \quad \rho^* = \frac{\rho}{\rho_\infty} \quad , \quad P^* = \frac{P}{\rho_\infty U_\infty^2} \quad , \quad e^* = \frac{e}{U_\infty^2} \\Et^* &= \frac{Et}{\rho_\infty U_\infty^2} \quad , \quad \mu^* = \frac{\mu}{\mu_\infty} \quad , \quad \varepsilon^* = \frac{\varepsilon}{\mu_\infty} \quad , \quad q^* = \frac{q}{q_\infty} \\t^* &= \frac{tU_\infty}{L} \quad , \quad L^* = \frac{L}{L} = 1\end{aligned}\tag{A-1}$$

and the non-dimensional Reynolds number is defined as

$$Re = \frac{\rho_\infty U_\infty L}{\mu_\infty}\tag{A-2}$$

The temperature, pressure, and energy equations can be expressed in terms of the Mach number

$$M_{\infty} = \frac{U_{\infty}}{a_{\infty}} \quad (\text{A-3})$$

where a is the local speed of sound

$$a_{\infty} = \sqrt{\gamma R T_{\infty}} \quad (\text{A-4})$$

pressure can be written using the equation of state

$$P = \rho R T \quad (\text{A-5})$$

$$P^* = \frac{P}{\rho_{\infty} U_{\infty}^2} = \frac{P}{\rho_{\infty} U_{\infty}^2 \frac{\gamma R T_{\infty}}{a_{\infty}^2}} = \frac{P}{P_{\infty} \gamma M_{\infty}^2} \quad (\text{A-6})$$

Temperature and energy can be modified in the same way

$$T^* = \frac{T}{T_{\infty}} = \frac{\frac{P}{\rho R}}{\frac{P_{\infty}}{\rho_{\infty} R}} = \frac{\rho_{\infty} P}{\rho P_{\infty}} = \frac{P^* \gamma M_{\infty}^2}{\rho^*} \quad (\text{A-7})$$

$$E_t^* = \frac{E_t}{\rho_{\infty} U_{\infty}^2} = \frac{E_t}{P_{\infty} \gamma M_{\infty}^2} \quad (\text{A-8})$$

$$e^* = \frac{Et}{\rho U_\infty} = \frac{Et}{\rho \gamma RT_\infty M_\infty^2} = \frac{Et}{\rho \gamma P_\infty M_\infty^2} = \frac{Et^*}{\rho^*} \quad (A-9)$$

An example of how the NS equations are non-dimensionalized is demonstrated on the continuity equation below

$$\frac{\partial \rho^*}{\partial t^*} + \frac{\partial(\rho^* u^*)}{\partial x^*} + \frac{\partial(\rho^* v^*)}{\partial y^*} = 0 \quad (A-10)$$

$$\frac{\partial \left(\frac{\rho}{\rho_\infty} \right)}{\partial \left(\frac{t U_\infty}{L} \right)} + \frac{\partial \left(\frac{\rho u}{\rho_\infty U_\infty} \right)}{\partial \left(\frac{x}{L} \right)} + \frac{\partial \left(\frac{\rho v}{\rho_\infty U_\infty} \right)}{\partial \left(\frac{y}{L} \right)} = 0 \quad (A-11)$$

The constants can come out of the derivatives and divide through leaving

$$\frac{\partial \rho}{\partial t} + \frac{\partial(\rho u)}{\partial x} + \frac{\partial(\rho v)}{\partial y} = 0 \quad (A-12)$$

In the momentum and energy equations the constants do not divide out. They form the Reynolds number presented above.

Appendix B: Jacobian Matrices for the Navier-Stokes

Equations (35:45-46)

The Jacobian matrices presented in equations (72-73) are defined below. They are obtained by differentiating the vectors E_1 , E_2 , V_1 and W_2 defined in equations (49-52)

(B-1)

$$A = \begin{bmatrix} 0 & \xi_x & \xi_y & 0 \\ \xi_x \phi - uu & u - (\gamma-2)\xi_x u & \xi_y u - (\gamma-1)\xi_x v & (\gamma-1)\xi_x \\ \xi_y \phi - vu & \xi_x v - (\gamma-1)\xi_y u & u - (\gamma-2)\xi_y v & (\gamma-1)\xi_y \\ (2\phi - \gamma e)u & (\gamma e - \phi)\xi_x - (\gamma-1)uu & (\gamma e - \phi)\xi_y - (\gamma-1)vu & \gamma u \end{bmatrix}$$

(B-2)

$$B = \begin{bmatrix} 0 & \eta_x & \eta_y & 0 \\ \eta_x \phi - uv & v - (\gamma-2)\eta_x u & \eta_y u - (\gamma-1)\eta_x v & (\gamma-1)\eta_x \\ \eta_y \phi - vu & \eta_x v - (\gamma-1)\eta_y u & v - (\gamma-2)\eta_y v & (\gamma-1)\eta_y \\ (2\phi - \gamma e)v & (\gamma e - \phi)\eta_x - (\gamma-1)uv & (\gamma e - \phi)\eta_y - (\gamma-1)vu & \gamma v \end{bmatrix}$$

where

$$\phi = 1/2 (\gamma-1) (u^2 + v^2) \quad (B-3)$$

and the Jacobian Matrix M and N are defined by

(B-4)

$$M = \frac{1}{\rho} \begin{bmatrix} 0 & 0 & 0 & 0 \\ -(b_1 u + b_2 v) & b_1 & b_2 & 0 \\ -(b_2 u + b_3 v) & b_2 & b_3 & 0 \\ -(b_1^2 + 2b_2 uv + b_3 v^2) & b_1 - b_4 \gamma (\gamma - 1) u & b_2 u + b_3 & b_4 \gamma (\gamma - 1) \\ +b_4 \gamma (\gamma - 1) (u^2 + v^2 - e) & +b_2 v & -b_4 \gamma (\gamma - 1) & \end{bmatrix}$$

(B-4)

$$N = \frac{1}{\rho} \begin{bmatrix} 0 & 0 & 0 & 0 \\ -(d_1 u + d_2 v) & d_1 & d_2 & 0 \\ -(d_2 u + d_3 v) & d_2 & d_3 & 0 \\ -(d_1^2 + 2d_2 uv + d_3 v^2) & d_1 - d_4 \gamma (\gamma - 1) u & d_2 u + d_3 & d_4 \gamma (\gamma - 1) \\ +d_4 \gamma (\gamma - 1) (u^2 + v^2 - e) & +d_2 v & -d_4 \gamma (\gamma - 1) & \end{bmatrix}$$

Appendix C: Boundary and Initial Conditions

Boundary Conditions Without Blowing. (35:10:11)

The boundary conditions on the C-grid and on the airfoil surface must be completely specified. In the code used the boundary conditions are explicit as opposed to implicit. This makes it easier to define and alter the conditions; but, requires a separate routine to reinitialize the conditions after each iteration. Referring to the airfoil computational domain shown in Figure 10, the following boundary conditions are prescribed.

Free stream conditions are given in non-dimensional form for all the flow variables along the outer boundary ABC.

$$P = P_{\infty} = \frac{1}{\gamma M_{\infty}^2}, \quad \rho = \rho_{\infty} = 1, \quad \varepsilon = \varepsilon_{\infty} = 0 \quad (C-1)$$

$$u = U_{\infty} \cos(\alpha), \quad v = U_{\infty} \sin(\alpha), \quad U_{\infty} = 1 \quad (C-2)$$

This is the only way in which angle of attack enters the problem and as such requires that restart solutions must be at the same angle of attack. Also, pressure P is

uniquely defined by Mach Number and requires all restart solutions to share the same Mach number.

On the downstream or far field boundaries AD and HC the flow variables are computed by the following relationships

$$P = P_{\infty} \quad (C-1)$$

$$\frac{\partial}{\partial \xi} \begin{pmatrix} \rho \\ \epsilon \\ u \\ v \end{pmatrix} = 0 \quad (C-3)$$

This allows for compressible non-uniform flow at the boundary and loss in momentum due to skin friction at the airfoil surface.

Along the airfoil surface EFG, the no-slip adiabatic conditions are assumed

$$u = v = 0 \quad (C-4)$$

and the gradient of pressure and temperature normal to the surface is assumed to be zero, where surface density is a function of surface pressure and temperature.

$$\frac{\partial}{\partial \eta} \begin{pmatrix} P \\ T \end{pmatrix} = 0 \quad , \quad \rho = \rho(P, T) \quad (C-5)$$

Finally, through the Wake cut ED and EH continuity is

assured by

$$\frac{\partial}{\partial \eta} \begin{pmatrix} P \\ \rho \\ \epsilon \\ u \\ v \end{pmatrix}_{\text{Lower Wake}} = \frac{\partial}{\partial \eta} \begin{pmatrix} P \\ \rho \\ \epsilon \\ u \\ v \end{pmatrix}_{\text{Upper Wake}} \quad (\text{C-6})$$

which reduces to a three point averaging

$$\begin{pmatrix} P \\ \rho \\ \epsilon \\ u \\ v \end{pmatrix}_{\text{Wake}} = \frac{1}{2} \begin{pmatrix} P \\ \rho \\ \epsilon \\ u \\ v \end{pmatrix}_{\text{Lower Wake}} + \frac{1}{2} \begin{pmatrix} P \\ \rho \\ \epsilon \\ u \\ v \end{pmatrix}_{\text{Upper Wake}} \quad (\text{C-7})$$

Boundary Conditions for Suction and Blowing (32)

Since the boundary conditions only affect specific sections of the airfoil section, refer to Figure 46, all other boundaries will be calculated as above. On the suction surface (s_u) P , ρ and T are calculated the same as the solid surface; however, u and v are determined by the constraint that \bar{V}_{s_u} be normal to the surface and is given by the slope, θ at the surface

$$e = \frac{dy}{dx} \quad (\text{C-8})$$

$$u = V_{s_u} \sin(\theta), \quad v = -V_{s_u} \cos(\theta) \quad (\text{C-9})$$

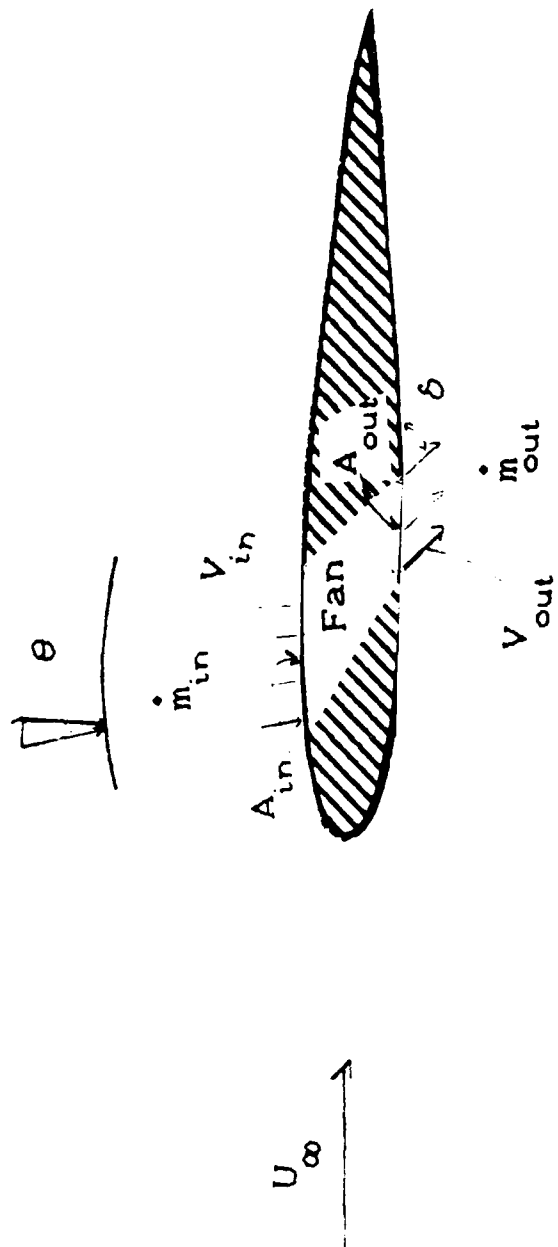


Figure 46. Boundary Conditions

where the magnitude V_{su} is a constant equal to some fraction of the free stream velocity

$$V_{su} = CvU_{\infty} = Cv, \quad U_{\infty} = 1 \quad (C-10)$$

In order to prescribe conditions on the lower blowing surface (bl) the mass flow \dot{m} must be determined and is done in the following manner (12)

$$\dot{m}_{su} = \dot{m}_{bl} = \dot{m} = \rho AV \quad (C-11)$$

where A is the area of the opening and V is the velocity magnitude normal to the surface. On the upper surface ρ is averaged and changes with each iteration, A is assumed to be ΔX and for this analysis was picked to be 0.25 or 25 percent of the airfoil cord and V is a known constant Cv . On the lower surface P is determined as above and ρ is fixed and assumed to be compressed by the action of the fan and is how work done by the fan is introduced into the model (11:4-5)

$$de = dq - Pd(1/\rho) = Pd(1/\rho) \quad (C-12)$$

for no heat transfer, $dq = 0$

and

$$\rho_{bl} = C_r \text{ avg } (\rho)_{su} \quad (C-13)$$

where C_r is a constant and equal to 1.1 for this analysis.

Using the above relationships the magnitude of the normal velocity on the lower surface, V_{bl} can be determined. If vanes are assumed on the lower surface and A_{bl} is assumed to be equal to dx , where dx is picked to be 0.125 for this analysis, then the boundary conditions simplify to the following equations

$$\rho_{avg} C_r A_{bl} V_{bl} = \rho_{avg} A_{su} C_v \quad (C-14)$$

$$v = -V_{bl} = \frac{C_a C_v}{C_r}, \quad u = V_{bl} \tan(\delta) \quad (C-15)$$

$$C_a = \frac{A_{su}}{A_{bl}} \quad (C-16)$$

where δ is the angle of the vane with respect to the airfoil cord and is equal to 90 degrees for blowing normal to the lower surface area A_{bl} .

Initial Conditions

For this code the first run made for a particular angle of a attack and Mach Number assumes a Uniform flow field, where the non-dimensional flow variables are given by the following relationships

$$P = P_{\infty} = \frac{1}{\gamma M_{\infty}^2} , \quad \rho = \rho_{\infty} = 1 \quad (C-1)$$

$$u = U_{\infty} \cos(\alpha) , \quad v = U_{\infty} \sin(\alpha) , \quad U_{\infty} = 1 \quad (C-2)$$

An initial run of one hundred iterations with turbulence turned off is made in order to develop the flow and a solution or restart file is saved. Additional runs can then be made using the restart file as long as the angle of attack, Mach Number and grid are not changed. The variables which can be manipulated include the transition points, Reynolds Number, C_v , C_r , δ and the damping coefficients. A considerable number of iterations can be saved by using a near convergent solution as a restart for a new problem within the above Constraints.

Appendix D: Derivation of the Force Coefficients

C_l and C_d

The Calculation of lift and drag on an airfoil surface with non-zero surface velocity and mass flux can be accomplished through a special application of the NS equations. Starting with the linear momentum equation in integral form. (41:)

$$\frac{D}{Dt} \iiint (\rho \bar{V}) d\nu = \iiint (\bar{f}_b + \nabla \cdot \underline{\underline{\sigma}}) d\nu \quad (D-1)$$

By assuming a constant control volume with respect to time and applying the material derivative equation. The above equation the reduces to the following form.

$$\iiint \frac{\partial(\rho \bar{V})}{\partial t} d\nu = \iiint (-(\rho \bar{V} \cdot \bar{\nabla}) \bar{V} + \bar{f}_b + \bar{\nabla} \cdot \underline{\underline{\sigma}}) d\nu \quad (D-2)$$

$$\begin{aligned} \iiint \left[\frac{\partial(\rho \bar{V})}{\partial t} - \bar{f}_b \right] d\nu & \quad (D-3) \\ & = \iint (-(\rho \bar{V} \bar{V}) \cdot \hat{n} + \underline{\underline{\sigma}} \cdot \hat{n}) ds \end{aligned}$$

Where ds represents a spatial increment on the airfoil surface. In 2-d cartesian coordinates the components reduce to (42)

$$\hat{n} = \frac{-y_{\xi} \hat{i} + x_{\xi} \hat{j}}{\sqrt{x_{\xi}^2 + y_{\xi}^2}} = \frac{-y_{\xi} \hat{i} + x_{\xi} \hat{j}}{ds} \quad (D-4)$$

$$\bar{V} = u \hat{i} + v \hat{j} \quad (D-5)$$

$$\iiint \frac{\partial(\rho \bar{V})}{\partial t} d\nu = \iiint \left[\rho \frac{\partial \bar{V}}{\partial t} + \bar{V} \frac{\partial \rho}{\partial t} \right] d\nu = 0 \quad (D-6)$$

$$\rho \bar{V} \cdot \hat{n} = \rho(u \hat{i} + v \hat{j}) \left[\frac{-uy_{\xi} + vx_{\xi}}{ds} \right] \quad (D-7)$$

$$\begin{aligned} \sigma \cdot \hat{n} &= \left[P y_{\xi} - \tau_{xx} y_{\xi} + \tau_{xy} x_{\xi} \right] \hat{i} \\ &+ \left[-P x_{\xi} + \tau_{yy} x_{\xi} - \tau_{yx} y_{\xi} \right] \hat{j} \end{aligned} \quad (D-8)$$

for velocity and density on the airfoil boundary equal to either a constant value or zero.

$$\begin{aligned} \iiint \bar{f}_b d\nu &= \bar{F}_b = F_b \hat{i} + F_b \hat{j} \\ &= -F_x - F_y \end{aligned} \quad (D-9)$$

Putting it all together and summing over the airfoil surface $\iint () ds = \Sigma ds$ the equations reduce to

$$F_x = - \sum \rho u \left[\frac{-uy_\xi + vx_\xi}{ds} \right] \quad (D-10)$$

$$+ \sum \left[-P_{x\xi} + \tau_{yy}x_\xi - \tau_{yx}y_\xi \right]$$

$$F_y = - \sum \rho v \left[\frac{-uy_\xi + vx_\xi}{ds} \right] \quad (D-11)$$

$$+ \sum \left[-P_{y\xi} + \tau_{yy}x_\xi - \tau_{yx}y_\xi \right]$$

and by using Stokes approximation $\lambda = -2/3\mu$ the non-dimensional shear stress terms become

$$\tau_{xx} = \frac{1}{R_\bullet} \mu \left[\frac{4}{3} \frac{\partial u}{\partial x} - \frac{2}{3} \frac{\partial v}{\partial y} \right] \quad (D-12)$$

$$\tau_{yy} = \frac{1}{R_\bullet} \mu \left[\frac{4}{3} \frac{\partial v}{\partial y} - \frac{2}{3} \frac{\partial u}{\partial x} \right] \quad (D-13)$$

$$\tau_{xy} = \tau_{yx} = \frac{1}{R_\bullet} \mu \left[\frac{\partial u}{\partial y} + \frac{\partial v}{\partial x} \right] \quad (D-14)$$

Lift and drag can be related to the body forces and the angle attack by the following relationships

$$\text{Lift} = -F_x \sin(\alpha) + F_y \cos(\alpha) \quad (D-15)$$

$$\text{Drag} = F_x \cos(\alpha) + F_y \sin(\alpha) \quad (D-16)$$

and the coefficients are

$$C_l = \frac{\text{Lift}}{\frac{1}{2} \rho_{\infty} U_{\infty}^2} \quad C_d = \frac{\text{Drag}}{\frac{1}{2} \rho_{\infty} U_{\infty}^2} \quad (\text{D-17})$$

and for non-dimensional variables $\rho_{\infty} = U_{\infty} = 1$ and equation (D-17) reduces to

$$C_l = 2 \text{ Lift} \quad , \quad C_d = 2 \text{ Drag} \quad (\text{D-18})$$

Appendix E: Computer Resource Requirements

The model simulations were accomplished by using the NS code as discussed in section III and in appendix F. The code was run on the Cray XMP computer located at Wright-Patterson Air Force Base. Table 13 compares the memory and CPU requirements for the original and modified codes.

Version	Grid		Memory	CPU/100
	IL	JL		
Unmodified	199	50	780,800	31.157
Modified	199	50	611,328	29.991
Modified	299	100	1,397,760	71.202

Table 13. Computer Resource Comparisons

The memory modifications to the code reduced the memory requirements by 27.7 percent and the CPU requirements by 4.1 percent. The memory improvements were necessary in order to decrease turn around time for the larger grid used in the analysis. The maximum available core memory on the Cray is 1,860,000 words. The unmodified code memory requirements for the larger grid would have been close to this value. The main reason the improvement was needed is based on how the priority system on the Cray works. Each job with the same priority is rotated in the queue and, if memory is available, is allowed to run for a

set number of CPUs. If no memory is available, then the job is passed over. This pattern continues until the job is completed.

For jobs requiring a lot of memory (50% core), the availability of memory goes down. Jobs with higher priority maintain their memory and it is not available for jobs of a lower priority. However, lower priority jobs requiring less memory than that being used by the higher priority jobs can run. For this reason, the turn around time for a job with the larger grid at regular day priority was approximately 1.4 minutes per 100 iterations, while at an overnight priority it was between 1 hour and 3 days.

Appendix F: Navier-Stokes, Fortran Listing (36)

The attached fortran listing is the modified version of the code used in this work. The original code was supplied by the Air Force Wright Aerodynamics Laboratories, Flight Dynamics Laboratory, Computational Fluid Dynamics Group. The Code was developed by Dr. Miguel Visbal. It uses the Beam-Warming approximate factorization algorithm to solve the two-dimensional, mass-averaged, compressible Navier-Stokes equations for viscous, unsteady flows.

Modifications, made by the author, for this study involved the boundary conditions for the fan, the turbulence model for blowing effects, the force and residual calculations, input/output and loop structure to reduce memory requirements (see appendix E). The Code was run on the Cray XMP Computer.

VECTORIZED NAVIER-STOKES CODE ——— BEAM-HARMING ALGORITHM
 CONFIGURATION: AIRFOIL, C-GRID; AUG. 1985
 BY MICHAEL R. VISBA
 PROGRAM MODIFIED TO INCLUDE INJECTION AND EJECTION ON THE AIRFOIL
 SURFACE. THIS ALLOWED SIMULATION OF A FAN IN THE WING CONCEPT. CHANGES
 WERE MADE IN THE SUBROUTINE BNDY. THESE CHANGES WERE MADE BY
 CAPT PAUL D BOYLES IN SUPPORT OF AN AFIT THESIS. AUG 1988

***** I M P O R T A N T *****
 BEFORE USING THIS PROGRAM :
 MODIFY DIMENSION STATEMENTS
 CHECK BOUNDARY CONDITIONS SUBROUTINE
 CHECK INPUT DATA

THIS PROGRAM SOLVES THE COMPRESSIBLE NAVIER-STOKES EQUATIONS
 IN ARBITRARY TWO-DIMENSIONAL DOMAINS USING BODY-FITTED (TIME-
 INVARIANT) CURVILINEAR COORDINATES AND THE IMPLICIT FACTORED
 SCHEME OF BEAM & HARMING. *****
 TIME DIFFERENCING : EULER IMPLICIT
 SPATIAL DIFFERENCING : SECOND ORDER CENTERED DIFFERENCES
 IN THIS PROGRAM THE SPACE INCREMENTS OF THE TRANSFORMED
 VARIABLES XI AND ETA ARE BOTH ASSUMED EQUAL TO ONE (I.E.,
 DEL(XI)=DEL(ETA)=1.0).

LIST OF SYMBOLS

X,Y : CARTESIAN COORDINATES
 XI,ETA : TRANSFORMED COORDINATES
 XJAC : JACOBIAN OF INVERSE TRANSFORMATION:D(X,Y)/D(XI,ETA).
 XXI,YXI,XYETA,YETA : TRANSFORMATION DERIVATIVES
 U,V : VELOCITY COMPONENTS
 RHO : DENSITY
 P : PRESSURE . IS NON DIMENSIONALIZED BY 1/(GMX*MACH**2)
 XMU : VISCOSITY
 RE : REYNOLDS NO.
 XM1 : MACH NO.
 PR : PRANDTL NO.
 S1 : NON-DIMENSIONAL PARAMETER FOR SUTHERLAND'S LAW
 PRT : TURBULENT PRANDTL NO.
 EDDY : TURBULENT EDDY VISCOSITY
 S1I,J : DISTANCE ALONG THE XI-LINES FROM ETA=0.
 NCONV : THE CONVERGENCE TEST IS APPLIED EVERY NCONV STEPS
 IL : NO. OF POINTS IN XI-DIRECTION
 JL : NO. OF POINTS IN ETA-DIRECTION
 ME,MI : DAMPING COEFFICIENTS
 INMAX : MAX. NO. OF TIME STEPS ALLOWED
 JLAST : LOCATION IN THE GRID ABOVE WHICH TURB IS NOT APPLIED
 ILE : I LOCATION OF THE LEADING EDGE
 ITEU : I LOCATION OF THE TRAILING EDGE ON THE UPPER SURFACE
 ITEL : I LOCATION OF THE TRAILING EDGE ON THE LOWER SURFACE
 ITRSU : I LOCATION OF TRANSITION ON THE UPPER SURFACE
 ITRSL : I LOCATION OF TRANSITION ON THE LOWER SURFACE
 INKST : I LOCATION WHERE MODIFIED TRANSITION IN THE WAKE STARTS
 INKKE : I LOCATION WHERE MODIFIED TRANSITION IN THE WAKE ENDS

MAIN PROGRAM

PARAMETER(IM=299, JM=100)
 COMMON /FLOW/ U(IM, JM), V(IM, JM), P(IM, JM), RHO(IM, JM),
 XMU(IM, JM), EDDY(IM, JM)
 COMMON /GRID/ X(IM, JM), Y(IM, JM), XXI(IM, JM), YXI(IM, JM),
 XETA(IM, JM), YETA(IM, JM), XJAC(IM, JM), S(IM, JM), SSI(IM)
 COMMON /MATRIX/ A(IM, JM, 4, 4), RHS(IM, JM, 4)
 COMMON /P/ IL, JL, ILE, ITEL, ITEU
 COMMON /PR/ GAM, PR, XM1, RE, TM, S1, ALFA, ANGLE
 COMMON /MISC/ IL1, IL2, IL3, JL1, JL2, JL3, ILEP1, ILEM1,
 ITEL1, ITEL2, ITEUP1, ITEL3, GAM1, GAM2, GAM3, GMX, S1P,
 PINF, SINA, COSA, PR1, PRT1, RE1, XL, XL1, XLN, PI
 COMMON /DMHY/ TEMP(IM, JM, 4)
 COMMON /TIME/ DTAU(IM, JM), CFL, DTMIN, DTMAX, BETA, DTVIS
 COMMON /DAMP/ ME, MI, WPE, WPI, ISPECT
 COMMON /TURB1/ ITRSU, ITRSL, INKST, INKKE, JLAST,
 XRELAX
 COMMON /TURB2/ XMUT1(JM), XMUT2(JM), D1(JM), M(2*JM), F(2*JM),
 GAMMA(IM)
 COMMON /SPECTR/ SPECT(IM, JM), PSMU(IM, JM)
 COMMON /NORM/ UNORM, VNORM
 COMMON /BND/ NBND, XMREF, TREF, TIMF, CV, CR, CT, DEL, L1, L2, L3, L4

INPUT DATA

OPEN(UNIT=5, FILE='DATA', STATUS='OLD')
 OPEN(UNIT=1, FILE='GRID', STATUS='OLD')
 OPEN(UNIT=6, FILE='OUTPUT', STATUS='NEW')
 OPEN(UNIT=2, FILE='SOLN', STATUS='NEW')
 OPEN(UNIT=3, FILE='STUFF', STATUS='NEW')

READ (5, 510) NSTEPJ
 READ (5, 520) TAU
 READ (5, 510) IL
 READ (5, 510) JL
 READ (5, 510) ILE
 READ (5, 510) ITEL
 READ (5, 510) ITEU
 510 FORMAT(I10)
 READ (5, 520) XM1
 READ (5, 520) RE
 READ (5, 520) IM
 READ (5, 520) S1
 READ (5, 520) ALFA
 520 FORMAT(F15.10)
 READ (5, 510) NTURB
 READ (5, 510) IFREQ
 READ (5, 510) ITRSU
 READ (5, 510) ITRSL
 READ (5, 510) INKST
 READ (5, 510) INKKE
 READ (5, 510) JLAST
 READ (5, 520) XRELAX
 READ (5, 510) NOTAU
 READ (5, 520) CFL
 READ (5, 520) BETA
 READ (5, 520) DTVIS
 READ (5, 510) ISPECT
 READ (5, 520) ME
 READ (5, 520) MI

```

READ (5,520) MPE
READ (5,520) MPI
READ (5,520) EDST
READ (5,510) INMAX
READ (5,510) WCONV
C IF RESTART THEN IREST = 1 ELSE = 0
C IPILOT = 1 TURNS PRINT ROUTINES ON FOR DEBUGGING
READ (5,510) IPILOT
READ (5,510) IPILOT1
C FAN INFORMATION
READ (5,510) NBND
READ (5,520) XMREF
READ (5,520) CV
READ (5,520) CR
READ (5,520) CT
READ (5,520) DEL
READ (5,510) L1
READ (5,510) L2
READ (5,510) L3
READ (5,510) L4

```

CONSTANTS FOR AIR

```

GAM=1.40
PR=0.720
PRT=0.90
PRES = 1. / ( GAM*XM1*XM1 )
RHO = 1
TINF = 1
TREF = XM1*XM1/(XMREF*XMREF)
ICHECK = 0

```

INITIALIZATION

CALL INITIA

```

UINF = COS(ANGLE)
VINF = SIN(ANGLE)

```

PRINT OUT THE INPUT DATA

```

WRITE (6,*) 'C'
WRITE (6,*) 'C'
WRITE (6,202)
WRITE (6,203)
WRITE (6,204) IL,JL,ILE,ITEL,ITEU
WRITE (6,205) NDTAU,CFL,BETA,DTVIS
WRITE (6,206) XM1,RE,S1,ALFA
WRITE (6,213) ITRSU,ITRSL,IMKST,IMKE,
- JLAST,XRELAX
WRITE (6,214) NTURB,IFREQ
WRITE (6,208) ME,MI,MPE,MPI,ISPECT
WRITE (6,*) RESTART (Y/N, I/O) => ',IREST'
WRITE (6,*)
IF (NBND .EQ. 2) THEN
WRITE (6,*) SUCTION ONLY

```

```

END IF
IF (NBND .EQ. 3) THEN
WRITE (6,*) BLOWING ONLY
END IF
IF (NBND .EQ. 0) THEN
WRITE (6,*) FAN IS TURNED OFF
GOTO 111
END IF
WRITE (6,*) FAN INFORMATION
WRITE (6,209) L1,L2,L3,L4,DEL
WRITE (6,210) CV,CR,CT
WRITE (6,215) XMREF,XM1,TREF,TINF

```

INPUT RESTART SOLUTION (I.E. X,Y,U,V,P,RHO,EDDY)

```

111 REMIND 1
DO 281 J=1,JL
DO 281 I=1,IL
IF (IREST .EQ. 0) GOTO 382
READ (1,1000) X(I,J),Y(I,J),U(I,J),V(I,J),
- P(I,J),RHO(I,J),EDDY(I,J)
GOTO 281
382 READ(1,1001) X(I,J),Y(I,J)
P(I,J) = PRES
RHO(I,J) = 1.0
U(I,J) = UINF
V(I,J) = VINF
EDDY(I,J) = 0.0
IF (J .LE. JLAST) EDDY(I,J) = EDST
281 CONTINUE
1000 FORMAT (1X,7E16.8)
1001 FORMAT (2E15.8)

```

COMPUTE TRANSFORMATION METRICS

CALL METRIC

```

INITIALIZE SPECTRAL RADIUS SPECT(I,J)
DO 282 J=1,JL
DO 282 I=1,IL
SPECT(I,J)=XJAC(I,J)
282 CONTINUE

```

COMPUTE TIME STEP (DTAU)

```

CALCULATE MOLECULAR VISCOSITY XMU(I,J)
CALL CXMU(ICHECK)
CALL TMSTEP
WRITE (6,211) DTMIN,DTMAX

```

PREPARE FOR FIRST ITERATION

```

608 NSTEP=NSTEP1
INDEA=0

```

```

ICNV=0
IDT=0
ITURB=0
C COMPUTE TURBULENCE TRANSITION FACTOR GAMMA(J)
CALL TRANSI
ADVANCE TIME STEP
100 NSTEP=NSTEP+1
INDEX=INDEX+1
ICNV=ICNV+1
IF (ICNV.EQ.NCONV) ISMTC=1
IDT=IDT+1
TAU=TAU+DTMIN
ITURB=ITURB+1
IF (INDEX.GT.INMAX) GO TO 200
C COMPUTE NEW DTAU IF DESIRED
IF (IDT.LT.NDTAU) GO TO 400
IDT=0
CALL TMSTEP
WRITE(6,212) NSTEP,DTMIN,DTMAX
400 CONTINUE
STEP 1 : XI - SNEEP
CALL STEPX (ISMTC,DRMAX,RMSDR)
STEP 2 : ETA - SNEEP
CALL STEPY
UPDATE VARIABLES AT INTERIOR POINTS
CALL CONVRT
DO 25 K=1,4
DO 25 J=2,JL1
DO 25 I=2,IL1
TEMP(I,J,K)=TEMP(I,J,K)+RHS(I,J,K)
25 CONTINUE
CALL UCONVRT
IMPLEMENT BOUNDARY CONDITIONS
CALL BNDRY
CALL CXMU(ICHECK)
IF (ICHECK.EQ.1) GOTD 200
UPDATE TURBULENT EDDY VISCOSITY
IF (ITRSU.GT.IL) GO TO 256
IF (INDEX.LT.NTURB) GO TO 256
IF (ITURB.LT.IFREQ) GO TO 256
ITURB=0
IF (INDEX.EQ.INMAX) IPILOT=1
IF (INDEX.EQ.INMAX) IPLOT1=1
CALL TURB (IPILOT,IPILOT1)
256 CONTINUE
CONVERGENCE CRITERIA
IF (ICNV.LT.NCONV) GO TO 100
ICNV=0
CALL MONTR (NSTEP,TAU,DRMAX,RMSDR)
GO TO 100
SAVE CURRENT SOLUTION.
200 CONTINUE
REMIND 2
DO 257 J=1,JL
DO 257 I=1,IL
WRITE (2,1000) X(I,J),Y(I,J),U(I,J),V(I,J),
P(I,J),RHO(I,J),EDDY(I,J)
257 CONTINUE
PRINT OUT SOLUTION
CALL OUTPUT
FORMATS
202 FORMAT (1H1,30X,'==== BEAM-WARNING METHOD ====',//)
203 FORMAT (10X,' NACA 0012 AIRFOIL',//)
204 FORMAT (10X,' IL=',13.3X,' JL=',13.3X,
' ILE=',13.3X,' ITEL=',13.3X,' ITEU=',13.3X,
' ILE=',13.3X,' ITEL=',13.3X,' ITEU=',13.3X,
205 FORMAT (15X,' NDTAU=',15.5X,' CFL=',12.3,5X,' BETA=',12.3,
5X,' DTMIN=',12.5,/)
206 FORMAT (1X,' REFERENCE MACH NO.=',12.5,3X,
1 ' REYNOLDS NO.=',12.1,3X,' VISCOSITY PARAMETER=',12.5,
1 3X,' ANGLE OF ATTACK.=',12.4,/)
208 FORMAT (15X,' DAMPING PARAMETERS',5X,' ME=',12.5,
5X,' MI=',12.5,5X,' MPE=',12.5,5X,
' MPI=',12.5,5X,' ISPECT=',15.5,/)
211 FORMAT (10X,' DTMIN=',12.5,5X,' DTMAX=',12.5,/)
215 FORMAT (2X,' HREF=',12.3,5X,' HMIN=',12.3,5X,' HREF=',12.3,5X,

```



```

DO 8 J=2,JL1
XXI(1,J)=-.5*(-X(3,J)+4.*X(2,J)-3.*X(1,J))
YXI(1,J)=-.5*(-Y(3,J)+4.*Y(2,J)-3.*Y(1,J))
XETA(1,J)=-.5*(X(1,J+1)-X(1,J-1))
YETA(1,J)=-.5*(Y(1,J+1)-Y(1,J-1))
8 CONTINUE
C
C XI=XIMAX
DO 9 J=2,JL1
XXI(IL,J)=-.5*(-X(IL2,J)+4.*X(IL1,J)-3.*X(IL,J))
YXI(IL,J)=-.5*(-Y(IL2,J)+4.*Y(IL1,J)-3.*Y(IL,J))
XETA(IL,J)=-.5*(X(IL,J+1)-X(IL,J-1))
YETA(IL,J)=-.5*(Y(IL,J+1)-Y(IL,J-1))
9 CONTINUE
C
C ETA=0.0
DO 10 I=2,IL1
XXI(1,I)=-.5*(X(I+1,1)-X(I-1,1))
YXI(1,I)=-.5*(Y(I+1,1)-Y(I-1,1))
XETA(1,I)=-.5*(X(1,3)+4.*X(1,2)-3.*X(1,1))
YETA(1,I)=-.5*(Y(1,3)+4.*Y(1,2)-3.*Y(1,1))
10 CONTINUE
C
C ETA=ETAMAX
DO 11 I=2,IL1
XXI(1,IL)=-.5*(X(I-1,IL)-X(I-1,JL))
YXI(1,IL)=-.5*(Y(I-1,IL)-Y(I-1,JL))
XETA(1,IL)=-.5*(-X(1,IL2)+4.*X(1,IL1)-3.*X(1,IL))
YETA(1,IL)=-.5*(-Y(1,IL2)+4.*Y(1,IL1)-3.*Y(1,IL))
11 CONTINUE
C
C CORNER POINTS
DO 99 I=1,1
XXI(1,1)=-.5*(-X(3,1)+4.*X(2,1)-3.*X(1,1))
YXI(1,1)=-.5*(-Y(3,1)+4.*Y(2,1)-3.*Y(1,1))
XETA(1,1)=-.5*(-X(1,3)+4.*X(1,2)-3.*X(1,1))
YETA(1,1)=-.5*(-Y(1,3)+4.*Y(1,2)-3.*Y(1,1))
C
XXI(1,JL)=-.5*(-X(3,JL)+4.*X(2,JL)-3.*X(1,JL))
YXI(1,JL)=-.5*(-Y(3,JL)+4.*Y(2,JL)-3.*Y(1,JL))
XETA(1,JL)=-.5*(-X(1,JL2)+4.*X(1,JL1)-3.*X(1,JL))
YETA(1,JL)=-.5*(-Y(1,JL2)+4.*Y(1,JL1)-3.*Y(1,JL))
C
XXI(IL,1)=-.5*(-X(IL2,1)+4.*X(IL1,1)-3.*X(IL,1))
YXI(IL,1)=-.5*(-Y(IL2,1)+4.*Y(IL1,1)-3.*Y(IL,1))
XETA(IL,1)=-.5*(-X(IL,3)+4.*X(IL,2)-3.*X(IL,1))
YETA(IL,1)=-.5*(-Y(IL,3)+4.*Y(IL,2)-3.*Y(IL,1))
C
XXI(IL,JL)=-.5*(-X(IL2,JL)+4.*X(IL1,JL)-3.*X(IL,JL))
YXI(IL,JL)=-.5*(-Y(IL2,JL)+4.*Y(IL1,JL)-3.*Y(IL,JL))
XETA(IL,JL)=-.5*(-X(IL,JL2)+4.*X(IL,JL1)-3.*X(IL,JL))
YETA(IL,JL)=-.5*(-Y(IL,JL2)+4.*Y(IL,JL1)-3.*Y(IL,JL))
C
C EVALUATE JACOBIAN
DO 12 J=1,JL
DO 12 I=1,IL
XJAC(I,J)=XXI(I,J)*YETA(I,J)-XETA(I,J)*YXI(I,J)
12 CONTINUE
C
XJMIN=1.0E+10
DO 122 J=1,JL
DO 122 I=1,IL
IF ( XJAC(I,J) .LT. XJMIN ) THEN
II = I
JJ = J
END IF
IF ( ABS(XJAC(I,J)) .LT. 1.0E-8 )
+ WRITE (6,211) I,J,XJAC(I,J),X(I,J),Y(I,J)
XJMIN=AMINI(XJAC(I,J),XJMIN)
122 CONTINUE
IF(XJMIN.GT.0.0) GO TO 500
WRITE(6,205) XJMIN
WRITE(6,206) II,JJ,X(II,JJ),Y(II,JJ)
C
211 FORMAT (2X,'I,J,XJAC,X(I,J),Y(I,J) = ',2I5,E10.5,2F7.3)
C PRINT METRICS IF DESIRED
WRITE (6,207)
DO 13 I=1,IL
WRITE (6,200) I
WRITE (6,201)
DO 13 J=1,JL
WRITE (6,202) J,X(I,J),Y(I,J),XJAC(I,J),XXI(I,J),XETA(I,J),
1 YXI(I,J),YETA(I,J)
13 CONTINUE
C
C FORMATS
200 FORMAT (20X,'COLUMN',I3)
201 FORMAT (4X,'J',5X,'X',8X,'Y',5X,'XJAC(I,J)',6X,'XXI(I,J)',
1 6X,'XETA(I,J)',6X,'YXI(I,J)',6X,'YETA(I,J)')
202 FORMAT (2X,I3,7(3X,E10.3))
205 FORMAT (10X,'*** WARNING *** JACOBIAN LESS OR EQUAL TO ZERO',
1 3X,'MIN(JACOBIAN)=' ,E15.7,/)
206 FORMAT (3X,'LOCATION IS AT I,J = ',2I3,2X,' AND X,Y = ',2F7.3,/)
207 FORMAT (10I,10X,'TRANSFORMATION DERIVATIVES',/)
500 RETURN
END
C
C *****
C
C SUBROUTINE "TMSTEP" COMPUTES LOCAL TIME STEP (DTAU(I,J)).
C IF BETA=0, DTAU(I,J) IS A CONSTANT EQUAL TO DTMIN.
C IF BETA.NE.0., LOCAL CFL NUMBER IS USED.
C
C SUBROUTINE TMSTEP
C
C PARAMETER(IM=299, JM=100)
C COMMON /FLOWV/ U(IM, JM), V(IM, JM), P(IM, JM), RHO(IM, JM),
C 1XNU(IM, JM), EDDY(IM, JM)
C COMMON /GRID/ X(IM, JM), Y(IM, JM), XXI(IM, JM), YXI(IM, JM),
C 1XETA(IM, JM), YETA(IM, JM), XJAC(IM, JM), S(IM, JM), SSI(IM)
C COMMON /P1/ IL, JL, ILE, ITEL, ITEU
C COMMON /P2/ GAM, PR, PRI, XMI, RE, TM, S1, ALFA, ANGLE
C COMMON /MISC/ ILL, IL2, IL3, JLL, JL2, JL3, ILEP1, ILEM1,
C 1 ITEL P1, ITEL M1, ITEU P1, ITEU M1, GAM1, GAM2, GAM I1, GRM, S1 P,
C 1 P1 F, S1 M, COSA, PRI, PRI1, RE1, XL, XL1, XL M, P1
C COMMON /DUMMY/ TEMP, IM, JM, 4
C COMMON /TIMEN/ DTAU(IM, JM), CFL, DTMIN, DTMAX, BETA, DTVIS
C
C X1=2.*GAM*REI
C
C DO 1 J=1,JL
C DO 1 I=1,IL

```

```

UC=(YETA(I,J)*U(I,J)-XETA(I,J)*V(I,J))/XJAC(I,J)
VC=(-YXI(I,J)*U(I,J)+XXI(I,J)*V(I,J))/XJAC(I,J)
DSET2=XETA(I,J)*YETA(I,J)**2
DSX12=XXI(I,J)**2+YXI(I,J)**2
T=GM*P(I,J)*RHO(I,J)
DTAU(I,J)=1./ABS(UC)-ABS(VC)+SQRT(T*1./DSET2+1./DSX12)/XMI
+X(I)*(XMI(I,J)*PRI+EDDY(I,J)*PRTI)/(RHO(I,J)*DSET2)
DTAU(I,J)=CFL*DTAU(I,J)
1 CONTINUE
C
C FIND DTMIN,DTMAX
DTMAX=C.
DTMIN=1.0E+20
DO 2 J=1,JL
DO 2 I=1,IL
DTMIN=AMIN1(DTMIN,DTAU(I,J))
DTMAX=AMAX1(DTMAX,DTAU(I,J))
2 CONTINUE
C
C OVERRIDE CFL-CONDITION .THIS IS DESIRABLE FOR VERY FINE
C GRIDS AND/OR IN VISCOUS REGIONS
DO 22 J=1,JL
DO 22 I=1,IL
IF(DTAU(I,J).GT.DTVIS) GO TO 22
DTAU(I,J)=DTVIS
22 CONTINUE
C
IF(BETA.NE.0.0) GO TO 100
DO 3 J=1,JL
DO 3 I=1,IL
DTAU(I,J)=DTVIS
3 CONTINUE
C
100 RETURN
END
C
C *****
C
C SUBROUTINE "STEPX", PERFORMES XI - SWEEP
C
C SUBROUTINE STEPX(ISMTC,DRMAX,RMSDR)
C
C PARAMETER(IM=299,JM=100)
COMMON /FLOWV/ U(IM,JM),V(IM,JM),P(IM,JM),RHO(IM,JM),
IXMU(IM,JM),EDDY(IM,JM)
COMMON /GRID/ X(IM,JM),Y(IM,JM),XXI(IM,JM),YXI(IM,JM),
IXETA(IM,JM),YETA(IM,JM),XJAC(IM,JM),S(IM,JM),SS(IM)
COMMON /MATRIX/ A(IM,JM,4),RMS(IM,JM,4)
COMMON /P1/ IL,JL,ILE,ITEL,ITEU
COMMON /P2/ GAM,PR,PRT,XMI,RE,TN,S1,ALFA,ANGLE
COMMON /MISC/ IL1,IL2,IL3,JL1,JL2,JL3,ILEP1,ILEM1,
- ITELP1,ITELM1,ITEUP1,ITEUM1,GAM2,GAM3,GAM4,GXM,SIP,
- P1F,SINA,COSA,PRI,PRTI,REI,XL,XL1,XLM,P1
COMMON /TIMER/ DTAU(IM,JM),CFL,DTMIN,DTMAX,BETA,DTVIS
COMMON /DUMMY/ TEMPI(IM,JM,4)
COMMON /DAMP/ ME,WI,WPE,WPI,ISPECT
COMMON /SPECTR/ SPECTR(IM,JM),PSMU(IM,JM)
C
C COMPUTE INVISCID JACOBIAN MATRIX A=DF/DO
CALL CHATA
C
C COMPUTE RHS-VECTOR
C
C CALL RHSV
C
C ADD FOURTH-ORDER EXPLICIT DAMPING
C
CALL CONVRT1
IF(ISPECT.EQ.0) GO TO 10
CALL SPECTR
10 CONTINUE
CALL DAMPEY (ME,WPE)
CALL DAMPEX (ME,WPE)
C
MULTIPLY RHS-VECTOR BY -DTAU
C
DO 1 K=1,4
DO 1 J=2,JL1
DO 1 I=2,IL1
RHS(I,J,K)=-DTAU(I,J)*RHS(I,J,K)
1 CONTINUE
C
C COMPUTE MAX. & L2-NORM OF RESIDUAL
IF(ISMTC.EQ.0) GO TO 20
CALL CONVRG(DRMAX,RMSDR)
20 CONTINUE
C
C SOLVE BLOCK-TRIDIAGONAL LINEAR SYSTEM
C
CALL BTRIDX
C
RETURN
END
C
C *****
C
C SUBROUTINE "STEPY", PERFORMES ETA - SWEEP
C
C SUBROUTINE STEPY
C
C PARAMETER(IM=299,JM=100)
COMMON /DAMP/ ME,WI,WPE,WPI,ISPECT
C
C COMPUTE INVISCID JACOBIAN MATRIX B=DG/DO
CALL CHATB
C
C SOLVE BLOCK-TRIDIAGONAL LINEAR SYSTEM
C
IF(WPE.LT.1.0E-05) GO TO 10
CALL PSMOOTH(2)
10 CONTINUE
CALL BTRIDY
C
RETURN
END
C
C *****
C
C SUBROUTINE "DAMPX" IMPLEMENTS FOURTH-ORDER EXPLICIT
C DAMPING IN XI-DIRECTION
C
C SUBROUTINE DAMPEX (M,WPI)
C PARAMETER(IM=299,JM=100)
COMMON /FLOWV/ U(IM,JM),V(IM,JM),P(IM,JM),RHO(IM,JM),
- XMU(IM,JM),EDDY(IM,JM)

```

```

COMMON /GRID/ X(IM,JM),Y(IM,JM),XX1(IM,JM),YY1(IM,JM),
- XETA(IM,JM),YETA(IM,JM),XJAC(IM,JM),S(IM,JM),SS1(IM)
COMMON /MATRIX/ A(IM,JM,4),RHS(IM,JM,4)
COMMON /P1/ IL,JL,ILE,ITEU,ITEU
COMMON /P2/ GAM,PR,PRT,XM1,RE,TH,S1,ALFA,ANGLE
COMMON /MISC/ IL1,IL2,IL3,JL1,JL2,JL3,ILEP1,ILEM1,
- ITEU1,ITEU2,ITEU3,ITEU4,GAM1,GAM2,GAM3,GAM4,GAM5,GAM6,
- P1NF,S1NA,COSA,PRT1,PRT2,REI,XL,XL1,XLW,P1
COMMON /SPECTR/ SPECTR(IM,JM),PSMU(IM,JM)
COMMON /DUMMY/ TEMP(IM,JM,4)
C
IF(IMP.LT.1.0E-05) GO TO 10
CALL PSMOOTH(1)
10 CONTINUE
C
DO 1 K=1,4
DO 1 J=2,JL1
DO 1 I=3,IL2
C
RHS(I,J,K)=RHS(I,J,K)+SPECT(I,J)*(TEMP(I+2,J,K)
-4.*TEMP(I+1,J,K)+6.*TEMP(I,J,K)-4.*TEMP(I-1,J,K)
+TEMP(I-2,J,K))-MP*PSMU(I,J)*TEMP(I+1,J,K)
-2.*TEMP(I,J,K)+TEMP(I-1,J,K))
C
1 CONTINUE
C
I = 2
C
DO 2 K=1,4
DO 2 J=2,JL1
C
RHS(2,J,K)=RHS(2,J,K)+SPECT(2,J)*(TEMP(4,J,K)
-3.*TEMP(3,J,K)+3.*TEMP(2,J,K)-TEMP(1,J,K))
-MP*PSMU(2,J)*TEMP(3,J,K)-2.*TEMP(2,J,K)
+TEMP(1,J,K))
C
2 CONTINUE
C
I = IL-1
C
DO 3 K=1,4
DO 3 J=2,JL1
C
RHS(IL-1,J,K)=RHS(IL-1,J,K)+SPECT(IL-1,J)*(TEMP(IL-1,J,K)
-3.*TEMP(IL-2,J,K)+3.*TEMP(IL-1,J,K)-TEMP(IL-3,J,K))
-MP*PSMU(IL-1,J)*TEMP(IL-2,J,K)-2.*TEMP(IL-1,J,K)
+TEMP(IL-3,J,K))
C
3 CONTINUE
RETURN
END
*****
SUBROUTINE "DAMPEY" IMPLEMENTS FOURTH-ORDER EXPLICIT
DAMPING IN ETA-DIRECTION.
C
SUBROUTINE DAMPEY (IM,MP)
PARAMETER IM=299,JM=100
COMMON /FLOWV/ U(IM,JM),V(IM,JM),P(IM,JM),RHO(IM,JM),
- KMU(IM,JM),EDDY(IM,JM)
COMMON /GRID/ X(IM,JM),Y(IM,JM),XX1(IM,JM),YY1(IM,JM),
- XETA(IM,JM),YETA(IM,JM),XJAC(IM,JM),S(IM,JM),SS1(IM)
COMMON /MATRIX/ A(IM,JM,4,4),RHS(IM,JM,4)
COMMON /P1/ IL,JL,ILE,ITEU,ITEU
COMMON /P2/ GAM,PR,PRT,XM1,RE,TH,S1,ALFA,ANGLE
COMMON /MISC/ IL1,IL2,IL3,JL1,JL2,JL3,ILEP1,ILEM1,
- ITEU1,ITEU2,ITEU3,ITEU4,GAM1,GAM2,GAM3,GAM4,GAM5,GAM6,
- P1NF,S1NA,COSA,PRT1,PRT2,REI,XL,XL1,XLW,P1
COMMON /SPECTR/ SPECTR(IM,JM),PSMU(IM,JM)
COMMON /DUMMY/ TEMP(IM,JM,4)
C
IF(IMP.LT.1.0E-05) GO TO 10
CALL PSMOOTH(2)
10 CONTINUE
C
DO 1 K=1,4
DO 1 J=3,JL2
DO 1 I=2,IL1
C
RHS(I,J,K)=RHS(I,J,K)+SPECT(I,J)*(TEMP(I,J+2,K)
-4.*TEMP(I,J+1,K)+6.*TEMP(I,J,K)-4.*TEMP(I,J-1,K)
+TEMP(I,J-2,K))-MP*PSMU(I,J)*TEMP(I,J+1,K)
-2.*TEMP(I,J,K)+TEMP(I,J-1,K))
C
1 CONTINUE
C
J = 2
C
DO 2 K=1,4
DO 2 I=2,IL1
C
RHS(I,2,K)=RHS(I,2,K)+SPECT(I,2)*(TEMP(I,4,K)
-3.*TEMP(I,3,K)+3.*TEMP(I,2,K)-TEMP(I,1,K))
-MP*PSMU(I,2)*TEMP(I,3,K)-2.*TEMP(I,2,K)
+TEMP(I,1,K))
C
2 CONTINUE
C
J = JL-1
C
DO 3 K=1,4
DO 3 I=2,IL1
C
RHS(I,JL-1,K)=RHS(I,JL-1,K)+SPECT(I,JL-1)*(TEMP(I,JL-3,K)
-3.*TEMP(I,JL-2,K)+3.*TEMP(I,JL-1,K)-TEMP(I,JL,K))
-MP*PSMU(I,JL-1)*TEMP(I,JL-2,K)-2.*TEMP(I,JL-1,K)
+TEMP(I,JL-3,K))
C
3 CONTINUE
RETURN
END
*****
SUBROUTINE "RMSV"
COMPUTES THE RMS-VECTOR FOR STEP #1
I.E. RMS=DF/DX1+DG/DETA-DV1/DX1-DV2/DX1-DW1/DETA-DW2/DETA
C
SUBROUTINE RMSV

```

```

C
PARAMETER IM=299, JM=100
COMMON /FLOW/ U(IM, JM), V(IM, JM), P(IM, JM), RHO(IM, JM),
XMU(IM, JM), EDDY(IM, JM)
COMMON /GRID/ X(IM, JM), Y(IM, JM), XXI(IM, JM), YXI(IM, JM),
XETA(IM, JM), YETA(IM, JM), XJAC(IM, JM), S(IM, JM), SSI(IM,
COMMON /MATRIX/ A(IM, JM, 4, 4), RHS(IM, JM, 4)
COMMON /P1/ IL, JL, ILE, ITEL, ITEU
COMMON /P2/ GAM, PR, PRT, XM1, RE, TM, S1, ALFA, ANGLE
COMMON /MISC/ I1, I2, IL3, JL1, JL2, JL3, ILEP1, ILEM1,
- ITEL1, ITEL11, ITEUP1, ITEU1, GAM1, GAM11, GAM, S1P,
- P1NF, S1NA, COSA, PRI, PRT1, RE1, XL, XL1, XLM, PI
COMMON DUMMY, TEMP(IM, JM, 4)
COMMON /DX/ DX1, DX2, DX3, DX4, DX5, DX6, DX7, DX8, DX9, DX10

```

----- COMPUTE RHS-VECTOR -----

PART #1.. INVISCID TERMS : OF/DX1+OG/DETA

```

C ***** DF / DX1 *****
C
DO 1 J=2, JL1
C
DO 1 I=1, IL
DX1=YETA(I, J)*U(I, J)-XETA(I, J)*V(I, J)
DX2=-1.*GAM11)*P(I, J)+.5*(U(I, J)**2+V(I, J)**2)
- RHO(I, J)
C
TEMP(I, J, 1)=RHO(I, J)*DX1
TEMP(I, J, 2)=RHO(I, J)*U(I, J)*DX1+YETA(I, J)*P(I, J)
TEMP(I, J, 3)=RHO(I, J)*V(I, J)*DX1-XETA(I, J)*P(I, J)
TEMP(I, J, 4)=DX1*DX2
1 CONTINUE
C
DO 3 K=1, 4
DO 3 J=2, JL1
DO 3 I=2, IL1
RHS(I, J, K)=.5*(TEMP(I+1, J, K)-TEMP(I-1, J, K))
3 CONTINUE
C
C ***** OG / DETA *****
C
DO 4 J=1, JL
C
DO 4 I=2, IL1
DX1=XXI(I, J)*V(I, J)-YXI(I, J)*U(I, J)
DX3=-1.*GAM11)*P(I, J)+.5*(U(I, J)**2
+V(I, J)**2)*RHO(I, J)
C
TEMP(I, J, 1)=RHO(I, J)*DX1
TEMP(I, J, 2)=RHO(I, J)*U(I, J)*DX1-YXI(I, J)*P(I, J)
TEMP(I, J, 3)=RHO(I, J)*V(I, J)*DX1+XXI(I, J)*P(I, J)
TEMP(I, J, 4)=DX1*DX3
4 CONTINUE
C
DO 5 K=1, 4
DO 5 J=2, JL1
DO 5 I=2, IL1
RHS(I, J, K)=RHS(I, J, K)+.5*(TEMP(I, J+1, K)-TEMP(I, J-1, K))
5 CONTINUE

```

PART #2 . VISCOUS TERMS : DV1/DX1+DV2/DX1+DM1/DETA+DM2/DETA

```

C ***** DV2 / DX1 *****
C
DO 6 J=2, JL1
C
DO 7 I=1, IL
DX1=XMU(I, J)+EDDY(I, J)
DX2=XXI(I, J)*XETA(I, J)
DX3=YXI(I, J)*YETA(I, J)
DX4=XXI(I, J)*YETA(I, J)
DX5=XETA(I, J)*YXI(I, J)
DX6=-DX1*(DX2+XL)*DX3
DX7=DX1*(DX5+XL)*DX4
DX8=DX1*(DX4+XL)*DX5
DX9=-DX1*(XL)*DX2+DX3
DX10=-GAM11)*XMU(I, J)*PRI+EDDY(I, J)*PRT1)
- (DX2+DX3)
C
DX1=REI/XJAC(I, J)
DX2=.5*(U(I, J+1)-U(I, J-1))
DX3=.5*(V(I, J+1)-V(I, J-1)
DX4=.5*(GAM)*P(I, J+1)/RHO(I, J+1)
- P(I, J-1)/RHO(I, J-1)
C
TEMP(I, J, 1)=0.0
TEMP(I, J, 2)=DX1*(DX6+DX2+DX7+DX3)
TEMP(I, J, 3)=DX1*(DX8+DX2+DX9+DX3)
TEMP(I, J, 4)=TEMP(I, J, 2)*U(I, J)+TEMP(I, J, 3)*V(I, J)
- DX1*DX10*DX4
7 CONTINUE
C
6 CONTINUE
C
DO 9 K=1, 4
DO 9 J=2, JL1
DO 9 I=2, IL1
RHS(I, J, K)=RHS(I, J, K)+.5*(TEMP(I+1, J, K)-TEMP(I-1, J, K))
9 CONTINUE
C
C ***** DM1 / DETA *****
C
DO 10 J=1, JL
C
DO 11 I=2, IL1
DX1=XMU(I, J)+EDDY(I, J)
DX2=XXI(I, J)*XETA(I, J)
DX3=YXI(I, J)*YETA(I, J)
DX4=XXI(I, J)*YETA(I, J)
DX5=XETA(I, J)*YXI(I, J)
DX6=-DX1*(DX2+XL)*DX3
DX7=DX1*(DX5+XL)*DX4
DX8=DX1*(DX4+XL)*DX5
DX9=-DX1*(XL)*DX2+DX3
DX10=-GAM11)*XMU(I, J)*PRI+EDDY(I, J)*PRT1)
- (DX2+DX3)
C
DX1=REI/XJAC(I, J)

```

```

DX2=.5*(U(I-1,J)-U(I-1,J))
DX3=.5*(V(I-1,J)-V(I-1,J))
DX4=.5*(GAM*P(I-1,J)/RHO(I-1,J)-
P(I-1,J)/RHO(I-1,J))
C
TEMP(I,J,1)=0.0
TEMP(I,J,2)=DX1*(DX6*DX2+DX8*DX3)
TEMP(I,J,3)=DX1*(DX7*DX2+DX9*DX3)
TEMP(I,J,4)=TEMP(I,J,2)+U(I,J)+TEMP(I,J,3)+V(I,J)
- DX1*DX10*DX4
11 CONTINUE
C
10 CONTINUE
C
DO 13 K=1,4
DO 13 J=2,IL1
DO 13 I=2,IL1
RHS(I,J,K)=RHS(I,J,K)-.5*(TEMP(I,J+1,K)-TEMP(I,J-1,K))
13 CONTINUE
C
***** DY1 / DX1 *****
C
DO 14 J=2,IL1
DO 15 I=2,IL1
DX1=.5*(XMU(I,J)+XMU(I-1,J)+EDDY(I,J)+EDDY(I-1,J))
DX2=.5*(XETA(I,J)+XETA(I-1,J))
DX3=.5*(YETA(I,J)+YETA(I-1,J))
DX4=DX2**2
DX5=DX3**2
DX6=DX1*(DX4+XLM*DX5)
DX7=XL1*DX1*DX2*DX3
DX8=DX1*(XLM*DX4+DX5)
DX9=GAM11*.5*(PRI*(XMU(I,J)+XMU(I-1,J))+
PRI*(EDDY(I,J)+EDDY(I-1,J)))*(DX4+DX5)
C
DX1=REI/(.5*(XJAC(I,J)+XJAC(I-1,J)))
DX2=U(I,J)-U(I-1,J)
DX3=V(I,J)-V(I-1,J)
DX4=GAM*(P(I,J)/RHO(I,J)-P(I-1,J)/RHO(I-1,J))
C
TEMP(I,J,1)=0.0
TEMP(I,J,2)=DX1*(DX6*DX2+DX7*DX3)
TEMP(I,J,3)=DX1*(DX7*DX2+DX8*DX3)
TEMP(I,J,4)=TEMP(I,J,2)+.5*(U(I,J)+U(I-1,J))
- TEMP(I,J,3)+.5*(V(I,J)+V(I-1,J))
- DX1*DX9*DX4
15 CONTINUE
C
14 CONTINUE
C
DO 17 K=1,4
DO 17 J=2,IL1
DO 17 I=2,IL1
RHS(I,J,K)=RHS(I,J,K)-(TEMP(I+1,J,K)-TEMP(I,J,K))
17 CONTINUE
C
***** DM2 / DETA *****
C
DO 18 J=2,IL1
DO 19 I=2,IL1
DX1=.5*(XMU(I,J)+XMU(I-1,J)+EDDY(I,J)+EDDY(I-1,J))
DX2=.5*(XMI(I,J)+XMI(I-1,J))
DX3=.5*(YMI(I,J)+YMI(I-1,J))
DX4=DX2**2
DX5=DX3**2
DX6=DX1*(DX4+XLM*DX5)
DX7=XL1*DX1*DX2*DX3
DX8=DX1*(XLM*DX4+DX5)
DX9=GAM11*.5*(PRI*(XMU(I,J)+XMU(I-1,J))+
PRI*(EDDY(I,J)+EDDY(I-1,J)))*(DX4+DX5)
C
DX1=REI/(.5*(XJAC(I,J)+XJAC(I-1,J)))
DX2=U(I,J)-U(I-1,J)
DX3=V(I,J)-V(I-1,J)
DX4=GAM*(P(I,J)/RHO(I,J)-P(I-1,J)/RHO(I-1,J))
C
TEMP(I,J,1)=0.0
TEMP(I,J,2)=DX1*(DX6*DX2+DX7*DX3)
TEMP(I,J,3)=DX1*(DX7*DX2+DX8*DX3)
TEMP(I,J,4)=TEMP(I,J,2)+.5*(U(I,J)+U(I-1,J))
- TEMP(I,J,3)+.5*(V(I,J)+V(I-1,J))
- DX1*DX9*DX4
19 CONTINUE
C
18 CONTINUE
C
DO 21 K=1,4
DO 21 J=2,IL1
DO 21 I=2,IL1
RHS(I,J,K)=RHS(I,J,K)-(TEMP(I,J+1,K)-TEMP(I,J,K))
21 CONTINUE
C
RETURN
END
C
*****
C
SUBROUTINE 'CHATA'. COMPUTES JACOBIAN MATRIX A= DF/DQ
SUBROUTINE CHATA
C
PARAMETER IM=299, JM=100)
COMMON /FLOWY/ U(IM,JM),V(IM,JM),P(IM,JM),RHO(IM,JM),
1XMU(IM,JM),EDDY(IM,JM)
COMMON /GRID/ X(IM,JM),Y(IM,JM),XMI(IM,JM),YMI(IM,JM),
1XETA(IM,JM),YETA(IM,JM),XJAC(IM,JM),S1(IM,JM),SS1(IM,
COMMON /MATRIX/ A(IM,JM,4,4),RHS(IM,JM,4)
COMMON /PI/ IL,IL1,ILE,ITEL,ITEU
COMMON /P2/ GAM,PR,PRI,XMI,RF,TM,S1,ALFA,ANGLE
COMMON /MISC/ IL1,IL2,IL3,IL4,IL5,IL6,ILEP1,ILEM1,
- ITEL1,ITELM1,ITEUP1,ITELM1,GAM1,GAM2,GAM11,GAM,S1P,
- P1,P2,S1M,COS4,PRI,PRI1,REI,XL,XL1,XLM,PI
COMMON /DX/ DX1,DX2,DX3,DX4,DX5,DX6,DX7,DX8,DX9,DX10
COMMON /DUMMY/ TEMP(IM,JM,4)
C
DO 2 J=2,IL1
DO 1 I=1,IL
DX1=.5*(XJAC(I,J)
DX2=YETA(I,J)+U(I,J)-XETA(I,J)+V(I,J)
DX3=.5*(GAM11*(U(I,J)**2+V(I,J)**2)

```

```

DX4=GAM*(P(I,J)*GAM1/RHO(I,J)+.5*(U(I,J)**2
-V(I,J)**2))
C
A(I,J,1,1)=0.
A(I,J,1,2)=-DX1*YETA(I,J)
A(I,J,1,3)=-DX1*XETA(I,J)
A(I,J,1,4)=0.
C
A(I,J,2,1)=DX1*YETA(I,J)+DX3-DX2*U(I,J)
A(I,J,2,2)=DX1*(DX2-GAM2*YETA(I,J)+U(I,J))
A(I,J,2,3)=-DX1*(XETA(I,J)+U(I,J)+GAM1*YETA(I,J)+V(I,J))
A(I,J,2,4)=-DX1*(GAM1*YETA(I,J))
C
A(I,J,3,1)=-DX1*(DX3*XETA(I,J)+DX2*V(I,J))
A(I,J,3,2)=DX1*(GAM1*XETA(I,J)+U(I,J)+YETA(I,J)+V(I,J))
A(I,J,3,3)=DX1*(DX2-GAM2*XETA(I,J)+V(I,J))
A(I,J,3,4)=-DX1*(GAM1*XETA(I,J))
C
A(I,J,4,1)=DX1*(DX2*(2.0-DX3-DX4))
A(I,J,4,2)=DX1*(YETA(I,J)*(DX4-DX3)-GAM1*(DX2*U(I,J)))
A(I,J,4,3)=-DX1*(XETA(I,J)*(DX4-DX3)+GAM1*(DX2*V(I,J)))
A(I,J,4,4)=-DX1*(GAM*DX2)
C
1 CONTINUE
2 CONTINUE
C
RETURN
END
C
*****
C SUBROUTINE 'CHATB', COMPUTES JACOBIAN MATRIX A= DG/DO
SUBROUTINE CHATB
C
PARAMETER(IM=299, JM=100)
COMMON /FLOWV/ U(IM, JM), V(IM, JM), P(IM, JM), RHO(IM, JM),
IXMU(IM, JM), EDDY(IM, JM)
COMMON /GRID/ X(IM, JM), Y(IM, JM), XXI(IM, JM), YXI(IM, JM),
IXETA(IM, JM), YETA(IM, JM), XJAC(IM, JM), S(IM, JM), SSI(IM,
COMMON /MATRIX/ A(IM, JM, 4, 4), RHM(IM, JM, 4)
COMMON /P1/ IL, JL, IL2, ITEL, ITEU
COMMON /P2/ GAM, PR, PRT, XN1, RE, TM, S1, ALFA, ANGLE
COMMON /MISC/ IL1, IL2, IL3, JL1, JL2, JL3, ILEP1, ILEM1,
- ITELPI, ITELMI, ITEUPI, ITEUMI, GAM1, GAM2, GAM11, GXM, S1P,
- PINF, SINA, COSA, PRI, PRTI, REI, XL, XL1, XLM, PI
COMMON /DUMMY/ TEMP(IM, JM, 4)
C
DO 2 J=1, JL
C
DO 1 I=2, IL1
C
DX1=1.0/XJAC(I, J)
DX3= .5*(GAM1*(U(I, J)**2+V(I, J)**2))
DX2=XXI(I, J)+V(I, J)-YXI(I, J)+U(I, J)
DX4=GAM*(GAM1*(P(I, J)/RHO(I, J)+.5*(U(I, J)**2+
V(I, J)**2))
C
A(I, J, 1, 1)=0.
A(I, J, 1, 2)=-DX1*YXI(I, J)
A(I, J, 1, 3)=DX1*XXI(I, J)
A(I, J, 1, 4)=0.
C
A(I, J, 2, 1)=-DX1*(YXI(I, J)+DX3-U(I, J)+DX2)
A(I, J, 2, 2)=DX1*(DX2+GAM2*YXI(I, J)+U(I, J))
A(I, J, 2, 3)=DX1*(GAM1*YXI(I, J)+V(I, J)+XXI(I, J)+U(I, J))
A(I, J, 2, 4)=-DX1*(GAM1*YXI(I, J))
C
A(I, J, 3, 1)=DX1*(XXI(I, J)+DX3-V(I, J)+DX2)
A(I, J, 3, 2)=-DX1*(GAM1*XXI(I, J)+U(I, J)+YXI(I, J)+V(I, J))
A(I, J, 3, 3)=DX1*(DX2-GAM2*XXI(I, J)+V(I, J))
A(I, J, 3, 4)=DX1*(GAM1*XXI(I, J))
C
A(I, J, 4, 1)=DX1*(DX2*(2.0-DX3-DX4))
A(I, J, 4, 2)=-DX1*(YXI(I, J)*(DX4-DX3)+GAM1*(U(I, J)+DX2))
A(I, J, 4, 3)=DX1*(XXI(I, J)*(DX4-DX3)-GAM1*(V(I, J)+DX2))
A(I, J, 4, 4)=-DX1*(GAM*DX2)
C
1 CONTINUE
2 CONTINUE
C
RETURN
END
C
*****
C SUBROUTINE 'CHATR', COMPUTES JACOBIAN MATRIX R= DV1/DQX1
SUBROUTINE CHATR(I, R)
C
PARAMETER(IM=299, JM=100)
COMMON /FLOWV/ U(IM, JM), V(IM, JM), P(IM, JM), RHO(IM, JM),
IXMU(IM, JM), EDDY(IM, JM)
COMMON /GRID/ X(IM, JM), Y(IM, JM), XXI(IM, JM), YXI(IM, JM),
IXETA(IM, JM), YETA(IM, JM), XJAC(IM, JM), S(IM, JM), SSI(IM,
COMMON /MATRIX/ A(IM, JM, 4, 4), RHM(IM, JM, 4)
COMMON /P1/ IL, JL, IL2, ITEL, ITEU
COMMON /P2/ GAM, PR, PRT, XN1, RE, TM, S1, ALFA, ANGLE
COMMON /MISC/ IL1, IL2, IL3, JL1, JL2, JL3, ILEP1, ILEM1,
- ITELPI, ITELMI, ITEUPI, ITEUMI, GAM1, GAM2, GAM11, GXM, S1P,
- PINF, SINA, COSA, PRI, PRTI, REI, XL, XL1, XLM, PI
COMMON /DUMMY/ TEMP(IM, JM, 4)
COMMON /DX/ DX1, DX2, DX3, DX4, DX5, DX6, DX7, DX8, DX9, DX10
DIMENSION R(IM, 4, 4)
C
DO 2 J=2, JL1
C
DX6=XETA(I, J)**2
DX7=YETA(I, J)**2
DX8=XMU(I, J)+EDDY(I, J)
DX1=REI/(RHO(I, J)*XJAC(I, J)**2)
DX2=(DX6-XL*DD7)*DX8
DX3=XL*(DX8*XETA(I, J)+YETA(I, J))
DX4=(XL*(DX6+DX7)+DX8)
DX5=GAM*(XMU(I, J)*PRI+EDDY(I, J)+PRTI)*(DX6+DX7)
C
R(I, J, 1, 1)=0.
R(I, J, 1, 2)=0.
R(I, J, 1, 3)=0.
R(I, J, 1, 4)=0.
C
R(I, J, 2, 1)=-DX1*(DX2*U(I, J)+DX3*V(I, J))
R(I, J, 2, 2)=DX1*(DX2)
R(I, J, 2, 3)=DX1*(DX3)

```

```

C      R(I,2,4)=0.
C      R(I,3,1)=-DX1*(DX3=U(I,J)+DX4=V(I,J))
C      R(I,3,2)=-DX1*DX3
C      R(I,3,3)=-DX1*DX4
C      R(I,3,4)=0.
C      R(I,4,1)=-DX1*(DX2=U(I,J)**2+2.*DX3=U(I,J)*V(I,J)
C      -DX4=V(I,J)**2-DX5=(.5*(U(I,J)**2+V(I,J)**2)
C      -P(I,J)*GAM1/RHO(I,J)))
C      R(I,4,2)=-DX1*(U(I,J)*(DX2-DX5)+DX3=V(I,J))
C      R(I,4,3)=-DX1*(DX3=U(I,J)+V(I,J)*(DX4-DX5))
C      R(I,4,4)=-DX1*DX5
C
C      2 CONTINUE
C
C      RETURN
C      END
C
C *****
C SUBROUTINE 'CMATS', COMPUTES JACOBIAN MATRIX S= DN2/DQETA
C SUBROUTINE CMATS(J,R)
C
C      PARAMETER IM=299, JM=100
C      COMMON /FLOWV/ U(IM, JM), V(IM, JM), P(IM, JM), RHO(IM, JM),
C      IXMU(IM, JM), EDDY(IM, JM)
C      COMMON /GRID/ X(IM, JM), Y(IM, JM), XXI(IM, JM), YXI(IM, JM),
C      IXETA(IM, JM), YETA(IM, JM), XJAC(IM, JM), S(IM, JM), SS1(IM)
C      COMMON /MATRIX/ A(IM, JM, 4, 4), RHS(IM, JM, 4)
C      COMMON /P1/ IL, JL, ILE, ITEL, ITEU
C      COMMON /P2/ GAM, PR, PRT, XMI, RE, TM, S1, ALFA, ANGLE
C      COMMON /MISC/ IL1, IL2, IL3, JL1, JL2, JL3, ILEP1, ILEM1,
C      - ITELPI, ITELMI, ITEUPI, ITEUMI, GAM1, GAM2, GAM11, GXM, S1P,
C      - PINF, SINA, COSA, PRI, PRTI, REI, XL, XL1, XLM, PI
C      COMMON /DUMMY/ TEMP(IM, JM, 4)
C      COMMON /DX/ DX1, DX2, DX3, DX4, DX5, DX6, DX7, DX8, DX9, DX10
C      DIMENSION R(IM, 4, 4)
C
C      DO 1 I=2, IL1
C
C      DX6=XXI(I, J)**2
C      DX7=YXI(I, J)**2
C      DX8=XMU(I, J)+EDDY(I, J)
C
C      DX1=REI/RHO(I, J)*XJAC(I, J)**2)
C      DX2=(DX6+XL*DX7)*DX8
C      DX3=-XL*DX8*XXI(I, J)*YXI(I, J)
C      DX4=XL*DX6+DX7*DX8
C      DX5=(XMU(I, J)+PRI*EDDY(I, J)+PRTI)*(DX6
C      -DX7)*GAM
C
C      R(I,1,1)=0.
C      R(I,1,2)=0.
C      R(I,1,3)=0.
C      R(I,1,4)=0.
C
C      R(I,2,1)=-DX1*(DX2=U(I,J)+DX3=V(I,J))
C      R(I,2,2)=-DX1*DX2
C      R(I,2,3)=-DX1*DX3
C      R(I,2,4)=0.
C
C
C      R(I,3,1)=-DX1*(DX3=U(I,J)+DX4=V(I,J))
C      R(I,3,2)=-DX1*DX3
C      R(I,3,3)=-DX1*DX4
C      R(I,3,4)=0.
C
C      R(I,4,1)=-DX1*(DX2=U(I,J)**2+2.*DX3=U(I,J)*V(I,J)
C      -DX4=V(I,J)**2-DX5=(.5*(U(I,J)**2+V(I,J)**2)
C      -GAM1=P(I, J)/RHO(I, J)))
C      R(I,4,2)=-DX1*(U(I,J)*(DX2-DX5)+DX3=V(I,J))
C      R(I,4,3)=-DX1*(U(I,J)+DX3=V(I,J)*(DX4-DX5))
C      R(I,4,4)=-DX1*DX5
C
C      1 CONTINUE
C
C      RETURN
C      END
C
C *****
C SUBROUTINE "CKMU", COMPUTES MOLECULAR DYNAMIC VISCOSITY USING
C SUTHERLAND'S FORMULA
C SUBROUTINE CKMU(ICHECK)
C
C      PARAMETER IM=299, JM=100
C      COMMON /FLOWV/ U(IM, JM), V(IM, JM), P(IM, JM), RHO(IM, JM),
C      IXMU(IM, JM), EDDY(IM, JM)
C      COMMON /P1/ IL, JL, ILE, ITEL, ITEU
C      COMMON /P2/ GAM, PR, PRT, XMI, RE, TM, S1, ALFA, ANGLE
C      COMMON /MISC/ IL1, IL2, IL3, JL1, JL2, JL3, ILEP1, ILEM1,
C      - ITELPI, ITELMI, ITEUPI, ITEUMI, GAM1, GAM2, GAM11, GXM, S1P,
C      - PINF, SINA, COSA, PRI, PRTI, REI, XL, XL1, XLM, PI
C
C      DO 1 J=1, JL
C      DO 1 I=1, IL
C      T=GX*P(I, J)/RHO(I, J)
C      XMU(I, J)=SQRT(T**3)*S1P/(T+S1)
C      1 CONTINUE
C
C      500 FORMAT (2X, 'T,P,RHO = ',3F10.4, ' AT I, J ',2I4)
C      RETURN
C      END
C
C *****
C SUBROUTINE "CONVRT", COMPUTES RHO/J, RHO=U/J, ETC. USING PRIMITIVE
C VARIABLES RHO, U, V AND P.
C SUBROUTINE CONVRT
C
C      PARAMETER IM=299, JM=100)
C      COMMON /FLOWV/ U(IM, JM), V(IM, JM), P(IM, JM), RHO(IM, JM),
C      IXMU(IM, JM), EDDY(IM, JM)
C      COMMON /GRID/ X(IM, JM), Y(IM, JM), XXI(IM, JM), YXI(IM, JM),
C      IXETA(IM, JM), YETA(IM, JM), XJAC(IM, JM), S(IM, JM), SS1(IM)
C      COMMON /P1/ IL, JL, ILE, ITEL, ITEU
C      COMMON /P2/ GAM, PR, PRT, XMI, RE, TM, S1, ALFA, ANGLE
C      COMMON /MISC/ IL1, IL2, IL3, JL1, JL2, JL3, ILEP1, ILEM1,
C      - ITELPI, ITELMI, ITEUPI, ITEUMI, GAM1, GAM2, GAM11, GXM, S1P,
C      - PINF, SINA, COSA, PRI, PRTI, REI, XL, XL1, XLM, PI
C      COMMON /DUMMY/ TEMP(IM, JM, 4)

```

```

DO 1 J=1,JL
DO 1 I=1,IL
  TEMP(I,J,1)=XJAC(I,J)*RHO(I,J)
  TEMP(I,J,2)=TEMP(I,J,1)*U(I,J)
  TEMP(I,J,3)=TEMP(I,J,1)*V(I,J)
  TEMP(I,J,4)=XJAC(I,J)*GAM1*P(I,J)
  S=RHO(I,J)*(U(I,J)**2+V(I,J)**2)
1 CONTINUE
C
RETURN
END
C
C-----
SUBROUTINE "UCONVRT", COMPUTES PRIMITIVE VARIABLES RHO, U, V AND P
USING RHO, J, RHO=U/J, ETC.
SUBROUTINE UCONVRT
C
PARAMETER (IM=299, JM=100)
COMMON /FLOWV/ U(IM, JM), V(IM, JM), P(IM, JM), RHO(IM, JM),
IXMU(IM, JM), EDDY(IM, JM)
COMMON /GRID/ X(IM, JM), Y(IM, JM), XXI(IM, JM), YXI(IM, JM),
IXETA(IM, JM), YETA(IM, JM), XJAC(IM, JM), S(IM, JM), SSI(IM)
COMMON /P1/ IL, JL, ILE, ITEL, ITEU
COMMON /P2/ GAM, PR, PRI, XMI, RE, TM, S1, ALFA, ANGLE
COMMON /MISC/ IL1, IL2, IL3, JL1, JL2, JL3, ILEP1, ILEM1,
- ITEL1, ITEL1, ITEUP1, ITEUM1, GAM1, GAM2, GAM11, GXM, S1P,
- P1NF, S1NA, COSA, PRI, PRT1, RE1, XL, XL1, XLM, P1
COMMON /NORM/ UNORM, VNORM
COMMON /DUMMY/ TEMP(IM, JM, 4)
C
UNORM = 0.0
VNORM = 0.0
DO 1 J=1,JL
DO 1 I=1,IL
C
  ULAST = U(I,J)
  VLAST = V(I,J)
  RHO(I,J)=TEMP(I,J,1)/XJAC(I,J)
  RR=1/TEMP(I,J,1)
  U(I,J)=TEMP(I,J,2)*RR
  V(I,J)=TEMP(I,J,3)*RR
  P(I,J)=GAM1*RHO(I,J)*(TEMP(I,J,4)*RR-
  S*(U(I,J)**2+V(I,J)**2))
  UNORM = UNORM + ( ULAST - U(I,J) )**2
  VNORM = VNORM + ( VLAST - V(I,J) )**2
C
1 CONTINUE
UNORM = SQRT(UNORM / FLOAT((IL-1)*(JL-1)))
VNORM = SQRT(VNORM / FLOAT((IL-1)*(JL-1)))
C
RETURN
END
C
C-----
SUBROUTINE "CONVRT1" FORMS CONSERVATION VARIABLES USING
THE AVAILABLE PRIMITIVE VARIABLES RHO,U,V,P
SUBROUTINE CONVRT1
PARAMETER (IM=299, JM=100)
COMMON /FLOWV/ U(IM, JM), V(IM, JM), P(IM, JM), RHO(IM, JM),
IXMU(IM, JM), EDDY(IM, JM)
COMMON /GRID/ X(IM, JM), Y(IM, JM), XXI(IM, JM), YXI(IM, JM),
IXETA(IM, JM), YETA(IM, JM), XJAC(IM, JM), S(IM, JM), SSI(IM)
COMMON /P1/ IL, JL, ILE, ITEL, ITEU
COMMON /P2/ GAM, PR, PRI, XMI, RE, TM, S1, ALFA, ANGLE
COMMON /MISC/ IL1, IL2, IL3, JL1, JL2, JL3, ILEP1, ILEM1,
- ITEL1, ITEL1, ITEUP1, ITEUM1, GAM1, GAM2, GAM11, GXM, S1P,
- P1NF, S1NA, COSA, PRI, PRT1, RE1, XL, XL1, XLM, P1
COMMON /DUMMY/ TEMP(IM, JM, 4)
C
DO 1 J=1,JL
DO 1 I=1,IL
  TEMP(I,J,1)=RHO(I,J)
  TEMP(I,J,2)=RHO(I,J)*U(I,J)
  TEMP(I,J,3)=RHO(I,J)*V(I,J)
  TEMP(I,J,4)=GAM11*P(I,J)+S*RHO(I,J)*(U(I,J)**2
  +V(I,J)**2)
1 CONTINUE
C
RETURN
END
C
C-----
SUBROUTINE "MONITR", COMPUTES INFORMATION REQUIRED DURING
TIME INTEGRATION. THIS INCLUDES:
A) CONVERGENCE CRITERIA
B) AIRFOIL LIFT AND DRAG COEFFICIENTS
SUBROUTINE MONITR (NSTEP,TAU,DRMAX,RMSDR)
C
PARAMETER (IM=299, JM=100)
COMMON /FLOWV/ U(IM, JM), V(IM, JM), P(IM, JM), RHO(IM, JM),
IXMU(IM, JM), EDDY(IM, JM)
COMMON /GRID/ X(IM, JM), Y(IM, JM), XXI(IM, JM), YXI(IM, JM),
IXETA(IM, JM), YETA(IM, JM), XJAC(IM, JM), S(IM, JM), SSI(IM)
COMMON /P1/ IL, JL, ILE, ITEL, ITEU
COMMON /P2/ GAM, PR, PRI, XMI, RE, TM, S1, ALFA, ANGLE
COMMON /MISC/ IL1, IL2, IL3, JL1, JL2, JL3, ILEP1, ILEM1,
- ITEL1, ITEL1, ITEUP1, ITEUM1, GAM1, GAM2, GAM11, GXM, S1P,
- P1NF, S1NA, COSA, PRI, PRT1, RE1, XL, XL1, XLM, P1
COMMON /TIMEH/ DTAU(IM, JM), CFL, DTMIN, DTMAX, BETA, DTVIS
COMMON /DUMMY/ TEMP(IM, JM, 4)
COMMON /NORM/ UNORM, VNORM
C
COMPUTE AIRFOIL LIFT AND DRAG COEFFICIENTS
C
CALL LIFT (CLIFT,CDRAG)
C
OUTPUT
WRITE(6,200) NSTEP,TAU,DRMAX,RMSDR,UNORM,VNORM,CLIFT,CDRAG
CP = P(ITEU,1) - 1./GXM
XN=FLOAT(NSTEP)
XLOGM=ALOG10(DRMAX)
XLOGR=ALOG10(RMSDR)
WRITE(3,201) XN,TAU,XLOGM,XLOGR,CLIFT,CDRAG,UNORM,VNORM,
RMSDR,CP
C
FORMATS

```

```
200 FORMAT(1X 'T =',15 'TAU=',E10.3,  
- 'AE12.5', CL=',E12.5', CD=',E12.6)  
201 FORMAT(10E13.5)
```

```
C  
RETURN  
END
```

```
-----  
SUBROUTINE "CONVRC"  
SUBROUTINE CONVRC (DRMAX,RMSDR)
```

```
PARAMETER (IM=299, JM=100)  
COMMON /FLOW/ U(IM, JM), V(IM, JM), P(IM, JM), RHO(IM, JM),  
- XMU(IM, JM), EDDY(IM, JM)  
COMMON /GRID/ X(IM, JM), Y(IM, JM), XXI(IM, JM), YXI(IM, JM),  
- XETA(IM, JM), YETA(IM, JM), XJAC(IM, JM), S(IM, JM), SS1(IM, JM),  
COMMON /MATRIX/ A(IM, JM, 4, 4), RHS(IM, JM, 4)  
COMMON /P1/ IL, JL, ILE, ITEL, ITEU  
COMMON /TIME/ DTAU(IM, JM), CFL, DTMIN, DTMAX, BETA, DTVIS
```

```
C  
SUMR=0.  
DRMAX=0.  
IL1=IL-1  
JL1=JL-1  
FN=FLOAT((IL-2)*(JL-2))
```

```
C  
DO 1 I=2, IL1  
DO 1 J=2, JL1  
DR=ABS(RHS(I, J, 1))  
DRMAX=AMAX1(DRMAX, DR)  
SUMR=SUMR+DR
```

```
1 CONTINUE  
RMSDR=SQRT(SUMR/FN)  
RETURN  
END
```

```
-----  
SUBROUTINE "BTRIDX" SOLVES BLOCK-TRIDIAGONAL SYSTEMS  
FOR THE XI - SHEEP  
SUBROUTINE BTRIDX
```

```
C  
PARAMETER (IM=299, JM=100)  
COMMON /GRID/ X(IM, JM), Y(IM, JM), XXI(IM, JM), YXI(IM, JM),  
1 XETA(IM, JM), YETA(IM, JM), XJAC(IM, JM), S(IM, JM), SS1(IM, JM),  
COMMON /MATRIX/ A(IM, JM, 4, 4), RHS(IM, JM, 4)  
COMMON /P1/ IL, JL, ILE, ITEL, ITEU  
COMMON /MISC/ ILS, ILS2, ILS3, JL1, JL2, JL3, ILEP1, ILEM1,  
- ITEL1, ITEL2, ITEL3, ITEU1, ITEU2, GAM1, GAM2, GAM3, GAM4, GAM5, S1P,  
- P1NF, S1NA, COSA, PRI, PART, REI, XL, XL1, XLM, PI  
COMMON /TIME/ DTAU(IM, JM), CFL, DTMIN, DTMAX, BETA, DTVIS  
COMMON /DUMMY/ TEMP(IM, JM, 4)  
COMMON /DAMP/ WE, W1, WPE, WPI, ISPECT  
COMMON /SPECTR/ SPECT(IM, JM), PSMU(IM, JM)  
COMMON /DX/ DX1, DX2, DX3, DX4, DX5, DX6, DX7, DX8, DX9, DX10  
COMMON /BTRID/ AA(IM, 4, 4), BB(IM, 4, 4), CC(IM, 4, 4),  
- HRK(IM, 4, 4), L11(IM), L21(IM), L22(IM), L31(IM),  
- L32(IM), L33(IM), L41(IM), L42(IM),  
- L43(IM), L44(IM), U12(IM), U13(IM), U14(IM),
```

```
- U23(IM), U24(IM), U34(IM)
```

```
C  
REAL L11, L21, L22, L31, L32, L33, L41, L42, L43, L44,  
- U12, U13, U14, U23, U24, U34
```

```
-----  
PART 1. FORWARD SHEEP
```

```
-----  
PREPARE FOR FIRST ITERATION  
CALL FILLMX(2)
```

```
C  
DO 1 I=2, IL1
```

```
C  
IF (I.EQ.2) GO TO 100
```

```
C  
DO 2 L=1, 4  
DO 2 J=2, JL1
```

```
C  
RHS(I, J, L)=RHS(I, J, L)-BB(J, L, 1)*RHS(I-1, J, 1)  
1 -BB(J, L, 2)*RHS(I-1, J, 2)  
2 -BB(J, L, 3)*RHS(I-1, J, 3)  
3 -BB(J, L, 4)*RHS(I-1, J, 4)
```

```
C  
AA(J, L, 1)=AA(J, L, 1)-BB(J, L, 1)*A(I-1, J, 1, 1)  
1 -BB(J, L, 2)*A(I-1, J, 2, 1)  
2 -BB(J, L, 3)*A(I-1, J, 3, 1)  
3 -BB(J, L, 4)*A(I-1, J, 4, 1)
```

```
C  
AA(J, L, 2)=AA(J, L, 2)-BB(J, L, 1)*A(I-1, J, 1, 2)  
1 -BB(J, L, 2)*A(I-1, J, 2, 2)  
2 -BB(J, L, 3)*A(I-1, J, 3, 2)  
3 -BB(J, L, 4)*A(I-1, J, 4, 2)
```

```
C  
AA(J, L, 3)=AA(J, L, 3)-BB(J, L, 1)*A(I-1, J, 1, 3)  
1 -BB(J, L, 2)*A(I-1, J, 2, 3)  
2 -BB(J, L, 3)*A(I-1, J, 3, 3)  
3 -BB(J, L, 4)*A(I-1, J, 4, 3)
```

```
C  
AA(J, L, 4)=AA(J, L, 4)-BB(J, L, 1)*A(I-1, J, 1, 4)  
1 -BB(J, L, 2)*A(I-1, J, 2, 4)  
2 -BB(J, L, 3)*A(I-1, J, 3, 4)  
3 -BB(J, L, 4)*A(I-1, J, 4, 4)
```

```
C  
2 CONTINUE
```

```
C  
100 CONTINUE
```

```
-----  
USE CROUT'S METHOD TO SOLVE 4 X 4 SYSTEMS OF EQUATIONS
```

```
C  
DO 3 J=2, JL1
```

```
L11(J)=1./AA(J, 1, 1)  
U12(J)=AA(J, 1, 2)*L11(J)  
U13(J)=AA(J, 1, 3)*L11(J)  
U14(J)=AA(J, 1, 4)*L11(J)  
L21(J)=AA(J, 2, 1)  
L22(J)=1./(AA(J, 2, 2)-L21(J)*U12(J))  
U23(J)=L22(J)*(AA(J, 2, 3)-L21(J)*U13(J))  
U24(J)=L22(J)*(AA(J, 2, 4)-L21(J)*U14(J))
```

```

L31(J)=AA(J,3,1)
L32(J)=AA(J,3,2)-L31(J)*U12(J)
L33(J)=1./AA(J,3,3)-L31(J)*U13(J)-L32(J)*U23(J)
U34(J)=L33(J)*AA(J,3,4)-L31(J)*U14(J)
1 -L32(J)*U24(J)
1 L41(J)=AA(J,4,1)
L42(J)=AA(J,4,2)-L41(J)*U12(J)
L43(J)=AA(J,4,3)-L41(J)*U13(J)-L42(J)*U23(J)
L44(J)=1./AA(J,4,4)-L41(J)*U14(J)
1 -L42(J)*U24(J)-L43(J)*U34(J)
C
C
C SOLVE FOR INTERMEDIATE VECTOR
C
DX1=L11(J)*RHS(I,J,1)
DX2=L22(J)*RHS(I,J,2)-L21(J)*DX1
DX3=L33(J)*RHS(I,J,3)-L31(J)*DX1
1 -L32(J)*DX2
DX4=L44(J)*RHS(I,J,4)-L41(J)*DX1
1 -L42(J)*DX2-L43(J)*DX3
C
RHS(I,J,4)=DX4
RHS(I,J,3)=DX3-U34(J)*DX4
RHS(I,J,2)=DX2-U23(J)*RHS(I,J,3)
1 -U24(J)*DX4
RHS(I,J,1)=DX1-U12(J)*RHS(I,J,2)
1 -U13(J)*RHS(I,J,3)-U14(J)*DX4
C
3 CONTINUE
C
IF (I.EQ.II1) GO TO 1
C
C COMPUTE GAMMA(I,J) (SEE NOTES FOR DEF.)
C
DO 4 M=1,4
DO 4 J=2,JL1
C
DX1=L11(J)*CC(J,1,M)
DX2=L22(J)*CC(J,2,M)-L21(J)*DX1
DX3=L33(J)*CC(J,3,M)-L31(J)*DX1
1 -L32(J)*DX2
DX4=L44(J)*CC(J,4,M)-L41(J)*DX1
1 -L42(J)*DX2-L43(J)*DX3
C
MRK(J,4,M)=DX4
MRK(J,3,M)=DX3-U34(J)*DX4
MRK(J,2,M)=DX2-U23(J)*MRK(J,3,M)
1 -U24(J)*DX4
MRK(J,1,M)=DX1-U12(J)*MRK(J,2,M)
1 -U13(J)*MRK(J,3,M)-U14(J)*DX4
C
4 CONTINUE
C
C COMPUTE AA,BB,CC FOR NEXT ITERATION
C
CALL FILLM(I+1)
C
C SAVE GAMMA(I,J)'S ON JACOBIAN MATRIX A
C
DO 5 L=1,4
DO 5 M=1,4
DO 5 J=2,JL1
C
A(I,J,L,M)=MRK(J,L,M)
5 CONTINUE
C
1 CONTINUE
C
C PART 2. BACKWARD SWEEP
C
C
IIE=II1-2
DO 6 II=1,IIE
I=II1-II
C
DO 7 L=1,4
DO 7 J=2,JL1
C
RHS(I,J,L)=RHS(I,J,L)-A(I,J,L,1)*RHS(I+1,J,1)
1 -A(I,J,L,2)*RHS(I+1,J,2)
2 -A(I,J,L,3)*RHS(I+1,J,3)
3 -A(I,J,L,4)*RHS(I+1,J,4)
C
7 CONTINUE
6 CONTINUE
C
RETURN
END
C
C-----
C
SUBROUTINE "FILLM" FORMS 4X4 BLOCKS AA, BB, CC
REQUIRED IN XI - SWEEP (INCLUDES IMPLICIT DAMPING)
SUBROUTINE FILLM (I)
C
PARAMETER (IM=299, JM=100)
COMMON /GRID/ X(IM, JM), Y(IM, JM), X1(IM, JM), Y1(IM, JM),
1 XETA(IM, JM), YETA(IM, JM), XJAC(IM, JM), S(IM, JM), SSI(IM)
COMMON /MATRIX/ A(IM, JM, 4, 4), RHS(IM, JM, 4)
COMMON /PI/ IL, JL, ILE, ITEL, ITEU
COMMON /MISC/ IL1, IL2, IL3, JL1, JL2, JL3, ILEP1, ILEM1,
- ITELPI, ITELM1, ITEUP1, ITEUM1, GAM1, GAM2, GAM11, GAM, S1P,
- P1NF, S1NA, COSA, PRI, PATI, REI, XL, XLI, XLM, PI
COMMON /TIME/ DTAU(IM, JM), CFL, DTMIN, DTMAX, BETA, DTVIS
COMMON /DUMP/ TEMP(IM, JM, 4)
COMMON /DAMP/ ME, MI, WPE, MPI, ISPECT
COMMON /SPECT/ SPECT(IM, JM), PSMU(IM, JM)
COMMON /STRID/ AA(IM, 4, 4), BB(IM, 4, 4), CC(IM, 4, 4),
- MRK(IM, 4), L11(IM), L21(IM), L22(IM), L31(IM),
- L32(IM), L33(IM), L41(IM), L42(IM),
- L43(IM), L44(IM), U12(IM), U13(IM), U14(IM),
- U23(IM), U24(IM), U34(IM)
COMMON /CMAT/ RR(IM, 4, 4), RP1(IM, 4, 4), RM1(IM, 4, 4)
C
REAL L11, L21, L22, L31, L32, L33, L41, L42, L43, L44,
- U12, U13, U14, U23, U24, U34
C
C COMPUTE VISCOUS JACOBIAN MATRIX 'R'
IP=I+1
IM=I-1
IF (I.GT.2) GOTO 100
CALL CMATRI, RR

```



```

C
L11(I)=1./AA(I,1,1)
U12(I)=AA(I,1,2)*L11(I)
U13(I)=AA(I,1,3)*L11(I)
U14(I)=AA(I,1,4)*L11(I)
L21(I)=AA(I,2,1)
L22(I)=1./AA(I,2,2)-L21(I)*U12(I)
U23(I)=L22(I)*AA(I,2,3)-L21(I)*U13(I)
U24(I)=L22(I)*AA(I,2,4)-L21(I)*U14(I)
L31(I)=AA(I,3,1)
L32(I)=AA(I,3,2)-L31(I)*U12(I)
L33(I)=1./AA(I,3,3)-L31(I)*U13(I)-L32(I)*U23(I)
U34(I)=L33(I)*AA(I,3,4)-L31(I)*U14(I)
1 -L32(I)*U24(I)
L41(I)=AA(I,4,1)
L42(I)=AA(I,4,2)-L41(I)*U12(I)
L43(I)=AA(I,4,3)-L41(I)*U13(I)-L42(I)*U23(I)
L44(I)=1./AA(I,4,4)-L41(I)*U14(I)
1 -L42(I)*U24(I)-L43(I)*U34(I)
C
SOLVE FOR INTERMEDIATE VECTOR
DX1=L11(I)*RHS(I,J,1)
DX2=L22(I)*(RHS(I,J,2)-L21(I)*DX1)
DX3=L33(I)*(RHS(I,J,3)-L31(I)*DX1
1 -L32(I)*DX2)
DX4=L44(I)*(RHS(I,J,4)-L41(I)*DX1
1 -L42(I)*DX2-L43(I)*DX3)
C
RHS(I,J,4)=DX4
RHS(I,J,3)=DX3-U34(I)*DX4
RHS(I,J,2)=DX2-U23(I)*RHS(I,J,3)
1 -U24(I)*DX4
RHS(I,J,1)=DX1-U12(I)*RHS(I,J,2)
1 -U13(I)*RHS(I,J,3)-U14(I)*DX4
C
3 CONTINUE
C
IF (J EQ JLI) GO TO 1
C
----- COMPUTE GAMMA(I,J) (SEE NOTES FOR DEF.) -----
C
DO 4 M=1,4
DO 4 I=2,IL1
C
DX1=L11(I)*CC(I,1,M)
DX2=L22(I)*(CC(I,2,M)-L21(I)*DX1)
DX3=L33(I)*(CC(I,3,M)-L31(I)*DX1
1 -L32(I)*DX2)
DX4=L44(I)*(CC(I,4,M)-L41(I)*DX1
1 -L42(I)*DX2-L43(I)*DX3)
C
WRK(I,4,M)=DX4
WRK(I,3,M)=DX3-U34(I)*DX4
WRK(I,2,M)=DX2-U23(I)*WRK(I,3,M)
1 -U24(I)*DX4
WRK(I,1,M)=DX1-U12(I)*WRK(I,2,M)
1 -U13(I)*WRK(I,3,M)-U14(I)*DX4
C
4 CONTINUE
C
----- COMPUTE AA,BB,CC FOR NEXT ITERATION -----
C
CALL FILLMY(J+1)
C
----- SAVE GAMMA(I,J)'S ON JACOBIAN MATRIX A -----
C
DO 5 L=1,4
DO 5 M=1,4
DO 5 I=2,IL1
A(I,J,L,M)=WRK(I,L,M)
5 CONTINUE
1 CONTINUE
C
----- PART 2. BACKWARD SWEEP -----
C
JJE=JLI-2
DO 6 JJ=1,JJE
J=JLI-JJ
C
DO 7 L=1,4
DO 7 I=2,IL1
C
RHS(I,J,L)=RHS(I,J,L)-A(I,J,L,1)*RHS(I,J+1,1)
1 -A(I,J,L,2)*RHS(I,J+1,2)
2 -A(I,J,L,3)*RHS(I,J+1,3)
3 -A(I,J,L,4)*RHS(I,J+1,4)
C
7 CONTINUE
6 CONTINUE
C
RETURN
END
C
-----
C
SUBROUTINE "FILLMY" FORMS 4X4 BLOCKS AA, BB, CC
REQUIRED IN ETA - SWEET (INCLUDES IMPLICIT DAMPING)
SUBROUTINE FILLMY (J)
C
PARAMETER IM=299, JM=100)
COMMON /GRID/ X(IM, JM), Y(IM, JM), XXI(IM, JM), YXI(IM, JM),
IXETA(IM, JM), YETA(IM, JM), XJAC(IM, JM), S(IM, JM), SSI(IM),
COMMON /MATRIX/ A(IM, JM, 4, 4), RHS(IM, JM, 4),
COMMON /PI/ IL, JL, IL2, ITEL, ITEU
COMMON /MISC/ IL1, IL2, IL3, JLI, JL2, JLS, ILEP1, ILEM1,
- ITEL1, ITEL2, ITEU1, ITEL3, GAM1, GAM2, GAM3, GAM4, S1P,
- P1P, S1M, COS4, PRT1, PRT2, SEI, XL, XLM, P1
COMMON /TIME/ DTAU(IM, JM), CFL, DTMIN, DTMAX, BETA, DTVIS
COMMON /DUMMY/ TEMP(IM, JM, 4)
COMMON /DAMP/ ME, MT, WPE, WPT, ISPECT
COMMON /SPECTR/ SPECT(IM, JM), PSMU(IM, JM)
COMMON /BTRID/ AA(IM, 4, 4), BB(IM, 4, 4), CC(IM, 4, 4),
- L11(IM), L21(IM), L31(IM), L41(IM), L22(IM), L32(IM),
- L42(IM), L33(IM), L43(IM), L44(IM), U12(IM), U13(IM), U14(IM),
- U23(IM), U24(IM), U34(IM)

```

```
COMMON/CHAT/ RR(IM,4,4),RP1(IM,4,4),RM1(IM,4,4)
C
REAL L11,L21,L22,L31,L32,L33,L41,L42,L43,L44,
  U12,U13,U14,U23,U24,U34
```

```
C COMPUTE VISCOUS JACOBIAN MATRIX 'R'
```

```
  JPI=J+1
  JMI=J-1
  IF ( J .GT. 2 ) GOTO 100
  CALL CHATS(J,RR)
  CALL CHATS(JMI,RM1)
  GOTO 200
100 DO 11 M=1,4
    DO 11 L=1,4
    DO 11 I=2,IL1
      RM1(I,L,M) = RR(I,L,M)
      RR(I,L,M) = RP1(I,L,M)
11 CONTINUE
C
200 CONTINUE
  CALL CHATS(JPI,RP1)
  DO 1 L=1,4
  DO 2 M=1,4
  DO 2 I=2,IL1
    AA(I,L,M)=2.*RR(I,L,M)
    BB(I,L,M)=-1.5*AA(I,J-1,L,M)+RM1(I,L,M)
    CC(I,L,M)=.5*AA(I,J+1,L,M)-RP1(I,L,M)
  2 CONTINUE
```

```
C ----- ADD IMPLICIT DAMPING -----
```

```
  DO 3 I=2,IL1
  WISP=SPEC7(I,J)**(NI*WPI*PSMU(I,J))
  AA(I,L,L)=AA(I,L,L)+2.*WISP/XJAC(I,J)
  BB(I,L,L)=BB(I,L,L)-WISP/XJAC(I,J-1)
  CC(I,L,L)=CC(I,L,L)-WISP/XJAC(I,J+1)
  3 CONTINUE
```

```
C ----- MULTIPLY BY DTAU(I,J) -----
```

```
  DO 4 M=1,4
  DO 4 I=2,IL1
  AA(I,L,M)=DTAU(I,J)*AA(I,L,M)
  BB(I,L,M)=DTAU(I,J)*BB(I,L,M)
  CC(I,L,M)=DTAU(I,J)*CC(I,L,M)
  4 CONTINUE
```

```
C ----- ADD IDENTITY MATRIX TO AA (DIAGONAL) -----
```

```
  DO 5 I=2,IL1
  AA(I,L,L)=AA(I,L,L)+1.0
  5 CONTINUE
```

```
C 1 CONTINUE
```

```
  RETURN
  END
```

```
C SUBROUTINE "BNDRY" IMPLEMENTS BOUNDARY CONDITIONS
C CASE : VISCOUS FLOW, AIRFOIL C-GRID
C SUBROUTINE BNDRY
```

```
  PARAMETER(IM=299, JM=100)
  COMMON /FLOWV/ U(IM,JM),V(IM,JM),P(IM,JM),RHO(IM,JM),
  IXMU(IM,JM),EDDY(IM,JM)
  COMMON /GRID/ X(IM,JM),Y(IM,JM),XXI(IM,JM),XXI(IM,JM),
  IYETA(IM,JM),YETA(IM,JM),XJAC(IM,JM),S(IM,JM),SS1(IM)
  COMMON /P1/ IL,JL,ILE,ITEL,ITEU
  COMMON /P2/ GAM,PR,PR1,XM1,RE,IM,S1,ALFA,ANGLE
  COMMON/MISC/IL1,IL2,IL3,JL1,JL2,JL3,ILEP1,ILEM1,
  ITELP1,ITELM1,ITEUP1,ITEUM1,GAM1,GAM2,GAM1,GKN,SIP,
  P1NF,S1NA,COSA,PR1,PR1,RE1,XL,XL1,XLM,PI
  COMMON/DUMMY/ TEND(IM,JM,4)
  COMMON/DX/ DX1,DX2,DX3,DX4,DX5,DX6,DX7,DX8,DX9,DX10
  COMMON/BNDR/ NBND,XMREF,TREF,TINF,CV,CR,CT,DEL,L1,L2,L3,L4
```

```
C DOWNSTREAM BOUNDARIES (XI=0, XI=MAX) : SUBSONIC OUTFLOW
C PEXIT SPECIFIED, EXTRAPOLATION FOR RHO,U,V.
```

```
  DO 12 J=2,JL1
  U(1,J)=U(2,J)
  V(1,J)=V(2,J)
  P(1,J)=PINF
  RHO(1,J)=RHO(2,J)
  EDDY(1,J)=EDDY(2,J)
  12 CONTINUE
```

```
  DO 22 J=2,JL1
  U(IL,J)=U(IL1,J)
  V(IL,J)=V(IL1,J)
  P(IL,J)=PINF
  EDDY(IL,J)=EDDY(IL1,J)
  RHO(IL,J)=RHO(IL1,J)
  22 CONTINUE
```

```
C ETA = ETAMAX, FREESTREAM VALUES SPECIFIED
```

```
  DO 25 I=1,IL
  U(1,JL)=COSA
  V(1,JL)=SINA
  P(1,JL)=PINF
  RHO(1,JL)=1.0
  25 CONTINUE
```

```
C AIRFOIL SURFACE AND MAKE CUT
```

```
C MAKE-CUT : AVERAGED EXTRAPOLATION
```

```
  DO 9 I=1,ITEL
  K=IL-I+1
  U(I,1)=.5*(U(I,2)+U(K,2))
  V(I,1)=.5*(V(I,2)+V(K,2))
  P(I,1)=.5*(P(I,2)+P(K,2))
  RHO(I,1)=.5*(RHO(I,2)+RHO(K,2))
  U(K,1)=U(I,1)
  V(K,1)=V(I,1)
  P(K,1)=P(I,1)
```


Appendix G: Hyperbolic Grid Generating Code,
Fortran Listing

The attached fortran listing is the original code used to generate the grids in this work as supplied by the Air Force Wright Aerodynamics Laboratories, Flight Dynamics Laboratory, Computational Fluid Dynamics Group. The code was developed jointly by Dr. Timothy Barth and Dr. Don Kinsey and described in reference (19). The code was run on the Cyber computer.

```

PROGRAM MAIN
C
C THIS PROGRAM GENERATES HYPERBOLIC C-MESHES ABOUT AIRFOILS
C WRITTEN BY TIM BARTH
C
OPEN(6,FILE='OUTPUT')
OPEN(5,FILE='INPUT')
CALL STARTE
CALL FOIL
CALL PARAM
CALL STRET
CALL MAKE
CALL GRIDGE
STOP
END
C
C-----
C
SUBROUTINE STARTE
C
COMMON/BASE/JMAX,KMAX,PI,SBODY,SMJ,SMJV,NBODY,NCLUST
COMMON/VARS/X(301),Y(301),XXI(301),XETA(301),YXI(301),
1 YETA(301),R(301),SCALE(100),SR(301,2),VOL(301)
COMMON /UNITS / BODYUN,GRIDUN,DOCU1
COMMON /FNAMES / BODYFI,GRIDFI,DOCFIL
COMMON /STRET / DS(100),CNTRLP(100),NBP(100),ARCLEN(301)
CHARACTER=80 BODYFI,GRIDFI,DOCFIL
INTEGER BODYUN,GRIDUN,DOCU1
C
C SET UP DOCUMENTATION FILE
C
1000 FORMAT(A)
10 CONTINUE
WRITE(6,*) ' INPUT DOC FILE NAME '
READ(5,1000)DOCFIL
DOCU1 = 1
OPEN(11,FILE=DOCFIL)
20 CONTINUE
WRITE(6,*) ' INPUT GRID FILE NAME '
READ(5,1000)GRIDFI
GRIDUN = 0
OPEN(9,FILE=GRIDFI)
RETURN
END
C
C-----
C
SUBROUTINE FOIL
C
COMMON/BASE/JMAX,KMAX,PI,SBODY,SMJ,SMJV,NBODY,NCLUST
COMMON/VARS/X(301),Y(301),XXI(301),XETA(301),YXI(301),
1 YETA(301),R(301),SCALE(100),SR(301,2),VOL(301)
COMMON /UNITS / BODYUN,GRIDUN,DOCU1
COMMON /FNAMES / BODYFI,GRIDFI,DOCFIL
COMMON /STRET / DS(100),CNTRLP(100),NBP(100),ARCLEN(301)
CHARACTER=80 BODYFI,GRIDFI,DOCFIL
CHARACTER=1 ANSWER
INTEGER BODYUN,GRIDUN,DOCU1
C
C SET UP FILE
C
1000 FORMAT(A)
WRITE(6,*) ' DO YOU HAVE BODY COORDINATES ON FILE (Y/N)? '
READ(5,1000)ANSWER
IF(ANSWER.EQ.'Y'.OR.ANSWER.EQ.'Y')THEN
C
WRITE(6,*) ' INPUT BODY FILE NAME '
READ(5,1000)BODYFI
BODYUN = 10
OPEN(10,FILE=BODYFI)
5 CONTINUE
KOUNT = 0
CONTINUE
10 READ(BODYUN,*,END=100)X(KOUNT+1),Y(KOUNT+1)
KOUNT=KOUNT+1
GO TO 10
100 CONTINUE
NBODY = KOUNT
WRITE(DOCUN1,2000)BODYFI,NBODY
2000 WRITE(6,2000)BODYFI,NBODY
FORMAT 'BODY FILE WAS USER INPUT ',A7,' WITH ',I5,' POINTS'
CLOSE (BODYUN)
C
ELSE
WRITE(6,*) ' *****MACADOXX AIRFOIL*****'
WRITE(6,*) ' *****CLOSED TE NORMALIZED*****'
WRITE(6,*) ' INPUT XX'
READ(5,*)TMAX
WRITE(DOCUN1,*) ' MACADOXX AIRFOIL: XX = ',TMAX
TMAX = TMAX/100.
NPTS = 300
NHALF = NPTS/2 + 1
NIMM = NHALF - 1
XINCP1 = 1.008930411365
DELX = 1./FLOAT(NIMM)
XX = 1. + DELX
DO 20 I=1,NIMM
XX = XX - DELX
X1 = .5*XINCP1*(1.0 - COS(3.1415926535*XX))
X1I = X1
Y1I = -.5*TMAX*(0.2969*SQRT(X1) - .126*X1 - 0.3516*X1*X1
+ 0.2843*X1**3 - 0.1015*X1**4)
20 CONTINUE
DO 21 I=1,NIMM
I1 = NHALF - I
I2 = NHALF + I
X'1I = X1I
Y'1I = -Y1I
21 CONTINUE
NPTS = NPTS + 1
DO 22 I=1,NPTS
X1I = X1I/XINCP1
Y1I = Y1I/XINCP1
22 CONTINUE
NBODY = NPTS
ENDIF
RETURN
END
C
C-----

```

SUBROUTINE PARAME

```

COMMON BASE JMAX,KMAX,PI,SBODY,SMU,SMUX,NBODY,NCLUST
COMMON VARS X,301,Y,301,XX,301,YY,301,ALFA,301,YP,301
: YETA,301,SR,301,100,SCALE,100,SR,301,21,VOL,301
COMMON /UNITS, BODYUN,GRIDUN,DOCFIL
COMMON /FNAMES, BODYFI,GRIDFI,DOCFI
COMMON /STRET, DS(100),CNTRLP(100),NBP,100,ARCLEN,301
DIMENSION XS(100)
CHARACTER=5 LOWER,UPPER,XXXXX
CHARACTER=80 BODYFI,GRIDFI,DOCFI
INTEGER BODYUN,GRIDUN,DOCFI
LOWER = 'LOWER'
UPPER = 'UPPER'

      FIND LE
      XMIN = 1000
      DO 9876 J=1,NBODY
      IF (X(J) .LT. XMIN) THEN
        XMIN = X(J)
      ENDIF
9876 CONTINUE
      JLE = JMIN

      NCLUST = 0
      WRITE(6,*) '*****AIRFOIL LOWER SURFACE*****'
10 CONTINUE
      WRITE(6,*) ' INPUT X LOCATION, MIN ARLENGTH SPACING, '
      WRITE(6,*) ' RETURN TO CONTINUE '
      READ(5,*) END=20, XS, NCLUST-1, DS, NCLUST-1
      NCLUST = NCLUST-1
      GO TO 10
20 REWIND 5

      BRUTE FORCE BUBBLE SORT
      DO9875 N=1,NCLUST
      DO9874 M=1,NCLUST
      IF (XS(M) .LT. XS(N)) THEN
        TEMP1 = XS(M)
        TEMP2 = DS(M)
        XS(M) = XS(N)
        DS(M) = DS(N)
        XS(N) = TEMP1
        DS(N) = TEMP2
      ENDIF
9874 CONTINUE
9875 CONTINUE

      FIND NEAREST BODY POINT
      DO9873 N=1,NCLUST
      RMAX = 1.E6
      DO9872 J=1,JLE
      RR = ABS(XS(N)-X(J))
      IF (RR .LT. RMAX) THEN
        RMAX = RR
      ENDIF
      JJ = J
9872 CONTINUE
      CNTRLP(N) = JJ
9873 CONTINUE
      NLOWER = NCLUST
      WRITE(6,*) '*****AIRFOIL UPPER SURFACE*****'
30 CONTINUE
      WRITE(6,*) ' INPUT Y LOCATION, MIN ARLENGTH SPACING, '
      WRITE(6,*) ' RETURN TO CONTINUE '
      READ(5,*) END=40, YS, NCLUST-1, DS, NCLUST-1
      NCLUST = NCLUST-1
      GO TO 30
40 REWIND 5

      BRUTE FORCE BUBBLE SORT
      DO9871 M=NLOWER-1,NCLUST
      DO9870 N=NLOWER-1,NCLUST
      IF (YS(M) .GT. YS(N)) THEN
        TEMP1 = YS(M)
        TEMP2 = DS(M)
        YS(M) = YS(N)
        DS(M) = DS(N)
        YS(N) = TEMP1
        DS(N) = TEMP2
      ENDIF
9870 CONTINUE
9871 CONTINUE

      FIND NEAREST BODY POINT
      DO9869 N=NLOWER-1,NCLUST
      RMAX = 1.E6
      DO9868 J=1,NBODY
      RR = ABS(YS(N)-Y(J))
      IF (RR .LT. RMAX) THEN
        RMAX = RR
      ENDIF
      JJ = J
9868 CONTINUE
      CNTRLP(N) = JJ
9869 CONTINUE

      ARCLEN(1) = 0
      DO9866 I=1,NBODY
      ARCLEN(I) = ARCLEN(I) +
      SORT((X(I)-X(I+1))**2 + (Y(I)-Y(I+1))**2)
9866 CONTINUE

      WRITE(DOCUNI,*) '***** CLUSTERINGS *****'
      DO9865 I=2,NCLUST
      IB1 = CNTRLP(I)
      IB2 = CNTRLP(I-1)
      XXXXX = UPPER
      IF (JLE NLOWER) XXXXX = LOWER
      ALENGT = ARCLEN(IB1) - ARCLEN(IB2)
      WRITE(6,2000) I, IB2, IB1, ALENGT, XXXXX

```

```

2000 > FORMAT(' INPUT NUMBER OF POINTS FOR THE INTERVAL X = ',
> F12.6, ' TO X = ', F12.6, '
> ARCLength = ', F12.6, ' ON THE 'A.' SURFACE')
READ(5, *INBP, I=1)
WRITE(DOCUNI, 3000) X(I B2), X(I B1), NBP(I-1), KXXX, DS(I),
3000 > DS, I=1
> FORMAT(' NUMBER OF POINTS FOR THE INTERVAL X = ',
> F12.6, ' TO X = ', F12.6, ' IS ', I5,
> ON THE 'A.' SURFACE. ' IS ', I5,
> ' MIN SPACING ON ENDS ARE ', F14.7, I X, F14.7)
9845 CONTINUE
RETURN
END

```

```

C
SUBROUTINE MAKE
C

```

```

COMMON /BASE/ JMAX, KMAX, PI, SBODY, SMU, SMUV, NBODY, MCLUST
COMMON /VARS/ X(301), Y(301), XX(301), YETA(301), YX(301),
1 YETA(301), R(301), 100, SCALE(100), SR(301,2), VOL(301)
COMMON /UNITS/ BODYUN, GRIDUN, DOCUNI
COMMON /FNAMES/ BODYFI, GRIDFI, DOCFIL
COMMON /STRET/ DS, 100, CNTRLP, 100, NBP, 100, ARCLEN, 301
CHARACTER*1 ANSWER
CHARACTER*80 BODYFI, GRIDFI, DOCFIL
INTEGER BODYUN, GRIDUN, DOCUNI
COMMON /BOO/ XINTER(301), YINTER(301), IMAX
COMMON /SOB/ SOB
DIMENSION XMAKE(301), YMAKE(301), XK(10), YK(10)

```

```

WRITE(6, *) '====OUTER DOMAIN LIMITS===='
WRITE(6, *) ' INPUT DISTANCE TO OUTER BOUNDARY'
READ(5, *) SOB
WRITE(DOCUNI, *) ' DISTANCE TO OUTER BOUNDARY = ', SOB
WRITE(6, *) ' INPUT NUMBER OF POINTS IN THE WAKE REGION'
READ(5, *) NMAKE
WRITE(DOCUNI, *) ' NMAKE = ', NMAKE

```

```

SLOPE ESTIMATION

```

```

THETA1 = ATAN2(YINTER(IMAX)-YINTER(IMAX-1),
> XINTER(IMAX)-XINTER(IMAX-1))
THETA2 = ATAN2(YINTER(1)-YINTER(2),
> XINTER(1)-XINTER(2))
SLOPE = TAN(.5*(THETA1-THETA2))
WRITE(6, *) ' TRAILING EDGE SLOPE = ', SLOPE
WRITE(6, *)
> ' DO YOU WISH TO CHANGE SLOPE ESTIMATION <Y/N>? '
READ(5, *) ANSWER
IF(ANSWER .EQ. 'Y' .OR. ANSWER .EQ. 'Y') THEN
WRITE(6, *) ' INPUT NEW SLOPE='
READ(5, *) SLOPE
ENDIF
YOPRIM = SLOPE
YIPRIM = 0.00000

```

```

START CUBIC PATCH AT X/C=1.05. END CUBIC AT X/C=1.5.

```

```

X0 = 1.01C
Y0 = YINTER(1) + YOPRIM*(X0-XINTER(1))
X1 = 1.2
Y1 = 2*(Y0-YINTER(1))
YINTER(1) = YOPRIM*(X0-XINTER(1))/2
WRITE(6, *) ' X0, Y0, X1, Y1 = ', X0, Y0, X1, Y1

```

```

FIND COEFFICIENTS A, B, C, D FOR POLYNOMIAL Y = A X/3 + B X/2 + C X + D

```

```

T1 = X0 - X1
T2 = X0**2 - X1**2
T3 = X0**3 - X1**3
T4 = YOPRIM - YIPRIM
T5 = Y0 - Y1
TL1 = 3.*T2
TL2 = 2.*T1
TL3 = 3.*T1*X1**2 - T3
TL4 = 2.*X1*T1 - T2
TL5 = YIPRIM*T1 - T5
D1 = TL1*TL4 - TL2*TL3
IF(ABS(D1) .LT. 1.E-26) THEN
WRITE(6, *) ' CAUTION MAKE CALCULATION D1 IN ERROR '
D1 = 1.E-26*SIGN(1., D1)
ENDIF

```

```

A = (T4*TL4 - TL2*TL5)/D1
D2 = T1
IF(ABS(D2) .LT. 1.E-26) THEN
WRITE(6, *) ' CAUTION MAKE CALCULATION D2 IN ERROR '
D2 = 1.E-26*SIGN(1., D2)
ENDIF

```

```

B = (TL5 - A*TL3)/D2
D3 = T1
IF(ABS(D3) .LT. 1.E-26) THEN
WRITE(6, *) ' CAUTION MAKE CALCULATION D3 IN ERROR '
D3 = 1.E-26*SIGN(1., D3)
ENDIF

```

```

C = (T5 - A*T3 - B*T2)/D3
D = Y1 - A*X1**3 - B*X1**2 - C*X1
WRITE(6, *) ' A, B, C, D = ', A, B, C, D
EPS = EPSIL/SOB, 0.0, DS(1), NMAKE, .00001, 40, 1)
XMAKE(1) = XINTER(1)
YMAKE(1) = (YINTER(1) + YINTER(IMAX))/2.0
DO 10 K=2, NMAKE
XMAKE(K) = XMAKE(K-1) + DS(1)*(1.+EPS)**(K-2)
IF(XMAKE(K) .LE. X1) THEN
YMAKE(K) = YMAKE(1) + YOPRIM*(XMAKE(K)-XMAKE(1))
ELSEIF(XMAKE(K) .GT. X1) THEN
YMAKE(K) = Y1
ELSE
Z = XMAKE(K)
YMAKE(K) = A*Z**3 + B*Z**2 + C*Z + D
ENDIF
WRITE(6, *) K, XMAKE(K), YMAKE(K)
10 CONTINUE

```

```

PIECE EVERYTHING TOGETHER

```

```

DO9844 I=1, NMAKE
X(I) = XMAKE(NMAKE-I+1)
Y(I) = YMAKE(NMAKE-I+1)

```

```

9860 CONTINUE
DO9863 I=NMMAKE-1,NMAKE-1,IMAX
  X(I) = XINTER / (NMMAKE - I)
  Y(I) = YINTER / (NMMAKE - I)
9863 CONTINUE
DO9862 J=NMMAKE-1,IMAX-2,NMAKE-1,IMAX-NMAKE-2
  X(I) = XMMAKE(I) - NMMAKE + 1 - IMAX + 3
  Y(I) = YMMAKE(I) - NMMAKE + 1 - IMAX + 3
9862 CONTINUE
JMAX = 2 * NMMAKE - IMAX - 2
JTAIL1 = NMMAKE
JTAIL2 = JMAX - JTAIL1 - 1
WRITE(6,*) JMAX = JMAX
WRITE(6,*) JTAIL1 = JTAIL1
WRITE(6,*) JTAIL2 = JTAIL2
WRITE(6,*) JMAX = JMAX
WRITE(6,*) JTAIL1 = JTAIL1
WRITE(6,*) JTAIL2 = JTAIL2
WRITE(DOCUM,*) JTAIL1 = JTAIL1
WRITE(DOCUM,*) JTAIL2 = JTAIL2

```

END

FUNCTION EPSIL, FMX, FMIN, DFM, NPT, FPCC, ICC, NCALL

THIS SUBROUTINE APPLIES A NEWTON-RAPHSON ROOT-FINDING TECHNIQUE TO FIND A VALUE OF EPSILON FOR A PARTICULAR USE OF THE EXPONENTIAL STRETCHING TRANSFORMATION.

FMX IS TOTAL ARC LENGTH ALONG COORDINATE
 FMIN IS STARTING VALUE OF ARC LENGTH SUCH AS 0.0
 DFM IS SPECIFIED INITIAL INCREMENT OF ARC LENGTH
 NPT IS NUMBER OF POINTS ALONG COORDINATE
 FPCC IS ITERATIVE ERROR BOUND E.G.C 0.00002
 ICC IS MAXIMUM NUMBER OF ITERATIONS
 NCALL IF NCALL=1 INITIAL GUESS FOR EPS IS USED
 IF NCALL.GT. 1, PREVIOUS EPS USED AS INITIAL GUESS

```

FMX=FMX
FMIN=FMIN
DFM=DFM
FPCC=FPCC
ICC=ICC

```

```

FNPTM2=NPT-2
IF(NCALL.EQ.1) EPS=(FMX/DFM)**1.0/FNPTM2-1.0

```

```

DO 3 NIT=1,ICC
  EP=EPS+1.0
  EPITN=EP**FNPTM2
  REPS=1.0/EP
  DFMOE=DFM*REPS
  F=FMX-FMIN-DFMOE*(EPITN-EP-1.0)
  IF(ABS(F).GT.FPCC) GO TO 4
  DFMOE2=DFMOE*REPS
  FNM=FMX-2.0*EPITN*(EPS-FNPTM2-1.0)
  DD = F/FNM

```

```

EPS=EPS+F/FNM
CONTINUE

```

```

EPSIL=EPS
WRITE(1,100)
RETURN

```

```

EPSIL=EPS
RETURN

```

```

100 FORMAT('42H EXCEEDED MAX. NO. OF ITERATIONS IN EPSIL.
101 FORMAT('7H EPSIL=',F12.5,'7H AND F=',F12.5,'7H AFTER 13.
12H ITERATIONS.

```

END

SUBROUTINE STRET

```

COMMON BASE, JMAX, KMAX, PI, SBODY, SMU, SHUY, NBODY, NCLUST
COMMON NARS, X(301), Y(301), XPI(301), YPI(301)
COMMON UNITS, BODYUN, GRIDUN, DOCUN
COMMON NAMES, BODYFI, GRIDFI, DOCFI
COMMON STRIP, DS(100), CNTRLP(100), NBP(100), ARCLEN(301)
CHARACTER*1 ANSWER
CHARACTER*80 BODYFI, GRIDFI, DOCFI
INTEGER BODYUN, GRIDUN, DOCUN
COMMON /BODY, XINTER(301), YINTER(301), IMAX
DIMENSION S(301), ARCDIS(301)

```

```

S(1)=0
N = 1
DO9861 N=1,NCLUST-1
  NODEI = CNTRLP(N)-1
  NODEJ = CNTRLP(N)
  ALENGT = ARCLEN(NODEI) - ARCLEN(NODEJ)
  DSI = DSI + ALENGT
  DSJ = DSJ + ALENGT
  CALL CLUSTARCD(S, DSI, DSJ, NL, NL + NBP(N))
DO9860 I=NL+1, NL + NBP(N)
  S(I) = ARCLEN(NODEJ) + ALENGT * ARCDIS(I)
CONTINUE

```

```

9860 CONTINUE
N = NL + NBP(N)
9861 CONTINUE
IMIN = 1
IMAX = N
WRITE(6,*) 'DO YOU WISH TENSIONED SPLINE FITS (Y/N)?'
READ(5,1000) ANSWER
1000 FORMAT(A)
IF(ANSWER.EQ.'N' OR ANSWER.EQ.'N' WITHIN)
  CALL CSPLIN(S, XINTER, ARCLEN, X, IMIN, IMAX, 1, NBODY)
  CALL CSPLIN(S, YINTER, ARCLEN, Y, IMIN, IMAX, 1, NBODY)
ELSE
  WRITE(6,*) 'INPUT TENSION '
  READ(5,*) SIGMA
  CALL TSPLIN(S, XINTER, ARCLEN, X, NBODY, IMAX, SIGMA)
  CALL TSPLIN(S, YINTER, ARCLEN, Y, NBODY, IMAX, SIGMA)
ENDIF

```



```

JA = J1 + 1
JE = J2 - 1
DC 10 J=JA,J2
M = 1
N = J2 - X(J-1)
DC 12 J=JA,J5
A(J) = M(J-1)
B(J) = 2.*M(J) + M(J+1)
C(J) = 3.*M(J)*D(J+1) + M(J+1)*D(J)
B(J) = 2.
M(J) = 1.
F(J) = 3.*D(JA)
A(J) = 1.
B(J) = 2.
C(J) = 3.*D(J2)
CALL TRIB(A,B,C,F,J1,J2,1)

```

INTERPOLATION . X(J) ARRAY MUST BE MONOTONE
FUJGE=1.E-8*ABS(X(J2)-A(J1))
J = J1
DC 20 J=J1,M2
28 IF X(J) - FUJGE.LE XX.N.AND.X(J) + FUJGE.GE.XX.N GO TO 30
IF X(J) - XX.N .22.22.2=
22 J = J + 1
IF J .GT. J2 GO TO 27
GO TO 28
24 J = J - 1
IF J .LT. J1 GO TO 27
GO TO 28
27 WRITE(6,600)
600 FORMAT(55H) FATAL ERROR IN CSP IN VALUE AT WHICH WE ARE SUPPOSED.
TO INTERPOLATE IS OUTSIDE OF GIVEN TABLE OF VALUES.
STOP
30 T = (XX/M) - X(J1)/M(J1)
YY(M) = T*Y(J) + TT*Y(J2) + M(J1)*T*TT*(F(J2) - D(J1))*TT
D(J1) - D(J2)) = T
20 CONTINUE
RETURN
END
SUBROUTINE TRIB(A,B,C,X,F,N1,MU,JINC
DIMENSION A(2),B(2),C(2),X(2),F(2)

```

THIS SUBROUTINE SOLVES A TRI-DIAGONAL SYSTEM OF LINEAR EQUATIONS.
X(N1)=C(N1)/B(N1)
F(N1)=F(N1)/B(N1)
N1=N1+JINC
DO 1 J=N1,P1,MU,JINC
JM=J-JINC
C(J)=B(J)-A(J)*X(JM)
X(J)=C(J)
1 F(J)=F(J)-A(J)*X(JM)
NUPN1=MU+N
DC 2 J=N1,P1,MU,JINC
JM=NUPN1-J1
JP=J+JINC
2 F(J)=F(J)-X(JM)*F(JP)
RETURN
END

```

```

SUBROUTINE TSPLIN,XX,YY,X,Y,N,NN,SIGMA

```

```

DRIVER FOR TENSION SPLINE
DIMENSION X(301),Y(301),A(301),B(301),C(301),R(301)
FDP(301)
DIMENSION XX(301),YY(301)
CALL SPLINE(X,Y,FDP,SIGMA)
CALL VALSPE(X,Y,FDP,NN,XX,YY,SIGMA)
RETURN
END

```

```

SUBROUTINE SPLINE(N,X,Y,FDP,SIGMA)
DIMENSION X(301),Y(301),A(301),B(301),C(301),R(301)
FDP(301)

```

```

ALAMBD = 1 ..... CARTELEVER END CONDITIONS
ALAMBD = 0 ..... PARABOLIC RUNOFF

ALAMBD = 0.
NM2 = N - 2
NM1 = N - 1
DC 1 I=2,NM1
DXM = Y(I) - Y(I-1)
DYM = X(I) - X(I-1)
DXP = Y(I+1) - Y(I)
DYM = Y(I) - Y(I-1)
SINHMP = SINH(SIGMA*DXP)
COSHP = COSH(SIGMA*DXP)
SINHMM = SINH(SIGMA*DYM)
COSHM = COSH(SIGMA*DYM)
IF(ABS(DXM) .LT. 1.E-8) THEN
WRITE(6,*) ' ERROR...DXM=0.0...I=',I
ENDIF
IF(ABS(DXP) .LT. 1.E-8) THEN
WRITE(6,*) ' ERROR...DXP=0.0...I=',I
ENDIF
A(I) = 1./DXM - SIGMA/SINHMP
B(I) = SIGMA*COSHMP/SINHMM - 1./DXM + SIGMA*COSHMP/SINHMP - 1./DXP
C(I) = 1./DXP - SIGMA/SINHMP
R(I) = SIGMA*SIGMA*(DYP/DXP - DYM/DXM)
1 CONTINUE
B(2) = B(2) + ALAMBD*(X(2)-X(1))
B(NM1) = B(NM1) + ALAMBD*(X(NM1))
DC 2 I=3,NM1
IF(ABS(B(I)) .LT. 1.E-9) THEN
WRITE(6,*) ' CAUTION... NEAR ZERO DIAGONAL... TSPLINE CONTINUES'
B(I) = SIGN(1.,B(I)-1) * 1.E-10
ENDIF
B(I) = B(I) - I*(C(I)-1)
B(I) = B(I) - I*(C(I)-1)

```

```

R(I) = R(I) - T*(R(I)-1)
2 CONTINUE
FDP(NM1) = R(NM1)/B(NM1)
DO 3 I=2,NM2
NM1 = N-I
FDP(NM1) = (R(NM1)-C(NM1)+FDP(NM1+1))/B(NM1)
3 CONTINUE
FDP(1) = ALAMBDA*(FDP(2) - SIGMA*SIGMA*Y(2))
FDP(N) = ALAMBDA*(FDP(NM1) - SIGMA*SIGMA*Y(NM1))
RETURN
END

```

```

SUBROUTINE VALSPE(N,X,Y,FDP,NM,XX,YY,SIGMA)

```

```

DIMENSION X(301),Y(301),FDP(301)
DIMENSION XX(301),YY(301)
NM1 = N - 1
DO 90 J=1,NM1
DO 1 I=1,NM1
IF(XX(J) .LE. X(I+1))GO TO 10
CONTINUE
10 DXM = XX(J) - X(I)
DXP = X(I+1) - XX(J)
DEL = X(I+1) - X(I)
SINHXP = SINH(SIGMA*DXP)
SINHXX = SINH(SIGMA*DEL)
IF(ABS(SINHXX) .LT. 1.E-10)THEN
WRITE(6,*) CAUTION IN SPLINE...SINHXX = 1,SINHXX
SINHXX = 1.E-10/SIGN(1,SINHXX)
ENDIF
SINHMX = SINH(SIGMA*DXM)
SIGZIN = 1./SIGMA/SIGMA
YY(J) = FDP(I)*SIGZIN+SINHXP/SINHXX
+ Y(I) - FDP(I)*SIGZIN+DXP/DEL
+ FDP(I+1)*SIGZIN+SINHMX/SINHXX
- Y(I+1) - FDP(I+1)*SIGZIN+DXM/DEL
50 CONTINUE
RETURN
END

```

```

SUBROUTINE GRIDGE

```

```

DEVELOPED BY TIM BARTH X-6417
NASA-AMES...WRIGHT-PATTERSON AFHS
TASK 933

```

```

COMMON /BASE/ JMAX,KNAX,PI,SBODY,SMU,SMUV,NBODY,NCLUST
COMMON /VARS/ X(301),Y(301),X1(301),XETA(301),YX1(301),
1 YETA(301),R(301,100),SCALE(100),SR(301,2),VOL(301)
COMMON /STORE/ XX(301,100),YY(301,100)
COMMON /ORDER/ ALPHA,ALPHAM,KM1,KM2
COMMON /UNITS / BODYUN,GRIDUN,DOCUM1
COMMON /FNAMES / BODYF1,GRIDF1,DOCFIL
COMMON /LAX/RELAX
INTEGER BODYUN,GRIDUN,DOCUM1

```

```

CHARACTER=80 BODY,GRID,INPUT

```

```

OPEN VARIOUS FILES FOR INPUT,OUTPUT,ETC

```

```

INITIALIZE

```

```

CALL INITIA

```

```

NOTE: SINCE THIS IS A MARCHING SCHEME, POINTS
NEED ONLY BE STORED FROM THE PREVIOUS K LEVEL.
THIS WOULD MEAN THAT THEY WOULD BE WRITTEN OUT
AFTER EVERY CALL TO STEP.....

```

```

BUT TO MAKE IT EASY TO USE THE BUNING GRAPHICS
PACKAGE, I WILL STORED THEM ALL AND WRITE
THEM OUT AT THE END

```

```

START BY LOADING BODY SURFACE POINTS INTO
XX,YY WHICH WILL STORE THE GRID AS WE MARCH OUT

```

```

DO 5 J=1,JMAX
XX(J,1) = X(J)
YY(J,1) = Y(J)
WRITE(GRIDUN,700)XX(J,1),YY(J,1)
5 CONTINUE

```

```

*****
***** MAIN LOOP TO MARCH GRID TO OUTER BOUNDARY *****
*****
DO 10 K=2,KNAX

```

```

ADVANCE GRID FROM K -> K+1

```

```

CALL STEP(K)

```

```

STORE SURFACE GRID PTS (MAY WISH TO WRITE OUT POINTS HERE)

```

```

DO 7 J=1,JMAX
XX(J,K) = X(J)
YY(J,K) = Y(J)

```

```

THIS WRITE PROVIDES DATA IN THE FORM THE NAVIER-STOKES SOLVER NEEDS.

```

```

WRITE(GRIDUN,700) XX(J,K),YY(J,K)
CONTINUE
700 FORMAT(2E15.9)

```

```

WRITE(6,*) '.....FINISHED LEVEL',K,' ALPHA=',ALPHA

```

```

10 CONTINUE

```

```

*****
***** END OF MAIN LOOP TO MARCH GRID TO OUTER BOUNDARY *****
*****

```

```

O.K. WE'RE DONE...LET'S WRITE OUT THAT GRID

```

```

WRITE(GRIDUN)JMAX,KNAX
WRITE(GRIDUN,250)((XX(J,K),J=1,JMAX),K=1,KNAX)

```

```

C      *          YY=J,K  ,J=1,JMAX,K=1,KMAX
250 FORMAT:2X,E20.10,2X,E20.10
      MASTA LA VISTA'
      STOP
1111 FORMAT(A)
      END
-----
C      SUBROUTINE SARC
-----
C      COMMON /BASE JMAX,KMAX,PI,SBODY,SMU,SMUJ,NBODY,NCLUST
C      COMMON VARS X,301,Y,302,XXI,303,XETA,304,YYI,305
C      I,YETA,306,R,307,100,SCALE,100,SR,308,2,VOL,309
C      INTEGRATE ARC LENGTH AROUND BODY
C
      S = 0.
      DO 10 J=1,JMAX-1
      JP = J-1
      S=S -SORT X JP -X,JP+2 + /Y JP -Y,JP+2
10 CONTINUE
      SBODY= S
      RETURN
      END
-----
C      SUBROUTINE INITIA
-----
C      COMMON /BASE JMAX,KMAX,PI,SBODY,SMU,SMUJ,NBODY,NCLUST
C      COMMON VARS X,301,Y,302,XXI,303,XETA,304,YYI,305
C      I,YETA,306,R,307,100,SCALE,100,SR,308,2,VOL,309
C      COMMON /ORDER ALPHA,ALPHAM,KM1,KM2
C      COMMON /DISS/SMUJ,SMUJIM
C      COMMON /SCALE/ DSETA
C      COMMON /SOB0/ SETAMX
C      COMMON /UNITS / BODYUN,GRIDUN,DOCUJ
C      COMMON /FRAMES / BODYFI,GRIDFI,DOCFI
C      LOGICAL VERBOS
C      CHARACTER=1 ANSMER
C      INTEGER BODYUN,GRIDUN,DOCUJ
C
      VERBOS = .TRUE.
      PI = 4.*ATAN(1.)
C
      JMAX :      NUMBER OF POINTS IN THE STREAMWISE DIRECTION
      KMAX :      NUMBER OF POINTS IN THE NORMAL DIRECTION
                  (NOTE: K=1 IS THE BODY SURFACE)
      DSETA :      APPROXIMATE CELL HEIGHT FOR K=1 TO K=2
      SETAMX :      APPROXIMATE DISTANCE TO OUTER BOUNDARY
                  (NOTE: THIS IS "EXACT" IF THE BODY IS A CIRCLE.
                  I'VE NEVER ACTUALLY CHECKED IF THIS IS TRUE)
C
      SCKMAX :      VALUE OF SCALING FUNCTION AT KMAX "SCALE(KMAX)"
                  SCALE IS THE FUNCTION THAT TRANSITIONS FROM
                  STREAMWISE CLUSTERED VOLUMES TO EQUAL-
                  SPACED VOLUMES AS MENTIONED IN THE
                  ORIGINAL PAPER BY STEGER AND CHAUSSEE
      SMU :      COEFFICIENT FOR EXPLICIT DISSIPATION
      SMUJIM :      COEFFICIENT FOR IMPLICIT DISSIPATION
      ALPHAM :      MAXIMUM ALPHA FOR MARCHING INTEGRATION
C
      -----
      * ALPHA = 0          EULER EXPLICIT
      * ALPHA = 1/2       TRAP RULE
      * ALPHA = 1          EULER IMPLICIT
      -----
      KM1 :      INNER VALUE OF K FOR VARIABLE ALPHA INTEGRATION
                  EXPLAINED BELOW
      KM2 :      OUTER VALUE OF K FOR VARIABLE ALPHA INTEGRATION
                  EXPLAINED BELOW
C
      THE ALPHA INTEGRATION SCHEME STARTS OUT AT THE BODY WITH
      ALPHA=1 (EULER IMPLICIT) AND LINEARLY INCREASES TO ALPHA AT
      X=KM1. FROM KM1 TO KM2 ALPHA REMAINS CONSTANT AT ALPHA.
      FROM KM2 TO KMAX, ALPHA LINEARLY DECREASES BACK TO 1 AT KMAX
C
      THIS VARIABLE ALPHA IS INCORPORATED TO ALLOW FOR ALPHA INTEGRATION
      GREATER THAN ONE. FOR ALPHA GREATER THAN ONE THE SCHEME
      BECOMES VERY TEMPORALLY-SPATIALLY DISSIPATIVE
      IF ETA IS VIEWED AS A TIME-LIKE DIRECTION,
      AND AS A RESULT GIVES VERY SMOOTH
      GRIDS WITH A SMALL DEGRADATION IN ORTHOGONALITY, INVERSE JACOBIAN ...ETC
C
      SMU,SMUJIM ARE SCALED LINEARLY FROM ZERO AT K=1 TO SMU,SMUJIM AT
      KM1 AND REMAIN CONSTANT FROM KM1 TO KMAX
C
      READ INPUTS
      WRITE(6,*) 'INPUT KMAX,NORMAL MALL SPACING'
      READ(5,*)KMAX,DSETA
      WRITE(DOCUN)=' KMAX,NORMAL MALL SPACING',KMAX,DSETA
      SCKMAX = .98
      SMU = .005
      SMUJIM = .005
      ALPHAM = 2.5
      KM1 = .25*KMAX
      KM2 = .75*KMAX

```

```

C      ECHO INPUTS
C
C      CONTINUE
C      WRITE(6,1000)JMAX,KMAX,DSETA,SETAMX,SCKMAX,
C      SMU,SMUIM,ALPHAM,KM1,KM2
1000  FORMAT(' JMAX=',I4,' KMAX=',I4,' DSETA=',E12.6,
C      ' SETAMX=',F12.6,' SCKMAX=',F12.6,
C      ' SMU=',F14.7,' SMUIM=',F14.7,' ALPHAM=',F14.7,
C      ' AT KM1=',I5,' KM2=',I5)
C      WRITE(6,*) ' DO YOU WISH TO CHANGE THE ABOVE DEFAULTS? (Y/N)'
C      READ(5,2222)ANSWER
2222  FORMAT(A)
C      IF(ANSWER.EQ.'Y'.OR.ANSWER.EQ.'Y')THEN
C      WRITE(6,*) ' CHANGE THE DEFAULT VALUES IN SUBROUTINE INITIA.'
C      STOP
C      ENDIF
C
C      READ IN BODY COORDINATES
C      FIND EPS FOR OUTER BOUNDARY APPROX
C      USES AN EXPONENTIAL STRETCHING IN THE NORMAL DIRECTION
C      EPSIL FIND THE COEFFICIENT FOR THE STRETCHING GIVEN
C      THE WALL SPACING AND THE OUTER BOUNDARY DISTANCE (APPROX)
C
C      EPS=EPSIL*(SETAMX,0.0,DSETA,KMAX,0.004,40.1)
C      DISTRIBUTE RADIAL POINTS
C
C      VERBOS = .FALSE.
C      IF(VERBOS)WRITE(6,*) ' INITIAL RADIAL SPACING'
C      DO 15 J=1,JMAX
C      R(J,1) = 0.00
15  CONTINUE
C      DC 16 K=2,KMAX
C      DO 16 J=1,JMAX
C      R(J,K)=R(J,K-1)+DSETA*(1.+EPS)**(K-2)
C      IF(VERBOS .AND. J.EQ.1)WRITE(6,*)K,R(1,K)
16  CONTINUE
C
C      SET SCALING FUNCTION SCKMAX = SCALE(KMAX)
C
C      SCALE(1)=1.
C      ESCAL = 1. - EXP(ALOG(SCKMAX)/FLOAT(KMAX-2))
C      DO 17 K=2,KMAX
C      SCALE(K) = 1. - ESCAL**K-2)
17  CONTINUE
C
C      RETURN
C      END
C
C-----
C      SUBROUTINE METRIC
C-----
C      COMMON/BASE/JMAX,KMAX,P1,SBODY,SMU,SMUV,NBODY,NCLUST
C      COMMON/VARS/X(301),Y(301),XXI(301),XETA(301),YXI(301),
C      YETA(301),R(301,100),SCALE(100),SR(301,2),VOL(301)
C      DO 10 J=2,JMAX-1
C      JP=J+1
C      JR=J-1
C
C      XXI(J)=(X(JP)-X(JR))/0.5
C      YXI(J)=(Y(JP)-Y(JR))/0.5
C      XXYY=XXI(J)**2-YXI(J)**2
C
C      NOTE: ETA METRICS ARE OBTAINED FROM DIFFERENTIAL
C      EQUATIONS AND ARE NONLINEAR AS SUCH
C
C      FROM THE CALLING SEQUENCE USED...
C      VOLUMES FROM THE UNKNOWN K LEVEL ARE BEING
C      USED (THIS IS EXPERIMENTALLY WORKS WELL)
C      .... THIS WHEN USED WITH ALPHA > 1
C      SEEMS TO HELP OUT IN REGIONS OF CONCAVE CURVATURE
C
C      XETA(J)=YXI(J)*VOL(J)/XXYY
C      YETA(J)=XXI(J)*VOL(J)/XXYY
10  CONTINUE
C      RETURN
C      END
C-----
C      SUBROUTINE STEP(K)
C-----
C      COMMON/BASE/JMAX,KMAX,P1,SBODY,SMU,SMUV,NBODY,NCLUST
C      COMMON/VARS/X(301),Y(301),XXI(301),XETA(301),YXI(301),
C      YETA(301),R(301,100),SCALE(100),SR(301,2),VOL(301)
C      COMMON /ORDER/ALPHA,ALPHAM,KM1,KM2
C      COMMON /DISS/SMUIM,SMUIMV
C      DIMENSION B(301,2,2),C(301,2,2),D(301,2,2),F(301,2)
C      DIMENSION A(301,2,2),E(301,2,2)
C
C      SET UP ALPHA VARIATION
C
C      IF(K.LE.KM1)THEN
C      SC1 = FLOAT(K-2)/FLOAT(KM1-2)
C      SC2=SC1
C      ELSEIF(K.GE.KM2)THEN
C      SC1 = 1. - FLOAT(K-KM2)/FLOAT(KMAX-KM2)
C      SC2 = 1.
C      ELSE
C      SC1 = 1.
C      SC2=SC1
C      ENDIF
C
C      ALPHA = 1. + (ALPHAM - 1.)*SC1
C
C      SCALE DISSIPATION
C
C      SMUV = SC2*SMU
C      SMUIMV = SC2*SMUIM
C
C      CALL VOLUME(K)
C      CALL METRIC
C      CALL RMSIK
C
C      INVERSION IN ETA DIRECTION

```

```

C      FILL A,B,C,F ARRAYS FOR BLOCK TRIDIAGONAL
C      CALL FILTRY(K,A,B,C,D,E,F)
C      CALL BPENTA(1,JMAX,A,B,C,D,E,F)
C      CALCULATE NEH X,Y COORDINATES
C      DO 5 J=1,JMAX
C      X(J) = X(J) + F(J,1)
C      Y(J) = Y(J) + F(J,2)
C      CONTINUE
C      RETURN
C      END
-----
C      SUBROUTINE FILTRY(K,A,B,C,D,E,F)
C      COMMON/BASE/JMAX,KMAX,P1,SBODY,SMU,SMUV,NBODY,NCLUST
C      COMMON/VARS/X(301),Y(301),XX(301),XETA(301),YXI(301),
C      I YETA(301),R(301),SCALE(100),SR(301),VOL(301)
C      DIMENSION B(301,2,2),C(301,2,2),D(301,2,2),F(301,2)
C      DIMENSION A(301,2,2),E(301,2,2)
C      COMMON/DISS/SMUIM,SMUIMV
C      COMMON/ORDER ALPHA,ALPHAM,KM1,KM2
C      DIMENSION AM(2,2)
-----
C      FILL TRIDIAGONAL MATRICES IN ETA-DIRECTION
-----
C      DO 5 N=1,2
C      DO 5 M=1,2
C      DO 5 J=1,JMAX
C      A(J,N,M) = 0.
C      E(J,N,M) = 0.
C      CONTINUE
C      DO 10 J=2,JMAX-1
C      METRIC TERMS IN B,-1A
C      R1=XETA(J)
C      R2=YETA(J)
C      R3=XX(J)
C      R4=YXI(J)
C      RME1=R3**2-R4**2
C      R1=RME1
C      R2=R2*RME1
C      CALL GMATRIX(AM,J,K,R1,R2,R3,R4)
C      LOAD B -1A INTO BANDS (ALLOW FOR GENERAL INTEGRATION..ALPHA)
C      C(J,1,1) = 1.
C      C(J,2,2) = 1.
C      C(J,1,2) = 0.
C      C(J,2,1) = 0.
C      DO 8 M=1,2
C      DO 8 N=1,2
C      B(J,N,M) = -.5*ALPHA*AM(N,M)
C      D(J,N,M) = .5*ALPHA*AM(N,M)
C      CONTINUE
C      DO 10 M=1,2
C      F(J,M)=SR(J,N)
C      CONTINUE
C      FULL IMPLICIT 4TH ORDER DISSIPATION
C      J=2
C      DO 12 N=1,2
C      A(J,N,N)=A(J,N,N)+0.*SMUIMV
C      B(J,N,N)=B(J,N,N)-2.*SMUIMV
C      C(J,N,N)=C(J,N,N)+5.*SMUIMV
C      D(J,N,N)=D(J,N,N)-4.*SMUIMV
C      E(J,N,N)=E(J,N,N)+1.*SMUIMV
C      CONTINUE
C      J=JMAX+1
C      DO 14 N=1,2
C      A(J,N,N)=A(J,N,N)+1.*SMUIMV
C      B(J,N,N)=B(J,N,N)-2.*SMUIMV
C      C(J,N,N)=C(J,N,N)+5.*SMUIMV
C      D(J,N,N)=D(J,N,N)-2.*SMUIMV
C      E(J,N,N)=E(J,N,N)+0.*SMUIMV
C      CONTINUE
C      DO 15 N=1,2
C      DO 15 J=3,JMAX-2
C      A(J,N,N)=A(J,N,N)+1.*SMUIMV
C      B(J,N,N)=B(J,N,N)-2.*SMUIMV
C      C(J,N,N)=C(J,N,N)+6.*SMUIMV
C      D(J,N,N)=D(J,N,N)-4.*SMUIMV
C      E(J,N,N)=E(J,N,N)+1.*SMUIMV
C      CONTINUE
C      IMPLICIT C-GRID B-C AT K=1,KMAX
C      DO 20 M=1,2
C      DO 20 N=1,2
C      J=1
C      A(J,N,M)=0.
C      B(J,N,M)=0.
C      C(J,N,M)=0.
C      D(J,N,M)=0.
C      E(J,N,M)=0.
C      F(J,N)=0.
C      J=JMAX
C      A(J,N,M)=0.
C      B(J,N,M)=0.
C      C(J,N,M)=0.
C      D(J,N,M)=0.
C      E(J,N,M)=0.
C      F(J,N)=0.
C      CONTINUE
C      J=1
C      C(J,1,1) = 1.
C      C(J,2,2) = 1.
C      D(J,2,2) = -2.
C      E(J,2,2) = 1.
C      J=JMAX
C      C(J,1,1) = 1.
C      C(J,2,2) = 1.
C      D(J,2,2) = -2.

```

```

A(J,2,2)= 1.
RETURN
END
-----
SUBROUTINE VOLUME(K)
-----
COMMON/BASE/JMAX,KMAX,P1,SBODY,SMU,SMUV,NBODY,NCLUST
COMMON/VARS/X(301),Y(301),XX(301),XETA(301),YX(301),
1 YETA(301),R(301,100),SCALE(100),SR(301,2),VOL(301)
COMMON /ORDER/ALPHA,ALPHAM,KM1,KM2
CALL SARC
DO 5 J=2,JMAX-1
JP = J+1
JR = J-1
DS = 5*(R(J-1,K)-R(J-1,K-1)) + R(J-1,K)-R(J+1,K-1)
DL = SQRT((5*(X(JP)-X(JR)))**2 + (5*(Y(JP)-Y(JR)))**2)
VOL(J)=DS*(SCALE(K)=DL *(1.-SCALE(K))=SBODY/FLOAT(JMAX-1))
CONTINUE
RETURN
END
-----
SUBROUTINE RMS(K)
-----
COMMON/BASE/JMAX,KMAX,P1,SBODY,SMU,SMUV,NBODY,NCLUST
COMMON/VARS/X(301),Y(301),XX(301),XETA(301),YX(301),
1 YETA(301),R(301,100),SCALE(100),SR(301,2),VOL(301)
COMMON /ORDER/ALPHA,ALPHAM,KM1,KM2
CALCULATE FORCING FUNCTION; CONSISTS OF NEW AND OLD
VOLUMES PLUS VARIABLES EVALUATED AT THE KTH LEVEL.
DO 5 J=2,JMAX-1
JP = J+1
JR = J-1
R1=XX(J)
R2=YX(J)
R3=XETA(J)
R4=YETA(J)
RMET=1./(R1**2+R2**2)
SR(J,1)=-R2*(ALPHA*VOL(J)+(1.-ALPHA)*(R1=R4-R2=R3))=RMET
SR(J,2)= R1*(ALPHA*VOL(J)+(1.-ALPHA)*(R1=R4-R2=R3))=RMET
-----
NUMERICAL DISSIPATION
IF(J .EQ. 2) THEN
JPP=J+2
SMX=-SMUV*(-2.*X(JR)+5.*X(J)-4.*X(JP)+X(JPP))
SMY=-SMUV*(-2.*Y(JR)+5.*Y(J)-4.*Y(JP)+Y(JPP))
ELSEIF(J .EQ. JMAX-1) THEN
JRR=J-2
SMX=-SMUV*(-2.*X(JP)+5.*X(J)-4.*X(JR)+X(JRR))
SMY=-SMUV*(-2.*Y(JP)+5.*Y(J)-4.*Y(JR)+Y(JRR))
ELSE
JPP=J+2
JRR=J-2
SMX=-SMUV*(X(JRR)+6.*X(J)+X(JPP)-4.*X(JP)+X(JR))
SMY=-SMUV*(Y(JRR)+6.*Y(J)+Y(JPP)-4.*Y(JP)+Y(JR))
ENDIF
SR(J,1)=SR(J,1)+SMX
SR(J,2)=SR(J,2)+SMY
CONTINUE
RETURN
END
-----
SUBROUTINE GMATRIX(A,J,K,R1,R2,R3,R4)
-----
COMMON/BASE/JMAX,KMAX,P1,SBODY,SMU,SMUV,NBODY,NCLUST
COMMON/VARS/X(301),Y(301),XX(301),XETA(301),YX(301),
1 YETA(301),R(301,100),SCALE(100),SR(301,2),VOL(301)
DIMENSION A(2,4)
FILL BINV=A
A(1,1)=R1-R3-R2=R4
A(1,2)=R2-R3+R4=R2
A(2,1)=R4-R1-R3=R2
A(2,2)=R4-R2-R3=R1
RETURN
END
-----
FUNCTION EPSIL(FMX,FMIN,DFM,NPT,FPCC,ICC, NCALL)
-----
THIS SUBROUTINE APPLIES A NEWTON-RAPHSON ROOT-FINDING
TECHNIQUE TO FIND A VALUE OF EPSILON FOR A PARTICULAR USE
OF THE EXPONENTIAL STRECHING TRANSFORMATION.
FMX IS TOTAL ARC LENGTH ALONG COORDINATE
FMIN IS STARTING VALUE OF ARC LENGTH SUCH AS 0.0
DFM IS SPECIFIED INITIAL INCREMENT OF ARC LENGTH
NPT IS NUMBER OF POINTS ALONG COORDINATE
FPCC IS ITERATIVE ERROR BOUND, E.G. 0.00002
ICC IS MAXIMUM NUMBER OF ITERATIONS
NCALL IF NCALL=1 INITIAL GUESS FOR EPS IS USED
IF NCALL .GT. 1, PREVIOUS EPS USED AS INITIAL GUESS
FMXL=FMX
FMINL=FMIN
DFML=DFM
FPCL=FPCC
ICCL=ICC
FNPTM2=FLOAT(NPT-2)
IF(NCALL.EQ.1) EPS=(FMXL/DFML)**(1.0/FNPTM2)-1.0
DO 3 HIT=1,ICCL
EP1=EPS+1.0
EP1N=EP1**FNPTM2
REPS=1.0/EP1

```



```

U(I,2,M) = D2
U(I,1,M) = D1 - U12*U(I,2,M)
45 CONTINUE
IF (I.EQ. IU-1) GO TO 80
DO 46 M=1,2
D1 = V1*E(I,1,M)
D2 = V2*E(I,2,M) - L21*D1
V(I,2,M) = D2
V(I,1,M) = D1 - U12*V(I,2,M)
46 CONTINUE
80 CONTINUE
50 CONTINUE
C
BACK SWEEP
I = IU - 1
DO 60 M=1,2
F(I,M) = F(I,M) - U(I,M,1)*F(I+1,1) - U(I,M,2)*F(I+1,2)
60 CONTINUE
DO 65 I = IU-2,IL,-1
DO 65 M=1,2
F(I,M) = F(I,M) - U(I,M,1)*F(I+1,1) - U(I,M,2)*F(I+1,2)
65 CONTINUE
RETURN
END
SUBROUTINE LUDECA
DIMENSION A(2,2)
COMMON/LUD/ L11,L21,L22,U12,V1,V2
REAL L11,L21,L22
C SUBROUTINE COMPUTES L-U DECOMPOSITION ELEMENTS
L11 = A(1,1)
V1 = 1./L11
U12 = V1*A(1,2)
L21 = A(2,1)
L22 = A(2,2) - L21*U12
V2 = 1./L22
RETURN
END

```



```

DO 33 J=2,JLAST
JJ=JL+J
UXI=.5*(U(I+1,J)-U(I-1,J))
VXI=.5*(V(I+1,J)-V(I-1,J))
YETA=.5*(U(I,J+1)-U(I,J-1))
VETA=.5*(V(I,J+1)-V(I,J-1))
N(JJ)=XII(I,J)*YETA-XETA(I,J)*UXI-YETA(I,J)*VXI
+YXI(I,J)*VETA/XJAC(I,J)
YMK=S(I,J)-YMKC
F(JJ)=ABS(YMK*M(JJ))
33 CONTINUE
C LOWER PART
DO 34 J=2,JLAST
JJ=JL+J+1
UXI=.5*(U(ILM+1,J)-U(ILM-1,J))
VXI=.5*(V(ILM+1,J)-V(ILM-1,J))
YETA=.5*(U(ILM,J+1)-U(ILM,J-1))
VETA=.5*(V(ILM,J+1)-V(ILM,J-1))
N(JJ)=XII(ILM,J)*YETA-XETA(ILM,J)*UXI-YETA(ILM,J)*VXI
+YXI(ILM,J)*VETA/XJAC(ILM,J)
YMK=S(ILM,J)+YMKC
F(JJ)=ABS(YMK*M(JJ))
34 CONTINUE
C MAKE-CUT POINTS
UXI=.5*(U(I+1,1)-U(I-1,1))
VXI=.5*(V(I+1,1)-V(I-1,1))
YETA=.5*(U(I,2)-U(I,1))
VETA=.5*(V(I,2)-V(ILM,2))
XE=.5*(X(I,2)-X(ILM,2))
YE=.5*(Y(I,2)-Y(ILM,2))
XJ=XI(I,1)*YE-XE*YXI(I,1)
N(JL)=XII(I,1)*YETA-XE*UXI-YE*VXI
+YXI(I,1)*VETA/XJ
YMK=YMKC
F(JL)=ABS(YMK*M(JL))
M(JL+1)=M(JL)
F(JL+1)=F(JL)
C COMPUTE FMAX, YMAX
FMAX=0
JJS=JL-JLAST+1
JJE=JL+JLAST
DO 341 JJ=JJS,JJE
IF(F(JJ).LE..MAX) GO TO 341
FMAX=F(JJ)
IF(JJ.GT.JL) GO TO 342
JMAX=JL-JJ+1
IMAX=ILM
YMAX=S(IMAX,JMAX)+YMKC
GO TO 341
342 JMAX=JJ-JL
IMAX=J
YMAX=S(IMAX,JMAX)-YMKC
341 CONTINUE
C COMPUTE FMAKE
FMAKE=ABS(YMAX)/(UDIF=2)/FMAX
C COMPUTE EDDY VISCOSITY
DO 37 J=1,JLAST
YMK=ABS(S(I,J))-YMKC
FKLEB=1./1.-.5*(CKLEB*YMK/ABS(YMAX))**.6
37 EDDY(I,J)=RE*CHAKE*RHO I,J)*FMAKE*FKLEB
DO 39 J=1,JLAST
YMK=ABS(S(ILM,J))-YMKC
FKLEB=1./1.-.5*(CKLEB*YMK/ABS(YMAX))**.6
39 EDDY(ILM,J)=RE*CHAKE*RHO ILM,J)*FMAKE*FKLEB
C OUTPUT
IF(IPLOT.EQ.0) GO TO 30
WRITE(209)X(IMIN,JMIN),IMAX,JMAX,YMAX,FMAX,FMAKE,YMKC,IMIN,JMIN,
UDIF
IF(IPLOT1.EQ.0) GO TO 30
KLAST=J-JLAST
WRITE(6,210)
DO 42 K=1,KLAST
JJ=JL+JLAST-K+1
JL=JJ
IF(JJ.LE.JL) J=JL-JJ+1
II=1
IF(JJ.LE.JL) II=ILM
WRITE(6,204)1.5(I,J),U(I,J),M(JJ),F(JJ),EDDY(II,J)
42 CONTINUE
30 CONTINUE
-----
NEAR-MAKE
DO 40 I=ITEUP1,INKST1
ILM=I-1+1
XL=CSCALE*(S(I)-S(I+1))/XRLX)/XRELAX
FACTOR=TANH(XL)
DO 40 J=1,JLAST
EDDY(I,J)=.5*(EDDY(ITEU,J)+EDDY(INKST,J))+FACTOR*
(EDDY(INKST,J)-EDDY(ITEU,J))
EDDY(ILM,J)=.5*(EDDY(ITEU,J)+EDDY(INKSTL,J))+FACTOR*
(EDDY(INKSTL,J)-EDDY(ITEU,J))
40 CONTINUE
-----
REGION OF CONSTANT EDDY VISCOSITY (VERY FAR FROM AIRFOIL)
IF(INKG.GE.IL1) GO TO 3000
DO 41 I=INKEP1,IL1
ILM=I-1+1
DO 41 J=1,JLAST
EDDY(I,J)=EDDY(INKG,J)
EDDY(ILM,J)=EDDY(INKEL,J)
41 CONTINUE
C ***** FORMATS *****
202 FORMAT (1X,'I=',I4,2X,'YMAX=',F11.4,2X,'FMAX=',F11.4,2X,
-'FMAKE=',F11.4,2X,'JMAX=',I3,2X,'JTRAN=',I3,2X,'YZPLUS=',F11.4,
-12)
203 FORMAT(4X,'J',6X,'S(I,J)',6X,'F(J)',6X,'VORT.',6X,'DAMP.',
-6X,'XMU(I)',6X,'XMU(T)')
204 FORMAT(2X,'I',3,6,2X,E10.4)
209 FORMAT(2X,'X/C=',F7.4,2X,'IMAX=',I4,2X,'JMAX=',I4,2X,'YMAX=',
-F7.4,2X,'FMAX=',F7.4,2X,'FMAKE=',F7.4,2X,
-'YMKC=',F7.4,2X,'IMIN=',I4,2X,'JMIN=',I4,2X,'UDIF=',F7.4,
210 FORMAT(4X,'I',6X,'S(I,J)',6X,'U(I,J)',6X,'VORT.',6X,'F(J)',
-6X,'EDDY')
3000 RETURN

```

```

END
C
C *****
C SUBROUTINE "LIFT" COMPUTES AIRFOIL LIFT AND DRAG COEFFICIENTS
C VISCOUS CASE
C SUBROUTINE LIFT (CL,CD)
C
C PARAMETER (IN=299, JM=100)
COMMON /FLOWV/ U(IM, JM), V(IM, JM), P(IM, JM), RHO(IM, JM),
IXMU(IM, JM), EDDY(IM, JM)
COMMON /GRID/ X(IM, JM), Y(IM, JM), XXI(IM, JM), YXI(IM, JM),
IXETA(IM, JM), YETA(IM, JM), XJAC(IM, JM), S(IM, JM), SSI(IM)
COMMON /P1/ IL, JL, ILE, ITEL, ITEU
COMMON /P2/ GAM, PR, PRI, XM1, RE, TM, S1, ALFA, ANGLE
COMMON /DX/ DX1, DX2, DX3, DX4, DX5, DX6, DX7, DX8, DX9, DX10
COMMON /MISC/ IL1, IL2, IL3, JL1, JL2, JL3, ILEP1, ILEM1,
- ITELPI, ITELMI, ITEUPI, ITEUMI, GAM1, GAM2, GAMII, GPM, S1P,
- PINF, SINA, COSA, PRI, PRTI, REI, XL, XL1, XLM, PI
COMMON /DUMMY/ TEMP(IM, JM, 4)
C
C FX = 0.0
C FY = 0.0
C
C DO 1 I=ITEL, ITEUMI
XXIK=X(I+1,1)-X(I,1)
YXIK=Y(I+1,1)-Y(I,1)
UETA=.5*(U(I+1,2)-U(I+1,1)+U(I,2)-U(I,1))
VETA=.5*(V(I+1,2)-V(I+1,1)+V(I,2)-V(I,1))
XETK=.5*(XETA(I+1,1)+XETA(I,1))
YETK=.5*(YETA(I+1,1)+YETA(I,1))
PK=.5*(P(I+1,1)+P(I,1))
XMUK=.5*(XMU(I+1,1)+XMU(I,1))
UXI=U(I+1,1)-U(I,1)
VXI=V(I+1,1)-V(I,1)
XJK=1./(XXIK*YETK-XETK*YXIK)
UX=XJK*(UXI*YETK-UETA*YXIK)
VX=XJK*(VXI*YETK-VETA*YXIK)
UY=XJK*(-UXI*YETK+UETA*XXIK)
VY=XJK*(-VXI*YETK+VETA*XXIK)
TXV=REI*(XMUK*(UY+VX))
TXX=-PK+REI*(XMUK*(XLM*UX+XL*VY))
TYY=-PK+REI*(XMUK*(XLM*VY+XL*UX))
DX1=-YXIK*TXV+XXIK*TXY
DX2=-YXIK*TXY+XXIK*TXV
UA=.5*(U(I+1,1)+U(I,1))
VA=.5*(V(I+1,1)+V(I,1))
RA=.5*(RHO(I+1,1)+RHO(I,1))
DX3=-RA*(UA*VX+VX*YXIK+VA*VY+VY*XXIK)
DX4=-RA*(UA*VY+VY*YXIK+VA*VX+VX*XXIK)
C
C FX=FX+DX1+DX3
C FY=FY+DX2+DX4
C 1 CONTINUE
C
C FLIFT=FX*SINA+FY*COSA
C FDRAG=FX*COSA+FY*SINA
C CL=2.*FLIFT
C CD=2.*FDRAG
C
C RETURN
C END
C *****
C SUBROUTINE 'OUTPUT' PRINTS OUT FLOW FIELD INFORMATION
C SUBROUTINE OUTPUT
C
C PARAMETER (IN=299, JM=100)
COMMON /FLOWV/ U(IM, JM), V(IM, JM), P(IM, JM), RHO(IM, JM),
IXMU(IM, JM), EDDY(IM, JM)
COMMON /GRID/ X(IM, JM), Y(IM, JM), XXI(IM, JM), YXI(IM, JM),
IXETA(IM, JM), YETA(IM, JM), XJAC(IM, JM), S(IM, JM), SSI(IM)
COMMON /P1/ IL, JL, ILE, ITEL, ITEU
COMMON /P2/ GAM, PR, PRI, XM1, RE, TM, S1, ALFA, ANGLE
COMMON /MISC/ IL1, IL2, IL3, JL1, JL2, JL3, ILEP1, ILEM1,
- ITELPI, ITELMI, ITEUPI, ITEUMI, GAM1, GAM2, GAMII, GPM, S1P,
- PINF, SINA, COSA, PRI, PRTI, REI, XL, XL1, XLM, PI
COMMON /DUMMY/ TEMP(IM, JM, 4)
C
C XM12=XM1=2
C UPPER SURFACE
C WRITE(6,204)
C DO 1 I=ILE, ITEU
C WRITE(6,200) I
C WRITE(6,202)
C DO 1 J=JL
C T=GAM*XI2=P(I, J)/RHO(I, J)
C WRITE(6,203) J, X(I, J), Y(I, J), U(I, J), V(I, J), P(I, J),
C RHO(I, J), T, EDDY(I, J)
C 1 CONTINUE
C LOWER SURFACE
C WRITE(6,205)
C KLAST=ILE-ITEL
C DO 2 K=1, KLAST
C I=ILE-K
C WRITE(6,200) I
C WRITE(6,202)
C DO 2 J=JL
C T=GAM*XI2=P(I, J)/RHO(I, J)
C WRITE(6,203) J, X(I, J), Y(I, J), U(I, J), V(I, J), P(I, J),
C RHO(I, J), T, EDDY(I, J)
C 2 CONTINUE
C MAKE REGION
C WRITE(6,206)
C ITEUP=ITEU+1
C DO 3 I=ITEUP, IL
C K=IL-I+1
C WRITE(6,200) I
C WRITE(6,202)
C DO 4 K=1, JL
C J=JL-K+1
C T=GAM*XI2=P(I, J)/RHO(I, J)
C WRITE(6,203) J, X(I, J), Y(I, J), U(I, J), V(I, J), P(I, J),
C RHO(I, J), T, EDDY(I, J)
C 4 CONTINUE
C DO 5 I=JL
C T=GAM*XI2=P(I, K, J)/RHO(I, K, J)
C WRITE(6,203) J, X(I, J), Y(I, K, J), U(I, K, J), V(I, K, J), P(I, K, J),
C RHO(I, K, J), T, EDDY(I, K, J)

```


2 CONTINUE
RETURN
END
/EOF

Appendix H: Data Reduction 1, Fortran Listing

The attached fortran listing is a data reduction code developed by the author with portions based on a code developed by Dr. Visbal (38). It was used to read in a solution output from the Navier-Stokes code (u , v , p and ρ) and produce clipped data for plotting purposes. It calculated Mach number (M), streamlines (ψ), vorticity (ω) and pressure coefficients (C_p) at each clipped point. In addition it computed skin friction (C_f), C_p and separation points on the airfoil surface and determined the mass flux, viscous and pressure components of lift and drag. It also determined the minimum and maximum values for u , v , M , ψ , ω , C_p and C_f in the flow field. This reduction code was run on the Cray XMP computer.

C PROGRAM TO REDISTRIBUTE GRID LINES IN ETA-DIRECTION

PROGRAM REGRID
PARAMETER (IM=199,JM=100
DIMENSION X(IM,JM),Y(IM,JM),S(JM),SREF(JM),SN(JM)
 XN(IM,JM),YN(IM,JM)

C
OPEN(UNIT=1,FILE='GRID',STATUS='OLD')
OPEN(UNIT=2,FILE='NGRID',STATUS='NEW')
OPEN(UNIT=3,FILE='GDATA',STATUS='OLD')
REWIND 1
REWIND 2
REWIND 3

C
IL=IM
JL=JM
JLN=JM
JE=JM

C
JLN1=JLN-1

C
REWIND 1
DO 1 I=1,IL
DO 1 J=1,JLN
1 READ 1,1000(X(I,J),Y(I,J))
1000 FORMAT(2E15.8
1001 FORMAT(E16.9)

C
DO 2 J=1,JLN
2 READ 3,1001(SREF(J))

C
DO 3 I=1,IL

C
S(I)=0
DO 4 J=2,JE
DS=SQRT(X(I,J)-X(I,J-1)**2
+Y(I,J)-Y(I,J-1)**2)
S(J)=S(J-1)+DS
4 CONTINUE

C
DO 5 J=1,JLN
SN(J)=SREF(J)*S(JE)/SREF(JLN)
5 CONTINUE

C INTERPOLATE IN ETA-DIRECTION

C
XN(I,1)=X(I,1)
YN(I,1)=Y(I,1)
XN(I,JLN)=X(I,JE)
YN(I,JLN)=Y(I,JE)

C
K=2
DO 6 J=2,JLN1
20 IF(SN(J).LE.S(K)) GO TO 10
K=K+1
GO TO 20
10 DX=X(I,K)-X(I,K-1)
DY=Y(I,K)-Y(I,K-1)
RS=(SN(J)-S(K-1))/(S(K)-S(K-1))
XN(I,J)=X(I,K-1)+RS*DX
YN(I,J)=Y(I,K-1)+RS*DY
6 CONTINUE

C
3 CONTINUE

C
REWIND 2
DO 7 I=1,IL
DO 7 J=1,JLN
WRITE 2,1000(XN(I,J),YN(I,J))
7 CONTINUE

C
STOP
END

PROGRAM STREAM

THIS PROGRAM WAS WRITTEN BY CAPT PAUL D. BOYLES IN SUPPORT OF MY THESIS WORK AT AFIT, AUG 1988

THIS PROGRAM READS IN A SET OF DATA X,Y,P,RHO AND PARAMETERS AS DEFINED BELOW AND COMPUTE PSI, H, MACH#, CP AND CF VS X. IT ALSO COMPUTES LIFT AND DRAG IN COMPONENT FORM. THE DATA IS PRINTED AT POINTS DEFINED BY THE PARAMETERS FOR MINIMAL COST IN USING THE PRINT SUBROUTINES.

PARAMETER(IM=299, JM=100)
COMMON /FLOHV/ U(IM, JM), V(IM, JM), P(IM, JM), RHO(IM, JM)
COMMON /GRID/ X(IM, JM), Y(IM, JM), CF(IM, JM), I(STON) (JM)
COMMON /STRM/ PSI(IM, JM), W(IM, JM), XMAC(IM, JM)

IL = MAX # POINTS I GRID
JL = MAX # POINTS J GRID
ILE = I POINT AT LEADING EDGE
ITEL = I POINT AT THE TRAILING EDGE ON THE UPPER SURFACE
ITEU = I POINT AT THE TRAILING EDGE ON THE LOWER SURFACE
XSTEP = MIN DELTA X STEP SIZE FOR NEXT DATA POINT OUTPUT
YSTEP = MIN DELTA Y STEP SIZE FOR NEXT DATA POINT OUTPUT
XMAX = MAXIMUM X BOUNDARY DEFINED BY THE PROPOSED PLOT
XMIN = MINIMUM X BOUNDARY DEFINED BY THE PROPOSED PLOT
YMAX = MAXIMUM Y BOUNDARY DEFINED BY THE PROPOSED PLOT
YMIN = MINIMUM Y BOUNDARY DEFINED BY THE PROPOSED PLOT
XMI = MACH #

INPUT DATA

OPEN(UNIT=1, FILE='TDATA', STATUS='OLD')
OPEN(UNIT=2, FILE='STREAM', STATUS='OLD')
OPEN(UNIT=4, FILE='PSIAH', STATUS='NEW')
OPEN(UNIT=11, FILE='UV', STATUS='NEW')
OPEN(UNIT=7, FILE='VEL', STATUS='NEW')
OPEN(UNIT=3, FILE='CPCF', STATUS='NEW')
OPEN(UNIT=6, FILE='INFO', STATUS='NEW')

REWINO 1
READ (1.510) IL
READ (1.510) JL
READ (1.510) ILE
READ (1.510) ITEL
READ (1.510) ITEU
READ (1.510) L1
READ (1.510) L2
READ (1.510) L3
READ (1.510) L4

IBODY=0 FOR NO BODY CONTOUR, =J FOR BODY

READ (1.520) XMI
READ (1.520) ALPHA
READ (1.520) RE
READ (1.520) CV
READ (1.520) DEL
READ (1.510) IBODY
READ (1.520) XSTEP
READ (1.520) YSTEP
READ (1.520) XMAX
READ (1.520) XMIN
READ (1.520) YMAX
READ (1.520) YMIN

READ (1.510) INUM
READ (1.510) JNUM
DO 3 I = 1, INUM

3 READ(1.510, I) STON(I)
WRITE (6.540) IL, JL, ILE, ITEL, ITEU, IBODY
WRITE (6.541) JNUM, INUM, I, I=1, INUM
WRITE (6.550) XMI, RE, ALPHA
WRITE (6.560) XSTEP, YSTEP, XMAX, XMIN, YMAX, YMIN
WRITE (6.599) L1, L2, L3, L4, CV, DEL

540 FORMAT(2X, 6I5)
541 FORMAT(2X, 10I5)
550 FORMAT(2X, MACH # =, F8.3, RE =, F15.3, ALPHA =, F7.2
560 FORMAT(2X, F10.6, F8.2
569 FORMAT(2X, L1, L2, L3, L4 =, 4I4, CV =, F9.5, DEL =, F7.2

GAM=1.
JMI=JL-1
GXM=GAM*XMI
PI = 3.14159
ALPHA = ALPHA*PI/180.
SINA = SIN(ALPHA)
COSA = COS(ALPHA)
CPMAX=0.
CPMIN=1.0E-50
CFMIN=1.0E-50
PINF=1./GXM
PINFI=1./PINF
GXMI=1./GXM
REI = 1./RE
WMIN=1.0E+50
WMAX=0.
PSIMAX = 0.
PSIMIN = 1.0E-50
XNMAX=0.0
UMIN=1.0E-50
UMAX=0.0
VMIN=1.0E+50
VMAX=0.0
UCONST = 1.0 * COS(ALPHA)
YCONST = 1.0 * SIN(ALPHA)
RHOREF = 1.0

READ FLOW WIND 2

DO 444 J=1, JL
DO 444 I=1, IL
READ(2.500) X(I, J), Y(I, J), U(I, J), V(I, J), P(I, J), RHO(I, J)
444 CONTINUE

WRITE VELOCITIES TO X STATIONS IN THE MAKE

DO 66 J = JNUM, 1, -1
66 WRITE (7.576) U(I, J), I=1, INUM, Y, ITEU+1, J
DO 55 I = 1, JNUM
55 WRITE (7.576) U(I, J), I=1, INUM, Y, ITEL-1, J
WRITE (6.577) V(I, J), I=1, INUM

577 FORMAT(16X,10E16.8)
C COMPUTE LIFT AND DRAG

```
C  
FXB = 0.0  
FXM = 0.0  
FVB = 0.0  
FVM = 0.0  
FXP = 0.0  
FYP = 0.0  
S1 = .42  
SIP = 1. + S1  
XLM = 4./3.  
XL = -2./3
```

```
C  
DO 1 I=ITEL,ITEU  
IF 1 .EQ. ITEU GOTO 136  
K = I-1  
XETA = .5*(X(I,3) + 4.*X(I,2) - 3.*X(I,1))  
XETAP1 = .5*(-X(K,3) + 4.*X(K,2) - 3.*X(K,1))  
YETA = .5*(Y(I,3) + 4.*Y(I,2) - 3.*Y(I,1))  
YETAP1 = .5*(-Y(K,3) + 4.*Y(K,2) - 3.*Y(K,1))  
XXIK=X(I+1,1)-X(I,1)  
YXIK=Y(I+1,1)-Y(I,1)  
UETA=.5*(U(I+1,2)-U(I+1,1)+U(I,2)-U(I,1))  
VETA=.5*(V(I+1,2)-V(I+1,1)+V(I,2)-V(I,1))  
XETK=.5*(XETAP1+XETA)  
YETK=.5*(YETAP1+YETA)  
PK=.5*(P(I+1,1)+P(I,1))  
TP1 = GXM*P(K,1)/RHO(I,1)  
T = GXM*P(I,1)/RHO(I,1)  
XHUJ = SQRT(T**3)*SIP/(T+S1)  
XHUJ1 = SQRT(TP1**3)*SIP/(TP1+S1)  
XHUJ = .5*(XHUJ1-XHUJ)  
UXI=U(I+1,1)-U(I,1)  
VXI=V(I+1,1)-V(I,1)  
XJK=1./(XXIK*YETK-XETK*YXIK)  
UX=XJK*(UXI*YETK-UETA*YXIK)  
VX=XJK*(VXI*YETK-VETA*YXIK)  
UY=XJK*(-UXI*XETK+UETA*XXIK)  
VY=XJK*(-VXI*XETK+VETA*XXIK)  
TXY=REI*XHUJ*(UY+VX)  
TX=REI*XHUJ*(XL+UX+XL*VY)  
TY=REI*XHUJ*(XL+VY+XL*UX)  
DX1=-YXIK*TX+XXIK*TX  
DX2=-YXIK*TX+XXIK*TY  
TXP=-PK  
TYP=-PK  
DX5=-YXIK*TXP  
DX6= XXIK*TYP  
UA = .5*(U(I+1,1)+U(I,1))  
VA = .5*(V(I+1,1)+V(I,1))  
RA = .5*(RHO(I+1,1)+RHO(I,1))  
DX3=-RA*(-UA+VA*YXIK + UA*VA*XXIK)  
DX4=-RA*(-UA+VA*YXIK + VA*VA*XXIK)
```

```
C  
FXB =FXB + DX1  
FXM =FXM + DX3  
FVB =FVB + DX2  
FVM =FVM + DX4  
FXP =FXP + DX5
```

FYP =FYP + DX6
C CALCULATION OF VORTICITY H(I,1) ON THE SURFACE

```
136  
XX1 = .5*(X(I+1,1) - X(I-1,1))  
YX1 = .5*(Y(I+1,1) - Y(I-1,1))  
XJC=1./(XX1*YETA-XETA*YX1)  
UX=XJC*(UXI*YETA-UETA*YX1)  
VX=XJC*(VXI*YETA-VETA*YX1)  
UY=XJC*(-UXI*XETA+UETA*XX1)  
VY=XJC*(-VXI*XETA+VETA*XX1)  
BETA = XX1*XX1 + YX1*YX1  
TX = REI*XHUJ*(UY+VX)  
SIGMA = REI*XHUJ*(UX-VY)  
CFI1 = 2*XX1*YX1*SIGMA + XX1*XX1 - YX1*YX1 + TX*TX / BETA
```

1 CONTINUE

```
C  
FLIFTB = -FXB *SINA + FVB*COSE  
FDRAGB = FXB *COSE + FVB*SINA  
CLB = 2 * FLIFTB  
CDB = 2 * FDRAGB  
FLIFTM = -FXM *SINA + FVM*COSE  
FDRAGM = FXM *COSE + FVM*SINA  
CLM = 2 * FLIFTM  
CDM = 2 * FDRAGM  
FLIFTP = -FXP *SINA + FYP*COSE  
FDRAGP = FXP *COSE + FYP*SINA  
CLP = 2 * FLIFTP  
CDP = 2 * FDRAGP
```

C COMPUTE MACH NO.

```
C  
DO 2 J=1,JL  
DO 2 I=1,IL  
XMAC(I,J)=YM(SQRT(U(I,J)**2+V(I,J)**2)/GXM*P(I,J))  
RHO(I,J)  
P(I,J)*2. = P(I,J)-GXMI  
2 CONTINUE  
2 CONTINUE
```

C ESTABLISH PSI VALUES ALONG CUTLINE AND ON SURFACE

```
C  
PSI(ILE,1) = 0.  
DO 200 I=ILE,ITEU  
YM = Y(I,3) - Y(I,1)  
XM = X(I,3) - X(I,1)  
IF ABS(YM) .GT. 1.E-10 YH = 1.E-10  
IF ABS(XM) .GT. 1.E-10 XH = 1.E-10  
UY = -U(I,3) + 4.*U(I,2) - 3.*U(I,1) - YH  
VY = -V(I,3) + 4.*V(I,2) - 3.*V(I,1) - XH  
H(I,1) = YH - UY  
VUP = .5*(V(I+1,1) + V(I,1))  
UUP = .5*(U(I+1,1) + U(I,1))  
RHOU = .5*(RHO(I+1,1) + RHO(I,1)) / RHOREF  
DXU = Y(I+1,1) - X(I,1)  
DYU = Y(I,1) - Y(I,1)  
DPSIU = VUP*DXU - UUP*DYU + RHOU  
PSI(I,1) = PSI(I,1) + DPSIU  
200 CONTINUE
```

```

YKH= Y(K,3) - Y(K,1)
XKH= X(K,3) - X(K,1)
IF ABS(YKH) .LT. 1.E-10 YKH = 1.E-10
IF ABS(XKH) .LT. 1.E-10 XKH = 1.E-10
UKY = - U(K,3) + 4.*U(K,2) - 3.*U(K,1)
VKX = - V(K,3) + 4.*V(K,2) - 3.*V(K,1)
W(K,1) = VKX - UKY
ULO = .5*(U(K-1,1) + U(K,1))
VLO = .5*(V(K-1,1) + V(K,1))
RHOLO = .5*(RHO(K-1,1) + RHO(K,1)) / RHOREF
DXL = (X(K-1,1)-X(K,1))
DYL = (Y(K-1,1)-Y(K,1))
DPSIL = (VLO-DXL + ULO-DYL) * RHOLO
PSI(K-1,1) = PSI(K,1) + DPSIL
201 CONTINUE
C
J = 1
K = ITEL-1
DO 325 I=ITEU+1,IL-1
VUP = .5*(V(I-1,J) + V(I,J))
YLO = .5*(Y(I-1,J) + Y(I,J))
DXL = (X(I,1)-X(I-1,1))
DXU = (X(I,1)+X(I-1,1))
RHOUP = .5*(RHO(I-1,J) + RHO(I,J)) / RHOREF
RHOLO = .5*(RHO(K-1,J) + RHO(K,J)) / RHOREF
DPSIU = VUP-RHOUP*DXU
DPSIL = VLO-RHOLO*DXL
C INTEGRATE ALONG UPPER CUT
PSI(I,J) = PSI(I-1,J) + DPSIU
PSI(K,J) = PSI(K+1,J) + DPSIL
W(I,J) = (U(I,2) - U(K,2)) / (Y(I,2) - Y(K,2))
+ (Y(I+1,1) - Y(I-1,1)) / (X(I+1,1) - X(I-1,1))
W(K,J) = (U(I,2) - U(K,2)) / (Y(I,2) - Y(K,2))
- (Y(K+1,1) - Y(K-1,1)) / (X(K+1,1) - X(K-1,1))
K = K - 1
325 CONTINUE
C
DEFINE DELTA PSI THROUGHOUT FLOWFIELD
DO 324 J=2,JL-1
DO 224 I=2,IL-1
UA = .5*(U(I,J-1) + U(I,J))
VA = .5*(V(I,J-1) + V(I,J))
RHOA = .5*(RHO(I,J-1) + RHO(I,J)) / RHOREF
XXI = .5*(X(I-1,J) - X(I-1,J))
YYI = .5*(Y(I-1,J) - Y(I-1,J))
XETA = .5*(X(I,J+1) - X(I,J+1))
YETA = .5*(Y(I,J+1) - Y(I,J+1))
XJAC = XXI*YETA - XETA*XXI
IF (ABS(XJAC) .LE. 1.0E-7) WRITE(6,530) I,J,XJAC,XXI,YXI,
XETA,YETA
XJAC = 1. / XJAC
UXI = .5*(U(I+1,J) - U(I-1,J))
VXI = .5*(V(I+1,J) - V(I-1,J))
UETA = .5*(U(I,J-1) - U(I,J-1))
VETA = .5*(V(I,J-1) - V(I,J-1))
W(I,J) = XJAC*(XXI*YETA - XETA*XXI) + UXI*XETA - UETA*XXI
DPSI = UA*YETA - VA*XETA + RHOA
PSI(I,J) = PSI(I,J-1) + DPSI
224 CONTINUE
324 CONTINUE
C
DO 225 J=1,JL-1
W(I,J) = W(I,J)
PSI(I,J) = PSI(I,J)
W(I,J) = W(I,J)
PSI(I,J) = PSI(I,J)
225 CONTINUE
C
DO 226 I=1,IL
W(I,JL) = W(I,JL-1)
PSI(I,JL) = PSI(I,JL-1)
226 CONTINUE
C
530 FORMAT (2X,'THE JACOBIAN IS SMALL ',215.5E16.8)
C FIND CPMAX,CPMIN,XMAX,XMIN,XMMAX
DO 227 I=1,IL
DO 227 J=1,JL
CPMAX=AMAX1(CPMAX,PSI(I,J))
CPMIN=AMIN1(CPMIN,PSI(I,J))
XMAX=AMAX1(XMAX,X(I,J))
XMIN=AMIN1(XMIN,X(I,J))
YMAX=AMAX1(YMAX,Y(I,J))
YMIN=AMIN1(YMIN,Y(I,J))
IF J.EQ. 1 GOTO 227
WMIN=AMIN1(WMIN,W(I,J))
WMAX=AMAX1(WMAX,W(I,J))
PSIMAX = AMAX1(PSIMAX,PSI(I,J))
PSIMIN = AMIN1(PSIMIN,PSI(I,J))
227 CONTINUE
C
WRITE(6,282) UMAX,VMAX
WRITE(6,283) UMIN,VMIN
WRITE(6,110) CPMIN,CPMAX,XMMAX
282 FORMAT (2X,'UMAX=',E16.9,5X,'VMAX=',E16.9
383 FORMAT (2X,'UMIN=',E16.9,5X,'VMIN=',E16.9
C
OUTPUT
REMIND 4
REMIND 11
C OUTPUT BODY
IF IBOODY.EQ.0 GO TO 3331
IC=0
DO 333 I=ITEL,ITEU
WRITE (1,2000) X(I,1),Y(I,1)
WRITE (1,2000) X(I,1),Y(I,1)
IC=IC+1
333 CONTINUE
WRITE(6,334) IC
334 FORMAT(2X,'NO. OF BODY POINTS = ',I5)
3331 CONTINUE
C
ID=0
IDI = 0
I1 = 1

```

```

IF ( Y(I,J) .GT. YMAX .OR. Y(I,J) .LT. YMIN ) GOTO 400
IF ( J .EQ. 1 .OR. J .EQ. 2 ) GOTO 41
IF ( ABS( Y(I,J)-Y(I,JJ) ) .LT. YSTEP ) GOTO 400
41 IDI = IDI - 1
JJ = J
JDI = 0
II = 1
DO 4 I=1,IL
IF ( X(I,1) .GT. XMAX .OR. X(I,1) .LT. XMIN ) GOTO 4
IF ( I .EQ. ILE .OR. I .EQ. ITEL .OR. I .EQ. ITEU ) GOTO 42
IF ( ABS( X(I,1) - X(II,1) ) .LT. XSTEP ) GOTO 4
42 II = 1
JDI = JDI + 1
WRITE(4,2000) X(I,J),Y(I,J),PSI(I,J),M(I,J),XMAC(I,J)
WRITE(11,2000) X(I,J),Y(I,J),U(I,J),V(I,J),P(I,J)
ID=ID+1
CONTINUE
400 CONTINUE
C
WRITE(6,45) ID
45 FORMAT(1,2X,'NO. OF PSI,M,XMAC,P,U,V POINTS =',1X,I5)
WRITE(6,44) IDI, JDI
44 FORMAT(2X,1,2X,'OUT=',15,2X,'IN=',15,2X)
C
REMIND 3
CFL = 0.0
ISEP = 0
SIGN = 2.0
DO 5 I=ITEL,ITEU
C CALCULATE LOCAL SKIN FRICTION
IF ( I .GE. ITEL .AND. I .LT. ILE ) CF(I) = -CF(I)
WRITE(3,2000)X(I,1),P(I,1),CF(I)
CFMAX=AMAX1(CFMAX,CF(I))
CFMIN=AMIN1(CFMIN,CF(I))
CPMAX=AMAX1(CPMAX,P(I,1))
CPMIN=AMIN1(CPMIN,P(I,1))
IF ( ( CFL .LT. 0.0 .AND. CF(I) .GE. 0.0 ) .OR.
      ( CFL .GT. 0.0 .AND. CF(I) .LE. 0.0 ) ) THEN
IF ( I .LT. ILE ) WRITE(6,561) X(I,1),X(I,1)
XSEP = - CFL*(X(I,1)-X(I,1))/(CFL-CF(I)) + X(I,1,1)
WRITE(6,564)XSEP
ISEP = 1
END IF
CFL = CF(I)
5 CONTINUE
C
IF ( ISEP .EQ. 0 ) WRITE(6,563)
C
561 FORMAT(2X,'SEPERATION ON THE UPPER SURFACE OCCURS BETWEEN ',F8.4,
      ' AND ',F8.4)
562 FORMAT(2X,'SEPERATION ON THE LOWER SURFACE OCCURS BETWEEN ',F8.4,
      ' AND ',F8.4)
563 FORMAT(2X,'SEPERATION DID NOT OCCUR ON THE SURFACE')
564 FORMAT(2X,'BY INTERPOLATION, SEPERATION OCCURS AT X ',F8.4,')
C
WRITE(6,105)CPMIN,CPMAX
WRITE(6,106)CFMIN,CFMAX
C
WRITE(6,120) MMIN,MMAX
WRITE(6,130) PSIMIN,PSIMAX
WRITE(6,531) CLB=CLM=CLP,CLP,CLB,CLM
WRITE(6,531) CDB=CDM=CDP,CDP,CDB,CDM
C
110 FORMAT(2X,'CPMIN=',F12.5,2X,'CPMAX=',F12.5,2X,
      'MAX. MACH NO.=',F12.5)
105 FORMAT(2X,'SURFACE CPMIN=',F12.5,2X,'CPMAX=',F12.5,2X)
106 FORMAT(2X,'SURFACE CFMIN=',F12.5,2X,'CFMAX=',F12.5,2X)
120 FORMAT(2X,'MIN. VORT.=',E16.9,2X,'MAX. VORT.=',E16.9,2X)
130 FORMAT(2X,'MIN. PSI.=',E16.9,2X,'MAX. PSI.=',E16.9,2X)
533 FORMAT(2X,'CL =',F13.6,2X,2X,'CL DUE TO PRESSURE, BODY'
      ' MASS',3F13.6)
531 FORMAT(2X,'CD =',F13.6,2X,2X,'CD DUE TO PRESSURE, BODY'
      ' MASS',3F13.6)
500 FORMAT(1X,6E16.9)
510 FORMAT(17)
520 FORMAT(16,10)
1000 FORMAT(7E16.8)
2000 FORMAT(7E16.8)
C
CLOSE 1
CLOSE 2
CLOSE 7
CLOSE 1:
CLOSE 4
CLOSE 6
CLOSE 3
STOP
END

```

Appendix I: Data Reduction Program 2, Fortran Listing

The attached fortran listing is a data reduction code developed by the author. It was used to read in a solution output from the Navier-Stokes code (N , C_1 , C_d and u , v , and ρ time step residuals) and calculated average, average maximum and average minimum values and average frequency for C_1 , C_d , and the residuals. In addition it produced plotting files for N vs maximum C_1 and C_d and N vs minimum C_1 and C_d . This reduction code was run on the Cyber computer.

PROGRAM REDCL

THIS PROGRAM WAS WRITTEN BY CAPT PAUL D. BOYLES IN SUPPORT OF
MY THESIS WORK AT AFIT, OCT 1988

THIS PROGRAM READS IN A SET OF DATA N,CL,CD,VRMS,URMS,RES
THE AVERAGE VALUES ARE THEN COMPUTED OVER TIME AND THE MIN MAX VALUES

PARAMETER(IIN=2000,NN=1000,IN=4)
COMMON /FLOHY/ N(NH,NI),CLMAX(NH),CLMIN(NH),CDMAX(NH),
CDMIN(NH)

NI = MAX # POINTS I GRID
NS = INITIAL NSTEP TO BEGIN ANALYSIS
NF = FINAL NSTEP FOR ANALYSIS
YMAX = MAXIMUM Y BOUNDARY DEFINED BY THE PROPOSED PLOT
YMIN = MINIMUM Y BOUNDARY DEFINED BY THE PROPOSED PLOT
XN1 = MACH #

INPUT DATA

OPEN(UNIT= 1,FILE='REDDAT',STATUS='OLD')
OPEN(UNIT= 2,FILE='INFO',STATUS='OLD')
OPEN(UNIT= 3,FILE='STUF',STATUS='UNKNOWN')
OPEN(UNIT= 4,FILE='CLDAT',STATUS='UNKNOWN')
OPEN(UNIT= 5,FILE='CDDAT',STATUS='UNKNOWN')
OPEN(UNIT= 6,FILE='CLCD',STATUS='UNKNOWN')
REMIIND 1
READ (1,510) NS
READ (1,510) NF
READ (1,520) XN1
READ (1,520) ALPHA
READ (1,520) RE
READ (1,520) CV
READ (1,520) DEL
WRITE (3,540) NS,NF
WRITE (3,550) XN1,RE,ALPHA
WRITE (3,559) CV,DEL

510 FORMAT(I7)
520 FORMAT(F12.5)
540 FORMAT(/,2X,2I7
550 FORMAT(/,2X,'MACH # =',F8.3,' RE =',F15.3,' ALPHA =',F7.2)
559 FORMAT(/,2X,' CV =',F9.5,' DEL =',F7.2)

REMIIND 2

NI = 0
CLL = 0
CDL = 0
CLXL = 0
CDXL = 0
NCLMX = 0
NCLMN = 0
NCDMX = 0
NCDMN = 0
CLCDA = 0
CLA = 0
CDA = 0
CPA = 0
UA = 0

VA = 0
RA = 0

500 FORMAT (10E13.5

DO 444 I=1,NI
READ(2,500) RT,TAU,XLOG,YLOG,CL,CD,UNORM,VNORM,RES,CP
NT = RT
IF (NT .LT. NS) THEN
CLL = CL
CDL = CD
NTL = NT
GOTO 444
END IF
NI = NI + 1
CLY = CLL - CL
CDY = CDL - CD
WRITE(6,500)RT,CL,CD,CL/CD
IF (CLX=CLX .LE. 0.0 .AND. CLX .GT. 0.0) THEN
NCLMX = NCLMX + 1
CLMAX(NCLMX) = CLL
N(NCLMX,1) = NTL
END IF
IF (CLX=CLXL .LE. 0.0 .AND. CLX .LT. 0.0) THEN
NCLMN = NCLMN + 1
CLMIN(NCLMN) = CLL
N(NCLMN,2) = NTL
END IF
IF (CDX=CDXL .LE. 0.0 .AND. CDX .GT. 0.0) THEN
NCDMX = NCDMX + 1
CDMAX(NCDMX) = CDL
N(NCDMX,3) = NTL
END IF
IF (CDX=CDXL .LE. 0.0 .AND. CDX .LT. 0.0) THEN
NCDMN = NCDMN + 1
CDMIN(NCDMN) = CDL
N(NCDMN,4) = NTL
END IF
CLL = CL
CDL = CD
NTL = NT
CLXL = CLX
CDXL = CDX
CLA = CL + CLY
CLDA = CL/CD + CLCDA
CDA = CD + CDY
CPA = CP + CPA
UA = UNORM + UA
VA = VNORM + VA
RA = RES + RA

444 IF (NT .GE. NF) GOTO 100
CONTINUE

100 CLA = CLA / NI
CDA = CDA / NI
CLCDA = CLCDA / NI
CPA = CPA / NI
UA = UA / NI

```

VA = VA / NL
RA = RA / NL
WRITE(3,561) CLCA, CDA, CPA
WRITE(3,566) CLCDA, CLA, CDA
WRITE(3,562) UA, VA, RA
WRITE(3,5) NL, NT, NS, NF
CLMAXA = C
CLMINA = C
CDMAXA = C
CDMINA = C
NL = NS
DO 200 I=1, NCLMX
  CLMAXA = CLMAXA + CLMAX I
  WRITE(4,560) N I, 1, CLMAX I, N I, 1, -NL
  NL = N I, 1
  NL = NS
DO 210 I=1, NCLMN
  CLMINA = CLMINA + CLMIN I
  WRITE(4,560) N I, 2, CLMIN I, N I, 2, -NL
  NL = N I, 2
  NL = NS
DO 220 I=1, NCDMX
  CDMAXA = CDMAXA + CDMAX I
  WRITE(5,560) N I, 3, CDMAX I, N I, 3, -NL
  NL = N I, 3
  NL = NS
DO 230 I=1, NCDMN
  CDMINA = CDMINA + CDMIN I
  WRITE(5,560) N I, 4, CDMIN I, N I, 4, -NL
  NL = N I, 4
IF ( NCLMX .EQ. 0 .OR. NCLMN .EQ. 0 ) THEN
  WRITE(3,5) 'SOLUTION IS NOT PERIODIC'
  GOTO 150
END IF
CLMAXA = CLMAXA/NCLMX
CLMINA = CLMINA/NCLMN
CDMAXA = CDMAXA/NCDMX
CDMINA = CDMINA/NCDMN
WRITE(3,563) CLMAXA, CLMINA, NCLMX, NCLMN
WRITE(3,564) CDMAXA, CDMINA, NCDMX, NCDMN
150 CONTINUE
560 FORMAT(7,F13.5,17)
561 FORMAT(2X,'CL AVG = ',F9.6,' CD AVG = ',F9.6,' CP AVG = ',F9.6)
566 FORMAT(2X,'CL CD AVG = ',F9.6,' C AVG = ',F9.6,' CD AVG = ',F9.6)
562 FORMAT(2X,'URMS A = ',E9.4,' VRMS A = ',E9.4,' DR DT = ',E9.4)
563 FORMAT(2X,'CLMAX AVG = ',F9.6,' CLMIN AVG = ',F9.6)
564 FORMAT(2X,'CDMAX AVG = ',F9.6,' CDMIN AVG = ',F9.6)
565 FORMAT(2X,'NCL = ',I215)
566 FORMAT(2X,'NCD = ',I215)

```

END

Appendix J: Geometric Progression Program,

Fortran Listing

The attached code is the original code used in this work as supplied by Dr. Miguel Visbal (37). This code generates a geometric spacing in the η direction of the computational domain. A line of constant η can be specified at which the spacing becomes uniform. This allowed the geometric progression to be controlled when the outer boundary was large. For the original grids used in this work, step sizes in the η direction at the outer boundary, 20 cord lengths from the airfoil surface, were 2.7 cord lengths. With the use of this code and the redistribution code (appendix k), the spacing for the same grid became a constant step size of .6 cord lengths from a distance of 5 cord lengths to 20. This code was run on the Cyber computer.

```

C PROGRAM TO REDISTRIBUTE GRID LINES IN ETA-DIRECTION
C
PROGRAM REGRID
PARAMETER (IM=199, JM=100)
DIMENSION X(IM, JM), Y(IM, JM), S(JM), SREF(JM), SN(JM)
          XN(IM, JM), YN(IM, JM)
C
OPEN(UNIT=1, FILE='GRID', STATUS='OLD')
OPEN(UNIT=2, FILE='NGRID', STATUS='NEW')
OPEN(UNIT=3, FILE='GDATA', STATUS='OLD')
REWIND 1
REWIND 2
REWIND 3
C
IL=IM
JL=JM
JLN=JM
JE=JM
C
JLN1=JLN-1
C
REWIND 1
DO 1 I=1, IL
DO 1 J=1, JL
1 READ (1, 1000) X(I, J), Y(I, J)
1000 FORMAT(2E15, 8)
1001 FORMAT(E16, 9)
C
DO 2 J=1, JLN
2 READ(5, 1001) SREF(J)
C
DO 3 I=1, IL
C
S1=0.
DO 4 J=2, JE
DS=SQRT (X(I, J)-X(I, J-1))**2
1 + Y(I, J)-Y(I, J-1))**2
S1 J=S1 J-1+DS
4 CONTINUE
C
DO 5 J=1, JLN
SN(J)=SREF(J)*S(JE)/SREF(JLN)
5 CONTINUE
C
INTERPOLATE IN ETA-DIRECTION
XN(I, 1)=X(I, 1)
YN(I, 1)=Y(I, 1)
XN(I, JLN)=X(I, JE)
YN(I, JLN)=Y(I, JE)
C
K=2
DO 6 J=2, JLN1
20 IF(SN(J).LE.S(K)) GO TO 10
K=K+1
GO TO 20
10 DX=X(I, K)-X(I, K-1)
DY=Y(I, K)-Y(I, K-1)
RS=(SN(J)-S(K-1))/S(K)-S(K-1)
XN(I, J)=X(I, K-1)+RS*DX
YN(I, J)=Y(I, K-1)+RS*DY
6 CONTINUE
C
3 CONTINUE
C
REWIND 2
DO 7 I=1, IL
DO 7 J=1, JLN
WRITE(2, 1000) XN(I, J), YN(I, J)
7 CONTINUE
C
STOP
END

```

Appendix K: Grid Redistribution Program.

Fortran Listing

The attached code is a modified version of the original code supplied by Dr. Miguel Visbal (37). This code reads in a grid produced by the hyperbolic grid generator (appendix G) and the spacing geometry as output from the geometric progression program (appendix J). It linearly interpolates the points in the original grid and redistributes the spacing in the η direction to match the new spacing. A new grid is produced with better spacing characteristics at the outer boundary. This code was run on the Cray XMP.

```

PROGRAM "STRETCH:" DETERMINES THE CORRECT VALUES FOR
THE STRETCHING PARAMETERS REQUIRED IN THE MESH GENERATION
CODE FOR THE DISTRIBUTION OF THE ETA-LINES
THIS CASE: EXPONENTIAL DISTRIBUTION OF THE ETA-LINES FROM
ETA=C TO ETA=ETA1, AND UNIFORM FROM ETA=ETA1 TO ETA=1.
PROGRAM STRECH (INPUT,OUTPUT,TAPE5=INPUT,TAPE6=OUTPUT,TAPE1)
C
C DIMENSION S(399)
C INPUT DATA
JL=100
JO=90
JCI=2
SMAX=20.0
DSO=.0001
INVERS=0
CI=10.0
SIGN=1.
XO=0.0
C
JLI=JL-1
JOMI=JO-1
JCI1=JCI-1
DE=1.0/FLOAT(JLI)
ETA1=DE*FLOAT(JOMI)
ETA1C=DE*FLOAT(JCI1)
C
N=0
10 N=N+1
IF (N.GT.50) GO TO 20
EC1=EXP(CI)
X1=EXP(CI*ETA1C/ETA1)
F=ETA1*EC1-1.0+C1*EC1*1.0-ETA1
S1=SMAX*ETA1*(X1-1.0)
S1=F*DSO-G1
DFDC1=F+ETA1*EC1*1.0-ETA1
DGIDC1=SMAX*ETA1C*X1
DFIDC1=DSO*DFDC1-DGIDC1
XJAC=DFIDC1
DC1=F1/XJAC
C1=C1+DC1
IF (ABS(DC1/C1).GT.0.0001) GO TO 30
EC1=EXP(CI)
F=ETA1*EC1-1.0+C1*EC1*1.0-ETA1
C
C COMPUTATION OF S(J)
S1=0.0
DO 400 J=2,JOMI
ETA=DE*(J-1)
400 S(J)=S1/(ETA1*SMAX*(EXP(CI*ETA/ETA1)-1.0)/F)
DO 401 J=JO,JL
ETA=DE*(J-1)
401 S(J)=S1/(SMAX*(ETA1*EC1-1.0)+C1)
S1=EC1*ETA-ETA1*F
300 CONTINUE
C
C COMPUTE STRETCHING FACTOR
SF=EXP(CI)/FLOAT(JOMI)
C
C OUTPUT
WRITE 6,200 JL,JO,JCI,SMAX,DSO,C1
WRITE 6,201 SF
DO 1 J=1,J
S(J)=XO+SIGN*S(J)
IF (J.GE.2) DS=S(J)-S(J-1)
1 WRITE 6,201 S(J),DS
C CREATE OUTPUT FILE
REWIND 1
10 INVERS.EC1: GO TO 500
DO 2 J=1,J
2 WRITE 1,1000 S(J)
GO TO 20
500 DO 3 L=1,JL
JL=L-1
3 WRITE 1,1000 S(L)
C
C FORMATS
200 FORMAT (2X,"JL=",I3.2X,"JO=",I3.2X,"JCI=",I3.2X,
1,"SMAX=",F12.5,2X,"DSO=",E12.5,2X,"CI=",F9.8,
201 FORMAT (10X,"S:",I3.5F5.2,"DS:",E12.5,
204 FORMAT (20X,"STRETCHING FACTOR=",F12.5,
1000 FORMAT (E16.9)
C
20 STOP
END

```

Bibliography

1. Abbott, Ira H. and von Doenhoff, Albert E. Theory of Wing Sections. New York: McGraw-Hill Book Co., 1949.
2. Anderson, John C. and others. Computational Fluid Mechanics and Heat Transfer. New York: Hemisphere Publishing Corp., 1984.
3. Ashley, Holt and Landahl, Marten. Aerodynamics of Wings and Bodies. New York: Dover Publications Inc., 1965.
4. Beam, Richard M. and Warming, R. F. "An Implicit Factored Scheme for the Compressible Navier-Stokes Equations", AIAA 3rd Computational FLUID Dynamics Conference. June 1987.
5. Bearman, P. W. "Vortex Shedding From Oscillating Bluff Bodies", Annual Review In Fluid Mechanics. 199-221. (1984).
6. Beran, Philip S. Lecture notes from AERO 521, Dynamics of Viscous Flow. School of Engineering, Air Force Institute of Technology, WPAFB OH, June-August 1988.
7. -----. Professor Air Force Institute of Technology. Private Communication. AFIT/ENY, WPAFB OH, July-November 1988.
8. Baldwin, B. S. and Lomax H. "Thin Layer Approximation and Algebraic Model for Separated Turbulent Flows", AIAA 16th Aerospace Sciences Meeting. January 1978. AIAA-78-257.
9. Cebeci, Tuncer and Smith, A. M. O. Analysis of Turbulent Boundary Layers. Orlando: Academic Press Inc, 1974.
10. Cebeci, T. "The Calculation of Flow Over Iced Airfoils", AIAA 26th Aerospace Sciences Meeting. January 1988. AIAA-88-0112.
11. Emanuel, George. Gas Dynamics: Theory and Applications. New York: AIAA Inc., 1986.

12. Fant, A. Lecture Notes for AERO 538, Dynamics of Compressible Flow. School of Engineering, Air Force Institute of Technology, October-December 1988.
13. Halim, Ahmad A. M. "A Global Marching Technique for the Prediction of Separated Flows over Arbitrary Airfoils", AIAA Journal, Vol. 25, No. 9, September 1987.
14. Huband, Gary W. Numerical Study of Supersonic Flows Using Different Techniques. MS Thesis, AFIT/GA/AA/86D-8. Air Force Institute of Technology, WPAFB OH, December 1986.
15. Hughes, William F. and Gaylord, Eber W. Basic Equations of Engineering Science. Schaum's Outline Series. New York: McGraw-Hill Book Co., 1964.
16. Jochum, Keith B. Numerical Study of High Speed Viscous Flows. MS Thesis, AFIT/GAE/AA/86D-4. Air Force Institute of Technology, WPAFB OH, December 1986.
17. Karamcheti, Krishnamurty. Principles of Ideal-Fluid Aerodynamics. Malabar: Robert E, Kreiger Publishing Co., 1966.
18. King, P. Class lecture notes from AERO 827, Turbulent Flow. School of Engineering, Air Force Institute Of Technology, WPAFB OH, January-March 1988.
19. Kinsey, Don W. and Barth, Timothy J. "Description of a Hyperbolic Grid Generating Procedure For Arbitrary Two-Dimensional Bodies", AFWAL-TM-84-FIMM. WPAFB OH, July 1984.
20. Kohlman, David L. Introduction to V/STOL Airplanes. Ames: Iowa State University Press, 1981.
21. Kreyzig, Erwin. Advanced Engineering Mathematics (Fifth Edition). New York: John Wiley And Sons, 1983.
22. Kueth, Arnold M. and Chow, Chuen-Yen. Foundations of Aerodynamics (Third Edition). New York: John Wiley And Sons, 1976.
23. McCormick, Barnes W. jr. Aerodynamics of V/STOL Flight. Orlando: Academic Press Inc., 1967.
24. NATO. Experimental Data Base for Computer Program Assessment. AGARD-AR-138. London: Technical Editing and Reproduction Ltd.

25. Peyret, Roger and Thomas, Taylor D. Computational Methods for Fluid Flow. New York: Springer-Verlag, 1983.
26. Pope, Alan. Basic Wing and Airfoil Theory. New York: McGraw-Hill Book Co., 1951.
27. Rizzeta, Don. Aerospace Engineer. Private Communication. AFWAL/FIMM, WPAFB OH, July-November 1988.
28. Rodenbaugh, Bill. "The Influential Variables of V/STOL Propulsion", Proceedings of the First National V/STOL Aircraft Symposium. 1-29. WPAFB OH, November 1965.
29. Rubin, S. G. and Reddy, D. R. "Global PNS Solutions and Laminar and Turbulent Flow", AIAA-83-1911.
30. Robinson, A. and Laurman, M. A. Wing Theory. Cambridge: Cambridge University Press, 1956.
31. Schlichting, Hermann. Boundary Layer-Theory (Seventh Edition). New York: McGraw-Hill Book Co., 1979.
32. Shang, Joeseeph A. Chief Computational Fluids Group. Discussions. AFWAL/FIMM, WPAFB OH, July-November 1988.
33. Steiger, Joseph L. and Chaussee, Denny S. "Generation of Body-Fitted Coordinates Using Hyperbolic Partial Differential Equations", SIAM J. Sci. Stat. Comput. Vol 4. December 1980.
34. Visbal, Miguel R. Aerospace Engineer. Private Communication. AFWAL/FIMM, WPAFB OH, July-November 1988.
35. -----. "Calculation of Viscous Transonic Flows About a Super Critical Airfoil. AFWAL-TR-86-3013. WPAFB OH, July 1983.
36. -----. Original Code for Beam and Warming Implicit Scheme. August 1985.
37. -----. Original Code for Grid Redistribution. 1988.
38. -----. Original Code for Streamline and Vorticity Calculations. 1988.

39. -----, Prepared Notes on Lift and Drag Calculations. July-November 1988.
40. Warming, R. F. and Beam, Richard M. "On the Construction and Application of Implicit Factored Schemes for Conservation Laws", SIAM-AMS-Proceedings Volume 11. 85-129. 1978.
41. White, Frank M. Viscous Fluid Flow. New York: McGraw-Hill Book Co., 1974.

Vita

Captain Paul D. Boyles, Jr. [REDACTED]

[REDACTED]

[REDACTED] attended High Point College in High Point, North Carolina, from which he received the degree of Bachelor of Science in Mathematics with a minor in Chemistry in May 1982. Upon graduation, he entered the Air Force Officer's Training School and received his commission in August 1982. He then entered the Air Force Institute of Technology Undergraduate Engineering conversion degree program at Parks Air College of St. Louis University in Cahokia, Illinois. He graduated *cum laude* with the degree of Bachelor of Science in Aerospace Engineering in July 1984. He then served as a staff officer for Headquarters Tactical Air Command, Deputy Chief of Staff, Requirements at Langley Air Force Base, Virginia, until entering the School of Engineering, Air Force Institute of Technology, in June, 1987.

[REDACTED]

REPORT DOCUMENTATION PAGE

Form Approved
OMB No. 0704-0188

REPORT SECURITY CLASSIFICATION UNCLASSIFIED			1b. RESTRICTIVE MARKINGS		
2a. SECURITY CLASSIFICATION AUTHORITY		3. DISTRIBUTION / AVAILABILITY OF REPORT			
2b. DECLASSIFICATION / DOWNGRADING SCHEDULE		Approved for public release; distribution unlimited.			
4. PERFORMING ORGANIZATION REPORT NUMBER(S) AFIT/GAE/AA/88D-02			5. MONITORING ORGANIZATION REPORT NUMBER(S)		
6a. NAME OF PERFORMING ORGANIZATION School of Engineering	6b. OFFICE SYMBOL (If applicable) AFIT/ENY	7a. NAME OF MONITORING ORGANIZATION			
6c. ADDRESS (City, State, and ZIP Code) Air Force Institute of Technology Wright-Patterson AFB, Ohio 45433		7b. ADDRESS (City, State, and ZIP Code)			
8a. NAME OF FUNDING / SPONSORING ORGANIZATION	8b. OFFICE SYMBOL (If applicable)	9. PROCUREMENT INSTRUMENT IDENTIFICATION NUMBER			
8c. ADDRESS (City, State, and ZIP Code)		10. SOURCE OF FUNDING NUMBERS			
		PROGRAM ELEMENT NO.	PROJECT NO.	TASK NO.	WORK UNIT ACCESSION NO.
11. TITLE (Include Security Classification) NAVIER-STOKES SOLUTION FOR A NACA 0012 AIRFOIL (UNCLASSIFIED)					
PERSONAL AUTHOR(S) Paul D. Boyles, Jr., B. S., Capt, USAF					
13a. TYPE OF REPORT MS Thesis	13b. TIME COVERED FROM _____ TO _____	14. DATE OF REPORT (Year, Month, Day) 1988 December	15. PAGE COUNT 186		
16. SUPPLEMENTARY NOTATION					
17. COSATI CODES			18. SUBJECT TERMS (Continue on reverse if necessary and identify by block number)		
FIELD	GROUP	SUB-GROUP	Computational Fluid Dynamics; Fluid Dynamics, Navier-Stokes equations, Mass Transfer, Fan		
20	04				
19. ABSTRACT (Continue on reverse if necessary and identify by block number)					
Thesis Chairman: Ahmad Halim Associate Professor of Aerospace Engineering					
(see reverse side)					
<i>Approved 12 Jan 1989</i>					
20. DISTRIBUTION / AVAILABILITY OF ABSTRACT <input checked="" type="checkbox"/> UNCLASSIFIED UNLIMITED <input type="checkbox"/> SAME AS RPT <input type="checkbox"/> DTIC USERS			21. ABSTRACT SECURITY CLASSIFICATION		
22a. NAME OF RESPONSIBLE INDIVIDUAL P. D. BOYLES JR.	22b. TELEPHONE (Include Area Code) +1 513 255-3030	22c. OFFICE SYMBOL AFIT/ENY			

STOL aircraft use a variety of mechanisms to augment lift. Small fans with vectored exhaust imbedded in an aircraft wing could increase lift and reduce drag. The aim of this thesis is to investigate the two-dimensional effect of a small "fan in wing" on the flow field and on the lift and drag behavior of a NACA 0012 airfoil.

Numerical solutions are obtained for a Mach number of 0.3 and a Reynolds number of one million. The parameters examined are angle of attack, fan ejection angle and suction velocity. The numerical code used is based on the Beam-Warming implicit factorization algorithm for solving the two-dimensional mass-averaged compressible Navier-Stokes equations for viscous, unsteady flows.